Pharmacological functions of multidrug transporters:
studies employing combination transporter knockout mice

ISBN/EAN 978-94-9012-223-2

Cover Art: Marinus Lagas, Alteveer (gem. Noordenveld)

Printed by: Gildeprint Drukkerijen, Enschede

Pharmacological functions of multidrug transporters:
studies employing combination transporter knockout mice

Farmacologische functies van multidrug transporters:
studies met combinatie transporter knockout muizen
(met een samenvatting in het Nederlands)

PROEFSCHRIFT

ter verkrijging van de graad van doctor
aan de Universiteit van Utrecht
op gezag van rector magnificus, prof. dr. J.C. Stoof,
ingevolge het besluit van het college van promoties
in het openbaar te verdedigen
op woensdag 17 juni 2009 des middags te 12.45 uur

door

Jurjen Sebastiaan Lagas

geboren op 10 oktober 1975 te Groningen

Promotor: Prof. dr. J.H. Beijnen

Co-promotor: Dr. A.H. Schinkel

Publication of this thesis was financially supported by:

The Netherlands Cancer Institute, Amsterdam, The Netherlands
The Netherlands Laboratory for Anticancer Drug Formulation (NLADF), Amsterdam, The Netherlands
Abbott, Hoofddorp, The Netherlands
AstraZeneca, Zoetermeer, The Netherlands
Boehringer Ingelheim, Alkmaar, The Netherlands
Merck Sharp & Dohme, Haarlem, The Netherlands

The research described in this thesis was performed at the Divisions of Experimental Therapy and Molecular Biology of the Netherlands Cancer Institute, Amsterdam, The Netherlands.

Aan mijn ouders

Voor Willemien,
Daniël en Ruben

CONTENTS

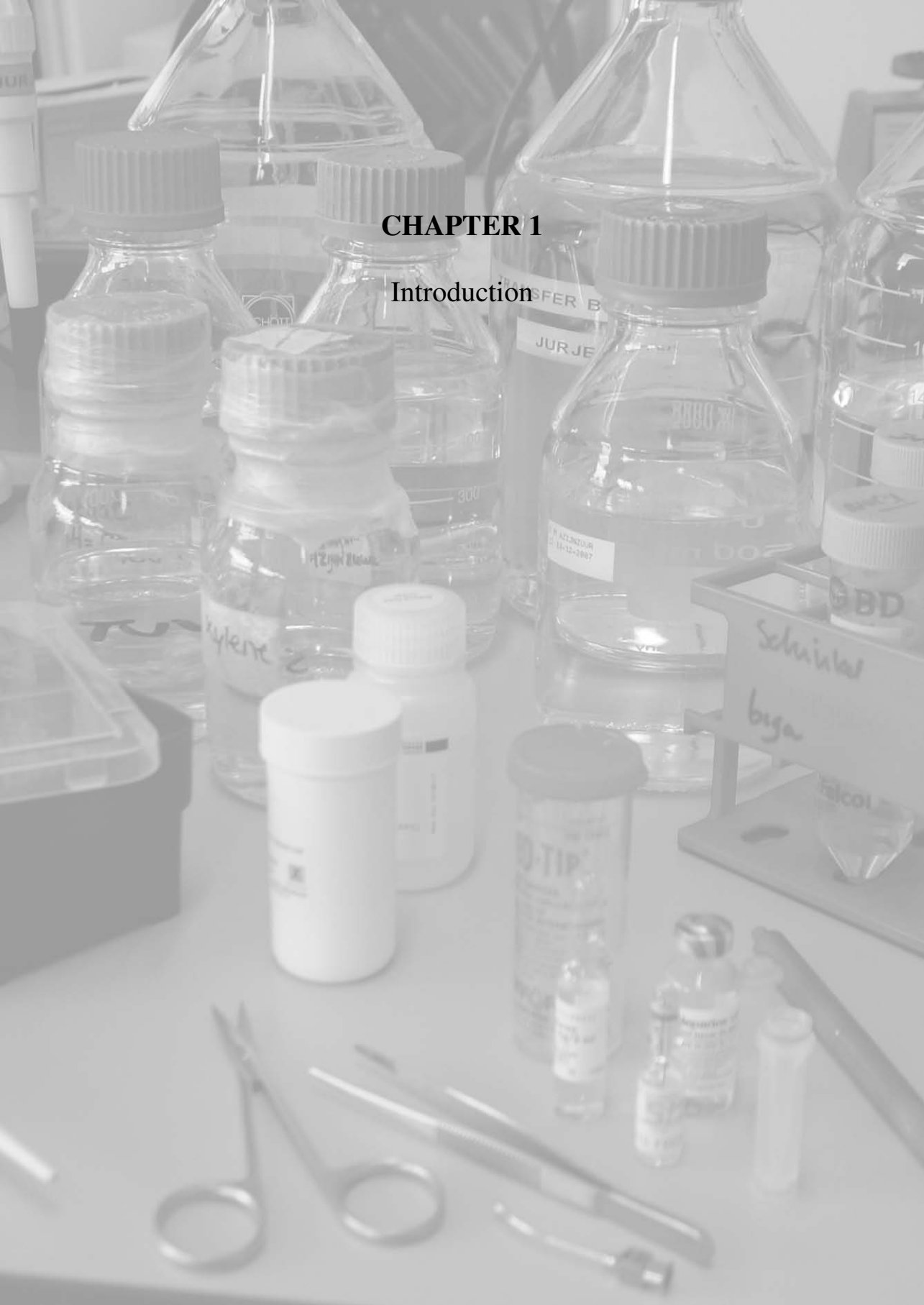

CHAPTER 1

Introduction

CHAPTER 1.1

Compound transporter knockout mice: powerful tools to unravel the pharmacological and physiological functions of ATP-binding cassette drug transporters

Jurjen S. Lagas*, Maria L.H. Vlaming* and Alfred H. Schinkel

* These authors contributed equally to this work.

To be submitted

ABSTRACT
ATP-binding cassette (ABC) transporters are cellular efflux pumps with broad and often widely overlapping substrate specificities, which can have a major impact on the pharmacology and pharmacokinetics of many drugs. To study their separate roles and functional overlap, a collection of mice deficient in two or more ABC transporters, termed "compound transporter knockout mice", has been generated and characterized. This review discusses recent findings obtained with these models, focusing on pharmacokinetic studies with a number of clinically relevant drugs. In addition, the characterization of these mice and some physiological aspects of ABC transporters are addressed.

INTRODUCTION
ATP-binding cassette (ABC) transporters, including the multidrug efflux transporters P-gp (ABCB1/MDR1), ABCC1-4 (MRP1-4) and ABCG2 (BCRP), are transmembrane proteins that can actively extrude a wide variety of endogenous and exogenous compounds from cells. Most multidrug ABC transporters have broad and substantially overlapping substrate specificities, and their substrates include many drugs and drug metabolites [extensively reviewed in (1;2)].

P-gp, ABCC2 and ABCG2 are localized at the canalicular membranes of hepatocytes and at the apical membrane of epithelial cells of kidneys and the intestinal tract where they pump their substrates into bile, urine and feces. Consequently, these efflux pumps can have an important impact on the elimination of many clinically relevant drugs and they can restrict their intestinal uptake (1;2). In addition, these transporters are found at the blood-placenta, blood-testis and blood-brain barriers, where they protect the corresponding tissue sanctuaries from the penetration of potentially harmful compounds (1;2).

ABCC3 is a basolateral transporter, predominantly present in liver, gut and kidney, where it transports its substrates towards the systemic circulation (1;2). In contrast, ABCC4 is expressed apically in brain capillaries and kidney proximal tubules, but in liver, prostate, urogenital tissues and choroid epithelial cells it is localized at the basolateral membrane, pumping its substrates into the circulation (1;2). The subcellular location in various tissues of the ABC transporters discussed in this review is depicted in Fig. 1. For most ABC transporters, transporter deficient (knockout) mouse models have been generated and these models have been and still are widely used to study the *in vivo* functions of these efflux pumps. However, due to the extensively overlapping substrate specificities of ABC transporters, it is often difficult to unravel their separate roles and functional overlap using single knockout mice. For example, when one transporter is absent,

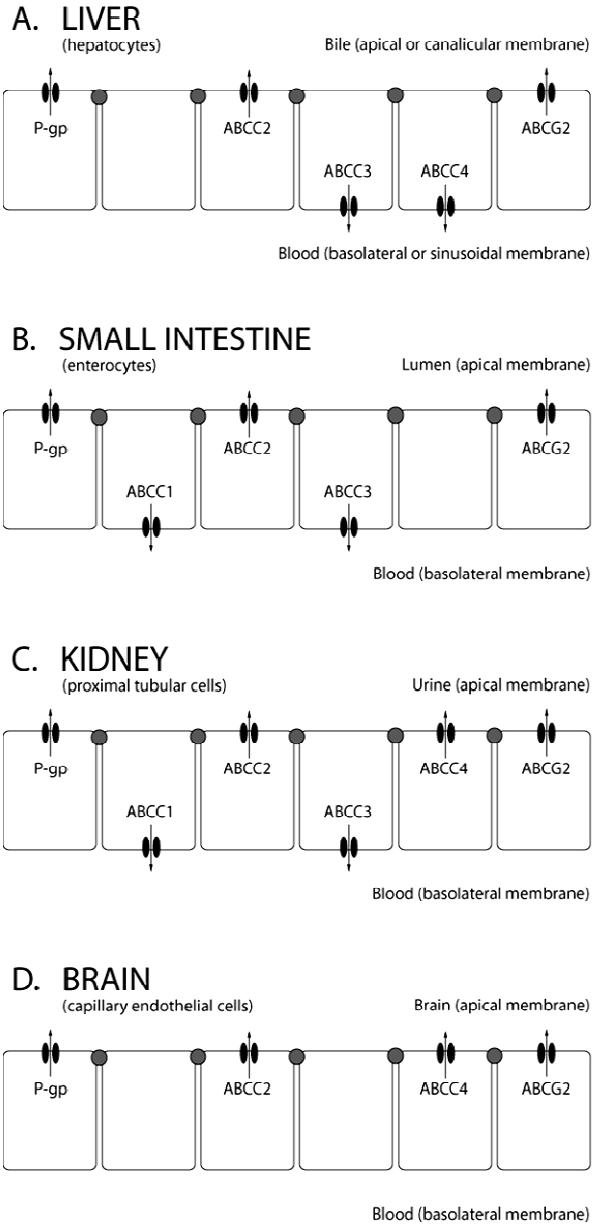

Fig. 1. Tissue distribution of the human ATP-binding cassette (ABC) transporters ABCB1 (P-gp), ABCG2 and ABCC1-4. **A)** ABC drug transporters in the liver. P-gp, ABCG2 and ABCC2 are located in the canalicular (apical) membrane of hepatocytes, pumping their substrates into bile. ABCC3 and ABCC4 are present in the sinusoidal (basolateral) membrane of hepatocytes, and pump their substrates towards the blood circulation. Notably, it was recently shown that Abcc1 is present in activated rat hepatic stellate cells (HSCs), but not in hepatocytes (73). **B)** ABC drug transporters in the small intestine. P-gp, ABCG2 and ABCC2 in the luminal (apical) membrane of enterocytes pump their substrates into the intestinal lumen. ABCC1 and ABCC3, located in the basolateral membrane of enterocytes pump their substrates towards the blood circulation. **C)** ABC drug transporters in the kidney. P-gp, ABCG2, ABCC2 and ABCC4 are localized in the apical membrane of proximal tubular cells and extrude their substrates into the urine. ABCC1 and ABCC3 are present at the basolateral membrane, pumping their substrates towards the blood circulation. **D)** ABC drug transporters at the BBB. P-gp, ABCG2, ABCC2 and ABCC4 are located at the apical membrane of capillary endothelial cells, pumping their substrates towards the blood. ABCC1 is also expressed in the basolateral membrane of epithelial cells of the choroid plexus, preventing the entry of its (potentially harmful) substrates in the cerebrospinal fluid (CSF) [not shown, reviewed in (1)].

another one may partly or completely compensate for its loss. As a consequence, often no or only minor effects of the single deletion are seen. Interestingly, a suggestion for overlapping functions of ABC transporters *in vivo* was recently seen in a clinical study that investigated the protective roles of ABCB1 (P-gp) and ABCG2 (BCRP) during cancer chemotherapy in children (3). This study showed that a combination of two SNP variants of ABCB1 and ABCG2 correlated with increased encephalopathy (brain toxicity), whereas patients with either one of these variants did not suffer from increased toxicity.

To study the functional overlap of ABC transporters *in vivo*, a set of mice deficient in two or more ABC transporters, also termed "compound transporter knockout mice", has been generated and characterized (4-13). This review discusses recent findings obtained with these compound transporter knockout mice. The main focus will be on pharmacokinetic studies with a number of clinically relevant drugs, illustrating that these models are powerful tools to study the separate roles and the functional overlap of ABC transporters. An overview of the generated compound knockout mice and the pharmacokinetic studies performed with these mice so far is given in Table 1. The ABC transporter compound knockout models will be discussed one by one in chronological order. For optimal understanding, the substrate specificity and tissue distribution of the particular ABC transporters will be briefly addressed in each section. In addition, for a number of compound knockout models the characterization and some physiological aspects will be addressed.

Abcb1a/1b$^{-/-}$ mice, the first compound ABC transporter knockout model

P-glycoprotein (P-gp/ABCB1) is the first discovered and most extensively studied member of the mammalian ATP binding cassette (ABC) multidrug transporter family (14). P-gp was discovered in cancer cells where it functions as an efflux pump and extrudes a wide variety of anticancer drugs. In addition to cancer cells, P-gp is also widely expressed in normal tissues, including the epithelial cells of intestine and kidneys and the canalicular membrane of hepatocytes, where it pumps its substrates into feces, urine and bile [Fig. 1; reviewed in (1)]. P-gp has a very broad substrate specificity, including bulky amphipathic anticancer drugs such as taxanes, anthracyclines and Vinca alkaloids. Consequently, (over)expression of P-gp in tumor cells can lead to multidrug resistance [MDR, (15)]. In contrast to humans, who have one *ABCB1* gene coding for P-gp, mice have two, *Abcb1a* and *Abcb1b*, and the products of these genes together appear to fulfill the same functions as the single human ABCB1 (P-gp).

Table 1. Impact of different ABC transporters on pharmacokinetics (PK) of drugs and endogenous substrates as analyzed using ABC transporter compound knockout mice.

Substrate	Compound knockout strain(s)	Findings	References
Etoposide	*Abcb1a/1b;Abcc1*$^{-/-}$	P-gp restricts the brain penetration. Abcc1 limits the accumulation in the cerebrospinal fluid. Both transporters protect against etoposide induced toxicity.	5,6
Topotecan	*Abcb1a/1b;Abcg2*$^{-/-}$	P-gp mediates the elimination and restricts the brain penetration. Abcg2 limits the oral uptake and mediates the elimination. Abcg2 also restricts the brain penetration when P-gp is absent.	39
Imatinib		P-gp mediates the fecal excretion and restricts the brain penetration. Abcg2 has a minor impact on the fecal excretion, but partially limits the brain penetration when P-gp is absent.	41
Dasatinib		P-gp limits the oral availability and restricts the brain penetration. Abcg2 partially restricts the brain penetration when P-gp is absent.	43
Lapatinib		P-gp restricts the brain penetration. Abcg2 partially restricts the brain penetration when P-gp is absent.	42
Sorafenib		Abcg2 restricts the brain penetration. P-gp partially restricts the brain penetration when Abcg2 is absent.	Lagas et al., unpublished results
Doxorubicin	*Abcb1a/1b;Abcc2*$^{-/-}$	P-gp is the main transporter for the biliary excretion. Abcc2 has a modest impact on biliary excretion, but can partly compensate for the absence of P-gp.	52
Paclitaxel		P-gp limits the oral uptake and facilitates the direct intestinal excretion. Abcc2 is the main transporter for the biliary excretion, and has an impact on the oral PK when P-gp is absent. Both transporters equally affect the iv PK.	8
PMEA	*Abcc4;Abcg2*$^{-/-}$	Abcc4 restricts the accumulation in the spleen. Abcc4 further restricts the liver, kidney and heart accumulation when Abcg2 is absent. Abcg2 restricts the liver, kidney, ovary and brain accumulation.	9
Methotrexate	*Abcc2;Abcc3*$^{-/-}$ and *Abcc2;Abcg2*$^{-/-}$	Abcc2 is the main transporter for biliary excretion. Abcg2 mediates the biliary and urinary excretion when Abcc2 is absent. Abcc3 mediates sinusoidal excretion from the liver when Abcc2 is absent.	12, 70, Vlaming et al., unpublished results
7-Hydroxy-methotrexate		Abcc2 is the main transporter for biliary excretion. Abcg2 mediates the biliary and urinary excretion when Abcc2 is absent. Abcc3 mediates the sinusoidal excretion from the liver when Abcc2 is absent.	
Morphine-3-glucuronide	*Abcc2;Abcc3*$^{-/-}$	Abcc2 is the main transporter for biliary excretion. Abcc3 mediates the sinusoidal excretion from the liver when Abcc2 is absent.	11
Fexofenadine		Abcc2 mediates the biliary excretion. Abcc3 mediates the sinusoidal excretion from the liver.	13

To study the *in vivo* functions of P-gp, *Abcb1a*$^{-/-}$ mice were initially established by inactivation of the *Abcb1a* gene via homologous recombination (16). Because *Abcb1a* is expressed at the blood–brain barrier (BBB) and in the intestinal epithelium, whereas *Abcb1b* is not, *Abcb1a*$^{-/-}$ mice proved to be a valuable tool to elucidate two important physiological functions of P-gp, namely restricting the brain penetration and limiting the oral uptake of potentially harmful compounds (16;17). Shortly after the generation of *Abcb1a*$^{-/-}$ mice, mice lacking *Abcb1b* were generated, but profound biological effects in this genotype were not observed (4). Therefore, a secondary targeting was performed and by disrupting both *Abcb1a* and *Abcb1b* in the same embryonic stem cell chromosome the first ABC transporter compound knockout mouse model was realized (4). Remarkably, *Abcb1a/1b*$^{-/-}$ mice had normal viability, fertility and life span and no apparent physiological abnormalities were observed, despite the complete absence of P-gp (4). Moreover, compound *Abcb1a/1b*$^{-/-}$ mice appeared to be a better model than the single knockout mice, and are still extensively used as a standard model for studies on the roles of P-gp in physiology, pharmacology and toxicology [reviewed in (18;19)]. Furthermore, these mice are also used as the basis for many other compound knockout mice (see below).

***Abcb1a/1b;Abcc1*$^{-/-}$ mice, the first triple ABC transporter knockout model**

ABCC1 (MRP1) is a versatile efflux transporter that can extrude a wide variety of endogenous and exogenous compounds from cells. In contrast to P-gp, which mainly transports non-conjugated neutral or weakly basic lipophilic substrates, ABCC1 is primarily an organic anion transporter, capable of transporting a broad spectrum of drugs conjugated to glutathione, glucuronic acid and sulfate. In addition, ABCC1 is the major transporter for the endogenous glutathione-conjugate leukotriene C_4 (LTC_4), an important mediator of the inflammatory response (20;21). Moreover, ABCC1 can also extrude lipophilic and amphipathic xenobiotics from cells as was shown for the anticancer drugs vincristine and etoposide (22;23). A number of experiments suggested that this transport was mediated by co-transport with glutathione. However, the presence of co-transport was later on questioned [reviewed in (24)].

ABCC1 is located basolaterally in polarized cells of many normal tissues, but it also occurs in some unpolarized cells. Expressing tissues include lung, heart, kidney, liver, muscle, colon, testes, bone marrow cells, blood erythrocytes and epithelial cells of the choroid plexus (see also Fig. 1). In addition, ABCC1 is found in tumor cells where it can contribute to multidrug resistance (1). The main function of ABCC1 seems to be the protection of individual cells from accumulation of toxic compounds (1). Two groups independently generated

Abcc1$^{-/-}$ mice (25;26), and both mutants had normal viability, fertility and life span. However, *Abcc1*$^{-/-}$ mice had an impaired response to inflammatory stimuli, which could be attributed to decreased secretion of LTC_4 from leukotriene secreting cells (25). Furthermore, tissue levels of glutathione were elevated in tissues that normally express substantial levels of Abcc1 (26). In addition, *Abcc1*$^{-/-}$ mice were found to be hypersensitive to the anticancer drugs etoposide and vincristine (25;26), indicating that Abcc1 plays an important role in drug detoxification. Moreover, absence of Abcc1 resulted in increased etoposide-induced damage to the mucosa of the oropharyngeal cavity and to the seminiferous tubules of the testis (27).

Both groups that had generated *Abcc1*$^{-/-}$ mice crossed these with the previously established *Abcb1a/1b*$^{-/-}$ mice (4) to obtain *Abcb1a/1b;Abcc1*$^{-/-}$ mice (5;6). These triple knockout (TKO) mice were more sensitive to toxicity induced by etoposide and vincristine than *Abcb1a/1b* $^{-/-}$ and *Abcc1*$^{-/-}$ mice (5;6), indicating that P-gp and ABCC1 had additive effects in the protection from toxicity. Importantly, *Abcb1a/1b;Abcc1*$^{-/-}$ mice also allowed investigators to demonstrate a protective function of ABCC1 in the choroid plexus (5). Etoposide was used as a probe drug. In P-gp deficient animals, the brain accumulation of etoposide was substantially higher than in their wild-type counterparts, whereas in *Abcc1*$^{-/-}$ mice brain accumulation was similar to the wild-type situation. However, mice deficient for both P-gp and Abcc1 had about 10-fold higher etoposide concentrations in their cerebrospinal fluid than mice only lacking P-gp. Apparently, absence of P-gp at the BBB allowed the drug to accumulate in the brain, and subsequently the important function of ABCC1 at the blood-cerebrospinal fluid barrier (preventing the accumulation of potentially harmful compounds in the cerebrospinal fluid) could be demonstrated. The latter finding is a nice example illustrating the power of compound transporter knockout models to elucidate novel transporter functions that otherwise would not have been found.

Abcb1a/1b;Abcg2$^{-/-}$ mice, a useful tool to study the functional overlap of P-gp and ABCG2

ABCG2 (BCRP) can transport a broad range of endogenous and exogenous substrates and shares a substantial overlap in substrate specificity with P-gp (1). Furthermore, in contrast to ABCC1, the tissue distribution of ABCG2 is roughly equal to that of P-gp, including expression at apical membranes of excretory organs (Fig.1). Consequently, ABCG2 limits the oral availability and tissue penetration of its substrates and mediates their excretion into bile, feces and urine. In addition, ABCG2 can confer multidrug resistance to tumor cells. Recent work, relying

mainly on the use of *Abcg2*$^{-/-}$ mice, has revealed important contributions of ABCG2 to the blood-brain, blood-testis and blood-fetal barriers (28-31).

Compound *Abcb1a/1b;Abcg2*$^{-/-}$ mice were generated by crossing the established *Abcb1a/1b*$^{-/-}$ (4) and *Abcg2*$^{-/-}$ mice (32). Despite the fact that these mice lack two important apical efflux transporters, normal viability, fertility and life span and no apparent physiological abnormalities were observed (7). These TKO mice thus seemed amenable for physiological and pharmacological analyses. The first study employing these mice was conducted to establish the respective contributions of P-gp and ABCG2 to the side population (SP) phenotype in mammary gland and bone marrow of mice (7;33). Many tissues contain a SP (or side population) of cells with stem cell characteristics, that can be identified by the ability of these cells to export the dye Hoechst 33342. Both P-gp and ABCG2 had been implicated to be responsible for this Hoechst 33342 export (33;34). By comparing *Abcb1a/1b*$^{-/-}$, *Abcg2*$^{-/-}$ and *Abcb1a/1b;Abcg2*$^{-/-}$ mice, it was found that Abcg2 is almost exclusively responsible for the SP phenotype in bone marrow, whereas both transporters contributed to the SP in the mammary gland (7). However, it was recently also shown that mouse mammary stem cells are Hoechst 33342 positive, and therefore likely not components of the SP (35;36).

In addition to normal tissues, it has been found that cancer cell lines and primary tumor cells also contain a SP. This has led to the hypothesis that expression of P-gp and/or ABCG2 in cancer stem cells may render these cells multidrug resistant and possibly explains their poor tractability. Although there remains controversy whether the SP is a universal stem cell marker, knowledge of the contribution of P-gp and ABCG2 to drug-resistance of specific tumor SPs may be useful to optimize cancer chemotherapy. *Abcb1a/1b;Abcg2*$^{-/-}$ mice may be useful to further address these issues.

Abcb1a/1b;Abcg2$^{-/-}$ mice have also been extensively used to study the overlapping functions of P-gp and ABCG2 at the BBB. Like P-gp (desribed above), ABCG2 is also abundant in the apical membranes of endothelial cells that form the BBB (37). However, in contrast to P-gp, for ABCG2 it was not as straightforward to establish a functional role at the BBB, despite the availability of Abcg2-deficient mice (32;38). In fact, retrospectively, most early studies used shared P-gp and ABCG2 substrates and failed to show higher brain penetration in single *Abcg2*$^{-/-}$ mice than in their wild-type counterparts [reviewed in (28)]. However, when the brain penetration in compound *Abcb1a/1b;Abcg2*$^{-/-}$ mice was compared to that in *Abcb1a/1b*$^{-/-}$ mice, a clear function of Abcg2 at the BBB could be demonstrated. This was first shown for the anticancer drug topotecan, which is a good substrate of ABCG2/Abcg2 and a weaker P-gp substrate. Compared to wild-type mice, the brain-to-plasma AUC ratios were not significantly different in

Abcg2$^{-/-}$ mice, whereas these ratios were 2.0-fold higher in *Abcb1a/1b*$^{-/-}$ mice and 3.2-fold higher in *Abcb1a/1b;Abcg2*$^{-/-}$ mice (39). Although topotecan appears to be a better substrate for ABCG2 than for P-gp *in vitro* as well as in the mouse intestine (40), apparently P-gp dominates at the BBB. Nonetheless, when P-gp is absent Abcg2 can partly take over the function of P-gp at the BBB and when both transporters are absent the brain penetration is highly increased. This clearly shows that, in addition to P-gp, Abcg2 also has a functional role at the BBB in restricting the entry of topotecan to the brain.

Using these compound knockout models, qualitatively similar results regarding brain penetration were recently obtained for the tyrosine kinase inhibitors imatinib, lapatinib and dasatinib (41-43). Although these three compounds are all good *in vitro* substrates for P-gp and ABCG2, a contribution of Abcg2 in restricting the brain penetration was only observed in *Abcb1a/1b;Abcg2*$^{-/-}$ mice, i.e. when P-gp is absent too. A possible explanation for this apparent discrepancy could be that Abcg2 expression at the BBB is lower than that of P-gp. Indeed, it was recently shown in mice of a ddy background that P-gp protein levels in brain capillaries were about 3-fold higher than protein levels of Abcg2 (44). This suggests that P-gp is the dominant player at the murine BBB and might explain why only when P-gp is absent the contribution of Abcg2 becomes visible. It must be noted, however, that the above described experiments on the brain penetration of tyrosine kinase inhibitors (41-43) were performed in mice of an FVB background and it was previously shown that the expression of ABC transporters at the murine BBB can differ dramatically between mouse strains (45). In addition, we checked the RNA expression of Mdr1a P-gp in the brain of *Abcg2*$^{-/-}$ mice, but found no difference compared to wild-type mice (Lagas et al, unpublished results). The relative contribution of Abcg2 at the BBB thus seems not to be underestimated by an increased expression of P-gp at the BBB of FVB *Abcg2*$^{-/-}$ mice.

Interestingly, examination of human brain capillaries revealed that mRNA levels of ABCG2 were about 8-fold higher than P-gp mRNA levels (46). It should be noted that the brain capillaries in that study were isolated from 7 patients who all suffered from brain disease (epilepsia or glioma), which might affect the RNA expression levels. However, there was more ABCG2 mRNA than ABCB1 mRNA in the microvessels from all patients, regardless of their pathology or treatment (46). If RNA levels correspond relatively well with protein levels of both transporters at the BBB, these studies might indicate that there are species differences in the relative expression of P-gp and ABCG2 at the BBB. In that case, the contribution of ABCG2 at the human BBB might be more important than thought thus far.

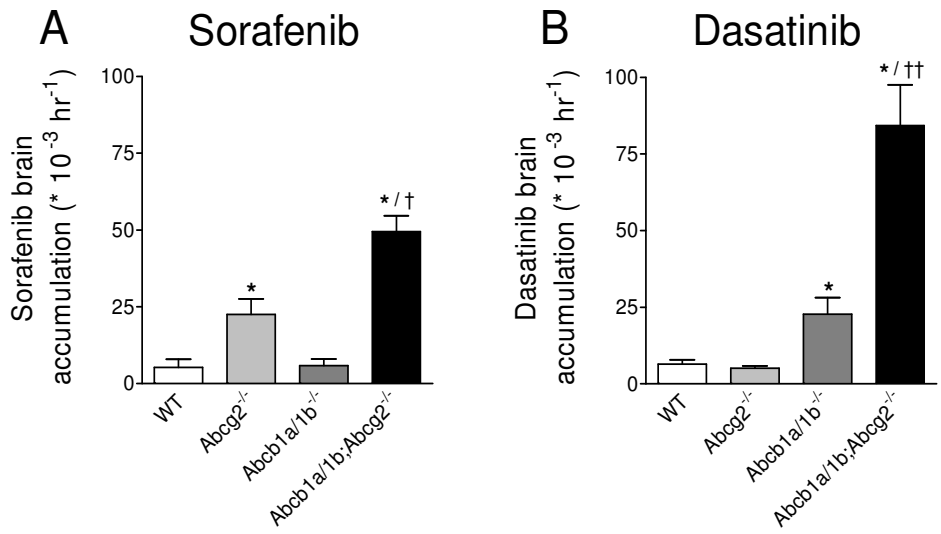

Fig. 2. Brain penetration of the tyrosine kinase inhibitor sorafenib (A) and dasatinib (B) in male wild-type, *Abcg2*$^{-/-}$, *Abcb1a/1b*$^{-/-}$, and *Abcb1a/1b;Abcg2*$^{-/-}$ mice, 6 hr after oral administration of sorafenib or dasatinib at a dose of 10 mg/kg. Data represent means ± SD, n = 5. * $P < 0.001$, compared to wild-type mice; † $P < 0.01$ and †† $P < 0.001$ compared to *Abcg2*$^{-/-}$ mice. Printed with permission (38) and (Lagas et al., unpublished results).

Although in mice P-gp thus seems to dominate at the BBB, we recently observed that the brain penetration of orally administered sorafenib, another tyrosine kinase inhibitor, was 4.3-fold increased in *Abcg2*$^{-/-}$ mice, not altered in *Abcb1a/1b*$^{-/-}$ mice and 9.3-fold higher in *Abcb1a/1b;Abcg2*$^{-/-}$ mice (Fig. 2A) (Lagas et al, unpublished results). In contrast, for orally administered dasatinib we previously found that Abcg2 deficiency did not affect the brain penetration, whereas absence of P-gp resulted in a 3.6-fold increase and *Abcb1a/1b;Abcg2*$^{-/-}$ mice had 13.2-fold higher brain penetration (Fig. 2B) (43). This discrepancy might simply be explained by the fact that sorafenib is a good Abcg2 substrate *in vitro*, but a very poor P-gp substrate (Lagas et al, unpublished results). This further

illustrates that for each substrate the interactions with ABC transporters in the BBB are unique, making it difficult to draw general conclusions on the pharmacological impact of ABC transporters.

Taken together, in addition to *Abcb1a/1b*$^{-/-}$ and *Abcg2*$^{-/-}$ mice, combination *Abcb1a/1b;Abcg2*$^{-/-}$ mice have proven to be a valuable tool to study the separate and combined impact of P-gp and ABCG2 at the BBB.

Abcb1a/1b;Abcc2$^{-/-}$ mice, a model to study hepatic versus intestinal elimination

Like P-gp and ABCG2, ABCC2 (MRP2) is expressed at the apical membranes of epithelial cells in kidney and intestine and at the canalicular membrane of hepatocytes (Fig. 1). Consequently, ABCC2 plays an important role in the hepatobiliary and renal excretion of its substrates, but, in contrast to P-gp and ABCG2, its contribution in restricting uptake of compounds from the intestine seems limited (1). ABCC2 was long thought to mainly affect organic anionic drugs *in vivo*, with a preference for substrates conjugated to glutathione, glucuronic acid and sulfate [reviewed in (47;48)]. Studies in two rat strains that naturally lack Abcc2 (EHBR and TR$^-$) and in humans suffering from Dubin-Johnson syndrome (a hereditary deficiency in ABCC2) revealed that ABCC2/Abcc2 plays an important role in the elimination of bilirubin glucuronides from hepatocytes into the bile (49-51). Recent work has shown that ABCC2 can also transport bulky amphipathic anticancer drugs *in vivo* (8;52), and ABCC2 thus has a substantial overlap in substrate specificity with P-gp. Recently, we and others independently generated *Abcc2*$^{-/-}$ mice (52;53), and we additionally crossed our *Abcc2*$^{-/-}$ mice with *Abcb1a/1b*$^{-/-}$ mice (4) to obtain compound *Abcb1a/1b;Abcc2*$^{-/-}$ mice (8;52). Similar to single *Abcc2*$^{-/-}$ mice, compound *Abcb1a/1b;Abcc2*$^{-/-}$ mice had a ~25% increased liver weight, and the bile flow was reduced by 40% to 50% due to absence of Abcc2-mediated biliary glutathione excretion (52). Furthermore, as a consequence of reduced biliary excretion of conjugated bilirubin caused by Abcc2-deficiency (52), conjugated bilirubin concentrations in plasma were ~3-fold elevated, compared to wild-type mice (8). Overall, *Abcb1a/1b;Abcc2*$^{-/-}$ mice appear in many respects very similar to *Abcc2*$^{-/-}$ mice and are likely as amenable to pharmacological analysis. We used the *Abcb1a/1b;Abcc2*$^{-/-}$ mice to study the separate and combined impact of P-gp and Abcc2 on the elimination of the lipophilic amphipathic anticancer drugs doxorubicin (52) and paclitaxel (8). The hepatobiliary excretion of doxorubicin was mainly dependent on P-gp, with a modest role for Abcc2 (52). In contrast, rather surprisingly, the excretion of paclitaxel into the bile was dominated by Abcc2, with a very minor contribution of P-gp (8). The abrogated biliary excretion of paclitaxel in *Abcc2*$^{-/-}$ mice resulted in a

1.3-fold higher area under the plasma concentration-time curve (AUC) upon intravenous paclitaxel administration. Interestingly, the $AUC_{i.v.}$ for paclitaxel in *Abcb1a/1b* $^{-/-}$ mice was also 1.3-fold higher. This could be explained by the dominant role of P-gp in the gut, where it mediates the direct intestinal excretion of paclitaxel from the blood across the intestinal wall into the gut lumen. Very likely it also restricts the intestinal re-uptake of paclitaxel after hepatobiliary secretion of the drug in the gut. Moreover, absence of both transporters resulted in an additive 1.7-fold higher $AUC_{i.v.}$ in *Abcb1a/1b;Abcc2*$^{-/-}$ mice [reviewed in (54)]. These studies demonstrate the power of this compound transporter knockout model to elucidate the tissue specific contribution as well as the separate and combined impact of P-gp and ABCC2 on the elimination of lipophilic amphipathic drugs.

Abcc4;Abcg2$^{-/-}$ mice, a model to study the impact of ABCC4 and ABCG2 on tissue accumulation of shared substrates

ABCG2 (BCRP) and ABCC4 (MRP4) are both expressed in liver and kidney, as well as in tissue sanctuaries such as brain, testis, prostate and ovary [Fig.1; (9;28;54)]. As described above, ABCG2 is present in the apical membranes of epithelial cells, pumping its substrates into bile, urine and feces (1). ABCC4 is expressed apically in brain capillaries and kidney proximal tubules, but in liver, prostate, urogenital tissues and choroid epithelial cells it is localized at the basolateral membrane, pumping its substrates into the circulation (54). In *Abcc4*$^{-/-}$ mice, Abcg2 expression is increased in spleen and brain, whereas thymus and spleen from *Abcg2*$^{-/-}$ mice had increased *Abcc4*$^{-/-}$ expression (9), suggesting compensatory changes in these tissues when either one of the transporters is absent.

Abcc4 and Abcg2 have broad and substantially overlapping substrate specificities. They both confer resistance to many (antiviral and anti-cancer) drugs such as PMEA (9-(2-(phosphonomethoxy)ethyl)-adenine) (9;55), camptothecin analogs (e.g. topotecan and irinotecan (56-58)), and methotrexate (59;60). Besides various drugs, Abcc4 and Abcg2 also transport endogenous compounds, such as cGMP (10) and steroid conjugates (61;62).

Recently, two research groups independently generated *Abcc4;Abcg2*$^{-/-}$ mice (in a mixed C57BL6;129SVJ and a mixed 129Ola/BL6;FVB background, respectively) (9;10). Both strains were viable and fertile. Clinical chemistry and hematologic analysis of the *Abcc4;Abcg2*$^{-/-}$ mice in C57BL6;129SVJ background did not reveal any specific aberrations due to absence of both transporters (9), suggesting that Abcc4 and Abcg2 do not have any vital, overlapping physiological functions. However, these mice appeared very useful to investigate the overlapping pharmacological functions of Abcc4 and Abcg2. Intravenous administration of the purine nucleoside phosphonate analogue [^{3}H]PMEA to *Abcc4*$^{-/-}$ mice resulted in

accumulation in the spleen but not in other tissues, suggesting that Abcc4 plays a modest role in limiting the tissue accumulation of PMEA. In contrast, in *Abcg2*$^{-/-}$ mice [^{3}H]PMEA accumulated in liver, kidney, brain and ovary, showing a significant effect of Abcg2 on the tissue accumulation of the drug. However, in *Abcc4;Abcg2*$^{-/-}$ mice [^{3}H]PMEA concentrations in liver, kidney and heart were even more increased than in *Abcg2*$^{-/-}$ mice (9). This suggests that when Abcg2 is absent, Abcc4 can also reduce [^{3}H]PMEA concentrations in these tissues, although it cannot completely compensate for the absence of Abcg2. On the other hand, [^{3}H]PMEA concentrations in the spleen were similarly increased in *Abcc4*$^{-/-}$ and *Abcc4;Abcg2*$^{-/-}$ mice, indicating that Abcg2 does not affect PMEA concentrations in this organ. This first pharmacological experiment employing *Abcc4;Abcg2*$^{-/-}$ mice shows that these are a valuable tool to elucidate the overlapping functions of both transporters in the pharmacokinetics of shared substrates. Therefore, it will be interesting to study the pharmacokinetics of additional common substrates in these mice.

Abcc2;Abcc3$^{-/-}$ mice, a useful tool to study the complementary functions of ABCC2 and ABCC3 in the liver

The ABC transporters ABCC2 (MRP2) and ABCC3 (MRP3) are both family members of the multidrug resistance protein (MRP) family and have similar structure and substrate specificities (48). They can both transport a range of physiological substrates, such as bilirubin glucuronides, estradiol-17β-glucuronide and some bile salts (48). Furthermore, ABCC2 and ABCC3 can transport many drugs, such as anthracyclines, epipodophyllotoxins and methotrexate, as well as a range of drug conjugates, in particular drug glucuronides such as morphine glucuronide (11;48). The tissue distribution of ABCC3 is quite similar to that of ABCC2 [Fig.1; (1)]. ABCC3 is additionally present in the adrenal glands and pancreas [Fig.1; (48)]. In contrast to the apical localization of ABCC2, ABCC3 is expressed basolaterally, pumping its substrates towards the circulation (1;48). Interestingly, in Abcc2/ABCC2-deficient mice, rats and humans, Abcc3/ABCC3 protein expression was significantly increased in the liver. This suggests a compensatory role of Abcc3/ABCC3 when Abcc2/ABCC2 is absent (52;63;64), transporting substrates that cannot be excreted into the bile back into the circulation, and hence leading to increased urinary excretion of these compounds.

Recently, *Abcc2;Abcc3*$^{-/-}$ mice have been generated, both in C57BL/6 and FVB background (11-13) and they have been used to study the overlapping physiological and pharmacological functions of both transporters *in vivo*. Physiological characterization of these mice in both backgrounds showed that *Abcc2;Abcc3*$^{-/-}$ had normal life spans and body weights, but that the liver weights

were significantly (36-49%) increased compared to wild-type mice (12;13), although the livers appeared normal, both macroscopically and microscopically (12). It could be that accumulation of shared Abcc2 and Abcc3 substrates in the liver induces liver proliferation. Furthermore, in *Abcc2;Abcc3*$^{-/-}$ mice of both backgrounds, the bile flow was significantly decreased compared to wild-type (12;13), as shown previously for *Abcc2*$^{-/-}$ mice (52;53).

It was previously hypothesized that (increased) Abcc3 protein in liver of Abcc2-deficient rats, mice and humans was, in combination with the decreased biliary clearance, responsible for the increased plasma levels and urinary excretion of conjugated bilirubin (52;63). Analysis of bilirubin concentrations in plasma, bile and urine of the *Abcc2;Abcc3*$^{-/-}$ mice indeed showed that Abcc3 in the liver of *Abcc2*$^{-/-}$ mice was necessary for the increased sinusoidal efflux of bilirubin glucuronides, and their increased plasma concentrations and urinary excretion (12). Similar observations using *Abcc2;Abcc3*$^{-/-}$ mice were made for the shared substrate drugs or drug metabolites methotrexate (12), 7-hydroxymethotrexate (12), morphine-3-glucuronide (11) and fexofenadine (13).

Administration of methotrexate to *Abcc2;Abcc3*$^{-/-}$ mice further led to significantly increased liver concentrations of methotrexate and its toxic metabolite 7-hydroxymethotrexate, which was not seen (or only to a minor extent) in the single knockout strains (12). Also treatment of the *Abcc2;Abcc3*$^{-/-}$ mice with morphine led to dramatic accumulation of its metabolite morphine-3-glucuronide (but not morphine itself) which was not found in the single knockout strains (11). This shows that Abcc2 and Abcc3 together are very important for reducing liver exposure of potentially toxic compounds, and that when one of them is absent or reduced, the other can (at least partly) compensate for this deficiency.

It was previously shown that co-administration of morphine to methotrexate-treated mice significantly reduced plasma clearance of methotrexate (65), which is of clinical interest because morphine and methotrexate are often co-administered in cancer treatment. The results obtained with the *Abcc2;Abcc3*$^{-/-}$ mice described above suggest that these effects could be caused by competition between methotrexate and morphine-3-glucuronide for elimination via Abcc2 and Abcc3. This would suggest that co-administration of these drugs to patients with reduced expression or activity of ABCC2 and/or ABCC3, or to Dubin-Johnson patients (66), should be done with caution. Overall, *Abcc2;Abcc3*$^{-/-}$ mice have already proven to be useful models for studying the overlapping and compensatory roles of Abcc2 and Abcc3 *in vivo*.

Abcc2;Abcg2$^{-/-}$ mice, a model to study the functional overlap of ABCG2 and ABCC2 in hepatobiliary excretion

As described above, the tissue distributions of ABCC2 and ABCG2 are quite similar (Fig. 1), and the substrate specificities of ABCC2 and ABCG2 are broad and substantially overlapping as well. Both proteins can transport many drugs, including anti-cancer drugs like methotrexate, doxorubicin and SN-38, as well as dietary toxins, e.g. the carcinogen PhIP (2-amino-1-methyl-6-phenylimidazo[4,5-*b*]pyridine), and a range of glucuronide and sulphate conjugates of endogenous and exogenous compounds (1;68;69).

The substantial overlap in substrate specificity and tissue distribution suggests that ABCC2 and ABCG2 are able to compensate for each other when one of the two proteins is absent or non-functional. Functions of transporters assessed with single knockout mice may therefore be obscured due to activity of the other transporter, which is still present. To investigate this, we have recently generated *Abcc2;Abcg2*$^{-/-}$ mice in 99% FVB background (70). Like the other ABC transporter compound knockout mice generated so far, these mice are viable and fertile and do not display any phenotypes other than what was seen previously in the single knockout mice, such as the hypersensitivity to the phototoxic dietary compound pheophorbide a of *Abcg2*$^{-/-}$ mice and the conjugated hyperbilirubinemia of *Abcc2*$^{-/-}$ mice (32;52). This suggests that the physiological functions of ABCC2 and ABCG2 are not overlapping, or may still be taken over by other systems such as enzymes or other transporters.

Because wild-type mice of an FVB background, in contrast to other genetic backgrounds, do not have Abcc2 protein in brain capillary endothelial cells, i.e., at the BBB (46), the *Abcc2;Abcg2*$^{-/-}$ mice we have generated can not be used to investigate overlapping functions of Abcc2 and Abcg2 in the BBB. However, we did use these mice to investigate the effect of Abcc2 and Abcg2 on the disposition of the anti-cancer drug methotrexate and its main (toxic) metabolite 7-hydroxymethotrexate *in vivo* (70). We found that Abcc2 and Abcg2 have additive effects on the plasma elimination of methotrexate, which was mainly caused by their impact on the biliary excretion of the drug. Whereas in both single knockout strains still substantial biliary excretion was present, in the double knockouts this was almost completely abolished, showing that Abcc2 and Abcg2 in mice are the main transporters for the excretion of methotrexate into the bile. Interestingly, in *Abcg2*$^{-/-}$ mice, we found no differences in the plasma concentration-versus-time curves for the toxic methotrexate metabolite 7-hydroxymethotrexate. However, compared to *Abcc2*$^{-/-}$ mice, an additional effect of Abcg2 absence on the plasma concentrations was found in *Abcc2;Abcg2*$^{-/-}$ mice, indicating that when Abcc2 is absent, Abcg2 can partly compensate for its loss. This clearly illustrates the value

of these compound transporter knockout mice to determine the relative impacts of both transporters on the elimination of shared substrates from the body. We therefore expect that *Abcc2;Abcg2*$^{-/-}$ mice will be extensively used to determine the *in vivo* effects on pharmacokinetics of known, but also of newly discovered drugs which are substrates of both transporters.

CONCLUSIONS

In the past few years, a large set of ABC transporter compound knockout mice have been generated and used for the analysis of overlapping effects of these proteins *in vivo*. The results obtained will be helpful to determine the consequences of reduced expression or activity of ABC transporters in patients treated with potentially toxic drugs. Furthermore, as ABC transporters can also transport endogenous compounds and food-derived toxins (e.g. carcinogens), these mice can be used to investigate the relative effects of ABC transporters on normal health. For example, ABC transporter (compound) knockout mice may be used to study whether loss of functional activity of one or more ABC transporters can influence the chance to develop cancer. Also studies on the overlapping or complementary effects of ABC transporters in multidrug resistance could be performed *in vivo* using these compound knockout strains.

The results obtained so far have shown that the relative effect of each ABC transporter on drug pharmacokinetics can be highly dependent on the substrate, administration route and the tissue or organ under investigation. Very likely, also the given dose determines which ABC transporter is more important for the pharmacokinetics of the drug. It is therefore very difficult to use *in vitro* assays to predict the *in vivo* effects of ABC transporters, and compound knockout mice are therefore invaluable tools for these types of studies.

So far, mainly combinations of two ABC transporters have been deleted simultaneously in mice. Because various drugs and toxins, as well as their metabolites, can be transported by more than two ABC transporters, it is obvious to extend the current set of models with triple, quadruple or even higher order compound knockout strains. Furthermore, crossing ABC transporter knockout mice with knockout models of other drug elimination mechanisms, such as drug-metabolizing enzymes, will give more insight into the interplay between these different systems *in vivo*.

Of course, as ABC transporters are involved in protection of the organism from endogenous and exogenous toxins, it will be interesting to see how many additional ABC transporter genes can be deleted without causing serious health problems to mice. Besides increasing fundamental knowledge on ABC transporter function, this is of interest because attempts are made to improve drug response in

patients by inhibition of one or more ABC transporters (71;72). We have recently even been able to generate *Abcb1a/b;Abcc2;Abcg2*$^{-/-}$ and *Abcc2;Abcc3;Abcg2*$^{-/-}$ mice which are viable, fertile and have normal life spans (Vlaming et al., unpublished results). This suggests that the physiological functions of these proteins are not essential, at least not in the protective environment of the lab. In the near future, these strains can be used for pharmacological analyses. Further investigation of the generated ABC transporter compound knockout mice will likely reveal more physiological and pharmacological functions of ABC transporters, and help to improve treatment of patients with drugs of which the efficacy and toxicity are influenced by ABC transporters.

ACKNOWLEDGMENTS

We thank our colleagues for critical reading of the manuscript. This work was supported in part by grant NKI 2003-2940 from the Dutch Cancer Society.

REFERENCES

(1) Borst P, Oude Elferink RP. Mammalian ABC transporters in health and disease. Annu Rev Biochem 2002;71:537-92.

(2) Schinkel AH, Jonker JW. Mammalian drug efflux transporters of the ATP binding cassette (ABC) family: an overview. Adv Drug Deliv Rev 2003;55:3-29.

(3) Erdilyi DJ, Kamory E, Csokay B, Andrikovics H, Tordai A, Kiss C et al. Synergistic interaction of ABCB1 and ABCG2 polymorphisms predicts the prevalence of toxic encephalopathy during anticancer chemotherapy. Pharmacogenomics J 2008;8:321-7.

(4) Schinkel AH, Mayer U, Wagenaar E, Mol CA, van Deemter L, Smit JJ et al. Normal viability and altered pharmacokinetics in mice lacking mdr1-type (drug-transporting) P-glycoproteins. Proc Natl Acad Sci U S A 1997;94:4028-33.

(5) Wijnholds J, de Lange EC, Scheffer GL, van den Berg DJ, Mol CA, van der Valk M et al. Multidrug resistance protein 1 protects the choroid plexus epithelium and contributes to the blood-cerebrospinal fluid barrier. J Clin Invest 2000;105:279-85.

(6) Johnson DR, Finch RA, Lin ZP, Zeiss CJ, Sartorelli AC. The pharmacological phenotype of combined multidrug-resistance mdr1a/1b- and mrp1-deficient mice. Cancer Res 2001;61:1469-76.

(7) Jonker JW, Freeman J, Bolscher E, Musters S, Alvi AJ, Titley I et al. Contribution of the ABC transporters Bcrp1 and Mdr1a/1b to the side population phenotype in mammary gland and bone marrow of mice. Stem Cells 2005;23:1059-65.

(8) Lagas JS, Vlaming ML, van Tellingen O, Wagenaar E, Jansen RS, Rosing H et al. Multidrug resistance protein 2 is an important determinant of paclitaxel pharmacokinetics. Clin Cancer Res 2006;12:6125-32.

(9) Takenaka K, Morgan JA, Scheffer GL, Adachi M, Stewart CF, Sun D et al. Substrate overlap between Mrp4 and Abcg2/Bcrp affects purine analogue drug cytotoxicity and tissue distribution. Cancer Res 2007;67:6965-72.

(10) De Wolf CJ, Yamaguchi H, van der Heijden I, Wielinga PR, Hundscheid SL, Ono N et al. cGMP transport by vesicles from human and mouse erythrocytes. FEBS J 2007;274:439-50.

(11) Van de Wetering K, Zelcer N, Kuil A, Feddema W, Hillebrand M, Vlaming ML et al. Multidrug resistance proteins 2 and 3 provide alternative routes for hepatic excretion of morphine-glucuronides. Mol Pharmacol 2007;72:387-94.

(12) Vlaming ML, Pala Z, van Esch A, Wagenaar E, van Tellingen O, de Waart DR et al. Impact of Abcc2 (Mrp2) and Abcc3 (Mrp3) on the in vivo elimination of methotrexate and its main toxic metabolite 7-hydroxymethotrexate. Clin Cancer Res 2008;14:8152-60.

(13) Tian X, Swift B, Zamek-Gliszczynski MJ, Belinsky MG, Kruh GD, Brouwer KL. Impact of basolateral multidrug resistance-associated protein (Mrp) 3 and Mrp4 on the hepatobiliary disposition of fexofenadine in perfused mouse livers. Drug Metab Dispos 2008;36:911-5.

(14) Juliano RL, Ling V. A surface glycoprotein modulating drug permeability in Chinese hamster ovary cell mutants. Biochim Biophys Acta 1976;455:152-62.

(15) Gottesman MM, Hrycyna CA, Schoenlein PV, Germann UA, Pastan I. Genetic analysis of the multidrug transporter. Annu Rev Genet 1995;29:607-49.

(16) Schinkel AH, Smit JJ, van Tellingen O, Beijnen JH, Wagenaar E, van Deemter L et al. Disruption of the mouse mdr1a P-glycoprotein gene leads to a deficiency in the blood-brain barrier and to increased sensitivity to drugs. Cell 1994;77:491-502.

(17) Sparreboom A, van Asperen J, Mayer U, Schinkel AH, Smit JW, Meijer DK et al. Limited oral bioavailability and active epithelial excretion of paclitaxel (Taxol) caused by P-glycoprotein in the intestine. Proc Natl Acad Sci U S A 1997;94:2031-5.

(18) Schinkel AH. Pharmacological insights from P-glycoprotein knockout mice. Int J Clin Pharmacol Ther 1998;36:9-13.

(19) Chen C, Liu X, Smith BJ. Utility of Mdr1-gene deficient mice in assessing the impact of P-glycoprotein on pharmacokinetics and pharmacodynamics in drug discovery and development. Curr Drug Metab 2003;4:272-91.

(20) Leier I, Jedlitschky G, Buchholz U, Cole SP, Deeley RG, Keppler D. The MRP gene encodes an ATP-dependent export pump for leukotriene C4 and structurally related conjugates. J Biol Chem 1994;269:27807-10.

(21) Müller M, Meijer C, Zaman GJR, Borst P, Scheper RJ, Mulder NH et al. Overexpression of the gene encoding the multidrug resistance-associated protein results in increased ATP-dependent glutathione S-conjugate transport. Proc Natl Acad Sci USA 1994; 91:13033-7.

(22) Loe DW, Deeley RG, Cole SP. Characterization of vincristine transport by the M(r) 190,000 multidrug resistance protein (MRP): evidence for cotransport with reduced glutathione. Cancer Res 1998;58:5130-6.

(23) Rappa G, Lorico A, Flavell RA, Sartorelli AC. Evidence that the multidrug resistance protein (MRP) functions as a co-transporter of glutathione and natural product toxins. Cancer Res 1997;57:5232-7.

(24) Borst P, Zelcer N, van de Wetering K, Poolman B. On the putative co-transport of drugs by multidrug resistance proteins. FEBS Lett 2006;580:1085-93.

(25) Wijnholds J, Evers R, van Leusden MR, Mol CA, Zaman GJ, Mayer U et al. Increased sensitivity to anticancer drugs and decreased inflammatory response in mice lacking the multidrug resistance-associated protein. Nat Med 1997;3:1275-9.

(26) Lorico A, Rappa G, Finch RA, Yang D, Flavell RA, Sartorelli AC. Disruption of the murine MRP (multidrug resistance protein) gene leads to increased sensitivity to etoposide (VP-16) and increased levels of glutathione. Cancer Res 1997;57:5238-42.

(27) Wijnholds J, Scheffer GL, van der Valk M, van der Valk P, Beijnen JH, Scheper RJ et al. Multidrug resistance protein 1 protects the oropharyngeal mucosal layer and the testicular tubules against drug-induced damage. J Exp Med 1998;188:797-808.

(28) Vlaming ML, Lagas JS, Schinkel AH. Physiological and pharmacological roles of ABCG2 (BCRP): recent findings in Abcg2 knockout mice. Advanced Drug Delivery Reviews 2009; 31;61(1):14-25

(29) Van Herwaarden AE, Schinkel AH. The function of breast cancer resistance protein in epithelial barriers, stem cells and milk secretion of drugs and xenotoxins. Trends Pharmacol Sci 2006;27:10-6.

(30) Polgar O, Robey RW, Bates SE. ABCG2: structure, function and role in drug response. Expert Opin Drug Metab Toxicol 2008;4:1-15.

(31) Sarkadi B, Ozvegy-Laczka C, Német K, Váradi A. ABCG2 – a transporter for all seasons. FEBS Lett 2004;567:116-20.

(32) Jonker JW, Buitelaar M, Wagenaar E, van der Valk MA, Scheffer GL, Scheper RJ et al. The breast cancer resistance protein protects against a major chlorophyll-derived dietary phototoxin and protoporphyria. Proc Natl Acad Sci U S A 2002;99:15649-54.

(33) Zhou S, Schuetz JD, Bunting KD, Colapietro AM, Sampath J, Morris JJ et al. The ABC transporter Bcrp1/ABCG2 is expressed in a wide variety of stem cells and is a molecular determinant of the side-population phenotype. Nat Med 2001;7:1028-34.

(34) Goodell MA, Brose K, Paradis G, Conner AS, Mulligan RC. Isolation and functional properties of murine hematopoietic stem cells that are replicating in vivo. J Exp Med 1996;183:1797-806.

(35) Shackleton M, Vaillant F, Simpson KJ, Stingl J, Smyth GK, Asselin-Labat ML et al. Generation of a functional mammary gland from a single stem cell. Nature 2006;439:84-88.

(36) Stingl J, Eirew P, Shackleton M, Vaillant F, Choi D, Li HI et al. Purification and unique properties of mammary epithelial stem cells. Nature 2006 ;439 :993-97.

(37) Cooray HC, Blackmore CG, Maskell L, Barrand MA. Localisation of breast cancer resistance protein in microvessel endothelium of human brain. Neuroreport 2002;13:2059-63.

(38) Zhou S, Morris JJ, Barnes Y, Lan L, Schuetz JD, Sorrentino BP. Bcrp1 gene expression is required for normal numbers of side population stem cells in mice, and confers relative protection to mitoxantrone in hematopoietic cells in vivo. Proc Natl Acad Sci U S A 2002;99:12339-44.

(39) de Vries NA, Zhao J, Kroon E, Buckle T, Beijnen JH, van Tellingen O. P-glycoprotein and breast cancer resistance protein: two dominant transporters working together in limiting the brain penetration of topotecan. Clin Cancer Res 2007;13:6440-9.

(40) Jonker JW, Smit JW, Brinkhuis RF, Maliepaard M, Beijnen JH, Schellens JH et al. Role of breast cancer resistance protein in the bioavailability and fetal penetration of topotecan. J Natl Cancer Inst 2000;92:1651-6.

(41) Oostendorp RL, Buckle T, Beijnen JH, van Tellingen O, Schellens JH. The effect of P-gp (Mdr1a/1b), BCRP (Bcrp1) and P-gp/BCRP inhibitors on the in vivo absorption, distribution, metabolism and excretion of imatinib. Invest New Drugs 2009; 27:31-40.

(42) Polli JW, Olson KL, Chism JP, John-Williams LA, Yeager RL, Woodard SM et al. An unexpected synergist role of P-glycoprotein and Breast Cancer Resistance Protein on the CNS penetration of the tyrosine kinase inhibitor lapatinib (GW572016). Drug Metab Dispos 2009; 37: 439-442

(43) Lagas JS, van Waterschoot RAB, van Tilburg VAC, Lankheet N, Rosing H, Beijnen JH et al. Brain accumulation of dasatinib is restricted by P-glycoprotein (ABCB1) and ABCG2 (BCRP) and can be enhanced by elacridar treatment. Clin Cancer Res. In press.

(44) Kamiie J, Ohtsuki S, Iwase R, Ohmine K, Katsukura Y, Yanai K et al. Quantitative atlas of membrane transporter proteins: development and application of a highly sensitive simultaneous LC/MS/MS method combined with novel *in-silico* peptide selection criteria. Pharm Res 2008;25:1469-83.

(45) Soontornmalai A, Vlaming ML, Fritschy JM. Differential, strain-specific cellular and subcellular distribution of multidrug transporters in murine choroid plexus and blood-brain barrier. Neuroscience 2006;138:159-69.

(46) Dauchy S, Dutheil F, Weaver RJ, Chassoux F, Damas-Duport C, Couraud PO et al. ABC transporters, cytochromes P450 and their main transcription factors: expression at the human blood-brain barrier. 2008;107:1518-28.

(47) Nies AT, Keppler D. The apical conjugate efflux pump ABCC2 (MRP2). Pflügers Arch 2007;453:643-59.

(48) Borst P, Zelcer N, van de Wetering K. MRP2 and 3 in health and disease. Cancer Lett 2006;234:51-61.

(49) Jansen PL, Peters WH, Lamers WH. Hereditary chronic conjugated hyperbilirubinemia in mutant rats caused by defective hepatic anion transport. Hepatology 1985;5:573-9.

(50) Hosokawa S, Tagaya O, Mikami T, Nozaki Y, Kawaguchi A, Yamatsu K et al. A new rat mutant with chronic conjugated hyperbilirubinemia and renal glomerular lesions. Lab Anim Sci 1992;42:27-34.

(51) Dubin IN, Johnson FB. Chronic idiopathic jaundice with unidentified pigment in liver cells; a new clinicopathologic entity with a report of 12 cases. Medicine (Baltimore) 1954;33:155-97.

(52) Vlaming ML, Mohrmann K, Wagenaar E, de Waart DR, Elferink RP, Lagas JS et al. Carcinogen and anticancer drug transport by Mrp2 in vivo: studies using Mrp2 (Abcc2) knockout mice. J Pharmacol Exp Ther 2006;318:319-27.

(53) Chu XY, Strauss JR, Mariano MA, Li J, Newton DJ, Cai X et al. Characterization of mice lacking the multidrug resistance protein MRP2 (ABCC2). J Pharmacol Exp Ther 2006;317:579-89.

(54) Kruh GD, Belinsky MG, Gallo JM, Lee K. Physiological and pharmacological functions of Mrp2, Mrp3 and Mrp4 as determined from recent studies on gene-disrupted mice. Cancer Metastasis Rev 2007;26:5-14.

(55) Schuetz JD, Connelly MC, Sun D, Paibir SG, Flynn PM, Srinivas RV et al. MRP4: A previously unidentified factor in resistance to nucleoside-based antiviral drugs. Nat Med 1999;5:1048-51.

(56) Tian Q, Zhang J, Tan TM, Chan E, Duan W, Chan SY et al. Human multidrug resistance associated protein 4 confers resistance to camptothecins. Pharm Res 2005;22:1837-53.

(57) Tian Q, Zhang J, Chan SY, Tan TM, Duan W, Huang M et al. Topotecan is a substrate for multidrug resistance associated protein 4. Curr Drug Metab 2006;7:105-18.

(58) Gradhand U, Kim RB. Pharmacogenomics of MRP transporters (ABCC1-5) and BCRP (ABCG2). Drug Metab Rev 2008;40:317-54.

(59) Volk EL, Schneider E. Wild-type breast cancer resistance protein (BCRP/ABCG2) is a methotrexate polyglutamate transporter. Cancer Res 2003;63:5538-43.

(60) Chen ZS, Lee K, Walther S, Raftogianis RB, Kuwano M, Zeng H et al. Analysis of methotrexate and folate transport by multidrug resistance protein 4 (ABCC4): MRP4 is a component of the methotrexate efflux system. Cancer Res 2002;62:3144-50.

(61) Zelcer N, Reid G, Wielinga P, Kuil A, van der Heijden I, Schuetz JD et al. Steroid and bile acid conjugates are substrates of human multidrug-resistance protein (MRP) 4 (ATP-binding cassette C4). Biochem J 2003;371:361-7.

(62) Imai Y, Asada S, Tsukahara S, Ishikawa E, Tsuruo T, Sugimoto Y. Breast cancer resistance protein exports sulfated estrogens but not free estrogens. Mol Pharmacol 2003;64:610-8.

(63) Donner MG, Keppler D. Up-regulation of basolateral multidrug resistance protein 3 (Mrp3) in cholestatic rat liver. Hepatology 2001;34:351-9.

(64) Nezasa K, Tian X, Zamek-Gliszczynski MJ, Patel NJ, Raub TJ, Brouwer KL. Altered hepatobiliary disposition of 5 (and 6)-carboxy-2',7'-dichlorofluorescein in Abcg2 (Bcrp1) and Abcc2 (Mrp2) knockout mice. Drug Metab Dispos 2006;34:718-23.

(65) Li Y, Looney GA, Hurwitz A. Effects of morphine on methotrexate disposition in mice. Clin Exp Pharmacol Physiol 2004;31:267-70.

(66) Zimniak P. Dubin-Johnson and Rotor syndromes: molecular basis and pathogenesis. Semin Liver Dis 1993;13:248-60.

(67) Bart J, Hollema H, Groen HJ, de Vries EG, Hendrikse NH, Sleijfer DT et al. The distribution of drug-efflux pumps, P-gp, BCRP, MRP1 and MRP2, in the normal blood-testis barrier and in primary testicular tumours. Eur J Cancer 2004;40:2064-70.

(68) Huang Y. Pharmacogenetics/genomics of membrane transporters in cancer chemotherapy. Cancer Metastasis Rev 2007;26:183-201.

(69) Leslie EM, Deeley RG, Cole SP. Multidrug resistance proteins: role of P-glycoprotein, MRP1, MRP2, and BCRP (ABCG2) in tissue defense. Toxicol Appl Pharmacol 2005;204:216-37.

(70) Vlaming ML, Pala Z, van Esch A, Wagenaar E, de Waart DR, van de Wetering K et al. Functionally overlapping roles of Abcg2 (Bcrp1) and Abcc2 (Mrp2) in the elimination of methotrexate and 7-hydroxymethotrexate *in vivo*. Clin Cancer Res 2009; *in press*.

(71) Breedveld P, Beijnen JH, Schellens JH. Use of P-glycoprotein and BCRP inhibitors to improve oral bioavailability and CNS penetration of anticancer drugs. Trends Pharmacol Sci 2006;27:17-24.

(72) Kuppens IE, Breedveld P, Beijnen JH, Schellens JH. Modulation of oral drug bioavailability: from preclinical mechanism to therapeutic application. Cancer Invest 2005;23:443-64.

(73) Hannivoort RA, Dunning S, van der Borght S, Schroyen B, Woudenberg J, Oakley F et al. Multidrug resistance-associated proteins are crucial for the viability of activated rat hepatic stellate cells. Hepatology 2008;48:624-34.

CHAPTER 1.2

Physiological and pharmacological roles of ABCG2 (BCRP): recent findings in Abcg2 knockout mice

Jurjen S. Lagas*, Maria L.H. Vlaming* and Alfred H. Schinkel

* These authors contributed equally to this work.

Modified from Advanced Drug Delivery Reviews 2009; 61:14-25

ABSTRACT

The multidrug transporter ABCG2 (BCRP/MXR/ABCP) can actively extrude a broad range of endogenous and exogenous substrates across biological membranes. ABCG2 limits oral availability and mediates hepatobiliary and renal excretion of its substrates, and thus influences the pharmacokinetics of many drugs. Recent work, relying mainly on the use of *Abcg2*$^{-/-}$ mice, has revealed important contributions of ABCG2 to the blood-brain, blood-testis and blood-fetal barriers. Together, these functions indicate a primary biological role of ABCG2 in protecting the organism from a range of xenobiotics. In addition, several other physiological functions of ABCG2 have been observed, including extrusion of porphyrins and/or porphyrin conjugates from hematopoietic cells, liver and harderian gland, as well as secretion of vitamin B_2 (riboflavin) and possibly other vitamins (biotin, vitamin K) into breast milk. However, the physiological significance of these processes has been difficult to establish, indicating that there is still a lot to learn about this intriguing protein.

CONTENTS

1. Introduction

The ATP-binding cassette (ABC) transporter ABCG2 (BCRP) is located at the apical membrane of hepatocytes and epithelial cells of intestine and kidney where it pumps a wide variety of endogenous and exogenous compounds out of the cell. Due to its activity in these excretory organs, ABCG2 can have a profound effect on the pharmacokinetics of many drugs and their metabolites, by enhancing their excretion and limiting their uptake from the intestinal lumen after oral administration. In addition, ABCG2 can confer multidrug resistance to tumor cells (1-5). ABCG2 might further be important for the pharmacological sanctuary properties of several tissues, due to its expression in the blood-brain, blood-placental and blood-testis barriers, where it could limit the penetration of its substrates into these critical tissues (1-7). ABCG2 is also found in stem cell-enriched cell populations and progenitor cells of a number of tissues, where it might potentially protect these important cells from insult by a variety of toxic or carcinogenic xenobiotics (2). A schematic overview of ABCG2 tissue distribution is shown in Figure 1. In general, ABCG2 appears to have a xenobiotic protective function, reducing levels of noxious compounds in individual cells, in certain organs, and in the body as a whole. Nevertheless, recently also high expression of ABCG2 in the lactating mammary gland was demonstrated, in the luminal membrane (Figure 1). Here ABCG2 concentrates its (often toxic) substrates into the milk (8), leading to the question whether ABCG2 may have additional, yet unrecognized physiological functions. The physiological and pharmacological roles of ABCG2/Abcg2 elucidated thus far have been extensively described in earlier reviews (1-5). Characterization of *Abcg2* knockout (*Abcg2*$^{-/-}$) mice has greatly contributed to the knowledge of *in vivo* ABCG2 functions (9;10). This review will focus on some of the more recently gained insights into the physiological and pharmacological functions of Abcg2, obtained using these valuable mouse models.

2. Recently established pharmacological functions of ABCG2/Abcg2

2.1. Functional role of Abcg2 at the blood-brain barrier; value of compound transporter knockout mice.

P-glycoprotein (P-gp, MDR1/ABCB1) was the first ABC multidrug transporter that was found to be highly expressed at the blood-brain barrier (BBB), where it efficiently restricts the entry of a wide variety of compounds into the brain (Figure 1) (11;12). More recently, ABCG2 was also identified at the BBB of humans, pigs and rodents, where it colocalizes with P-gp at the luminal side of endothelial cells of brain capillaries (13-17). *Mdr1a* knockout mice have proven to be a valuable tool to unravel the dominant function of P-gp at the BBB (11). In contrast, for ABCG2 it was not as straightforward to unequivocally establish a functional role at

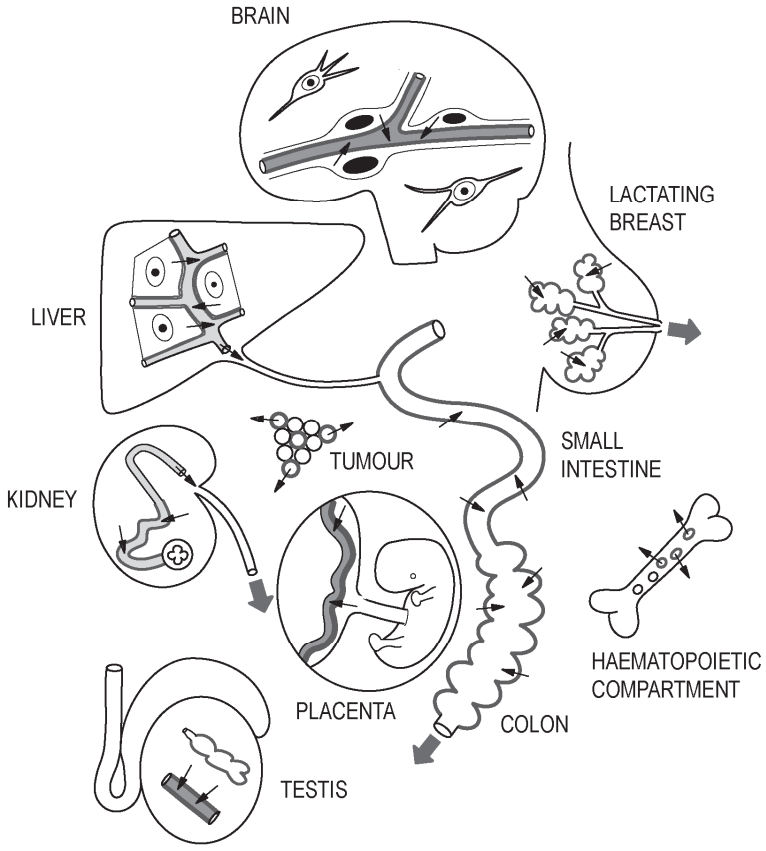

Figure 1. Schematic overview of ABCG2 expression throughout the body. Bold dark grey lines indicate the location of ABCG2. At all expression sites where small arrows indicate the direction of ABCG2-mediated transport, *in vivo* functionality of ABCG2/Abcg2 has been demonstrated. Wide arrows indicate net body excretion of ABCG2 substrates. For testis the situation in humans is depicted, where ABCG2 is found in both myoid cells of the seminiferous tubules and in blood capillary endothelial cells. However, only the Abcg2 barrier function of testis endothelial cells as demonstrated in mice is indicated with arrows. Expression of ABCG2 in endothelial cells of blood capillaries and veins, or in "side population" cells throughout many tissues in the body is not indicated. This figure was modified from reference [2].

the BBB, despite the availability of mouse models deficient in either P-gp or Abcg2 (9-11). This was illustrated by a number of studies, with sometimes contradicting outcomes. Shortly after the discovery of ABCG2 expression at the BBB, Cisternino *et al.* performed *in situ* brain perfusion experiments with the

prototypic ABCG2 substrates prazosin and mitoxantrone (18). To exclude involvement of P-gp, they used *Mdr1a*$^{-/-}$ mutant CF-1 mice and compared these to wild-type mice. Brain uptake of both compounds was not affected by the absence of P-gp, indicating that P-gp does not restrict the uptake of these compounds into the brain. Furthermore, elacridar, a dual P-gp and ABCG2 inhibitor, significantly increased the brain uptake of the studied compounds in wild-type and *Mdr1a*$^{-/-}$ CF-1 mice. Interestingly, elacridar increased the brain uptake of prazosin and mitoxantrone more in *Mdr1a*$^{-/-}$ mutant mice than in wild-type mice, which appeared to correlate with the observation that *Mdr1a*$^{-/-}$ mutant CF-1 mice had a threefold higher Abcg2 mRNA expression in their brain capillaries. From these somewhat indirect experiments it was inferred that Abcg2, and not P-gp, restricts the uptake of prazosin and mitoxantrone into the brain.

Contradicting results, however, were reported by Lee *et al.* (16), who performed similar in situ brain perfusion experiments with the ABCG2 model substrates mitoxantrone and dehydroepiandrosterone sulfate (DHEAS), using knockout mice in an FVB strain background (16). *Mdr1a/b*$^{-/-}$ mice displayed moderately but significantly higher brain uptake compared to wild-type mice for mitoxantrone and DHEAS, suggesting that brain penetration of both compounds is limited by P-gp. However, when *Abcg2*$^{-/-}$ mice were compared to wild-type mice, no difference in brain uptake of mitoxantrone and DHEAS was found. Furthermore, co-perfusion of the brains with elacridar resulted in a comparable and significantly increased brain uptake of mitoxantrone and DHEAS in all three genotypes. Based on these results, the authors concluded that one or more elacridar sensitive transporters are involved in the efflux of mitoxantrone and DHEAS at the BBB, but that no evidence was found for a functional role of Abcg2 at the BBB. Expression of ABC transporters in the BBB of mice (for instance, Abcc2) can sometimes vary markedly between different mouse strains (19). If this is also true for Abcg2, this could perhaps explain the contradicting outcomes of the described experiments. Whether indeed other ABC transporters than P-gp or Abcg2 are involved in limiting transport of mitoxantrone across the BBB may possibly be investigated in the future using (compound) knockout mice for different ABC transporters.

In another study addressing the functional role of Abcg2 at the BBB, Breedveld *et al.* used a different approach (20). Imatinib, a tyrosine kinase inhibitor anticancer drug and *in vitro* substrate of both P-gp and Abcg2 (21), was intravenously applied to wild-type, *Mdr1a/1b*$^{-/-}$ and *Abcg2*$^{-/-}$ mice and brain concentrations were determined 2 hours after administration. Consistent with a previous study (22), *Mdr1a/1b*$^{-/-}$ mice displayed 3.6-fold higher brain penetration compared to wild-type mice. Interestingly, for *Abcg2*$^{-/-}$ mice, which have functional

P-gp at the BBB, a 2.5-fold higher imatinib brain uptake was found. Furthermore, pharmacological inhibition of both P-gp and Abcg2 with the dual inhibitor elacridar resulted in a 4.2-fold increased brain penetration in wild-type mice. In addition, co-administration of imatinib with the Abcg2 inhibitor pantoprazole slightly increased the brain uptake in wild-type and *Mdr1a/1b*$^{-/-}$ mice, but did not affect brain penetration in *Abcg2*$^{-/-}$ mice. Collectively, these observations suggest that, in addition to P-gp, Abcg2 restricts the brain penetration of imatinib.

The roles of P-gp and Abcg2 in limiting the brain uptake of imatinib were also studied in a recent series of in situ brain perfusion experiments (23). In this study, brain uptake of imatinib was not different between wild-type and *Abcg2*$^{-/-}$ mice when it was perfused at non-saturating concentrations. However, when imatinib was perfused at higher (>1 μM) perfusate concentrations, increased brain penetration was found in both wild-type and *Abcg2*$^{-/-}$ mice, which suggests that saturation of one or more efflux processes occurred. The fact that this saturation phenomenon did not occur in *Mdr1a/1b*$^{-/-}$ mice, pointed towards saturation of P-gp. Interestingly, at imatinib concentrations exceeding ~20 μM, brain uptake was substantially more increased in *Abcg2*$^{-/-}$ than in wild-type mice. This suggests that, when P-gp is saturated in wild-type mice, the contribution of Abcg2 in reducing imatinib passage across the BBB becomes detectable. Saturation of P-gp might also explain the higher imatinib brain uptake that Breedveld *et al.* found in *Abcg2*$^{-/-}$ mice (20). Initial high plasma concentration in *Abcg2*$^{-/-}$ mice of ~15 mg/L (~25 μM), as applied in this study, indeed exceeded the saturation cut-off of ~20 μM that was found by Bihorel *et al.* (23).

The above summarized studies, employing mice that are deficient in either P-gp or Abcg2, suggest that P-gp is a dominant transporter at the BBB, which can even restrict brain penetration of comparatively poor P-gp substrates. Therefore, if one uses *Abcg2*$^{-/-}$ mice, in which P-gp is still present, it can be difficult to unequivocally demonstrate a functional role for Abcg2 at the BBB for shared P-gp/ABCG2 substrates. This was recently further supported by Enokizono *et al.*, who found that the brain uptake clearance of the dietary carcinogen and shared ABCG2 and P-gp substrate PhIP (2-amino-1-methyl-6-phenylimidazo[4,5-*b*]pyridine) in brain perfusion experiments was not different between wild-type and *Abcg2*$^{-/-}$ mice (7), whereas the ABCG2 (but not P-gp) substrates dantrolene and daidzein did show increased brain uptake clearance. Interestingly, however, when continuous infusion into the systemic circulation was applied, *Abcg2*$^{-/-}$ mice did show increased brain-to-plasma ratios even for the common ABCG2 and P-gp substrates PhIP and prazosin (7), although the differences were modest (1.5- to 2.5-fold). This discrepancy might be explained by the fact that in the brain perfusion experiments the compounds were perfused for only 1 minute, whereas in the

continuous infusion experiments the substrates were applied for 150 minutes before brain concentrations were measured. Consequently, prolonged exposure of the brain to relatively high plasma concentrations of these compounds may result in saturation of P-gp at the BBB and therefore a marked detectable effect on brain penetration of PhIP and prazosin in *Abcg2*$^{-/-}$ mice. Using these same continuous infusion conditions, the drug dantrolene and the phytoestrogens daidzein, genistein and coumestrol (Figure 3), which are ABCG2 but not P-gp substrates, did show very marked (up to 10-fold) increased brain penetration in *Abcg2*$^{-/-}$ mice (7;24).

Considering the complications described above, an elegant model to study the overlapping functions of P-gp and ABCG2 at the BBB for shared substrates is the compound P-gp and Abcg2 knockout mouse (*Mdr1a/1b/Abcg2*$^{-/-}$) (25). Recently, de Vries *et al.* used this model to study the brain uptake of the anticancer drug topotecan, which is a good substrate of ABCG2 and a weaker P-gp substrate (26). Compared to wild-type mice, brain-to-plasma AUC ratios were 2.0-fold higher in *Mdr1a/1b*$^{-/-}$ mice, not significantly different in *Abcg2*$^{-/-}$ mice, and 3.2-fold higher in *Mdr1a/1b/Abcg2*$^{-/-}$ mice. This study shows that, although topotecan appears to be a better ABCG2 substrate *in vitro* and in the mouse intestine (27), P-gp still dominates at the BBB. Nonetheless, Abcg2 also has a functional role and restricts the brain uptake of topotecan when P-gp is absent. Similarly, Oostendorp *et al.* recently used the *Mdr1a/1b/Abcg2*$^{-/-}$ mouse model to establish the restricting roles of P-gp and Abcg2 for the brain penetration of imatinib (28). The brain-to-plasma ratios of imatinib were highly (>10-fold) increased in *Mdr1a/1b/Abcg2*$^{-/-}$ mice, whereas for *Mdr1a/1b*$^{-/-}$ mice a modest (~2-fold) increase and for *Abcg2*$^{-/-}$ mice no increase in brain-to-plasma ratios was found. These latter two studies illustrate the value of compound transporter knockout mouse models to study the overlapping roles of Abcg2 and P-gp in the brain. To further illustrate the usefulness of compound knockout mice, recently also *Abcg2/Abcc4*$^{-/-}$ mice have been generated and these could be similarly used to elucidate the overlapping functions of both transporters in the disposition of the purine analogue drug PMEA (9-(2-(phosphonomethoxy)ethyl)-adenine) to various tissues (29). However, in this case brain penetration was not affected by the combination knockout in comparison to the single knockouts.

Taken together, Abcg2 appears to play a significant role at the BBB, where it can effectively restrict the brain penetration of potentially harmful compounds, especially those that are good ABCG2 substrates and not P-gp substrates. For shared substrates, Abcg2 and P-gp can (partially) take over each other's function at the BBB, although P-gp often dominates, whereas absence of both transporters can result in a drastically increased brain penetration.

2.2. Functional role of ABCG2/Abcg2 in the placenta and fetal membranes.

One of the main expression sites for ABCG2/Abcg2 is the placenta, where it is, like P-gp and MRP2 (ABCC2), expressed at the apical membrane of syncytiotrophoblasts (Figure 1) (6). The syncytiotrophoblast cellular layer forms the main barrier between the maternal and fetal blood circulations, and virtually all exchange of nutrients and waste products between mother and fetus occurs across these cells. Here ABCG2, which faces the maternal blood, could be involved in transport of its substrates from fetal to maternal blood, likely protecting the fetus from toxic compounds in the maternal circulation (6). Interestingly, the expression of Abcg2 changes with gestational age. In mice and rats Abcg2 mRNA expression peaks at mid-gestation (day 12-15) and decreases thereafter (6). However, from gestation day 9.5 on, protein levels of murine Abcg2 did not change significantly over time, although there was a tendency of a decrease after mid-gestation (30). Whether this is similar in humans is not completely clear, as contradictory results have been reported (6). The physiological function of the variable RNA expression of Abcg2 during gestation is not known (6). If the protein levels remain similar, it may simply reflect a lower turnover rate of placental Abcg2 protein at later gestational stages.

The first evidence that ABCG2 in the placenta limited fetal penetration of drugs was found in *Mdr1a/b*$^{-/-}$ mice that were treated with the Abcg2 and P-gp inhibitor elacridar. The fetal penetration of the anti-cancer drug topotecan was 2-fold increased in *Mdr1a/b*$^{-/-}$ mice that were treated with elacridar compared to vehicle-treated mice (27). Using *Abcg2*$^{-/-}$ and/or *Mdr1a/b/Abcg2*$^{-/-}$ mice, the effect of Abcg2 on limiting fetal exposure has recently been more directly demonstrated for the drugs topotecan (9), nitrofurantoin (31) and glyburide (32), as well as for the phytoestrogen genistein (24). In these studies absence of Abcg2 led to 2- to 5-fold increased fetal-to-maternal plasma ratios of the tested compounds, indicating the relatively important role for Abcg2 in protecting the fetus from potential toxins. The functional role of placental ABCG2 in humans has been investigated *in vitro* by several studies on the anti-diabetic drug glyburide, which is used in gestational diabetes. Using right-side out vesicles that were derived from human placental brush border membranes a 1.4-fold increase of glyburide uptake was shown after adding the ABCG2 inhibitor novobiocin (33). Furthermore, an *ex vivo* placental perfusion study revealed that co-administration of the ABCG2-inhibitor nicardipine led to 2-fold increased fetal-to-maternal concentration ratios of glyburide as measured in the respective perfusates (34). These data suggest a barrier function of ABCG2 in the human placenta as well. However, it cannot be excluded that the used inhibitors may have inhibitory or stimulating effects on other efflux and/or uptake transporters. This complicates the interpretation of these results.

Furthermore, *ex-vivo* studies may not completely reflect what happens *in vivo*. To address such issues, the complementary use of *Abcg2*$^{-/-}$ mice for studies on Abcg2-mediated transplacental transport remains invaluable.

Recently, expression of Abcg2 and other ABC transporters in murine fetal membranes, in particular the visceral yolk sac, has been detected. mRNA expression was higher than in the placental membrane and, like for placental expression of murine Abcg2, peaked at mid-gestation (35). Protein levels of Abcg2 in the yolk sac could only be measured after gestational day 12 and did not change up to 18 days after gestation (30). Similar high expression of ABCG2 protein and RNA was recently demonstrated in human fetal membranes (36). For the mouse, immunolocalization of Abcg2 in the yolk sac indicated that it faces the maternal side, leading to the speculation that it might have a protective function for the fetus, in analogy to the placental Abcg2 (30). Interestingly, the multidrug transporter Mrp2/Abcc2 colocalizes with Abcg2 at the apical (maternal) side of the visceral yolk sac membrane (35). However, whether Abcg2/ABCG2 expression at this site has any physiological or pharmacological significance remains to be investigated in functional studies.

Altogether, there is strong evidence that placental ABCG2/Abcg2 can have a marked protective effect for the fetus against numerous xenobiotics, in analogy to the function of placental P-gp. A possible protective contribution of ABCG2/Abcg2 in fetal membranes remains to be established.

2.3. Functional role of ABCG2/Abcg2 at the blood-testis barrier.

The testis is another sanctuary site where ABCG2 is highly expressed (Figure 1). Immunohistochemical analysis of human testis sections revealed that ABCG2, like P-gp, is expressed in the luminal membranes of endothelial cells of blood capillaries (Figure 2). In analogy to endothelial cells at the blood-brain barrier, testis endothelial cells form tight junctions with each other, providing a continuous cellular layer that could contribute to the blood-testis barrier (37). However, testis capillary endothelial cells (at least in the rat) are not as tightly linked as those in the brain, which has raised doubts about an optimal barrier function (38). Obviously, when the physical barrier is not completely closed, the impact of drug transporters may be limited. Furthermore, ABCG2 and P-gp are strongly expressed in the apical membranes of myoid cells surrounding the seminiferous tubules (Figure 2) (39). The transport direction of both transporters in myoid and endothelial cells is outward from the seminiferous tubuli, which suggests that ABCG2 and P-gp protect the developing germ cells by restricting testicular penetration of potentially harmful substrates (Figure 2). It should be noted, though, that myoid cells too are not consistently joined by tight junctions (at least, in the rat), which might hamper

their function as an effective barrier (38). In addition, the ABC multidrug transporter MRP1/ABCC1 is expressed in the basal membrane of the Sertoli cells of the seminiferous tubules (Figure 2), where it can protect the seminiferous tubules from drug induced damage, as was shown for the anticancer agent etoposide (40). Sertoli cells are consistently joined by tight junctions. It is noteworthy, however, that the progenitor spermatogenic cells (i.e., germ line cells) are located just outside the Sertoli cells (41) and are thus not protected by MRP1 (Figure 2). Theoretically there is therefore a need for an additional protective barrier between blood and these critical germline cells, which could be situated in the myoid and/or capillary endothelial cells expressing ABCG2 and P-gp.

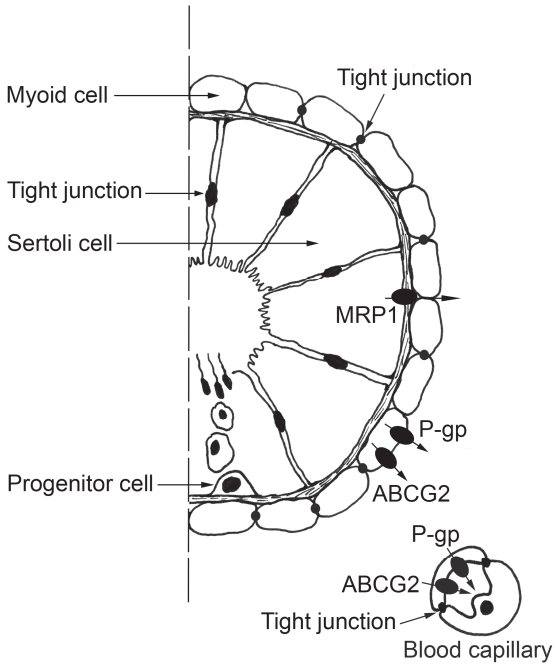

Figure 2. Schematic representation of a cross-section through a seminiferous tubule and a blood capillary in the testis. The strategic localization of drug efflux transporters in the blood-testis barrier is depicted. In humans ABCG2 and P-gp (ABCB1) are found in the apical (luminal) membrane of blood capillary endothelial cells and in the apical membranes of myoid cells surrounding the seminiferous tubules. In addition, MRP1 (ABCC1) is expressed in the basal membrane of Sertoli cells. Note that the myoid cells are not consistently connected by tight junctions, whereas the endothelial cells of the testis blood capillaries are connected by tight junctions, but not as consistently as in brain capillaries. Sertoli cells are consistently joined by tight junctions.

Also in the mouse testis, Abcg2 expression was recently demonstrated in the luminal membranes of endothelial cells of blood capillaries (24). In contrast to the human testis, however, Abcg2 expression in the apical membranes of myoid cells was not observed (24). In the same study, expression of ABCG2/Abcg2 in the murine and human epididymis was investigated. The epididymis is part of the male reproductive system that is attached to the testis and used for maturation and storage of spermatozoa after production in the testis (42). In the body region of the mouse epididymis (i.e., somewhat distal from the testis), Abcg2 was observed in the endothelial cells of the blood capillaries, whereas in the epididymis head region (i.e., most proximal to the testis) Abcg2 was expressed in both the luminal and abluminal membranes of the ducts that contain spermatozoa. Expression of Abcg2 in the blood capillaries of the epididymis head and in the abluminal membranes of the ducts in the epididymis body might restrict penetration of potentially harmful Abcg2 substrates and thus protect the spermatozoa in the ducts. However, expression of Abcg2 in the luminal membrane of the ducts in the epididymis head seems paradoxical, because the transport direction is towards the spermatozoa in the lumen. A physiological function cannot be excluded, but male fertility (and hence sperm function) in *Abcg2*$^{-/-}$ mice does not seem to be compromised (9;10). In the human epididymis, mRNA expression of BCRP was demonstrated, but no immunohistochemical analysis was reported yet (24).

Using *Abcg2*$^{-/-}$ mice, it was recently demonstrated that penetration of a number of exogenous compounds (all Abcg2 substrates) into the testis was indeed efficiently restricted by Abcg2 (7;24). When these compounds were systemically infused under steady state conditions, the testis-to-plasma ratios were markedly (up to 15-fold) higher in *Abcg2*$^{-/-}$ mice compared to WT mice. This was shown for PhIP, two metabolites of PhIP, MeIQx (2-amino-3,8-dimethylimidazo[4,5-f]quinoxaline), dantrolene, prazosin and for the phytoestrogens daidzein, genistein and coumestrol (7;24). In addition, genistein penetration into the epididymis was also higher in *Abcg2*$^{-/-}$ mice (2.5-fold). Together, these data indicate a prominent role of ABCG2 in reducing testis and epididymis exposure to numerous xenobiotics.

As pointed out by Enokizono *et al.* (7), the pronounced effect of Abcg2 knockout on testis penetration of a range of substrates provides strong evidence for a substantial role of testis capillary endothelial cells in the blood-testis barrier, at least in the mouse, as these cells are the only location where testicular Abcg2 could be detected.

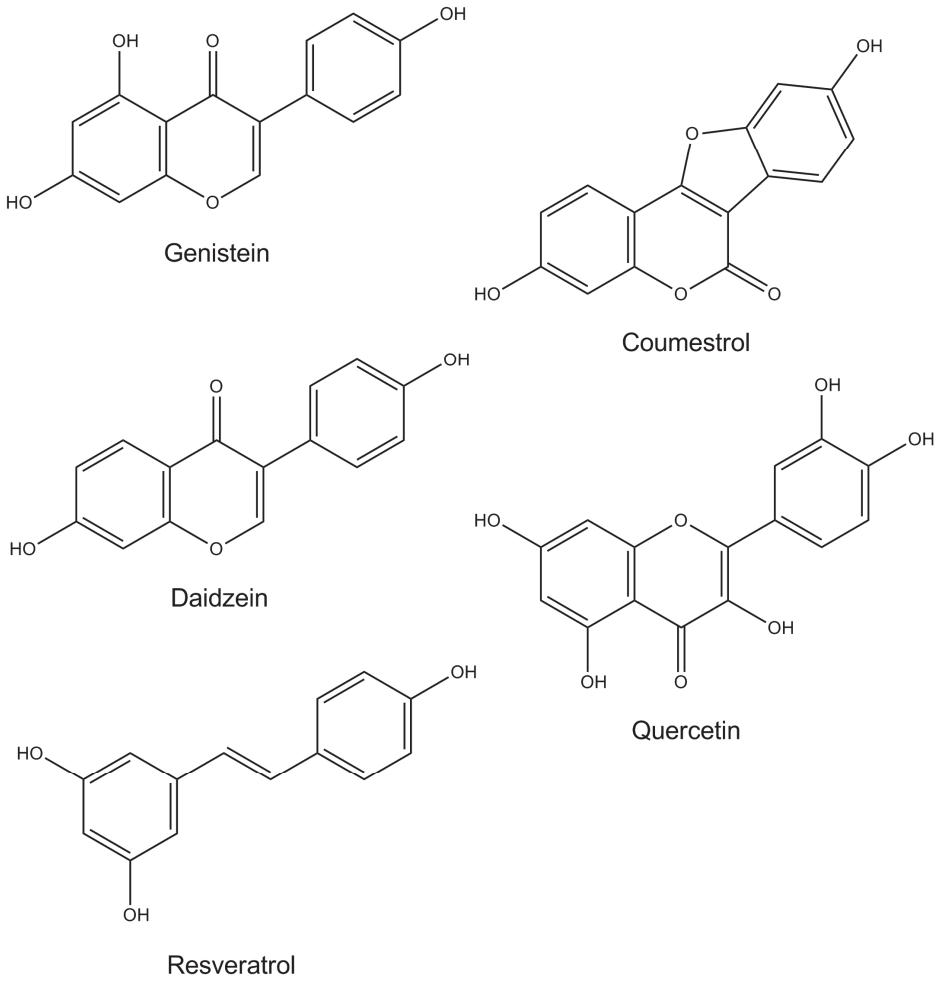

Figure 3. Phytoestrogens that are transported by Abcg2/ABCG2. An effect of murine and human Abcg2/ABCG2 *in vitro* and murine Abcg2 *in vivo* has been shown for transport of genistein, daidzein and coumestrol (24). Quercetin is transported *in vitro* by murine Abcg2, and an *in vivo* effect of rat intestinal Abcg2 on quercetin glucuronide excretion was demonstrated (43). Resveratrol transport by human ABCG2 has been shown *in vitro*, but only at low pH and not at physiological pH (44).

The physiological function of Abcg2 at the blood-testis and blood-epididymis-barriers might be particularly important with respect to (phyto)estrogens, many of which have been identified as Abcg2 substrates (Figure 3) (24;43;44), because these compounds are known to influence reproductive functions, e.g. reducing testicular weight and sperm count (45;46).

In conclusion, at all three of the above discussed blood-tissue barriers, ABCG2 appears to play an important role in restricting the uptake of (potentially harmful) substrates. It is interesting to note that for shared substrates of ABCG2 and P-gp, the restricting role of P-gp at the BBB appears more pronounced than that of ABCG2. Even for very good ABCG2 substrates *in vitro* and in the intestine, such as topotecan (27), penetration into brain is predominantly limited by P-gp and an effect of ABCG2 could only be demonstrated under P-gp deficient conditions (9;26). Nonetheless, deficiency of both P-gp and Abcg2 results in higher brain penetration than observed for P-gp deficient animals (9;26). This illustrates that Abcg2 can be an important backup mechanism for shared substrates, which can partially take over the function of P-gp at the sanctuary site barriers.

3. Physiological functions of ABCG2/Abcg2

3.1.1. Abcg2 pumps vitamins into milk.

In addition to its expression in excretory organs such as liver, kidney and small intestine, and its function in protecting the brain, testis and fetus from xenobiotics, it was recently found that Abcg2 is also expressed in the lactating mammary gland of mice, sheep, cows and humans (Figure 1) (8;47). Abcg2 localizes here to the apical side of alveolar epithelial cells, the main site of milk production. Mammary Abcg2 expression is strongly induced during pregnancy and lactation, and only falls back upon weaning of the pups (8). As a consequence, (potentially toxic) Abcg2 substrates in the maternal circulation are actively pumped into the milk, leading to the exposure of suckling infants and dairy consumers to a wide range of xenobiotics. This intriguing finding therefore has major pharmacological and toxicological consequences for breast-feeding infants and dairy consumers (and producers), which are discussed in more detail in a recent review (2). The fact that Abcg2/ABCG2 is expressed in the lactating mammary gland led to the hypothesis that besides a xenobiotic efflux transporter, Abcg2 may also be involved in the transfer of nutrients from mother to pup via the milk (2).

Recently, it was indeed found that an important nutrient, namely riboflavin (vitamin B_2) (Figure 4A), is a transported substrate for mouse and human Abcg2/ABCG2 *in vitro* (48). Riboflavin is necessary to form the enzyme cofactors FMN and FAD (Figure 4A), which function as electron carriers in many essential redox reactions in the body (49). Using *Abcg2*$^{-/-}$ mice it was shown that Abcg2 on

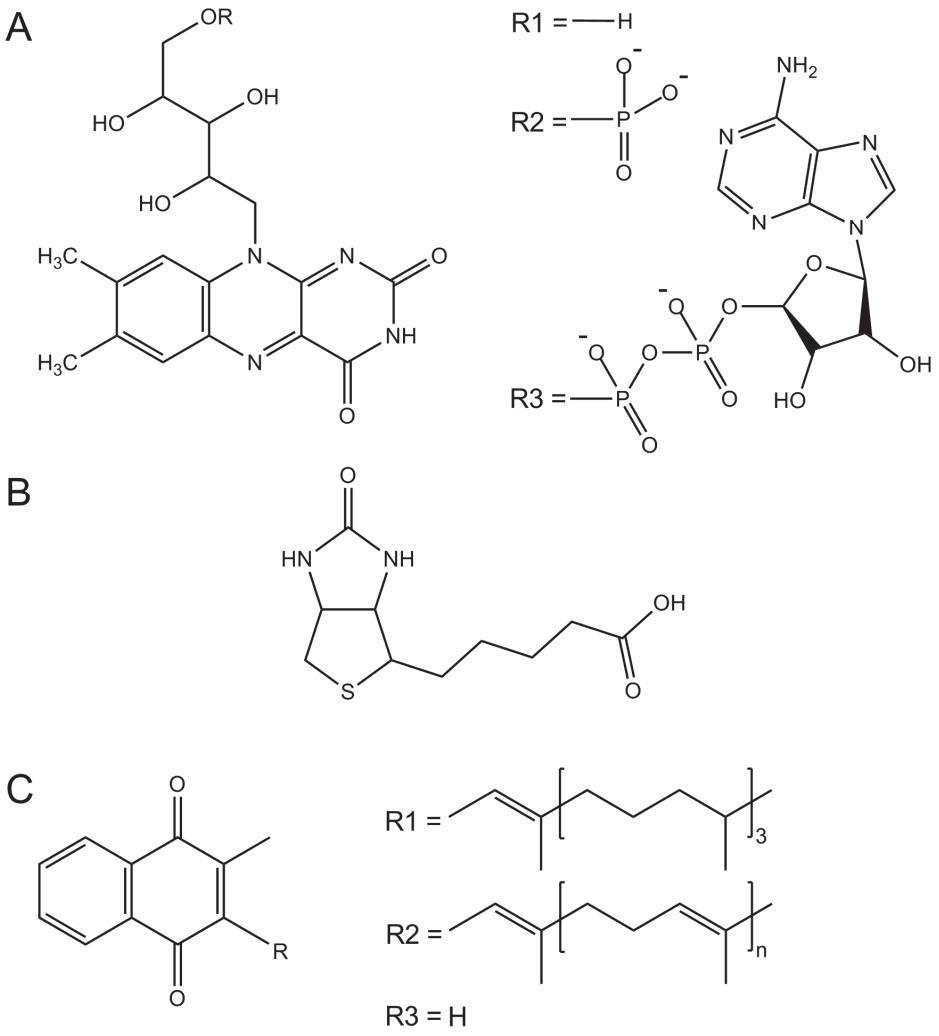

Figure 4. Vitamins of which the milk secretion can be affected by Abcg2. (A) Riboflavin (vitamin B_2) (R = R1) and FMN (R = R2), but not FAD (R = R3) are concentrated into milk by Abcg2. (B) Biotin (vitamin B_7) levels in milk are 3.5-fold decreased in *Abcg2*$^{-/-}$ mice. (C) Vitamin K_1 (R = R1) levels in milk are not affected by Abcg2 and vitamin K_2 (R = R2) or K_3 (R =R3) concentrations in *Abcg2*$^{-/-}$ milk have not been determined yet. Vitamin K_3 is transported by ABCG2 *in vitro* and therefore may be concentrated into milk by ABCG2/Abcg2.

the one hand limits the tissue distribution and plasma concentrations of dietary riboflavin, but on the other hand also actively pumps riboflavin into the milk. In fact, steady state milk secretion of riboflavin in *Abcg2*$^{-/-}$ mice was 60-fold reduced compared to wild-type mice. Additionally, the (already low) concentrations of FMN were ~6-fold reduced in milk of *Abcg2*$^{-/-}$ mice, suggesting that Abcg2 also pumps FMN into the milk. Nevertheless, pups from *Abcg2*$^{-/-}$ mothers do not display any phenotype associated with riboflavin-deficiency (e.g. growth retardation, skin lesions or neurodegenerative changes (50)), suggesting that Abcg2-mediated transport of riboflavin into milk is not essential for the health of suckling pups (48). This is most likely explained by the fact that substantial amounts of the cofactor FAD can still enter the milk independently of Abcg2 (48). FAD can be converted to riboflavin in the intestine before being absorbed, and this is probably sufficient to compensate for the riboflavin deficiency in the milk of *Abcg2*$^{-/-}$ mice, at least in the protective environment of the lab, with ample supplies of riboflavin-rich food. It could well be that under more natural conditions, such as a variable food supply, reduced dietary intake, or increased need for vitamins due to stress or disease, Abcg2-mediated transport of riboflavin into the milk will be essential for an optimal nutritional and health state of suckling pups.

After the mammary transport of riboflavin by Abcg2 was discovered, the milk of *Abcg2*$^{-/-}$ mice was analyzed for levels of other vitamins (48). In addition to riboflavin, the concentration of biotin (vitamin H, vitamin B_7) (Figure 4B) was reduced in milk of *Abcg2*$^{-/-}$ mice, although the difference was smaller than for riboflavin (~3.5-fold decrease). This suggests that Abcg2 may also be involved in the secretion of biotin into the milk. Direct transport of biotin by Abcg2/ABCG2, however, has not been shown yet, so decreased milk concentrations of biotin may also be caused by indirect effects of Abcg2 deficiency. Furthermore, no signs of biotin deficiency (dermatitis, hair loss and neurological signs (51)) in suckling *Abcg2*$^{-/-}$ pups have been reported. This may be due to the fact that a significant amount of biotin is still present in the milk of *Abcg2*$^{-/-}$ mothers (48), which may be sufficient for the pups, at least in the protective environment of the lab where the mice receive an excess of nutrients through the diet.

The fact that Abcg2/ABCG2 has a prominent effect on the elimination or transport of a variety of exogenous and endogenous porphyrins, such as pheophorbide a (9), PPIX (9;52;53) and PPIX glycoconjugates (53) and its interaction with hemin (54) (see also below), would suggest that vitamin B_{12}, a porphyrin-containing vitamin, could be transported into the milk by Abcg2. However, the analysis of milk of *Abcg2*$^{-/-}$ mice did not show decreased levels of this vitamin, suggesting that this is not the case, or at least that Abcg2 does not make a important contribution to vitamin B_{12} secretion into milk (48).

Folic acid (folate, vitamin B_9) is another vitamin that is directly transported by ABCG2 *in vitro* (55). It was therefore hypothesized that ABCG2 would transport folic acid into the milk. Nevertheless, studies under both steady-state conditions (48) as well as after i.v. administration of 1 mg/kg [^{3}H]folic acid (8) to lactating dams did not reveal any difference in folate levels between milk of wild-type and *Abcg2*$^{-/-}$ mice. This indicates that alternative, and quantitatively more important pathways of folate secretion into milk must exist in the mammary gland. Some other ABC transporters are also capable of folic acid transport, at least *in vitro* (55), and these might perhaps contribute, but various other transport processes may also be relevant. In fact, very little is known yet about milk secretion mechanisms of various vitamins, and this may be an interesting area for future research.

It was recently shown that ABCG2 expression in HEK 293 cells conferred resistance to vitamin K_3 (menadione, 2-methyl-1,4-naphtoquinone) (Figure 4C) *in vitro*, and that ABCG2-dependent efflux of mitoxantrone could be inhibited by vitamin K_3 (56). This suggests that this vitamin is a substrate for ABCG2 as well. Vitamin K_3 is a synthetic precursor of vitamin K_2 (menaquinone) (Figure 4C), and can be converted to K_2 in the body, although the biological significance of this conversion is unclear (57). Vitamin K_1 (phylloquinone) (Figure 4C) levels in milk were not different between *Abcg2*$^{-/-}$ and wild-type mice, suggesting that this compound is not a substrate of Abcg2, or that other transport processes dominate its milk secretion (48). Levels of vitamins K_2 and K_3 in milk of *Abcg2*$^{-/-}$ mice have not been analyzed thus far. Based on the *in vitro* experiments with vitamin K_3 this may be interesting to investigate, although also vitamin K deficiency (reflected by haemorrhagic disease (57)) has never been reported for *Abcg2*$^{-/-}$ pups. This might of course be explained by the fact that vitamin K_1 secretion into milk is normal in *Abcg2*$^{-/-}$ mothers, which could be sufficient to meet the required vitamin K intake of pups, at least in the favorable environment of the lab (see above).

Although these recent reports indicate that Abcg2 contributes to transport of some important nutrients into the milk, the question remains why pups fed by *Abcg2*$^{-/-}$ mothers do not show any abnormalities. Challenging *Abcg2*$^{-/-}$ mice with different types of diets containing low amounts of nutrients may shed more light on this. It appears that for many of these nutrients multiple (possibly redundant) pathways are available for transport into the milk. Investigation of other mechanisms of nutrient secretion into milk may also provide more insight into the relative contribution of Abcg2 to this process.

3.1.2. Secretory function of the multidrug resistance transporter ABCG2/Abcg2 in the mammary gland: a conundrum?

What is the biological meaning of ABCG2 function in the mammary gland? Clearly, the use of a multispecific xenobiotic transporter to secrete a number of vitamins into milk poses problems, both biological and conceptual. Based on the tissue distribution of ABCG2 (Figure 1), its extremely wide substrate specificity, and extensive functional studies in *Abcg2*$^{-/-}$ mice, there can be no doubt that one of the main biological functions of ABCG2 is protection from naturally occurring dietary xenobiotics. It limits oral uptake and bioavailability, mediates hepatobiliary and renal excretion, and restricts penetration of its substrates into critical tissues such as brain, testis, and fetus, as well as individual cells (e.g. hematopoietic progenitors) expressing ABCG2. It thus limits exposure to its substrates at the organismal (systemic), organ and cellular levels. This is all well and good for noxious xenobiotics, but at the same time ABCG2 will also limit uptake and availability of transported vitamins such as riboflavin, folate, and vitamin K_3. In theory this might compromise vitamin supply to the organism, to critical tissue and cell compartments, and to the developing fetus. We indeed observed higher levels of riboflavin in *Abcg2*$^{-/-}$ than in wild-type mice (48), but the differences were modest. It is therefore reasonable to assume that for critical nutrients that are ABCG2 substrates, efficient uptake and retention mechanisms exist in all relevant barriers (intestine, placenta and other blood-tissue barriers, cell membranes) that largely overrule the extruding function of ABCG2. This would make the vitamin extrusion function of ABCG2 tolerable for the organism.

Conversely, the active secretion of potentially noxious xenobiotics into the milk by ABCG2 seems difficult to reconcile with optimal protection of the newborn offspring. Altogether, the combination of properties of ABCG2 (tissue distribution, substrate specificity, established functions) seems highly paradoxical. Here we will consider some hypotheses on ABCG2 function in the mammary gland that might begin to explain this paradox.

A. ABCG2 expression in mammary gland is coincidental. This hypothesis assumes that there is no positive biological need for mammary gland ABCG2. This would be consistent with the lack of obvious deficiency phenotypes observed so far in pups nursed by *Abcg2*$^{-/-}$ mothers. The mammary gland expression of ABCG2 during pregnancy and lactation would merely be a consequence of the presence of transcriptional regulation elements that are necessary for proper expression and regulation of ABCG2 at other developmental stages or elsewhere in the body. The possible negative effects of pumping noxious dietary xenobiotics into the milk are mitigated by the fact that the nursing mother can itself prevent high systemic

accumulation of dietary ABCG2 substrates through her own ABCG2 functions (in liver, intestine, kidney). Only a limited amount of noxious ABCG2 substrates would therefore be secreted into the milk. The riboflavin and other vitamin secretion into milk would be a coincidental consequence of the very wide substrate specificity of ABCG2. Although we cannot exclude this coincidental hypothesis, we feel it is less likely. Mammary gland ABCG2 is consistently induced during pregnancy and lactation in at least four widely divergent mammalian species (mouse, man, sheep, cow) (8;47). This evolutionary conservation suggests some functional need. Moreover, Abcg2 expression elsewhere in the mouse body (liver, kidney, small intestine) is not altered during pregnancy and lactation (58), so there is also at least one tissue-specific factor in the mammary gland that allows specific induction of ABCG2. Altogether, the conserved presence of so many regulatory factors that allow specific mammary gland induction of ABCG2 in a variety of mammalian species suggests there is some biological need for it.

B. ABCG2 activity in the mammary gland is useful as a xenobiotic clearance mechanism for the mother. This hypothesis assumes that mammary gland Abcg2 is not necessary for transport of nutrients, but functions primarily as an "overflow mechanism". Lactating mothers are in general more vulnerable and may therefore need extra elimination routes for potentially toxic compounds. Abcg2 expression in the mammary gland may be used for this. Still then the question remains why it would be acceptable to expose suckling pups to these potentially toxic compounds. Abcg2 protein expression has been detected in the intestinal submucosa of the fetus recently (30). Abcg2 in the intestinal wall of the suckling pups may therefore be sufficient to restrict intestinal uptake of Abcg2 substrates from the milk. Even though we have observed that sometimes substantial fractions (up to 15% of the dose) of i.v. administered drugs are cleared via the milk (59), we consider this hypothesis unlikely as well. If the mother is compromised by xenobiotic exposure, so will the pup, and it is likely that the rapidly growing and developing pup is more susceptible to adverse effects of toxins than the mother. Moreover, there are highly efficient alternative clearance pathways available to the mother (liver, kidney, intestine). If need be, it would make more biological sense for the mother to optimize those clearance pathways, for instance by upregulating ABCG2 in these tissues, rather than endangering the well-being of the pups through the milk.

C. Xenobiotic exposure of suckling pups prepares them for the switch to solid food. This hypothesis assumes that deliberate transfer of moderate levels of dietary xenobiotics through the milk will induce proper detoxification systems in the pup (48). Very likely, upon weaning the pups will be eating the same solid food as the

mother, and therefore be exposed to the same dietary xenobiotics. It would make biological sense to preemptively upregulate the detoxification systems in the pup that are suited to handling these xenobiotics (e.g., xenobiotic-metabolizing, -conjugating and -transporting proteins), instead of challenging a "virgin" detoxification system. The preinduction through the milk xenobiotics, for instance via activation of the nuclear xenobiotic receptors PXR and CAR, will help the pups in dealing immediately with the solid food xenobiotics, and thus improve their overall fitness. We feel this hypothesis is conceptually attractive, and pilot experiments to test it are ongoing. A limitation that we have encountered here is, however, that there are not yet many ABCG2 substrates known that are also good activators of PXR and CAR, which would seem to be the most obvious mediators for preemptive upregulation of detoxification systems in pups (60).

D. Milk transfer of xenobiotics may reduce the chance of developing allergy against these molecules later in life. This hypothesis is based on the recent demonstration that, upon milk transfer of an allergen to which the lactating mother is exposed, the chance that the suckling pups will develop allergy against this compound later in life is reduced (61). This oral tolerance induction in the pups was dependent on the presence of TGF-β, which is normally present in breast milk. The presence of this protein suggests that oral tolerance induction is a natural function of milk. Milk transfer by ABCG2 of potentially allergenic compounds (either exogenous or endogenous) to which the mother is exposed might thus reduce the chance for the pups of developing allergy against these compounds later in life. A limitation of this hypothesis is that it would mainly apply to relatively small molecules (i.e., transported by ABCG2) whereas the experimental demonstration concerned a protein (ovalbumine). Proteins and protein conjugates are more usual allergens than small molecules. However, small molecules can also be highly allergenic (penicillin is a well-known example) (62), and true allergies to various other drugs (cephalosporins, sulfa drugs, anticonvulsants, neuromuscular blocking agents, novocaine) have been described (62-64). This hypothesis could be tested when a suitable allergenic small molecule is identified as an ABCG2 substrate.

E. Mammary gland ABCG2 is necessary for nutrient transfer in the milk. This assumes that we have not yet applied the proper conditions to nursing *Abcg2*$^{-/-}$ mice to reveal a strong need for ABCG2 in providing vitamins and perhaps other nutrients in milk. Testing this hypothesis may depend on finding the proper conditions in the lab, or perhaps identifying additional nutrients that might be transported by ABCG2 into the milk. Nevertheless, this hypothesis still begs the

question why mammals didn't evolve dedicated transport systems to pump the various nutrients into milk, rather than a multispecific xenobiotic transporter. This would circumvent the risk of xenobiotic exposure of pups through milk. Still, nature tends to be pragmatic, and it may have been relatively easy (in an evolutionary sense), sufficiently efficient and with acceptable risk to the pups to apply a multidrug transporter for simultaneously pumping a variety of nutrients into milk.

Of course other, even more tentative hypotheses can be formulated, but here we restrict ourselves to the most obvious ones. We further note that some possibilities are not mutually exclusive. For instance, it is quite possible that mammary gland ABCG2 is important for both preemptively inducing detoxification mechanisms in suckling pups (C), and in providing them with some nutrients (E). Even the allergen hypothesis (D) might apply in parallel to hypotheses C and E. We finally note that there may still be other, unrecognized functions for mammary gland ABCG2 that would clarify its presence in the breast. Clearly, much more work will need to be done to resolve these complex but intriguing questions.

3.2. Abcg2 is expressed in the harderian gland and involved in transport of conjugated protoporphyrin IX.

The tubulo-alveolar epithelial cells of the harderian gland have recently been identified as another site of high Abcg2 expression in the mouse (53). The harderian gland is a lipid-secreting exocrine gland located behind the eye, which is especially well developed in rodents and many other vertebrates (occupying about one third of the eye socket in mice), but appears to be absent in humans and other primates. Perhaps related to its absence in humans, the physiological function of the harderian gland is still unclear. Situated next to the tear gland, its secreta are released at the inner corner of the eye. In rodents it secretes lipids as well as large amounts of porphyrins, which are, amongst others, suggested to function as phototransducers capable of absorbing UV-light (65). Due to its high concentration and excretion of porphyrins, the harderian gland is an interesting organ for studies on porphyrin excretion mechanisms. It may be worth observing that substantial amounts of these porphyrins, which have a reddish colour, end up in the coat of rats through grooming. In white-coated animals they are responsible for the typical reddish coat glow that is often seen. Conversely, in sick animals harderian gland secreta accumulate in the eye corner due to lack of grooming, causing typical red crusts. A possible function of harderian gland secreta in rodent coat care or function should not be excluded.

One of the main porphyrins, protoporphyrin IX (PPIX), is a direct precursor of heme (Figure 5), which is an important cofactor in many essential biological processes (O_2 transport by hemoglobin, electron transfer in cytochrome P450s, etc). Nevertheless, porphyrins are highly efficient photosensitizers and an excess can cause severe cellular damage (66), so their synthesis and distribution must be carefully regulated. When harderian glands of *Abcg2*$^{-/-}$ mice were macroscopically investigated, it was found that they had a deep red-brown colour instead of the pale colour seen in wild-type mice. Fluorescence microscopy showed that this could be attributed to a vast increase in intracellular porphyrin levels, which suggested that Abcg2 is normally involved in secretion of porphyrins into the tubulo-alveolar lumen of the harderian gland (53).

The involvement of Abcg2/ABCG2 in endogenous porphyrin transport has previously been suggested based upon the fact that *Abcg2*$^{-/-}$ mice had increased erythrocyte PPIX levels (9). Subsequently, it was shown that progenitor cells from *Abcg2*$^{-/-}$ mice were more affected by hypoxic conditions (leading to increased intracellular heme concentrations) compared to wild-type progenitor cells, and that ABCG2 specifically could bind to hemin, a heme analogue (Figure 5) (54). This binding could be intensified by the presence of ABCG2 substrates. Presence of hemin on the other hand also increased ABCG2-mediated transport of estrone-3-sulfate (54). Furthermore, Zhou *et al.* (52) showed that ABCG2 overexpression in K562 cells led to reduced cellular PPIX levels, which could be reversed by the ABCG2 inhibitor Ko143. Also treatment of mature erythrocytes expressing ABCG2 with Ko143 could increase PPIX accumulation (52). These studies clearly suggested that ABCG2 is capable of transporting PPIX and that it can interact with heme under excess conditions. However, they did not distinguish between PPIX and its various conjugates.

Analysis of harderian gland extracts from *Abcg2*$^{-/-}$ mice showed that levels of the PPIX-glycoconjugates protoporphyrin-1-O-acyl-β-xyloside (penta) and to a minor extent protoporphyrin-1-O-acyl-β-glucoside (hexa) (Figure 5) were dramatically increased. No unconjugated PPIX was detected in harderian glands of *Abcg2*$^{-/-}$ mice, which suggested that PPIX is mainly excreted from harderian gland as a penta conjugate (53). Indeed, only the penta conjugate of PPIX (but not unconjugated PPIX) was detectable in tear fluid collected from wild-type mice. Furthermore, although *Abcg2*$^{-/-}$ mice still showed penta secretion in tear fluid, the tear/gland ratio of penta was 9-fold lower than in wild-type. Subsequent *in vitro* cellular accumulation experiments with MDCKII cells expressing murine Abcg2 or human ABCG2 suggested that the harderian gland PPIX glycoconjugates are indeed transported efficiently by Abcg2/ABCG2 (53).

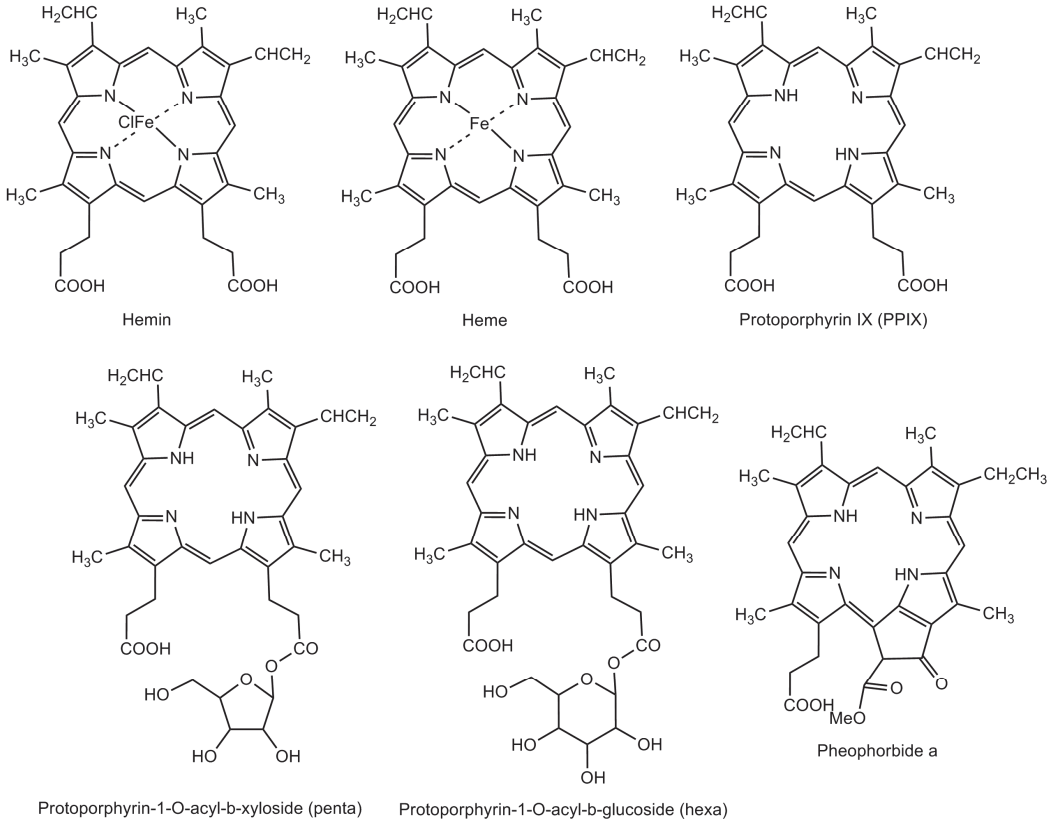

Figure 5. Physiological and exogenous porphyrins that interact with and/or are transported by ABCG2/Abcg2. Hemin, an analogue of heme, interacts with ABCG2 *in vitro* (54). The heme-precursor PPIX is likely transported by ABCG2 *in vitro* (52) and PPIX levels in erythrocytes of *Abcg2*$^{-/-}$ mice are elevated (9). The PPIX-glycoconjugates "penta" and "hexa" are likely transported *in vitro* and *in vivo* by Abcg2/ABCG2 (53). The exogenous porphyrin pheophorbide a is transported by Abcg2/ABCG2 *in vitro* and causes severe phototoxicity in *Abcg2*$^{-/-}$ mice (9).

Also in the liver of *Abcg2*$^{-/-}$ mice an accumulation of protoporphyrin-1-O-acyl-β-xyloside (penta) was found, but under normal conditions the total amounts of PPIX and its conjugates were only slightly increased in livers of *Abcg2*$^{-/-}$ mice. However, when a high PPIX dose was administered i.v. to wild-type and *Abcg2*$^{-/-}$ mice, the biliary excretion of total PPIX was dramatically reduced in the *Abcg2*$^{-/-}$ mice compared to wild-type (53). This suggests that although Abcg2/ABCG2 is likely an efficient transporter of PPIX-glycoconjugates, it is probably also a low-

affinity (but high capacity) transporter for PPIX, which may primarily be important under excess PPIX conditions.

The physiological function of Abcg2-mediated transport of PPIX (-conjugates) remains unclear, as no functional abnormalities have been described in *Abcg2*$^{-/-}$ mice that could be directly attributed to the altered PPIX levels. One possibility is that Abcg2 helps to reduce porphyrin toxicity in liver and other cells in situations of PPIX excess. Also, the PPIX-conjugates that are excreted from the harderian gland by Abcg2 will likely have a (so far unknown) exocrine or endocrine function. Considering that the whole heme biosynthetic pathway up till PPIX (i.e., the last step before insertion of Fe to generate heme, Figure 5) must be highly activated in the harderian gland in order to obtain the normal levels of PPIX conjugate secretion, it is difficult to imagine that there would not be a biological need for it. Be that as it may, the actual biological function of PPIX conjugate secretion (and thus of Abcg2) in the harderian gland remains a mystery.

3.3. Abcg2 is expressed at the murine blood-retinal barrier where it might protect the retina from circulating phototoxins.

Abcg2 is expressed in blood capillary endothelial cells of many so-called tissue sanctuaries (see above). Recently, also the murine blood-retinal barrier (BRB) has been identified as a site of Abcg2 expression, where it was detected at the luminal membrane of retinal capillary endothelial cells (67). Intrinsic to its function as a light-sensing organ, the retina is highly photosensitive and vulnerable to damage caused by circulating phototoxic compounds such as pheophorbide a and PPIX, which are both Abcg2 substrates (see also above) (9;53;68). Abcg2 expression was also detected in conditionally immortalized rat retinal capillary endothelial cells (TR-iBRB2 cells), in which the accumulation of pheophorbide a increased significantly by treatment with the Abcg2-inhibitor Ko143, suggesting that Abcg2 expression in these cells is functional (67). The physiological function of the Abcg2 expression in the BRB may be to protect the retina from phototoxicity induced by circulating PPIX(-conjugates), or phototoxins derived from the diet. It should be noted, though, that ABCG2 is generally expressed in endothelial cells of small veins and capillaries throughout the body, also in blood vessels where there are no tight junctions between endothelial cells (69). It is therefore uncertain whether endothelial ABCG2 expression always has to indicate a blood-tissue barrier function. Whether Abcg2 really limits the penetration of drug or phototoxic substrates into the retina should therefore be determined in future studies, possibly using *Abcg2*$^{-/-}$ mice.

4. Concluding remarks

The last 4-5 years have seen a significant increase in insights into possible pharmacological and physiological functions of ABCG2, many based on analyses of *Abcg2*$^{-/-}$ mice. These include a definitive demonstration of the impact of ABCG2 in protecting brain, testis, and fetus from various xenobiotics, and elucidation of the function of mammary gland ABCG2 in pumping various drugs, carcinogens and toxins into milk. These findings can have a wide range of clinical applications. For example, when pregnant women are treated with drugs that are potentially harmful to the fetus, it might be preferable to select drugs that are ABCG2 substrates, so the fetus is protected. Conversely, if a drug should enter the fetus for therapeutic purposes, it might be better to select non-, or poor ABCG2 substrates. A similar consideration would apply to drugs that should or should preferably not enter the brain. On the other hand, when drugs that are potentially dangerous to suckling infants are used for treatment of lactating mothers, it would be wise to select drugs that are not ABCG2 substrates, in order to reduce the amount of drug that is secreted into the milk. Of course, whether ABCG2 functions as efficiently at these sites in humans as in mice will first have to be investigated in more detail, before extrapolating directly from the mouse to humans. Nevertheless, we consider that *Abcg2*$^{-/-}$ and combination knockout mice are valuable tools to determine the *in vivo* effects of ABCG2 for many drugs that are currently used in the clinic, as well as for the characterization of newly discovered drugs.

As for the physiological functions of ABCG2, even though we have learnt many new aspects of both physiological ABCG2 substrates and new expression sites and functions, it seems that a straightforward picture is still lacking. Although we are convinced that one main physiological function of ABCG2 is protection from noxious dietary xenobiotics, there are many indications that there must be various additional physiological functions. Given the multispecificity of ABCG2, it may simply be that the body has applied this protein for a multitude of different functions, without an essential underlying common theme, except for the transport function. However, it would not surprise us if we are still lacking many pieces of the ABCG2 puzzle, which may one day come together to yield a comprehensive picture of the functions of this intriguing protein. We are convinced that *Abcg2*$^{-/-}$ mice will provide very useful tools in this process.

ACKNOWLEDGMENTS

We thank Evita van de Steeg and Robert van Waterschoot for critical reading of the manuscript. This work was supported by grant NKI 2003-2940 from the Dutch Cancer Society.

REFERENCES

(1) Hardwick LJ, Velamakanni S, van Veen HW. The emerging pharmacotherapeutic significance of the breast cancer resistance protein (ABCG2). Br J Pharmacol 2007;151:163-74.

(2) van Herwaarden AE, Schinkel AH. The function of breast cancer resistance protein in epithelial barriers, stem cells and milk secretion of drugs and xenotoxins. Trends Pharmacol Sci 2006;27:10-6.

(3) Polgar O, Robey RW, Bates SE. ABCG2: structure, function and role in drug response. Expert Opin Drug Metab Toxicol 2008;4:1-15.

(4) Sarkadi B, Ozvegy-Laczka C, Nemet K, Varadi A. ABCG2 -- a transporter for all seasons. FEBS Lett 2004;567:116-20.

(5) Sarkadi B, Homolya L, Szakacs G, Varadi A. Human multidrug resistance ABCB and ABCG transporters: participation in a chemoimmunity defense system. Physiol Rev 2006;86:1179-236.

(6) Mao Q. BCRP/ABCG2 in the Placenta: Expression, Function and Regulation. Pharm Res 2008; 25:1244-55.

(7) Enokizono J, Kusuhara H, Ose A, Schinkel AH, Sugiyama Y. Quantitative investigation of the role of breast cancer resistance protein (Bcrp/Abcg2) in limiting brain and testis penetration of xenobiotic compounds. Drug Metab Dispos 2008;36:995-1002.

(8) Jonker JW, Merino G, Musters S, van Herwaarden AE, Bolscher E, Wagenaar E et al. The breast cancer resistance protein BCRP (ABCG2) concentrates drugs and carcinogenic xenotoxins into milk. Nat Med 2005;11:127-9.

(9) Jonker JW, Buitelaar M, Wagenaar E, Van Der Valk MA, Scheffer GL, Scheper RJ et al. The breast cancer resistance protein protects against a major chlorophyll-derived dietary phototoxin and protoporphyria. Proc Natl Acad Sci U S A 2002;99:15649-54.

(10) Zhou S, Morris JJ, Barnes Y, Lan L, Schuetz JD, Sorrentino BP. Bcrp1 gene expression is required for normal numbers of side population stem cells in mice, and confers relative protection to mitoxantrone in hematopoietic cells in vivo. Proc Natl Acad Sci U S A 2002;99:12339-44.

(11) Schinkel AH, Smit JJ, van Tellingen O, Beijnen JH, Wagenaar E, van Deemter L et al. Disruption of the mouse mdr1a P-glycoprotein gene leads to a deficiency in the blood-brain barrier and to increased sensitivity to drugs. Cell 1994;77:491-502.

(12) Schinkel AH, Wagenaar E, Mol CA, van Deemter L. P-glycoprotein in the blood-brain barrier of mice influences the brain penetration and pharmacological activity of many drugs. J Clin Invest 1996;97:2517-24.

(13) Cooray HC, Blackmore CG, Maskell L, Barrand MA. Localisation of breast cancer resistance protein in microvessel endothelium of human brain. Neuroreport 2002;13:2059-63.

(14) Eisenblatter T, Huwel S, Galla HJ. Characterisation of the brain multidrug resistance protein (BMDP/ABCG2/BCRP) expressed at the blood-brain barrier. Brain Res 2003;971:221-31.

(15) Doyle LA, Ross DD. Multidrug resistance mediated by the breast cancer resistance protein BCRP (ABCG2). Oncogene 2003;22:7340-58.

(16) Lee YJ, Kusuhara H, Jonker JW, Schinkel AH, Sugiyama Y. Investigation of efflux transport of dehydroepiandrosterone sulfate and mitoxantrone at the mouse blood-brain barrier: a minor role of breast cancer resistance protein. J Pharmacol Exp Ther 2005;312:44-52.

(17) Yousif S, Marie-Claire C, Roux F, Scherrmann JM, Decleves X. Expression of drug transporters at the blood-brain barrier using an optimized isolated rat brain microvessel strategy. Brain Res 2007;1134:1-11.

(18) Cisternino S, Mercier C, Bourasset F, Roux F, Scherrmann JM. Expression, up-regulation, and transport activity of the multidrug-resistance protein Abcg2 at the mouse blood-brain barrier. Cancer Res 2004;64:3296-301.

(19) Soontornmalai A, Vlaming ML, Fritschy JM. Differential, strain-specific cellular and subcellular distribution of multidrug transporters in murine choroid plexus and blood-brain barrier. Neuroscience 2006;138:159-69.

(20) Breedveld P, Pluim D, Cipriani G, Wielinga P, van Tellingen O, Schinkel AH et al. The effect of Bcrp1 (Abcg2) on the in vivo pharmacokinetics and brain penetration of imatinib mesylate (Gleevec): implications for the use of breast cancer resistance protein and P-glycoprotein inhibitors to enable the brain penetration of imatinib in patients. Cancer Res 2005;65:2577-82.

(21) Ozvegy-Laczka C, Cserepes J, Elkind NB, Sarkadi B. Tyrosine kinase inhibitor resistance in cancer: role of ABC multidrug transporters. Drug Resist Updat 2005;8:15-26.

(22) Dai H, Marbach P, Lemaire M, Hayes M, Elmquist WF. Distribution of STI-571 to the brain is limited by P-glycoprotein-mediated efflux. J Pharmacol Exp Ther 2003;304:1085-92.

(23) Bihorel S, Camenisch G, Lemaire M, Scherrmann JM. Influence of breast cancer resistance protein (Abcg2) and p-glycoprotein (Abcb1a) on the transport of imatinib mesylate (Gleevec) across the mouse blood-brain barrier. J Neurochem 2007;102:1749-57.

(24) Enokizono J, Kusuhara H, Sugiyama Y. Effect of breast cancer resistance protein (Bcrp/Abcg2) on the disposition of phytoestrogens. Mol Pharmacol 2007;72:967-75.

(25) Jonker JW, Freeman J, Bolscher E, Musters S, Alvi AJ, Titley I et al. Contribution of the ABC transporters Bcrp1 and Mdr1a/1b to the side population phenotype in mammary gland and bone marrow of mice. Stem Cells 2005;23:1059-65.

(26) de Vries NA, Zhao J, Kroon E, Buckle T, Beijnen JH, van Tellingen O. P-glycoprotein and breast cancer resistance protein: two dominant transporters working together in limiting the brain penetration of topotecan. Clin Cancer Res 2007;13:6440-9.

(27) Jonker JW, Smit JW, Brinkhuis RF, Maliepaard M, Beijnen JH, Schellens JH et al. Role of breast cancer resistance protein in the bioavailability and fetal penetration of topotecan. J Natl Cancer Inst 2000;92:1651-6.

(28) Oostendorp RL, Buckle T, Beijnen JH, van Tellingen O, Schellens JH. The effect of P-gp (Mdr1a/1b), BCRP (Bcrp1) and P-gp/BCRP inhibitors on the in vivo absorption, distribution, metabolism and excretion of imatinib. Invest New Drugs 2009; 27: 31-40.

(29) Takenaka K, Morgan JA, Scheffer GL, Adachi M, Stewart CF, Sun D et al. Substrate overlap between Mrp4 and Abcg2/Bcrp affects purine analogue drug cytotoxicity and tissue distribution. Cancer Res 2007;67:6965-72.

(30) Kalabis GM, Petropoulos S, Gibb W, Matthews SG. Breast cancer resistance protein (Bcrp1/Abcg2) in mouse placenta and yolk sac: ontogeny and its regulation by progesterone. Placenta 2007;28:1073-81.

(31) Zhang Y, Wang H, Unadkat JD, Mao Q. Breast cancer resistance protein 1 limits fetal distribution of nitrofurantoin in the pregnant mouse. Drug Metab Dispos 2007;35:2154-8.

(32) Zhou L, Naraharisetti SB, Wang H, Unadkat JD, Hebert MF, Mao Q. The breast cancer resistance protein (Bcrp1/Abcg2) limits fetal distribution of glyburide in the pregnant mouse: an Obstetric-Fetal Pharmacology Research Unit Network and University of Washington Specialized Center of Research Study. Mol Pharmacol 2008;73:949-59.

(33) Gedeon C, Anger G, Piquette-Miller M, Koren G. Breast cancer resistance protein: mediating the trans-placental transfer of glyburide across the human placenta. Placenta 2008;29:39-43.

(34) Pollex E, Lubetsky A, Koren G. The Role of Placental Breast Cancer Resistance Protein in the Efflux of Glyburide across the Human Placenta. Placenta 2008; 29:734-7.

(35) Aleksunes LM, Cui Y, Klaassen CD. Prominent Expression of Xenobiotic Efflux Transporters in Mouse Extraembryonic Fetal Membranes Compared to Placenta. Drug Metab Dispos 2008; 36:960-70.

(36) Yeboah D, Kalabis GM, Sun M, Ou RC, Matthews SG, Gibb W. Expression and localisation of breast cancer resistance protein (BCRP) in human fetal membranes and decidua and the influence of labour at term. Reprod Fertil Dev 2008;20:328-34.

(37) Holash JA, Harik SI, Perry G, Stewart PA. Barrier properties of testis microvessels. Proc Natl Acad Sci U S A 1993;90:11069-73.

(38) Dym M, Fawcett DW. The blood-testis barrier in the rat and the physiological compartmentation of the seminiferous epithelium. Biol Reprod 1970;3:308-26.

(39) Bart J, Hollema H, Groen HJ, de Vries EG, Hendrikse NH, Sleijfer DT et al. The distribution of drug-efflux pumps, P-gp, BCRP, MRP1 and MRP2, in the normal blood-testis barrier and in primary testicular tumours. Eur J Cancer 2004;40:2064-70.

(40) Wijnholds J, Scheffer GL, van der Valk M, van der Valk P, Beijnen JH, Scheper RJ et al. Multidrug resistance protein 1 protects the oropharyngeal mucosal layer and the testicular tubules against drug-induced damage. J Exp Med 1998;188:797-808.

(41) Cooke HJ, Saunders PT. Mouse models of male infertility. Nat Rev Genet 2002;3:790-801.

(42) Jones RC. To store or mature spermatozoa? The primary role of the epididymis. Int J Androl 1999;22:57-67.

(43) Sesink AL, Arts IC, de Boer VC, Breedveld P, Schellens JH, Hollman PC et al. Breast cancer resistance protein (Bcrp1/Abcg2) limits net intestinal uptake of quercetin in rats by facilitating apical efflux of glucuronides. Mol Pharmacol 2005;67:1999-2006.

(44) Breedveld P, Pluim D, Cipriani G, Dahlhaus F, van Eijndhoven MA, de Wolf CJ et al. The effect of low pH on breast cancer resistance protein (ABCG2)-mediated transport of methotrexate, 7-hydroxymethotrexate, methotrexate diglutamate, folic acid, mitoxantrone, topotecan, and resveratrol in in vitro drug transport models. Mol Pharmacol 2007;71:240-9.

(45) Kyselova V, Peknicova J, Boubelik M, Buckiova D. Body and organ weight, sperm acrosomal status and reproduction after genistein and diethylstilbestrol treatment of CD1 mice in a multigenerational study. Theriogenology 2004;61:1307-25.

(46) Adeoya-Osiguwa SA, Markoulaki S, Pocock V, Milligan SR, Fraser LR. 17beta-Estradiol and environmental estrogens significantly affect mammalian sperm function. Hum Reprod 2003;18:100-7.

(47) Pulido MM, Molina AJ, Merino G, Mendoza G, Prieto JG, Alvarez AI. Interaction of enrofloxacin with breast cancer resistance protein (BCRP/ABCG2): influence of flavonoids and role in milk secretion in sheep. J Vet Pharmacol Ther 2006;29:279-87.

(48) van Herwaarden AE, Wagenaar E, Merino G, Jonker JW, Rosing H, Beijnen JH et al. Multidrug transporter ABCG2/breast cancer resistance protein secretes riboflavin (vitamin B2) into milk. Mol Cell Biol 2007;27:1247-53.

(49) Powers HJ. Riboflavin (vitamin B-2) and health. Am J Clin Nutr 2003;77:1352-60.

(50) Foraker AB, Khantwal CM, Swaan PW. Current perspectives on the cellular uptake and trafficking of riboflavin. Adv Drug Deliv Rev 2003;55:1467-83.

(51) Said HM. Biotin: the forgotten vitamin. Am J Clin Nutr 2002;75:179-80.

(52) Zhou S, Zong Y, Ney PA, Nair G, Stewart CF, Sorrentino BP. Increased expression of the Abcg2 transporter during erythroid maturation plays a role in decreasing cellular protoporphyrin IX levels. Blood 2005;105:2571-6.

(53) Jonker JW, Musters S, Vlaming ML, Plosch T, Gooijert KE, Hillebrand MJ et al. Breast cancer resistance protein (Bcrp1/Abcg2) is expressed in the harderian gland and mediates transport of conjugated protoporphyrin IX. Am J Physiol Cell Physiol 2007;292:C2204-C2212.

(54) Krishnamurthy P, Ross DD, Nakanishi T, Bailey-Dell K, Zhou S, Mercer KE et al. The stem cell marker Bcrp/ABCG2 enhances hypoxic cell survival through interactions with heme. J Biol Chem 2004;279:24218-25.

(55) Assaraf YG. The role of multidrug resistance efflux transporters in antifolate resistance and folate homeostasis. Drug Resist Updat 2006;9:227-46.

(56) Shukla S, Wu CP, Nandigama K, Ambudkar SV. The naphthoquinones, vitamin K3 and its structural analogue plumbagin, are substrates of the multidrug resistance linked ATP binding cassette drug transporter ABCG2. Mol Cancer Ther 2007;6:3279-86.

(57) Shearer MJ. Vitamin K. Lancet 1995;345:229-34.

(58) Merino G, van Herwaarden AE, Wagenaar E, Jonker JW, Schinkel AH. Sex-dependent expression and activity of the ATP-binding cassette transporter breast cancer resistance protein (BCRP/ABCG2) in liver. Mol Pharmacol 2005;67:1765-71.

(59) Merino G, Jonker JW, Wagenaar E, van Herwaarden AE, Schinkel AH. The breast cancer resistance protein (BCRP/ABCG2) affects pharmacokinetics, hepatobiliary excretion, and milk secretion of the antibiotic nitrofurantoin. Mol Pharmacol 2005;67:1758-64.

(60) Urquhart BL, Tirona RG, Kim RB. Nuclear receptors and the regulation of drug-metabolizing enzymes and drug transporters: implications for interindividual variability in response to drugs. J Clin Pharmacol 2007;47:566-78.

(61) Verhasselt V, Milcent V, Cazareth J, Kanda A, Fleury S, Dombrowicz D et al. Breast milk-mediated transfer of an antigen induces tolerance and protection from allergic asthma. Nat Med 2008;14:170-5.

(62) Greenberger PA. 8. Drug allergy. J Allergy Clin Immunol 2006;117:S464-S470.

(63) Schwartz A. Pathology of allergic diseases. Acta Univ Carol Med Monogr 1989;129:1-197.

(64) Bohan KH, Mansuri TF, Wilson NM. Anticonvulsant hypersensitivity syndrome: implications for pharmaceutical care. Pharmacotherapy 2007;27:1425-39.

(65) Payne AP. The harderian gland: a tercentennial review. J Anat 1994;185 (Pt 1):1-49.

(66) Krishnamurthy P, Xie T, Schuetz JD. The role of transporters in cellular heme and porphyrin homeostasis. Pharmacol Ther 2007;114:345-58.

(67) Asashima T, Hori S, Ohtsuki S, Tachikawa M, Watanabe M, Mukai C et al. ATP-binding cassette transporter G2 mediates the efflux of phototoxins on the luminal membrane of retinal capillary endothelial cells. Pharm Res 2006;23:1235-42.

(68) Boulton M, Rozanowska M, Rozanowski B. Retinal photodamage. J Photochem Photobiol B 2001;64:144-61.

(69) Maliepaard M, Scheffer GL, Faneyte IF, van Gastelen MA, Pijnenborg AC, Schinkel AH et al. Subcellular localization and distribution of the breast cancer resistance protein transporter in normal human tissues. Cancer Res 2001;61:3458-64.

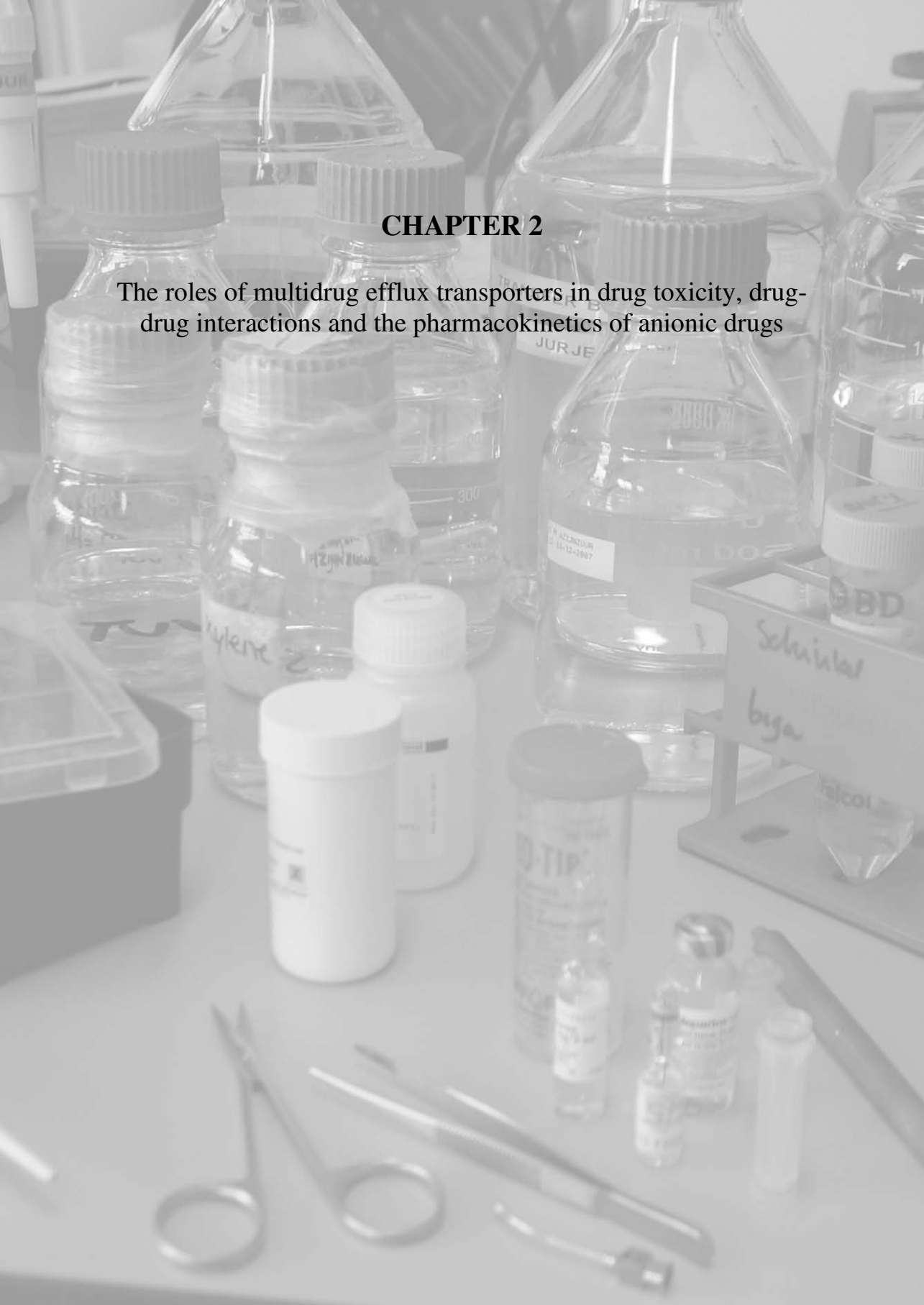

CHAPTER 2

The roles of multidrug efflux transporters in drug toxicity, drug-drug interactions and the pharmacokinetics of anionic drugs

CHAPTER 2.1

P-glycoprotein limits oral availability, brain penetration and toxicity of an anionic drug, the antibiotic salinomycin

Jurjen S. Lagas, Rolf W. Sparidans, Robert A.B. van Waterschoot, Els Wagenaar, Jos H. Beijnen and Alfred H. Schinkel

Antimicrobial Agents and Chemotherapy 2008; 52:1034-1039

ABSTRACT

Salinomycin is a polyether organic anion that is extensively used as a coccidiostatic antibiotic in poultry and commonly fed to ruminant animals to improve feed efficiency. However, salinomycin also causes severe toxicity when accidentally fed to animals in high doses. In addition, humans are highly sensitive to salinomycin and severe toxicity has been reported. Multidrug efflux transporters like P-glycoprotein, BCRP and MRP2 are highly expressed in the intestine and can restrict oral uptake and tissue penetration of xenobiotics. The purpose of this study was to investigate whether the anionic drug salinomycin is a substrate for one or more of these efflux pumps. Salinomycin was actively transported by human MDR1 P-gp expressed in polarized MDCK-II monolayers, but not by the known organic anion transporting human MRP2 and murine Bcrp1. Using P-gp-deficient mice we found a marked increase in salinomycin plasma concentrations after oral administration and a decreased plasma clearance after i.v. administration. Furthermore, absence of P-gp resulted in a significantly increased brain penetration. P-gp-deficient mice also displayed clearly increased susceptibility to salinomycin toxicity. Thus far, P-gp was thought to mainly affect hydrophobic, positively charged or neutral drugs *in vivo*. Our data show that P-gp can also be a major determinant of the pharmacokinetic behavior and toxicity of an organic anionic drug. Variation in P-gp activity might thus directly affect the effective exposure to salinomycin and possibly to other anionic drugs and toxin substrates. Individuals with reduced or absent P-gp activity could therefore be more susceptible to salinomycin toxicity.

INTRODUCTION

ATP binding cassette (ABC) multidrug transporters, like P-glycoprotein (P-gp, *ABCB1*), BCRP (*ABCG2*) and MRP2 (*ABCC2*), form important defense mechanisms against exogenous toxins and other potentially harmful compounds that can be encountered in daily life. Because of their strategic localization at apical membranes of important epithelial barriers and at the canalicular membrane of hepatocytes, they can mediate active excretion of transported substrates via liver, intestine and kidneys. Furthermore, efflux transporters can restrict small intestinal uptake of substrates after oral ingestion and overexpression of drug efflux transporters in tumor cells can confer resistance to cancer chemotherapy (1). The presence of these efflux transporters in blood-brain, blood-testis and maternofetal barriers also restricts penetration of substrates in brain, testis and fetus (pharmacological sanctuary sites). As many drugs and their metabolites are excellent substrates of these transporters, they can have a dramatic impact on the

oral availability, tissue distribution, elimination and excretion, and toxicity risks of drugs, with potentially profound positive or negative consequences for the clinical application of these drugs.

Salinomycin (Fig. 1) is a polyether antibiotic belonging to the group of ionophores. This natural toxin is produced by a *Streptomyces albus* strain (2). Salinomycin is extensively used as a coccidiostat in poultry and other livestock and is commonly fed to ruminant animals to improve feed efficiency (3;4). However, salinomycin can also cause severe toxicity when accidentally fed to animals in relatively high doses, as described for chickens (5-7), turkeys (8-10), cats (11), pigs (12-14), alpacas (15) and horses (16;17). Severe human poisoning with salinomycin has also been reported (18). Accidental ingestion of an estimated 1 mg/kg of salinomycin resulted in a 6-week hospital admission with prolonged rhabdomyolysis, pain and disability. In addition, human poisoning with fatal rhabdomyolysis has been reported for the polyether ionophore antibiotic monensin, illustrating that humans are highly vulnerable to the toxicity of these types of compounds (19;20).

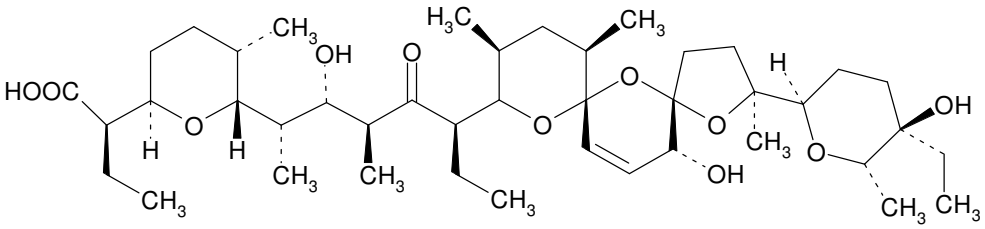

Fig. 1. Structural formula of salinomycin. MW = 751.02. The predicted *pKa* value of 4.4 was calculated by MarvinSketch software and by ACD/pKa 8.03 software.

Our interest in salinomycin was sparked by the widespread poisoning of cats with salinomycin that occurred in 1996 in the Netherlands and in Switzerland (11). Two brands of cat food from one manufacturer were contaminated with salinomycin, which resulted in an outbreak of acute polyneuropathy. In the Netherlands, an estimated 100.000 cats were exposed to the contaminated food and the reported number of cases of acute paralysis, many with fatal outcome, was 823. The incidence among exposed cats was thus about 1%. We wondered if salinomycin could be a substrate of one or more of the apical efflux transporters, as these can restrict oral uptake and reduce bioavailability of harmful substrate compounds, thus protecting the body. This was shown for the anti-cancer agents paclitaxel in *Mdr1a/1b*$^{-/-}$ mice and topotecan in *Bcrp1*$^{-/-}$ mice and for the carcinogen PhIP in MRP2 deficient rats (21-23).

Salinomycin is an organic anionic drug, with a pKa around 4.4 (Fig. 1), implying that at physiological pH >99% of the drug is present in its anionic form. With a molecular mass of 751 Da it is also relatively large. We therefore expected that salinomycin might be a substrate for MRP2 and/or Bcrp1, which are known to transport a broad spectrum of organic anions, in contrast to MDR1 P-gp, which primarily transports hydrophobic neutral or positively charged compounds (1). Nevertheless, we started out by testing whether salinomycin was transported by any of these three apical efflux transporters.

MATERIALS AND METHODS

Animals. Mice were housed and handled according to institutional guidelines complying with Dutch legislation. Animals used in this study were male wild-type (WT) and *Mdr1a/1b*$^{-/-}$ mice of a >99% FVB genetic background, between 9 and 15 weeks of age. Animals were kept in a temperature-controlled environment with a 12-hour light / 12-hour dark circle and received a standard diet (AM-II, Hope Farms, Woerden, The Netherlands) and acidified water *ad libitum*.

Chemicals. Salinomycin SV sodium salt pentahemihydrate was obtained from Sigma-Aldrich (Steinheim, Germany), heparin (5000 IE/ml) was from Leo Pharma BV (Breda, The Netherlands), methoxyflurane (Metofane) originated from Medical Developments Australia Pty. Ltd. (Springvale, Victoria, Australia) and bovine serum albumin (BSA), fraction V, was from Roche (Mannheim, Germany). The organic solvents methanol, acetonitril (both HPLC grade) and diethyl ether originated from Merck (Darmstadt, Germany). GlaxoSmithKline (Uxbridge, UK) kindly provided Elacridar (GF120918).

Transport assays. Polarized canine kidney MDCK-II cell lines were used in transport assays. Human MDR1-, MRP2- and murine Bcrp1-transduced MDCK-II subclones and their growth conditions were described previously (24;25). Transepithelial transport assays using Transwell plates were carried out as described previously with minor modifications (26). Experiments with MDCK-II-MRP2 cells were performed in the presence of 5 µM of Elacridar, to inhibit any endogenous P-glycoprotein activity. Elacridar does not affect MRP2 activity. Experiments were started (t = 0) by replacing the medium in the apical or basolateral compartment with fresh OptiMEM medium, either with or without 5 µM Elacridar and containing 5 µM salinomycin. Cells were incubated at 37°C in 5% CO_2, and 50 µl aliquots were taken at t = 2 and 4 h and stored at –20°C until LC-MS/MS analysis. The transport was calculated as the fraction salinomycin found in the acceptor compartment relative to the total amount added to the donor compartment at the beginning of the experiment. Membrane tightness was assessed in parallel, using the same cells seeded on the same day and at the same density, by

analyzing transepithelial [^{14}C]Inulin (approx. 3 kBq /well) leakage. Leakage had to remain <1% of the total added radioactivity per hour.

Plasma pharmacokinetic experiments and tissue distribution. For oral studies, salinomycin was formulated in absolute ethanol (10 mg/ml), diluted 10- or 100-fold with 0.9% NaCl (saline) to 1 and 0.1 mg/ml, respectively, and dosed at 1 or 10 mg/kg body weight (10 ml/kg). To minimize variation in absorption, mice were fasted for 3 hours, before salinomycin was administered by gavage into the stomach, using a blunt-ended needle (n = 5). Multiple blood samples (~30 µl) were collected from the tail vein at 0.25, 0.5, 1, 2, 4, and 6 h, using heparinized capillary tubes (Oxford Labware, St. Louis, USA). Blood samples were centrifuged at 2100 x *g* for 5 min at 4°C, the plasma fraction was collected and stored at -20°C until LC-MS/MS analysis. For intravenous studies, salinomycin formulated in absolute ethanol (10 mg/ml) was diluted 50-fold with saline to 0.2 mg/ml and injected as single bolus of 1 mg/kg body weight (5 ml/kg) into a tail vein (n = 5). Multiple blood samples (~30 µl) were collected from the tail vein at 0.125, 0.25, 0.5, 1, 2, 4, and 6 h, using heparinized capillary tubes. Blood samples were centrifuged at 2,100 x *g* for 5 min at 4°C, the plasma fraction was collected and stored at -20°C until LC-MS/MS analysis. For tissue distribution studies, salinomycin was injected i.v. as single bolus of 1 mg/kg body weight (5 ml/kg) into a tail vein (n = 4). After 180 min blood, liver, brain and small intestinal contents (SIC) were isolated, plasma was collected, and the samples were stored at -20°C until LC-MS/MS analysis.

LC-MS/MS analysis. For the quantitative analysis of salinomycin in OptiMEM-, plasma- and tissue samples fast and sensitive LC-MS/MS methods were developed and validated using simple sample pre-treatment procedures for all different matrices (27).

Pharmacokinetic calculations and statistical analysis. Pharmacokinetic parameters were calculated by noncompartmental methods using the software package WinNonlin Professional version 5.0. The area under the plasma concentration time curves (AUCs) were calculated using the trapezoidal rule. For oral experiments at a dose of 10 mg/kg, the AUC could not be reliably extrapolated to infinity as clearance up to 6 hours was very slow, so only the $AUC_{0\text{-}6}$ was calculated. For oral and i.v. experiments at a dose of 1 mg/kg, both the $AUC_{0\text{-}6}$ and the AUC extrapolated to infinity ($AUC_{(0\text{-}\infty)}$) were calculated. The peak plasma concentration (C_{max}) and the time of maximum plasma concentration (T_{max}) were estimated from the original data. Plasma clearance (CL) after i.v. administration was calculated by the formula $CL = Dose/AUC_{(0\text{-}\infty)}$. The Wilcoxon rank sum test was used for statistical analysis. Differences were considered statistically significant when $P < 0.05$. Data are presented as means ± SD.

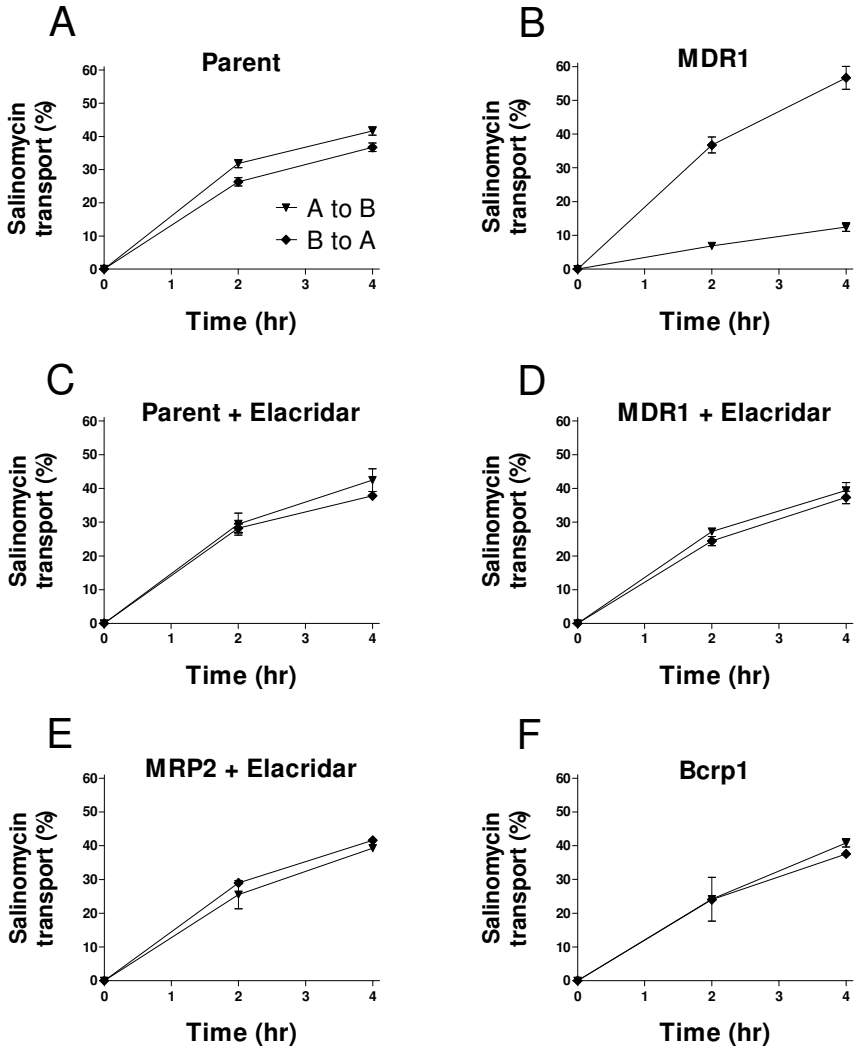

Fig. 2. Transepithelial transport of salinomycin (5 μM) in MDCK-II cells either non-transduced (*A & C*) or transduced with human *MDR1* (*B & D*), human *MRP2* (*E*) or murine *Bcrp1* (*F*) cDNAs, in the absence (*A, B & F*) or presence (*C, D & E*) of Elacridar (5 μM). At t = 0 h, salinomycin was applied in one compartment (apical or basolateral), and the percentage of salinomycin transported to the opposite compartment at t = 2 and t = 4 h was measured by LC-MS/MS and plotted (n = 3). Translocation from the basolateral to the apical compartment (♦); translocation from the apical to the basolateral compartment (▼). Data represent means ± SD.

RESULTS

In vitro transport of salinomycin. To determine whether the organic anion salinomycin was transported by one or more of the apical ATP Binding Cassette (ABC) multidrug transporters *in vitro*, we used the polarized canine kidney cell line MDCK-II and its subclones transduced with human MDR1 and MRP2, and murine Bcrp1. The parental and transduced cell lines were grown to confluent polarized monolayers on porous membrane filters, and vectorial transport of 5 μM salinomycin across the monolayers was determined. In the MDCK-II parental cell line, the translocation of salinomycin in the basolateral direction was slightly higher than in the apical direction (Fig. 2A). In MDR1-transduced MDCK-II cells, apically directed translocation was significantly increased and basolaterally directed translocation was markedly decreased (Fig. 2B). In the presence of 5 μM of the P-glycoprotein inhibitor Elacridar, this transport was completely inhibited, resulting in a translocation pattern similar to that of the MDCK-II parent cell line (Fig. 2C and D). In the murine Bcrp1- and the human MRP2-transduced MDCK-II cell lines, vectorial translocation of salinomycin was not different compared to parental MDCK-II cells (Fig. 2E and F). These results demonstrate efficient transport of salinomycin by human MDR1, but not by murine Bcrp1 and human MRP2.

Plasma pharmacokinetics of salinomycin in WT and Mdr1a/1b$^{-/-}$ mice. To test whether the *in vitro* observed MDR1 P-gp-mediated transport of salinomycin is also relevant *in vivo*, we studied salinomycin plasma pharmacokinetics in WT and *Mdr1a/1b*$^{-/-}$ mice. For oral administration, we performed an experiment at 10 mg/kg body weight (~ 20% of the published oral LD_{50} in mice). Fifteen to thirty min after administration, 4 out of 5 *Mdr1a/1b*$^{-/-}$ mice displayed symptoms of salinomycin poisoning, whereas these signs were absent in WT mice. The affected *Mdr1a/1b*$^{-/-}$ mice had paralyzed fore- and hindlimbs and their respiratory frequency was decreased. Therefore, we had to terminate this experiment for the *Mdr1a/1b*$^{-/-}$ mice. For WT mice the AUC from 0-6 hours was 2130 ± 178.0 hr.μg/L, with a C_{max} of 517.4 ± 152.4 μg/L at approximately 0.5 hr (Table 1). We repeated the oral study with 1 mg/kg salinomycin (Fig. 3). No signs of toxicity were observed at this dose. The $AUC_{0-\infty}$ for *Mdr1a/1b*$^{-/-}$ mice was 3.1-fold increased compared to WT mice (250.8 ± 27.3 versus 80.2 ± 12.3 hr.μg/L; $P < 0.01$, Table 1 and Fig. 3) and the C_{max} for both WT and *Mdr1a/1b*$^{-/-}$ mice was reached approximately 2 hr after administration. Comparison of the AUC_{0-6} for WT mice at 1 mg/kg or 10 mg/kg shows that a 10-fold increase in dose resulted in a 34-fold higher AUC (Table 1). This, together with the shift in the estimated T_{max}, suggests that plasma pharmacokinetics of salinomycin is non-linear in mice, which might be the result

of saturation of absorption-limiting, drug-metabolizing and/or drug-excreting systems at high salinomycin concentrations.

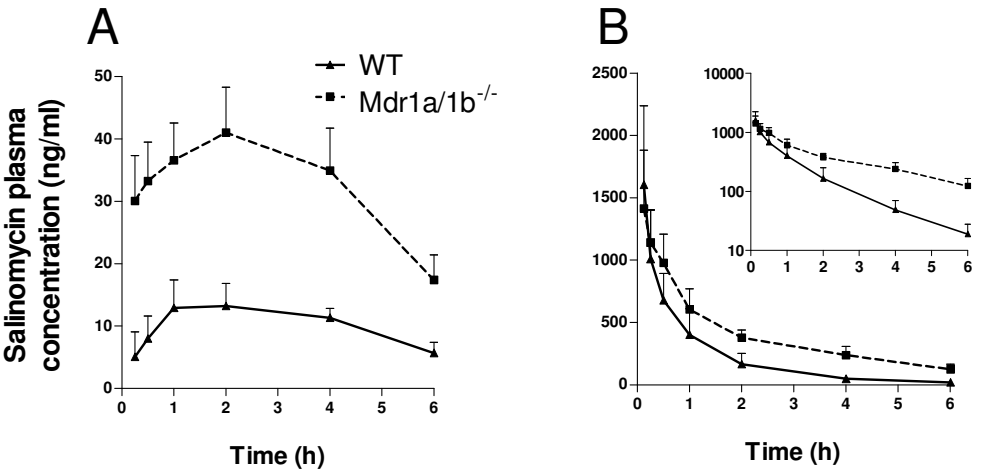

Fig. 3. Plasma concentration-time curves of salinomycin in male FVB wild-type (▲) and *Mdr1a/1b*$^{-/-}$ (■) mice, after oral (*A*) and i.v. (*B*) administration of salinomycin at a dose of 1 mg/kg. Data represent mean concentrations ± SD, n = 5 for oral and i.v. administration. Insert in B shows semilog plot of the data.

After i.v. administration of 1 mg/kg salinomycin there were no signs of toxicity, despite the high initial plasma concentrations. *Mdr1a/1b*$^{-/-}$ mice had a 2.0-fold higher $AUC_{0-\infty}$ compared to WT mice (2813 ± 318.1 versus 1374 ± 253.2 hr.µg/L; $P < 0.05$, Table 1 and Fig. 3). In addition, the plasma clearance for *Mdr1a/1b*$^{-/-}$ mice was 2.2-fold lower than for WT mice (0.37 ± 0.10 versus 0.82 ± 0.29 l/hr.kg; $P < 0.05$, Table 1). For *Mdr1a/1b*$^{-/-}$ mice receiving 1 mg/kg salinomycin, the oral $AUC_{0-\infty}$ was increased more than the i.v. $AUC_{0-\infty}$, i.e. 3.1-fold versus 2.0-fold. Taken together, these data suggest that in *Mdr1a/1b*$^{-/-}$ mice a decreased CL combined with an increased oral availability results in an overall higher exposure. P-gp thus seems not only an important determinant for the oral availability of salinomycin in mice, but also for its elimination.

Table 1. Plasma pharmacokinetic parameters after salinomycin administration at 1 mg/kg (oral and i.v.) and 10 mg/kg (oral).

	Strain		
	WT	***Mdr1a/1b*$^{-/-}$**	**Ratio KO / WT**
Oral (10 mg/kg)			
$AUC_{(0-6)}$, hr.µg/L	2130 ± 178.0	N.D.	-
C_{max}, µg /L	517.4 ± 152.4	N.D.	-
T_{max}, hr	0.5	N.D.	-
Oral (1 mg/kg)			
$AUC_{(0-6)}$, hr.µg/L	62.1 ± 7.5	196.1 ± 18.8**	3.2
$AUC_{(0-\infty)}$, hr.µg/L	80.2 ± 12.3	250.8 ± 27.3**	3.1
C_{max}, µg /L	13.2 ± 3.6	41.0 ± 7.3**	3.1
T_{max}, hr	2	2	1
i.v. (1 mg/kg)			
$AUC_{(0-6)}$, hr.µg/L	1310 ± 246.6	2374 ± 242.5*	1.8
$AUC_{(0-\infty)}$, hr.µg/L	1374 ± 253.2	2813 ± 318.1*	2.0
CL, l/hr.kg	0.82 ± 0.29	0.37 ± 0.10*	0.5

AUC, area under plasma concentration-time curve; C_{max}, maximum plasma concentration; T_{max}, time of maximum plasma concentration; CL, plasma clearance. N.D., not determined in view of toxicity. Data are means ± SD, n = 5 for both oral and i.v. administration. KO: knockout. * $P < 0.05$ and ** $P < 0.01$, compared to WT mice.

Brain penetration, liver accumulation and intestinal excretion of salinomycin. To investigate whether P-gp deficiency affects tissue distribution and disposition of salinomycin, we determined salinomycin concentrations in brain, liver and small intestinal contents at 180 min after i.v. administration of 1 mg/kg. The concentration of salinomycin in brain of *Mdr1a/1b*$^{-/-}$ mice was about 6-fold increased, whereas the plasma level in *Mdr1a/1b*$^{-/-}$ mice at this time point was 3.7-fold higher than in WT mice (Table 2). To correct for the higher plasma concentration in *Mdr1a/1b*$^{-/-}$ mice, we calculated the brain/plasma ratios. In *Mdr1a/1b*$^{-/-}$ mice this ratio was significantly greater than in WT mice (0.20 ± 0.03 versus 0.13 ± 0.01; $P < 0.05$, Table 2), suggesting that P-gp limits the brain penetration of salinomycin, albeit to a modest extent.

In livers and small intestinal contents, no differences in concentrations between WT and *Mdr1a/1b*$^{-/-}$ mice were found at 180 min after administration (Table 2), in spite of the clear differences in plasma concentration. Salinomycin concentration in the liver was 7.4 ± 1.0 µg/g in WT and 6.5 ± 1.1 µg/g in *Mdr1a/1b*$^{-/-}$ mice, representing 33.9 ± 4.2% and 29.5 ± 3.8% of the administered dose, respectively. These high amounts in the livers at 180 min suggest that initially high plasma concentrations of salinomycin upon i.v administration result in a substantial accumulation of salinomycin in the liver and that subsequent biliary excretion and/or sinusoidal clearance is relatively slow.

Table 2. Concentrations of salinomycin in plasma, brain, liver and small intestinal contents (S.I.C.) at t = 180 min after i.v. administration of 1 mg/kg.

	Strain		
Biological matrix	**WT**	***Mdr1a/1b*$^{-/-}$**	**Ratio KO / WT**
Plasma, ng/ml	72.5 ± 3.6	269.7 ± 13.9*	3.7
Brain, ng/g	9.2 ± 0.7	53.2 ± 10.1*	5.8
Ratio brain/plasma	0.13 ± 0.01	0.20 ± 0.03*	1.5
Liver, µg/g	7.4 ± 1.0	6.5 ± 1.1	0.9
S.I.C., µg/g	0.21 ± 0.06	0.29 ± 0.03	1.4

Plasma concentrations of salinomycin are expressed as ng/ml, brain concentrations as ng/g and liver and S.I.C. concentrations as µg/g (mean ± SD, n = 4). KO: knockout. * $P < 0.05$, compared to WT mice.

DISCUSSION

In this study we demonstrate that the organic anion salinomycin, belonging to the group of ionophore polyether antibiotics, is an efficiently transported substrate of human and murine P-gp, but not of MRP2 or Bcrp1, even though the latter two are known to transport many negatively charged compounds. From our studies with *Mdr1a/1b*$^{-/-}$ mice, it is clear that P-gp deficiency results in pronounced effects on the pharmacokinetics and toxicity of salinomycin in mice. *Mdr1a/1b*$^{-/-}$ mice displayed substantially increased oral bioavailability and toxicity of salinomycin, decreased plasma clearance and significantly increased salinomycin brain penetration.

Thus far, P-gp was thought to mainly affect hydrophobic, positively charged or neutral drugs *in vivo*. Although P-gp was shown to be a low affinity transporter for the negatively charged hydrophobic anti-cancer agent methotrexate *in vitro* (28), to date there are to the best of our knowledge no reports on P-gp affecting oral availability, plasma clearance, or toxicity of negatively charged compounds *in vivo*. Our data show that P-gp can be a major determinant of the pharmacokinetics and toxicity of an organic anionic drug. Variation in P-gp activity might thus directly affect the effective exposure to salinomycin and possibly other anionic drugs and toxin substrates, further expanding the already broad spectrum of compounds critically influenced by P-gp *in vivo*.

During preparation of this manuscript, Chen et al reported that the acidic (anionic) form of the statin drug lovastatin showed a significantly higher brain/plasma ratio in *Mdr1a/1b*$^{-/-}$ than WT mice (29). Although the neutral lactone form of lovastatin showed a markedly higher brain/plasma ratio, which was at least 8-fold increased in P-gp-deficient mice, this result may reflect reduced brain penetration of acidic lovastatin due to P-gp activity, in line with our observation for salinomycin brain penetration. Plasma clearance of lovastatin (lactone or acidic form) was not noticeably altered in this study. Oral availability and pharmacodynamic aspects were not assessed. Nonetheless, this study could illustrate the potential wider *in vivo* relevance of P-gp for anionic drugs.

Salinomycin and other anionic ionophore drugs, like monensin, narasin and lasalocid are extensively used as coccidiostats in poultry and other livestock and to improve feed efficiency in ruminant animals (3;4). However, ionophore antibiotics can also cause severe toxicity when accidentally fed to animals in relatively high doses. Acute toxicity studies in different animal species (mouse, rat, rabbit, chicken, dog, pig, bull, horse) revealed oral LD_{50} values ranging from 21-60 mg/kg body weight. Humans are also very sensitive to salinomycin and exposure via inhalation or ingestion can cause serious toxicity (18). Salinomycin is extensively used in animals and exposure of workers through handling animal feeds is a concern. Accordingly, an HPLC assay for the quantification of salinomycin in human plasma has been described (30).

Because P-gp can restrict oral uptake of salinomycin, reduced P-gp activity or complete P-gp deficiency may result in increased oral availability of salinomycin and thereby toxicity, as we observed in *Mdr1a/1b*$^{-/-}$ mice. Knowledge of anionic and other compounds that are affected by P-gp *in vivo* is useful for veterinary medicine, since there are domestic animals known to be deficient for P-gp. For example, some dog breeds (e.g., Collies) and their crosses were found to have a deletion mutation of the *Mdr1* gene, resulting in loss of protein activity and greatly increased sensitivity to neurotoxicity induced by the P-gp substrate ivermectin, a

drug used to treat worm infections (31). A spontaneous mutation in a subpopulation of outbred CF-1 mice also resulted in Mdr1a deficiency and ivermectin hypersensitivity (32). Interestingly, an isolated herd of Murray Grey cattle in Australia showed unusually high concentrations of the ivermectin analogue abamectin in their central nervous system, and corresponding toxicity (33). This strongly suggests a P-gp deficiency in some inbred populations of this species as well. It is therefore tempting to speculate that a possible low-frequency P-gp deficiency in domestic cats might explain the low-frequency hypersensitivity of cats exposed to salinomycin-contaminated food (11). Unfortunately, the currently available necropsy material of a limited number of cats that succumbed to salinomycin poisoning does not allow unambiguous assessment of their Mdr1-type P-gp status. If P-gp deficiency does indeed occur in a small subfraction of Dutch, Swiss and possibly other domestic cat populations, this might have implications for their treatment with veterinary drugs.

ACKNOWLEGMENTS

We thank Dr. J. van Nes for providing necropsy material of cats that succumbed to salinomycin poisoning (32). This work was supported in part by grant BFA.6165 of NWO/STW.

REFERENCES

(1) Borst P, Oude Elferink RP. Mammalian ABC transporters in health and disease. Annu Rev Biochem 2002;71:537-92.

(2) Miyazaki Y, Shibuya M, Sugawara H, Kawaguchi O, Hirsoe C. Salinomycin, a new polyether antibiotic. J Antibiot (Tokyo) 1974;27:814-21.

(3) Yvore P, Raynaud JP, Conan L, Naciri M. Evaluation of the efficacy of salinomycin in the control of coccidiosis in chicks. Poult Sci 1980;59:2412-6.

(4) Callaway TR, Edrington TS, Rychlik JL, Genovese KJ, Poole TL, Jung YS et al. Ionophores: their use as ruminant growth promotants and impact on food safety. Curr Issues Intest Microbiol 2003;4:43-51.

(5) Kamashi K, Reddy AG, Reddy KS, Reddy VR. Evaluation of zinc against salinomycin toxicity in broilers. Indian J Physiol Pharmacol 2004;48:89-95.

(6) Hoop RK. Salinomycin toxicity in layer breeders. Vet Rec 1998;142:550.

(7) Mezes M, Salyi G, Banhidi G, Szeberenyi S. Effect of acute salinomycin-tiamulin toxicity on the lipid peroxide and antioxidant status of broiler chicken. Acta Vet Hung 1992;40:251-7.

(8) Van Assen EJ. A case of salinomycin intoxication in turkeys. Can Vet J 2006;47:256-8.

(9) Andreasen JR, Jr., Schleifer JH. Salinomycin toxicosis in male breeder turkeys. Avian Dis 1995;39:638-42.

(10) Potter LM, Blake JP, Blair ME, Bliss BA, Denbow DM. Salinomycin toxicity in turkeys. Poult Sci 1986;65:1955-9.

(11) van der Linde-Sipman JS, van den Ingh TS, van nes JJ, Verhagen H, Kersten JG, Beynen AC et al. Salinomycin-induced polyneuropathy in cats: morphologic and epidemiologic data. Vet Pathol 1999;36:152-6.

(12) Plumlee KH, Johnson B, Galey FD. Acute salinomycin toxicosis of pigs. J Vet Diagn Invest 1995;7:419-20.

(13) Pott JM. Salinomycin toxicity in pigs. Vet Rec 1990;127:554.

(14) Kavanagh NT, Sparrow DS. Salinomycin toxicity in pigs. Vet Rec 1990;127:507.

(15) Kosal ME, Anderson DE. An unaddressed issue of agricultural terrorism: a case study on feed security. J Anim Sci 2004;82:3394-400.

(16) Nicpon J, Czerw P, Harps O, Deegen E. [Salinomycin poisoning in a Polish stud horse]. Tierarztl Prax Ausg G Grosstiere Nutztiere 1997;25:438-41.

(17) Rollinson J, Taylor FG, Chesney J. Salinomycin poisoning in horses. Vet Rec 1987;121:126-8.

(18) Story P, Doube A. A case of human poisoning by salinomycin, an agricultural antibiotic. N Z Med J 2004;117:U799.

(19) Kouyoumdjian JA, Morita MP, Sato AK, Pissolatti AF. Fatal rhabdomyolysis after acute sodium monensin (Rumensin) toxicity: case report. Arq Neuropsiquiatr 2001;59:596-8.

(20) Caldeira C, Neves WS, Cury PM, Serrano P, Baptista MA, Burdmann EA. Rhabdomyolysis, acute renal failure, and death after monensin ingestion. Am J Kidney Dis 2001;38:1108-12.

(21) Sparreboom A, van Asperen J, Mayer U, Schinkel AH, Smit JW, Meijer DK et al. Limited oral bioavailability and active epithelial excretion of paclitaxel (Taxol) caused by P-glycoprotein in the intestine. Proc Natl Acad Sci U S A 1997;94:2031-5.

(22) Dietrich CG, de Waart DR, Ottenhoff R, Schoots IG, Elferink RP. Increased bioavailability of the food-derived carcinogen 2-amino-1-methyl-6-phenylimidazo[4,5-b]pyridine in MRP2-deficient rats. Mol Pharmacol 2001;59:974-80.

(23) Jonker JW, Buitelaar M, Wagenaar E, Van Der Valk MA, Scheffer GL, Scheper RJ et al. The breast cancer resistance protein protects against a major chlorophyll-derived dietary phototoxin and protoporphyria. Proc Natl Acad Sci U S A 2002;99:15649-54.

(24) Evers R, Kool M, van Deemter L, Janssen H, Calafat J, Oomen LC et al. Drug export activity of the human canalicular multispecific organic anion transporter in polarized kidney MDCK cells expressing cMOAT (MRP2) cDNA. J Clin Invest 1998;101:1310-9.

(25) Jonker JW, Smit JW, Brinkhuis RF, Maliepaard M, Beijnen JH, Schellens JH et al. Role of breast cancer resistance protein in the bioavailability and fetal penetration of topotecan. J Natl Cancer Inst 2000;92:1651-6.

(26) Schinkel AH, Wagenaar E, van Deemter L, Mol CA, Borst P. Absence of the mdr1a P-Glycoprotein in mice affects tissue distribution and pharmacokinetics of dexamethasone, digoxin, and cyclosporin A. J Clin Invest 1995;96:1698-705.

(27) Sparidans RW, Lagas JS, Schinkel AH, Schellens JH, Beijnen JH. Liquid chromatography-tandem mass spectrometric assays for salinomycin in mouse plasma, liver, brain and small intestinal contents and in OptiMEM cell culture medium. J Chromatogr B Analyt Technol Biomed Life Sci 2007.

(28) de Graaf D, Sharma RC, Mechetner EB, Schimke RT, Roninson IB. P-glycoprotein confers methotrexate resistance in 3T6 cells with deficient carrier-mediated methotrexate uptake. Proc Natl Acad Sci U S A 1996;93:1238-42.

(29) Chen C, Lin J, Smolarek T, Tremaine L. P-glycoprotein has differential effects on the disposition of statin acid and lactone forms in mdr1a/b knockout and wild-type mice. Drug Metab Dispos 2007;35:1725-9.

(30) Karnes HT, Wei AT, Dimenna GP. HPLC analysis of salinomycin in human plasma using pre-column oxidation and automated heart cut column switching. J Pharm Biomed Anal 1993;11:823-7.

(31) Mealey KL, Bentjen SA, Gay JM, Cantor GH. Ivermectin sensitivity in collies is associated with a deletion mutation of the mdr1 gene. Pharmacogenetics 2001;11:727-33.

(32) Lankas GR, Cartwright ME, Umbenhauer D. P-glycoprotein deficiency in a subpopulation of CF-1 mice enhances avermectin-induced neurotoxicity. Toxicol Appl Pharmacol 1997;143:357-65.

(33) Seaman JT, Eagleson JS, Carrigan MJ, Webb RF. Avermectin B1 toxicity in a herd of Murray Grey cattle. Aust Vet J 1987;64:284-5.

CHAPTER 2.2

Transport of diclofenac by BCRP (ABCG2) and stimulation of MRP2 (ABCC2)-mediated drug transport by diclofenac and benzbromarone

Jurjen S. Lagas, Cornelia M. M. van der Kruijssen, Koen van de Wetering, Jos H. Beijnen and Alfred H. Schinkel

Drug Metabolism and Disposition 2009; 37:129-136

ABSTRACT

Diclofenac is an important analgesic and anti-inflammatory drug, widely used for treatment of post-operative pain, rheumatoid arthritis, and chronic pain associated with cancer. Consequently, diclofenac is often used in combination regimens and undesirable drug-drug interactions may occur. As many drug-drug interactions may occur at the level of drug transporting proteins, we studied interactions of diclofenac with apical ATP-binding cassette (ABC) multidrug efflux transporters. Using MDCK-II cells transfected with human P-glycoprotein (P-gp, MDR1/ABCB1), multidrug resistance protein 2 (MRP2/ABCC2) and breast cancer resistance protein (BCRP/ABCG2) and murine Bcrp1, we found that diclofenac was efficiently transported by murine Bcrp1 and moderately by human BCRP, but not by P-gp or MRP2. Furthermore, in Sf9-BCRP membrane vesicles diclofenac inhibited transport of MTX in a concentration-dependent manner. We next used MDCK-II-MRP2 cells to study interactions of diclofenac with MRP2-mediated drug transport. Diclofenac stimulated paclitaxel, docetaxel and saquinavir transport at only 50 μM. We further found that the uricosuric drug benzbromarone stimulated MRP2 at an even lower concentration, having maximal stimulatory activity at only 2 μM. Diclofenac and benzbromarone stimulated MRP2-mediated transport of amphipathic lipophilic drugs at 10- and 250-fold lower concentrations, respectively, than reported for other MRP2 stimulators. Because these concentrations are readily achieved in patients, adverse drug-drug interactions may occur. For instance during cancer therapy, when drug concentrations are often critical and stimulation of elimination via MRP2 may result in suboptimal chemotherapeutic drug concentrations. Moreover, stimulation of MRP2 activity in tumors may lead to increased efflux of chemotherapeutic drugs and thereby drug resistance.

INTRODUCTION

Diclofenac is a nonsteroidal anti-inflammatory drug (NSAID) that exhibits potent analgesic and anti-inflammatory properties and is extensively used to treat post-operative pain, rheumatoid arthritis, osteoarthritis and acute gouty arthritis (1). Diclofenac is also widely used to treat pain associated with cancer and treatment combinations of diclofenac with chemotherapeutic drugs are common. In addition, preclinical evidence is accumulating that NSAIDs, including diclofenac, have beneficial effects as adjuvant therapy in treatment of some types of cancer (2;3). Due to this wide-spread co-use of drugs, interactions of NSAIDs with chemotherapeutic drugs can result in unexpected toxicities or failure of chemotherapy. For example, NSAIDs are known to restrict plasma clearance of

methotrexate (MTX). When MTX is used at high-dose regimens for cancer treatment, interactions with NSAIDs can result in severe toxicity, with sometimes fatal outcome (4). Recently, using human kidney slides, it was demonstrated that diclofenac and its acyl-glucuronide can inhibit the luminal urinary efflux of MTX via the ATP binding cassette (ABC) multidrug transporters Mrp4 and Mrp2, respectively (5).

Because it is recognized more and more that many interactions of drugs occur at the level of drug transporting proteins, we investigated whether diclofenac is a substrate of one of the apical ABC transporters, using MDCK-II cells transfected with human P-gp, MRP2, BCRP or murine Bcrp1 cDNA. We further used the MDCK-II cells transduced with human and mouse MRP2/Mrp2 to examine whether diclofenac could modulate MRP2-mediated transport of taxane anti-cancer drugs. To date, a number of compounds, e.g. probenecid, sulfinpyrazone and sulfanitran, have been shown to stimulate the MRP2-mediated transport of lipophilic amphipathic drugs (6;7). Stimulation of MRP2-mediated transport can be of interest, because we recently demonstrated *in vivo* that Mrp2 is an important determinant for biliary excretion and thereby pharmacokinetics of the lipophilic amphipathic anticancer drug paclitaxel (8). Stimulation of Mrp2-mediated excretion of paclitaxel into the bile might thus seriously interfere with paclitaxel pharmacokinetics by enhancing its elimination. The same may apply to various other lipophilic amphipathic drugs transported by MRP2. Moreover, stimulation of MRP2 expressed in tumor cells may result in increased efflux of chemotherapeutics, thereby resulting in suboptimal drug concentrations and therapy failure.

MATERIALS AND METHODS

Chemicals. [^{3}H]etoposide, [^{3}H]paclitaxel, [^{3}H]MTX, [^{3}H]inulin and [^{14}C]inulin were from Amersham (Little Chalfont, UK). [^{3}H]docetaxel was obtained from Sankyo (Tokyo, Japan). [^{14}C]diclofenac was from Campro Scientific (Veenendaal, The Netherlands). [^{14}C]saquinavir originated from Roche Discovery Welwyn (Welwyn Garden City, UK). GlaxoSmithKline (Uxbridge, UK) kindly provided Elacridar (GF120918). The BCRP/Bcrp1 inhibitor Ko143 was described previously (9). All other chemicals and reagents were obtained from Sigma-Aldrich (Steinheim, Germany).

Transport across MDCK-II monolayers. Polarized canine kidney MDCK-II cell lines were used in transport assays. MDCK-II cells transduced with human MDR1, MRP2 or BCRP or murine Mrp2 and Bcrp1 were described (10-13). Transepithelial transport assays using Transwell plates were performed as described with minor modifications (14). Experiments with cells transfected with

human MRP2 or mouse Mrp2 were done in the presence of 5 μM of Elacridar, to inhibit any endogenous P-glycoprotein activity. Elacridar does not affect MRP2 activity (15). Experiments with MDCK-II-BCRP or MDCK-II-Bcrp1 cells were performed with or without 5 μM of the BCRP inhibitor Ko143. When applied, these inhibitors were present in both compartments during 2 hr preincubation and during the transport experiment. After preincubation, experiments were started (t = 0) by replacing the medium in either the apical or basolateral compartment with fresh OptiMEM medium, either with or without 5 μM Elacridar or Ko143 and containing 5 μM of the drug of interest (diclofenac, docetaxel, paclitaxel, saquinavir or etoposide), traced with radiolabeled drug (0.09 μCi/well). When stimulation of MRP2 was investigated, the stimulator was present in both compartments during preincubation as well as during the transport experiment. Cells were incubated at 37°C in 5% CO_2, and 50 μl aliquots were taken at t = 1, 2, 3 and 4 h. The samples were diluted with 4 ml of scintillation fluid (Ultima-Gold; Packard, Meriden CT) and radioactivity was measured using a dual channel scintillation counter. Transport was calculated as the fraction of drug found in the acceptor compartment relative to the total amount added to the donor compartment at the beginning of the experiment. Transport was given as mean percentage ± SD (n = 3). Membrane tightness was assessed using [^{14}C]inulin or [^{3}H]inulin (0.09 μCi/well), which was added to the donor compartment. Leakage was not allowed to be >1% of the total added radioactivity per hour.

Vesicular transport assays. Inside-out membrane vesicles were prepared from Sf9 insect cells overproducing human BCRP, as described previously (Zelcer et al., 2003). Transport of [^{3}H]MTX was studied at pH 7.4 and pH 5.5. The latter condition was included because the net transport of MTX by BCRP was reported to be higher at pH 5.5 (16). Vesicular uptake buffers for incubations with Sf9 vesicles consisted of 50 mM TRIS and 250 mM sucrose and the pH was adjusted with HCl to either 7.4 or 5.5. Both buffers also contained 10 mM MgCl, 10 mM creatine phosphate, and 100 μg/ml creatine. Uptake of MTX into membrane vesicles was assessed at 37°C in the presence or absence of 4 mM ATP, as described previously (17). ATP-dependent MTX transport was calculated by subtracting transport in the absence of ATP from that in its presence.

Relative transport ratio and statistical analysis. Active transport across MDCK-II monolayers was expressed by the relative transport ratio (r), defined as: r = percentage apically directed transport divided by percentage basolaterally directed translocation, after 4 hr (18). For statistical analysis, the two-sided unpaired Student's t-test was used. Differences were considered statistically significant when $P < 0.05$. Data are presented as means ± SD.

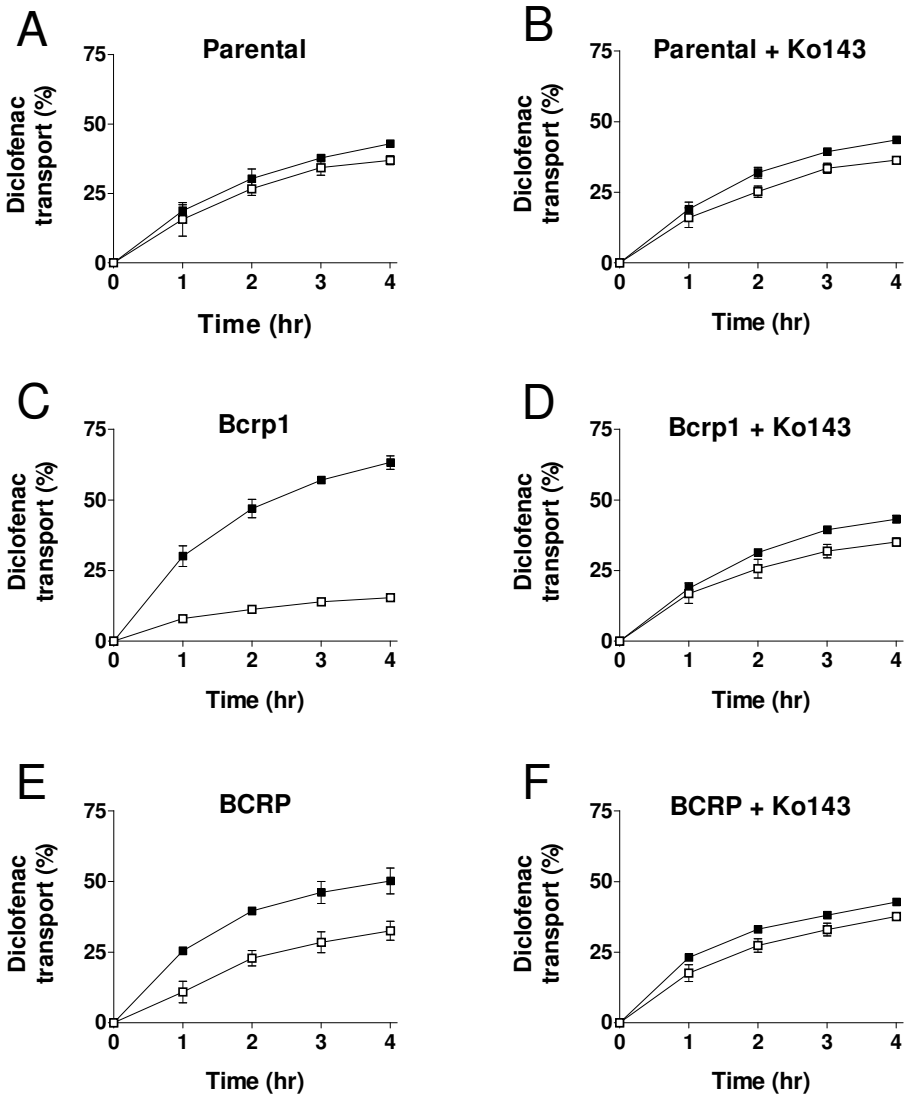

Fig. 1. Transepithelial transport of [^{14}C]diclofenac (5 μM) in MDCK-II cells either non-transduced (*A, B*) or transduced with murine Bcrp1 (*C, D*) or human BCRP (*E, F*) cDNA, in the absence (*A, C, E*) or presence (*B, D, F*) of Ko143 (5 μM). At t = 0 h, [^{14}C]diclofenac was applied in one compartment (apical or basolateral), and the percentage of radioactivity translocated to the opposite compartment at t = 1, 2, 3 and 4 h was measured by scintillation counting and plotted (n = 3). Translocation from the basolateral to the apical compartment (■); translocation from the apical to the basolateral compartment (□). Data represent means ± SD.

RESULTS

We used the polarized canine kidney cell line MDCK-II and its subclones transduced with human MDR1, MRP2 or BCRP or murine Bcrp1 to study vectorial transport of 5 μM diclofenac. In murine Bcrp1-transduced MDCK-II cells, apically directed translocation was markedly increased and basolaterally directed translocation was markedly decreased (Fig. 1C). MDCK-II cells overexpressing human BCRP also displayed directional transport of diclofenac, albeit less pronounced than Bcrp1-transduced cells (Fig. 1C, E). In the presence of 5 μM of the selective BCRP inhibitor Ko143 (9), net diclofenac transport in Bcrp1- and BCRP-transduced cells was effectively inhibited (Fig. 1B, D, F). In the MDCK-II cells transduced with human MDR1 or MRP2, no vectorial translocation of diclofenac was observed (data not shown). These results demonstrate efficient transport of diclofenac by murine Bcrp1, marked transport by human BCRP, and no transport by human MDR1 and MRP2. We also tested whether diclofenac could inhibit the transport of MTX by BCRP in vesicular uptake experiments performed at pH 7.4 and 5.5.

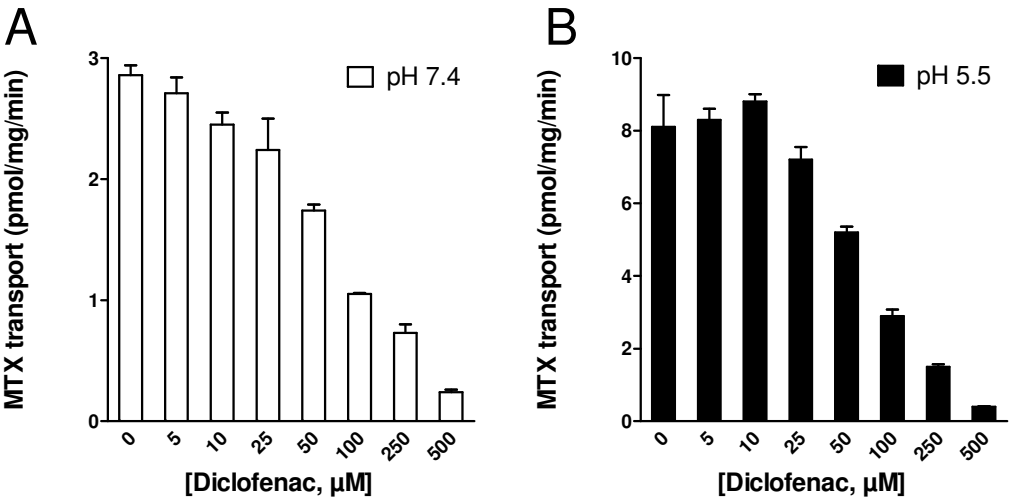

Fig. 2. Inhibition of BCRP-mediated transport of MTX by diclofenac. Sf9-BCRP membrane vesicles were incubated for 20 min at 37°C with 1 μM [^{3}H]MTX in the absence or presence of increasing diclofenac concentrations at pH 7.4 (*A*) or pH 5.5 (*B*). ATP-dependent MTX transport was calculated by subtracting transport in the absence of ATP from that in its presence. Each bar represents the mean transport value ± SD for experiments performed in triplicate.

Figure 2 shows that the net transport of MTX by BCRP was higher at pH 5.5 compared to pH 7.4, which is consistent with previous findings (16). The ATP-dependent transport of MTX by BCRP was inhibited by diclofenac in a concentration-dependent manner under both pH conditions, as shown in figure 2A and 2B. The inhibitor concentrations at which the effect was 50% of the maximal inhibitory effect (IC_{50}-values) were 78 µM (pH 7.4) and 71 µM (pH 5.5), respectively.

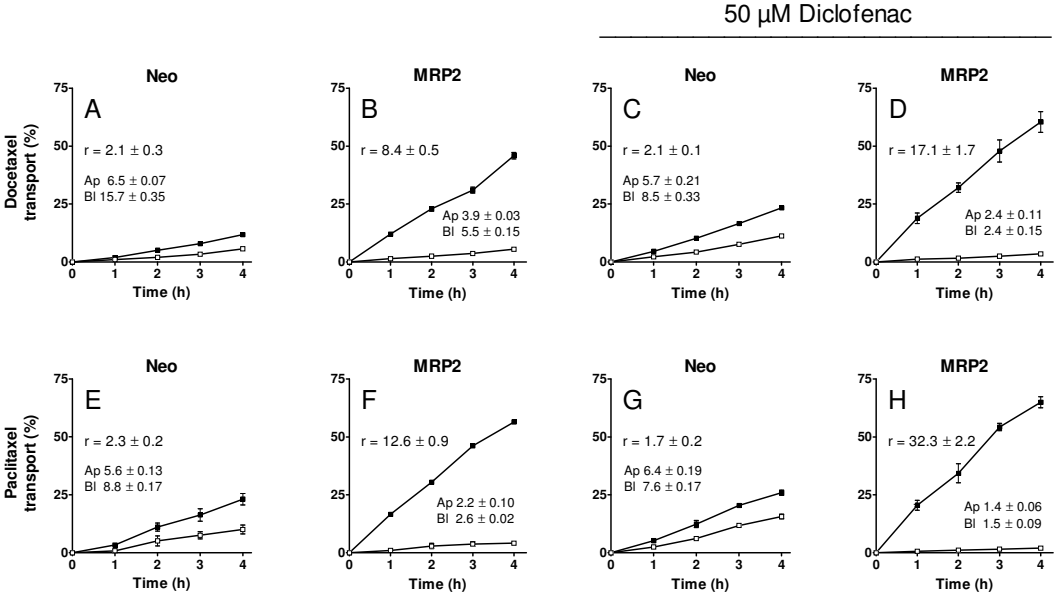

Fig. 3. Transepithelial transport of 5 µM [^{3}H]docetaxel or [^{3}H]paclitaxel in MDCK-II-*Neo* or MDCK-II-*MRP2* monolayers in the absence (*A, B, E, F*) and presence (*C, D, G, H*) of 50 µM diclofenac. Elacridar (5 µM) was present in all experiments to inhibit endogenous P-gp. At t = 0 h, the radioactive drug was applied in one compartment (apical or basolateral), and the percentage of radioactivity translocated to the opposite compartment at t = 1, 2, 3 and 4 h was measured by scintillation counting and plotted (n = 3). Translocation from the basolateral to the apical compartment (■); translocation from the apical to the basolateral compartment (□). Data represent means ± SD. Numbers in the panels indicate the percentage of radioactivity retrieved from the cell layer 4 hr after application of the drug to the apical (Ap) or basolateral (Bl) compartment. *r* represents the relative transport ratio (*i.e.,* the apically directed translocation divided by the basolaterally directed translocation) at t = 4 hr.

We next investigated whether diclofenac could modulate the transport of paclitaxel and docetaxel, using MDCK-II cells transfected with human MRP2. The MDCK-II-Neo cell-line was used as a control, because it contains only little endogenous canine Mrp2 (10). As shown previously (18), docetaxel and paclitaxel at 5 μM were efficiently transported by human MRP2 (Fig. 3A, B, E, F). This is evident from the increased relative transport ratios (*r*, defined in M&M section) and the decreased intracellular taxane concentration in MDCK-II-MRP2 cells (Fig. 3). In the presence of 50 μM diclofenac, transport of docetaxel and paclitaxel by MRP2 was markedly stimulated (Fig. 3). For docetaxel the transport ratio was increased 2.0-fold and the intracellular concentrations were 1.6-fold and 2.3-fold decreased for apically and basolaterally applied docetaxel, respectively (Fig. 3B, D). For paclitaxel the relative transport ratio was increased 2.6-fold and the intracellular concentrations were 1.6-fold and 1.7-fold decreased for apically and basolaterally applied paclitaxel, respectively (Fig. 3F, H). The stimulation of the relative transport ratio for paclitaxel was maximal for diclofenac concentrations ranging from 50-250 μM (Fig. 4A). Higher diclofenac concentrations (> 500 μM) were toxic for the monolayers, as indicated by an increased paracellular inulin leakage. These results show that diclofenac can stimulate MRP2-mediated transport of paclitaxel and docetaxel at a concentration of only 50 μM, which is 10-fold lower than the optimal stimulatory concentrations we previously found in MDCK-II-MRP2 cells for the established MRP2 stimulators probenecid, sulfinpyrazone and sulfanitran (6;7;18).

Partly based on structural similarities with established MRP2 stimulators and partly based on reported MRP2 modulator activities we tested four additional compounds for their ability to stimulate MRP2-mediated taxane transport. For the diuretic furosemide and the antidiabetic agents tolbutamide and glyburide we found at best only weak stimulatory activities (data not shown). The uricosuric drug benzbromarone (Fig. 4B), however, was found to stimulate MRP2 transport with a maximal stimulatory activity at only 2 μM (Fig. 4 and 5). Benzbromarone increased the transport ratio for docetaxel 3.3-fold and for paclitaxel 3.8-fold and the intracellular concentrations of both taxanes were markedly decreased in the presence of benzbromarone (Fig. 5B, D, F, H). The MRP2-mediated transport of paclitaxel was stimulated in a concentration-dependent manner by benzbromarone. The relative transport ratio was maximal at 2 μM and gradually decreased to control levels at 10 μM benzbromarone (Fig. 4B). Higher benzbromarone concentrations (> 10 μM) were toxic for the monolayers, as indicated by increased paracellular inulin leakage.

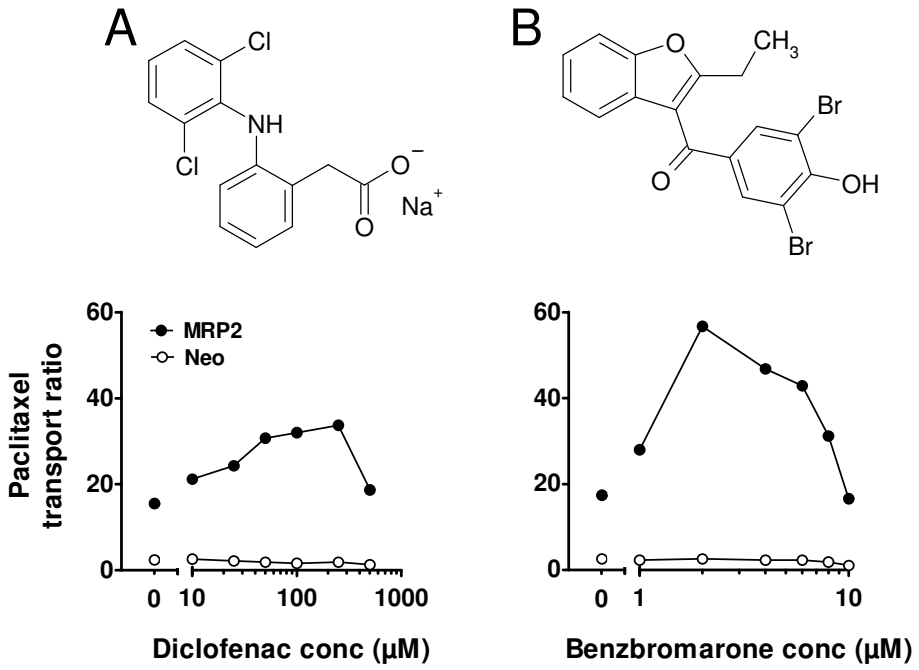

Fig. 4. Relative transport ratios of [^{3}H]paclitaxel (5 µM) in the presence of various concentrations of diclofenac (A) or benzbromarone (B), measured after 4 hr in MDCKII-*Neo* (○, very low expression of endogenous canine *Mrp2*) and MDCKII-*MRP2* (●, overexpression of human *MRP2*, n = 1). Elacridar (5 µM) was present to inhibit endogenous P-gp. Relative transport ratios were determined by dividing the percentage of apically directed translocation by the percentage of basolaterally directed translocation. Structural formulas of (*A*) diclofenac (MW = 318.13) and (*B*) benzbromarone (MW = 424.09) are indicated in the panels above.

Because benzbromarone could stimulate taxane transport by MRP2 at a very low concentration, we tested its stimulatory potency for two other clinically relevant MRP2 substrates, the HIV protease inhibitor saquinavir and the anticancer drug etoposide. In the presence of 2 µM benzbromarone we found pronounced stimulation of net saquinavir transport (4.8-fold), and modest stimulation of net etoposide transport (1.4-fold, Fig. 5, panels I-L and M-P). These levels of stimulation of MRP2 are quantitatively similar to those seen before with 500 µM probenecid, sulfinpyrazone and sulfanitran (6;7;18). These results thus demonstrate that benzbromarone is an effective MRP2 stimulator in MDCK-II-MRP2 cells for a wide range of drugs.

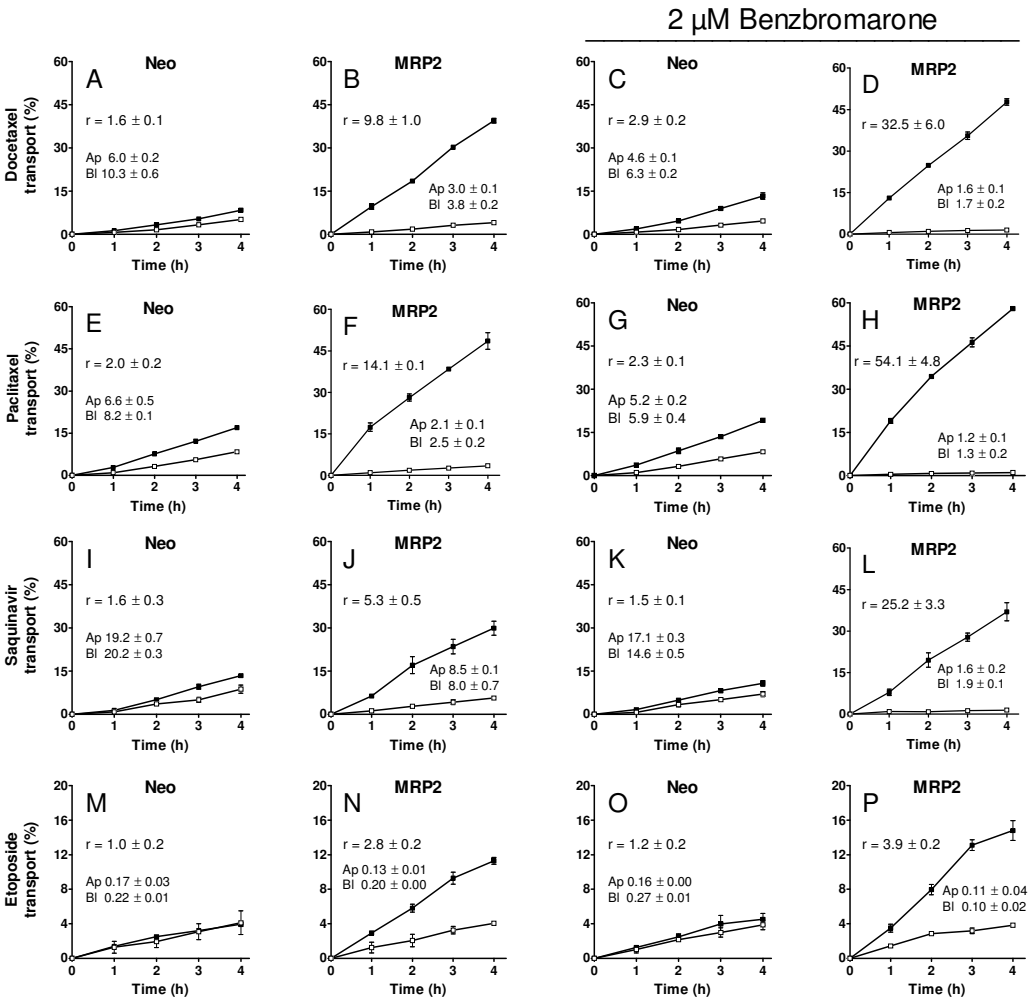

Fig. 5. Transepithelial transport of 5 µM [^{3}H]docetaxel, [^{3}H]paclitaxel, [^{14}C]saquinavir or [^{3}H]etoposide in MDCK-II-*Neo* or MDCK-II-*MRP2* monolayers in the absence (first 2 columns) and presence (last 2 columns) of 2 µM benzbromarone. Elacridar (5 µM) was present in all experiments to inhibit endogenous P-gp. For further experimental details, see legend of Figure 3.

We next addressed the relevance of drug-drug interactions via stimulation of MRP2 *in vivo*. Because we recently demonstrated that hepatobiliary excretion of paclitaxel in the mouse is almost exclusively dependent on Mrp2 (8), we tried to stimulate biliary paclitaxel excretion in mice by the coadministration of either diclofenac or benzbromarone. However, we were unable to show any *in vivo*

stimulation (Lagas et al., unpublished data). This discrepancy might be the result of species differences between human MRP2 and murine Mrp2 in their modulatory responsiveness (13). Therefore, we used the recently generated MDCK-II cells expressing murine Mrp2 cDNA (13) and tested whether diclofenac or benzbromarone could modulate transport of paclitaxel. In contrast to stimulating transport activity of human MRP2 (Fig. 3 and 5), diclofenac and benzbromarone inhibited the net transport of paclitaxel in cells transfected with murine Mrp2 by 2.2- and 1.7-fold, respectively (Fig. 6 B). As a result, intracellular accumulation of paclitaxel in MDCK-II-Mrp2 cells at 4 hr was significantly increased in the presence of diclofenac or benzbromarone (Fig 6C, $P < 0.05$). In contrast, intracellular paclitaxel accumulation in human MRP2-transfected cells was significantly lower when diclofenac or benzbromarone were applied (Fig. 6C, $P < 0.01$). Because benzbromarone showed most pronounced stimulation of human MRP2-mediated transport of saquinavir (Fig. 5L), we also tested the impact of diclofenac on saquinavir transport in both human- and mouse MRP2/Mrp2-transfected cells. We observed a similar modulation pattern as for paclitaxel. Diclofenac increased the net transport of saquinavir by human MRP2 3.4-fold, but decreased net saquinavir transport by murine Mrp2 2.1-fold (Fig. 7A, B). Furthermore, diclofenac markedly lowered the intracellular saquinavir concentrations in MDCK-II-MRP2 cells by 5.2-fold, whereas a 1.5-fold higher intracellular concentration was found in cells transfected with murine Mrp2. Taken together, these results show that profound species differences can occur in modulatory responsiveness of human MRP2 and murine Mrp2 for various compounds. The mouse therefore has limitations as a model to study drug-drug interactions that occur via stimulation of MRP2 by diclofenac and benzbromarone.

DISCUSSION

In the present study diclofenac was identified as an efficiently transported substrate for both murine and human BCRP. Diclofenac is often used to treat pain associated with cancer and co-administration of diclofenac with anticancer drugs is common. Because BCRP is an important determinant in the pharmacokinetics of many anticancer agents, interactions of diclofenac with chemotherapeutics drugs at the level of BCRP may occur. In patients, diclofenac can limit plasma clearance of MTX, which can result in severe toxicity, especially when MTX is used in high-dose regimens for cancer treatment (4). This interaction may be (partially) explained by the observation that diclofenac can inhibit luminal urinary efflux of MTX via Mrp4 in human kidney slices (5). In addition, MTX is a good substrate for BCRP (19) and, like MRP4, BCRP is expressed in the apical membrane of the proximal tubules of the human kidney (20). *In vivo* competition between diclofenac

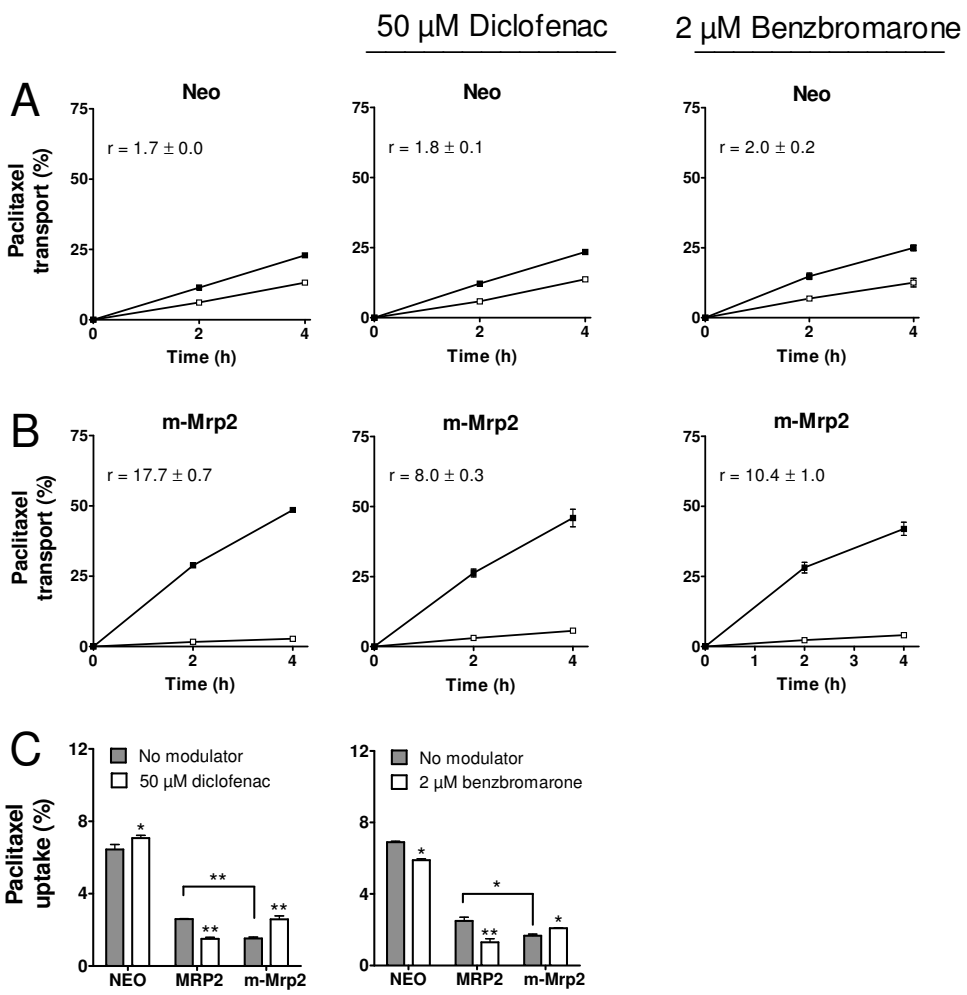

Fig. 6. Transepithelial transport of 5 µM [^{3}H]paclitaxel in MDCK-II-*Neo* (A) and MDCK-II-*Mrp2* (B) monolayers in the absence and presence of 50 µM diclofenac or 2 µM benzbromarone. Intracellular accumulation of 5 µM [^{3}H]paclitaxel after 4 hrs in MDCK-II-*Neo*, MDCK-II -*MRP2* or MDCK-II -*Mrp2* monolayers in the absence and presence of 50 µM diclofenac or 2 µM benzbromarone (C). * $P < 0.05$ and ** $P < 0.01$, uptake without modulator compared to uptake with modulator for the same cell lines. Note that the uptake without modulators was also compared between MDCK-II -*MRP2* and MDCK-II -*Mrp2* cells. Data for MDCK-II -*MRP2* were also presented in Fig. 3. Elacridar (5 µM) was present in all experiments to inhibit endogenous P-gp. For further experimental details, see legend of Figure 3.

and MTX for transport by BCRP may therefore be a clinically relevant drug-drug interaction, as this may contribute to lower renal clearance of MTX. Using inside-out Sf9-BCRP plasma membrane vesicles, we show that diclofenac indeed can inhibit the BCRP-mediated transport of MTX in a concentration-dependent manner. We note, however, that the IC_{50}-values of 78 µM (pH 7.4) and 71 µM (pH 5.5) indicate that diclofenac is not a very potent BCRP inhibitor *in vitro*. Therefore, the clinical significance of drug-drug interactions through inhibition of BCRP by diclofenac needs to be studied in patients.

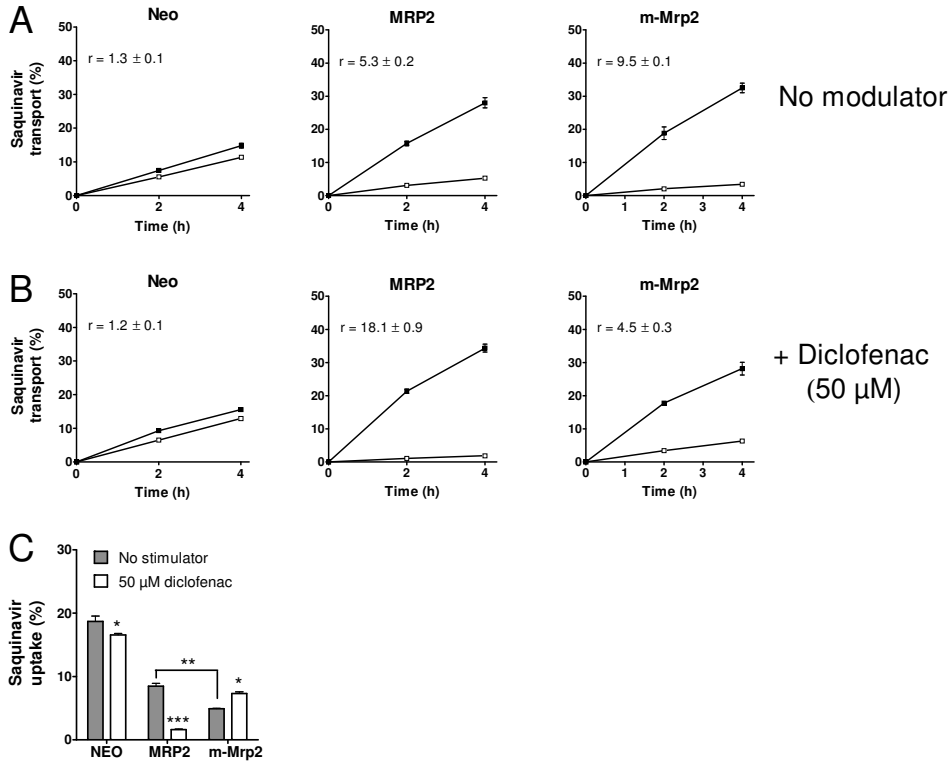

Fig. 7. Transepithelial transport of 5 µM [^{14}C]saquinavir in MDCK-II-*Neo*, MDCK-II-*MRP2* or MDCK-II-*Mrp2* monolayers in the absence (A) and presence (B) of 50 µM diclofenac. Intracellular accumulation of 5 µM [^{14}C]saquinavir after 4 hrs in MDCK-II-*Neo*, MDCK-II -*MRP2* or MDCK-II -*Mrp2* monolayers in the absence and presence of 5 µM diclofenac (C). * $P < 0.05$, ** $P < 0.01$, and *** $P < 0.001$, uptake without modulator compared to uptake with modulator for the same cell lines. Note that the uptake without modulators was also compared between MDCK-II -*MRP2* and MDCK-II -*Mrp2* cells. Elacridar (5 µM) was present in all experiments to inhibit endogenous P-gp. For further experimental details, see legend of Figure 3.

Using inside-out plasma membrane vesicles, extensive studies on the complex modulation (stimulation and/or inhibition) of MRP2/Mrp2-mediated transport of various anionic compounds have been performed (7;21-25). Transport studies with estradiol-17β-glucuronide ($E_2$17βG) revealed that $E_2$17βG can stimulate its own transport by MRP2 (7;22). This finding indicated that the MRP2 protein contains at least two binding sites that display a positive cooperative interaction, i.e. $E_2$17βG can bind to a substrate transport site and to a modulatory site which affects the transport rate allosterically by homotropic cooperative interaction (7;26). Notably, stimulation of its own transport, as was seen for $E_2$17βG, was recently also found for the bile salt tauroursodeoxycholate (25). In addition, many examples have been reported of other substrates that can stimulate the MRP2-mediated transport of $E_2$17βG in a positive cooperative manner. Several of these compounds are themselves transported substrates of MRP2 and inhibit $E_2$17βG transport at higher concentrations via competition for the substrate transport site (7). Thus at least a number of compounds can bind both the modulatory site and the substrate transport site.

Stimulated transport by MRP2 was also shown in intact MDCKII-cells overexpressing MRP2 (6;7;27). In this system, MRP2-mediated transport of the organic anion glutathione (GSH) could be stimulated at relatively low concentrations by indomethacine and sulfinpyrazone (27). Maximal stimulation of the MRP2-mediated transport of large lipophilic amphipathic drugs, however, was only observed at stimulator concentrations $\geq$ 500 μM (6;7). We here report that diclofenac and benzbromarone can markedly stimulate MRP2-mediated transport of a number of lipophilic amphipathic compounds, including taxane anticancer drugs, etoposide and saquinavir at respectively 10- and 250-fold lower concentrations than reported for other MRP2 stimulators (6;7). We note that it is difficult to compare the detailed kinetic properties of MRP2 stimulators when monolayers of intact MDCKII-cells are used, because kinetic parameters (such as K_m and V_{max}) cannot be directly determined in this system as the intracellular stimulator concentrations are unknown. In contrast, these parameters can be readily obtained from experiments with Sf9-MRP2 inside-out plasma membrane vesicles, because all applied transported substrates and stimulators have access to the transporters. However, transport of hydrophobic compounds, such as taxanes, etoposide and saquinavir, cannot be studied properly in inside-out plasma membrane vesicles, because these substrates easily diffuse back out and they also display extensive non-specific binding to membranes, resulting in a low signal-to-noise ratio (28). Detailed kinetic studies on stimulation of MRP2-mediated transport of amphipathic lipophilic compounds are therefore complicated. Our

observation, however, that diclofenac is not transported by MRP2 might indicate that diclofenac binds primarily to the modulator site of the MRP2 protein.

To date, there are a number of MRP2 modulator compounds known that inhibit MRP2-mediated transport of some anionic substrates, but stimulate the transport of lipophilic amphipathic compounds; e.g. probenecid inhibits transport of MTX by MRP2, but stimulates the MRP2-mediated transport of HIV protease inhibitors and taxanes (6;18;29). This might also be true for diclofenac and benzbromarone. Several studies show that benzbromarone and diclofenac can inhibit MRP2-mediated transport of hydrophilic anionic compounds (5;21;27;30;31). However, to our knowledge this is the first report showing that diclofenac and benzbromarone can stimulate MRP2-mediated transport of a number of clinically relevant lipophilic amphipathic drugs. Because the stimulator concentrations showing maximal stimulatory effect can be readily achieved in patients, confirmation of these results *in vivo* would indicate whether these drug-drug interactions are likely to be clinically relevant. Unfortunately, using mouse models we were unable to demonstrate stimulation with these compounds *in vivo*. We could attribute this to profound species differences in modulatory responsiveness for human MRP2 and murine Mrp2, which is in line with recent observations (13). We thus conclude that the mouse has limitations as a model to study drug-drug interactions that occur via stimulation of human MRP2 by diclofenac and benzbromarone. However, because we observed strong stimulation of human MRP2 *in vitro* at very low modulator concentrations, drug-drug interactions via this mechanism may be relevant for the clinical situation in humans. Especially in cancer therapy, when severe toxicity must be avoided and anticancer drugs are applied in a narrow therapeutic range, stimulation of MRP2 may result in suboptimal drug concentrations in the blood. Moreover, stimulation of MRP2 in tumors may result in increased drug efflux and thereby resistance against anticancer agents.

ACKNOWLEGMENTS

We thank Vicky van Tilburg for performing transwell experiments and our colleagues for critical reading of the manuscript.

REFERENCES

(1) Davies NM, Anderson KE. Clinical pharmacokinetics of diclofenac. Therapeutic insights and pitfalls. Clin Pharmacokinet 1997;33:184-213.

(2) Crokart N, Radermacher K, Jordan BF, Baudelet C, Cron GO, Gregoire V et al. Tumor radiosensitization by antiinflammatory drugs: evidence for a new mechanism involving the oxygen effect. Cancer Res 2005;65:7911-6.

(3) Johnsen JI, Lindskog M, Ponthan F, Pettersen I, Elfman L, Orrego A et al. NSAIDs in neuroblastoma therapy. Cancer Lett 2005;228:195-201.

(4) Thyss A, Milano G, Kubar J, Namer M, Schneider M. Clinical and pharmacokinetic evidence of a life-threatening interaction between methotrexate and ketoprofen. Lancet 1986;1:256-8.

(5) Nozaki Y, Kusuhara H, Kondo T, Iwaki M, Shiroyanagi Y, Nakayama H et al. Species difference in the inhibitory effect of nonsteroidal anti-inflammatory drugs on the uptake of methotrexate by human kidney slices. J Pharmacol Exp Ther 2007;322:1162-70.

(6) Huisman MT, Smit JW, Crommentuyn KM, Zelcer N, Wiltshire HR, Beijnen JH et al. Multidrug resistance protein 2 (MRP2) transports HIV protease inhibitors, and transport can be enhanced by other drugs. AIDS 2002;16:2295-301.

(7) Zelcer N, Huisman MT, Reid G, Wielinga P, Breedveld P, Kuil A et al. Evidence for two interacting ligand binding sites in human multidrug resistance protein 2 (ATP binding cassette C2). J Biol Chem 2003;278:23538-44.

(8) Lagas JS, Vlaming ML, van Tellingen O, Wagenaar E, Jansen RS, Rosing H et al. Multidrug resistance protein 2 is an important determinant of paclitaxel pharmacokinetics. Clin Cancer Res 2006;12:6125-32.

(9) Allen JD, van Loevezijn A, Lakhai JM, van der Valk M, van Tellingen O, Reid G et al. Potent and specific inhibition of the breast cancer resistance protein multidrug transporter in vitro and in mouse intestine by a novel analogue of fumitremorgin C. Mol Cancer Ther 2002;1:417-25.

(10) Evers R, Kool M, van Deemter L, Janssen H, Calafat J, Oomen LC et al. Drug export activity of the human canalicular multispecific organic anion transporter in polarized kidney MDCK cells expressing cMOAT (MRP2) cDNA. J Clin Invest 1998;101:1310-9.

(11) Jonker JW, Buitelaar M, Wagenaar E, Van Der Valk MA, Scheffer GL, Scheper RJ et al. The breast cancer resistance protein protects against a major chlorophyll-derived dietary phototoxin and protoporphyria. Proc Natl Acad Sci U S A 2002;99:15649-54.

(12) Pavek P, Merino G, Wagenaar E, Bolscher E, Novotna M, Jonker JW et al. Human breast cancer resistance protein: interactions with steroid drugs, hormones, the dietary carcinogen 2-amino-1-methyl-6-phenylimidazo(4,5-b)pyridine, and transport of cimetidine. J Pharmacol Exp Ther 2005;312:144-52.

(13) Zimmermann C, van de Wetering K, van de Steeg E, Wagenaar E, Vens C, Schinkel AH. Species-dependent transport and modulation properties of human and mouse multidrug resistance protein 2 (MRP2/Mrp2, ABCC2/Abcc2). Drug Metab Dispos 2008;36:631-40.

(14) Schinkel AH, Wagenaar E, van Deemter L, Mol CA, Borst P. Absence of the mdr1a P-Glycoprotein in mice affects tissue distribution and pharmacokinetics of dexamethasone, digoxin, and cyclosporin A. J Clin Invest 1995;96:1698-705.

(15) Evers R, Kool M, Smith AJ, van Deemter L, de Haas M, Borst P. Inhibitory effect of the reversal agents V-104, GF120918 and Pluronic L61 on MDR1 Pgp-. Br J Cancer 2000;83:366-74.

(16) Breedveld P, Pluim D, Cipriani G, Dahlhaus F, van Eijndhoven MA, de Wolf CJ et al. The effect of low pH on breast cancer resistance protein (ABCG2)-mediated transport of methotrexate, 7-hydroxymethotrexate, methotrexate diglutamate, folic acid, mitoxantrone, topotecan, and resveratrol in in vitro drug transport models. Mol Pharmacol 2007;71:240-9.

(17) van de Wetering K, Zelcer N, Kuil A, Feddema W, Hillebrand M, Vlaming ML et al. Multidrug resistance proteins 2 and 3 provide alternative routes for hepatic excretion of morphine-glucuronides. Mol Pharmacol 2007;72:387-94.

(18) Huisman MT, Chhatta AA, van Tellingen O, Beijnen JH, Schinkel AH. MRP2 (ABCC2) transports taxanes and confers paclitaxel resistance and both processes are stimulated by probenecid. Int J Cancer 2005;116:824-9.

(19) Volk EL, Rohde K, Rhee M, McGuire JJ, Doyle LA, Ross DD et al. Methotrexate cross-resistance in a mitoxantrone-selected multidrug-resistant MCF7 breast cancer cell line is attributable to enhanced energy-dependent drug efflux. Cancer Res 2000;60:3514-21.

(20) Huls M, Brown CD, Windass AS, Sayer R, van den Heuvel JJ, Heemskerk S et al. The breast cancer resistance protein transporter ABCG2 is expressed in the human kidney proximal tubule apical membrane. Kidney Int 2008;73:220-5.

(21) Bakos E, Evers R, Sinko E, Varadi A, Borst P, Sarkadi B. Interactions of the human multidrug resistance proteins MRP1 and MRP2 with organic anions. Mol Pharmacol 2000;57:760-8.

(22) Bodo A, Bakos E, Szeri F, Varadi A, Sarkadi B. Differential modulation of the human liver conjugate transporters MRP2 and MRP3 by bile acids and organic anions. J Biol Chem 2003;278:23529-37.

(23) Chu XY, Huskey SE, Braun MP, Sarkadi B, Evans DC, Evers R. Transport of ethinylestradiol glucuronide and ethinylestradiol sulfate by the multidrug resistance proteins MRP1, MRP2, and MRP3. J Pharmacol Exp Ther 2004;309:156-64.

(24) Gerk PM, Li W, Vore M. Estradiol 3-glucuronide is transported by the multidrug resistance-associated protein 2 but does not activate the allosteric site bound by estradiol 17-glucuronide. Drug Metab Dispos 2004;32:1139-45.

(25) Gerk PM, Li W, Megaraj V, Vore M. Human multidrug resistance protein 2 transports the therapeutic bile salt tauroursodeoxycholate. J Pharmacol Exp Ther 2007;320:893-9.

(26) Borst P, Zelcer N, van de Wetering K, Poolman B. On the putative co-transport of drugs by multidrug resistance proteins. FEBS Lett 2006;580:1085-93.

(27) Evers R, de Haas M, Sparidans R, Beijnen J, Wielinga PR, Lankelma J et al. Vinblastine and sulfinpyrazone export by the multidrug resistance protein MRP2 is associated with glutathione export. Br J Cancer 2000;83:375-83.

(28) Borst P, Oude Elferink RP. Mammalian ABC transporters in health and disease. Annu Rev Biochem 2002;71:537-92.

(29) Hooijberg JH, Broxterman HJ, Kool M, Assaraf YG, Peters GJ, Noordhuis P et al. Antifolate resistance mediated by the multidrug resistance proteins MRP1 and MRP2. Cancer Res 1999;59:2532-5.

(30) Prime-Chapman HM, Fearn RA, Cooper AE, Moore V, Hirst BH. Differential multidrug resistance-associated protein 1 through 6 isoform expression and function in human intestinal epithelial Caco-2 cells. J Pharmacol Exp Ther 2004;311:476-84.

(31) El Sheikh AA, van den Heuvel JJ, Koenderink JB, Russel FG. Interaction of nonsteroidal anti-inflammatory drugs with multidrug resistance protein (MRP) 2/A. J Pharmacol Exp Ther 2007;320:229-35.

CHAPTER 2.3

Hepatic clearance of reactive glucuronide metabolites of diclofenac is dependent on multiple ATP-binding cassette efflux transporters

Jurjen S. Lagas, Rolf W. Sparidans, Els Wagenaar,
Jos H. Beijnen and Alfred H. Schinkel

To be submitted

ABSTRACT
Diclofenac is an important analgesic and anti-inflammatory drug, widely used for treatment of post-operative pain, rheumatoid arthritis, and chronic pain associated with cancer. Diclofenac is extensively metabolized in the liver, and the main metabolites are hydroxylated and/or glucuronidated conjugates. We show here that loss of Multidrug Resistance Protein 2 (MRP2/ABCC2) and Breast Cancer Resistance Protein (BCRP/ABCG2) in mice results in highly increased plasma levels of diclofenac acyl glucuronide, both after oral and intravenous administration. Absence of Mrp2 and Bcrp1, localized at the canalicular membrane of hepatocytes, leads to impaired biliary excretion of acyl glucuronides, and consequently, to elevated liver and plasma levels. Mrp2 also mediates the biliary excretion of two hydroxylated diclofenac metabolites, 4'-hydroxydiclofenac and 5-hydroxydiclofenac. We further show that the sinusoidal efflux of diclofenac acyl glucuronide, from liver to blood, is largely dependent on Multidrug Resistance Protein 3 (MRP3/ABCC3). Diclofenac acyl glucuronides are chemically instable and reactive, and in patients these metabolites are associated with rare but serious idiosyncratic liver toxicity. This might explain why *Mrp2/Mrp3/Bcrp1*$^{-/-}$ mice, which have markedly elevated levels of diclofenac acyl glucuronides in their liver, display acute, albeit mild, hepatotoxicity. We believe that the handling of diclofenac acyl glucuronides by ABC transporters may be representative for the handling of acyl glucuronide metabolites of additional clinically relevant drugs.

INTRODUCTION
Diclofenac (DF, Fig. 1) is a nonsteroidal anti-inflammatory drug (NSAID) that exhibits potent analgesic and anti-inflammatory properties and is widely used to treat post-operative pain, rheumatoid arthritis, osteoarthritis and acute gouty arthritis (1). When given orally, absorption is rapid and complete (1-3). The metabolism of DF partitions between acyl glucuronidation and aryl hydroxylation (4), and the major metabolites are DF acyl glucuronide (DF-AG), 4'hydroxy DF (4OH-DF) and 5-hydroxy DF (5OH-DF; Fig 1). In humans, UDP-glucuronosyltransferase 2B7 (UGT2B7) catalyzes the glucuronidation of DF, whereas in rats this is Ugt2b1 (5). The hydroxylation of DF to 4OH-DF and 5OH-DF is catalyzed by CYP2C9 and 3A4, respectively (4). After glucuronidation, DF-AG can undergo further hydroxylation (6), and hydroxylated DF-AG conjugates are major urinary metabolites (2).

Extensive first-pass metabolism combined with low enterohepatic circulation reduces the oral bioavailability of DF in humans to 50-60% of the administered dose, and the metabolites of DF are predominantly eliminated in the urine (7-9). In

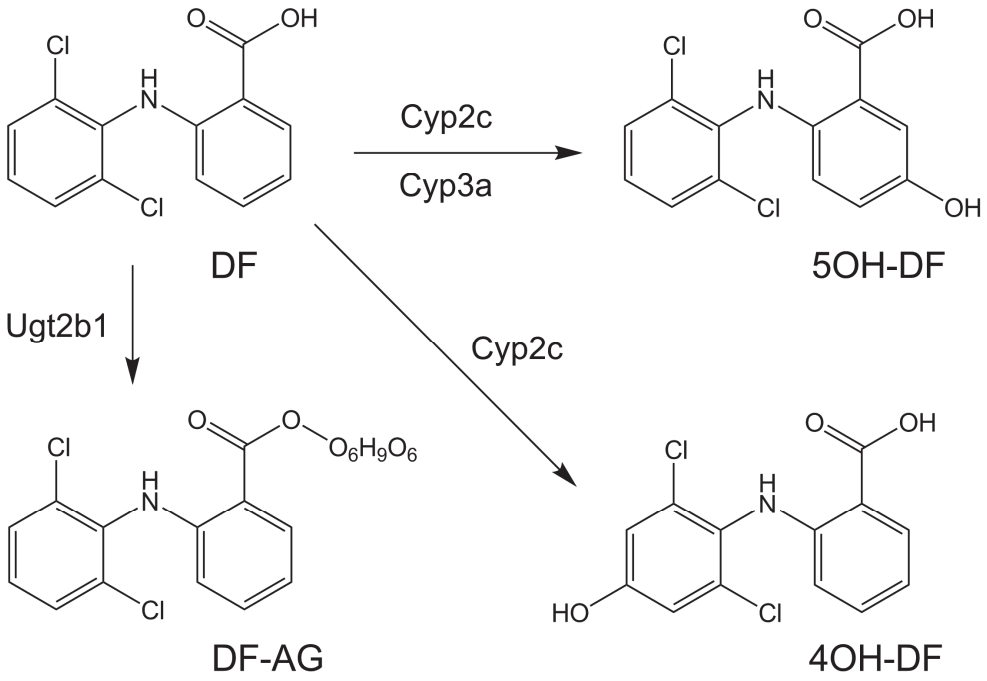

Fig. 1. Structures and biotransformation routes of DF and its three most predominant primary metabolites with the putative metabolic enzymes involved in the mouse. Cyp = Cytochrome P450; Ugt = UDP-glucuronosyltransferase.

contrast, in rats the biliary excretion of DF glucuronides plays an important role in the elimination of DF (3). Once excreted into the intestines, DF glucuronides can be hydrolyzed by bacterial β-glucuronidases, and reabsorption of DF results in significant enterohepatic circulation (3;10). However, acyl glucuronides are chemically unstable and can undergo epimerization by acyl migration to the 2-, 3-, or 4-O-glucuronide, especially in the alkaline environment of bile, and these isomers are resistant to cleavage by bacterial β-glucuronidases (10-13).

Multidrug Resistance Proteins 2 and 3 (MRP2/*ABCC2* and MRP3/*ABCC3*) and Breast Cancer Resistance Protein (BCRP/ABCG2) are ATP binding cassette (ABC) multidrug transporters that have broad and substantially overlapping substrate specificities (14;15). MRP2 and BCRP are situated at apical membranes of important epithelial barriers, such as intestine and kidney and at the canalicular membrane of hepatocytes. Consequently, they extrude their substrates into bile,

urine and feces, and restrict the (re)uptake of transported compounds from the gut (15). In contrast, MRP3 is located at the basolateral membrane of epithelial cells of kidney and intestine and at the sinusoidal membrane of hepatocytes, and pumps its substrates towards the blood circulation (16).

DF can cause rare but serious idiosyncratic hepatotoxicity and the formation of protein adducts with reactive DF glucuronides is believed to play a role herein [reviewed in (4;17)]. Using TR^- rats, that naturally lack Mrp2, Seitz and colleagues (1998) showed that hepatic Mrp2 mediates the efflux of DF glucuronides from the liver into the bile. Moreover, the formation of hepatic protein adducts by the reactive acyl glucuronides of DF was critically dependent on Mrp2, i.e. TR^- rats displayed no hepatic adducts, whereas control rats did (18), suggesting that Mrp2 deficiency might protect the liver from diclofenac-induced toxicity. This might explain why intra-hepatic protein adduct formation most frequently occurs in the biliary tree (13). Furthermore, DF glucuronides, excreted into the bile by Mrp2, were shown to be involved in the formation of ulcers in the small intestine (10). Although DF treatment in humans also leads to the formation of gastrointestinal ulcers, DF glucuronides are predominantly exported from the human liver to the blood circulation and subsequently excreted in the urine (2;7;8). The hepatic efflux pump(s) that is responsible for the sinusoidal transport of DF glucuronides remains to be identified. MRP3, localized in the sinusoidal membrane of hepatocytes, might be a candidate, as this transporter accepts organic anions with a preference for glucuronidated substrates (19).

In this study we investigated the impact of MRP2, MRP3 and BCRP on the pharmacokinetics of DF, using *Mrp2*$^{-/-}$, *Mrp3*$^{-/-}$ and *Bcrp1*$^{-/-}$ mice and all combination knockout strains. We included BCRP in this study, because we recently identified DF as a Bcrp1 substrate *in vitro* (20).

MATERIALS AND METHODS

Chemicals. DF (Voltaren; 25 mg/ml) was obtained from Novartis (Arnhem, The Netherlands). DF-AG originated from United States Biological (Swampscott, MA, USA). 5OH-DF was from Toronto Research Chemicals (North York, Canada). 4OH-DF was a kind gift from Becton Dickinson Bioscience (Breda, The Netherlands). [^{14}C]DF, specific activity 55 Ci/mol, was from Campro Scientific (Veendedaal, The Netherlands). Heparin (5000 IE/ml) originated from Leo Pharma BV (Breda, The Netherlands). Methoxyflurane (Metofane) was from Medical Developments Australia Pty. Ltd. (Springvale, Victoria, Australia). Bovine serum albumin (BSA), fraction V, was from Roche (Mannheim, Germany). Ketamine (Ketanest-S®) was from Pfizer (Cappelle a/d IJssel, the Netherlands). Xylazine was from Sigma Chemical Co (St. Louis, MO, USA). L(+)-ascorbic acid and

sodium acetate were of analytical grade and originated from Merck (Darmstadt, Germany). Acetic acid of analytical quality originated from Riedel-de Haën (Sigma Aldrich, Seelze, Germany).

Animals. Mice were housed and handled according to institutional guidelines complying with Dutch legislation. Animals used were male *Bcrp1*$^{-/-}$ (21), *Mrp2*$^{-/-}$ (22), *Mrp3*$^{-/-}$ (23), *Mrp2/Bcrp1*$^{-/-}$ (Vlaming et al., in press), *Mrp2/Mrp3*$^{-/-}$ (24), *Mrp3/Bcrp1*$^{-/-}$ (Vlaming et al., unpublished), *Mrp2/Mrp3/Bcrp1*$^{-/-}$ (Vlaming et al., unpublished) and wild-type (WT) mice, all of a >99% FVB genetic background, between 9 and 15 weeks of age. Animals were kept in a temperature-controlled environment with a 12-hour light / 12-hour dark cycle and received a standard diet (AM-II, Hope Farms, Woerden, The Netherlands) and acidified water *ad libitum*.

Plasma pharmacokinetic experiments and tissue distribution. For oral studies, DF (Voltaren; 25 mg/ml) was 50-fold diluted with a 5% glucose solution in water and a total volume of 10 ml/kg (5 mg/kg) body weight was administered by gavage into the stomach, using a blunt ended needle (n = 5). To minimize variation in absorption, mice were fasted 3 hours before drug administration. Blood samples (~30 µl) were collected in heparinized capillary tubes (Oxford Labware, St. Louis, USA) from the tail vein at 15 and 30 min and at 1, 2, 4, and 6 h after administration of the drug. For i.v. studies, DF (Voltaren; 25 mg/ml) was 25-fold diluted with a saline solution (0.9% NaCl) and a total volume of 5 ml/kg (5 mg/kg) body weight was injected into a tail vein (n = 5). Blood samples were collected by cardiac puncture under methoxyflurane anesthesia 60 minutes after administration of the drug. Blood samples were kept on melting ice. After centrifugation at 2,100 x *g* for 6 min at 4°C, plasma was supplemented with 4% (v/v) of 2 M acetic acid in water and 1% (v/v) of 0.5 M ascorbic acid in water and stored at -80°C until LC-MS/MS analysis. Acetic acid and ascorbic acid were used to improve the stability of DF-AG and 5OH-DF, respectively [see (25) for details about the stabilization of these metabolites]. In the i.v. experiments, livers were collected immediately after cardiac puncture and stored at -80°C until homogenization. Livers were homogenized in ice-cold 0.3 M sodium acetate, 20 mM ascorbic acid and 4% BSA (m/v) solution (pH 4.5) and homogenates were stored at -80°C until LC-MS/MS analysis.

Biliary excretion. Mice were anesthetized by intraperitoneal injection of a solution of ketamine (100 mg/kg) and xylazine (6.7 mg/kg), in a volume of 4.33 µl per gram body weight. After opening the abdominal cavity and distal ligation of the common bile duct, a polythene catheter (Portex limited, Hythe, UK) with an inner diameter of 0.28 mm, was inserted into the incised gall bladder and fixed with an additional ligation. Bile was collected for 60 min after i.v. injection of 5 mg/kg DF in a tube placed on ice, containing 10 µl 2M acetic acid and 1µl 0.5 M ascorbic

acid. At the end of the experiment, blood was collected under methoxyflurane anesthesia by cardiac puncture and processed as described above. Mice were sacrificed by cervical dislocation and livers were collected en processed as described above. To determine the total biliary output of DF and metabolites, biliary excretion after dosing of 5 mg/kg DF, supplemented with [^{14}C]DF (~0.5 μCi per animal), was assessed in WT mice (n = 4). The levels of radioactivity were determined by liquid scintillation counting.

LC-MS/MS analysis. For the quantitative analysis of DF and its three principal metabolites we set up and validated a fast and sensitive LC-MS/MS method (25).

Toxicity studies. WT and *Mrp2/Mrp3/Bcrp1*$^{-/-}$ mice were fasted overnight and i.p. injected with 5 ml/kg (25 mg/kg) body weight DF (Voltaren, 5-fold diluted with 0.9% NaCl solution to 5 mg/ml). Blood was collected from the tail vein 3 hr after administration, using heparinized capillary tubes (Oxford Labware, St. Louis, USA). Twenty-four hr after administration, blood was collected under methoxyflurane anesthesia by cardiac puncture and mice were sacrificed by cervical dislocation. Blood was centrifuged at 2,100 x *g* for 6 min at 4°C, plasma was collected and stored at -20 °C until analysis. Alanine aminotransferase (ALAT) levels in plasma were determined as a marker for hepatotoxicity, using a Roche Hitachi 917 analyzer (Roche diagnostics, Basel, Switzerland).

Pharmacokinetic calculations and statistical analysis. The area under the plasma concentration-time curve (AUC) was calculated using the trapezoidal rule, without extrapolating to infinity. To assess the statistical significance, we performed one-way ANOVA followed by Dunnett's multiple comparison test. Differences were considered statistically significant when $P < 0.05$. Data are presented as means ± SD.

RESULTS

DF plasma pharmacokinetics in *Mrp2*$^{-/-}$, *Bcrp1*$^{-/-}$ and *Mrp2/Bcrp1*$^{-/-}$ mice. To assess the roles of Mrp2 and Bcrp1 in the plasma pharmacokinetics of DF, we orally administered 5 mg/kg DF to WT, *Mrp2*$^{-/-}$, *Bcrp1*$^{-/-}$ and *Mrp2/Bcrp1*$^{-/-}$ mice and collected blood at multiple time points (Fig. 2). Mrp2 and Bcrp1 did not affect the oral uptake of DF, i.e. no differences in plasma concentrations were observed among all genotypes (Fig. 2A). In contrast, plasma concentrations of DF-AG, the main glucuronide metabolite of DF were highly increased in *Mrp2*$^{-/-}$ and *Mrp2/Bcrp1*$^{-/-}$ mice (Fig. 2B). Consequently, the area under the plasma-concentration time curve (AUC), which is a measure for the exposure to DF-AG, was 8.0-fold higher in *Mrp2*$^{-/-}$ mice (2.18 ± 0.60 mg.hr/L) and 13.9-fold elevated in *Mrp2/Bcrp1*$^{-/-}$ mice (3.79 ± 1.53 mg.hr/L), both compared to WT mice (0.27 ± 0.10

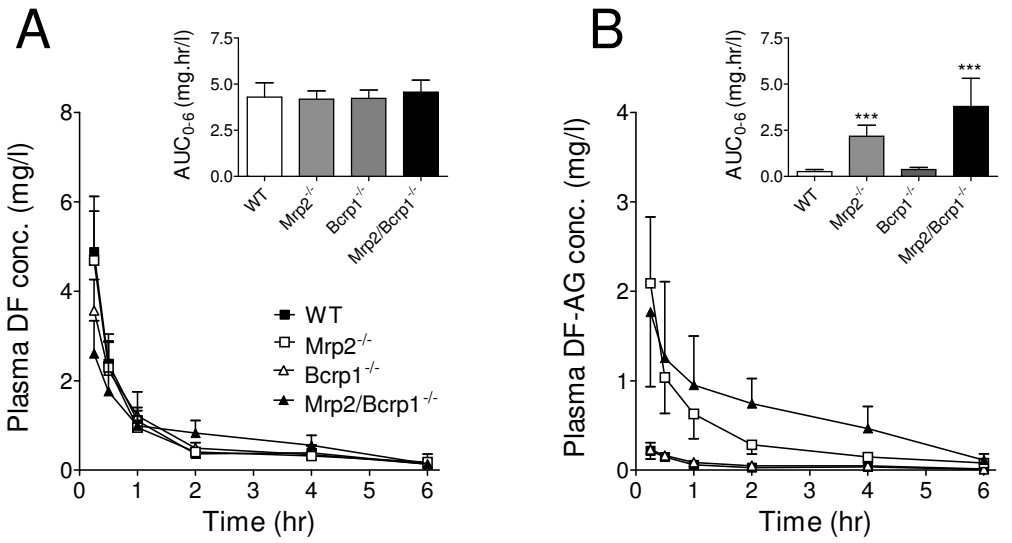

Fig. 2. Plasma concentration-time curves of DF (*A*) and DF-AG (*B*) in male FVB WT (■), *Mrp2*$^{-/-}$ (□), *Bcrp1*$^{-/-}$ (Δ), and *Mrp2/Bcrp1*$^{-/-}$ (▲) mice, after oral administration of 5 mg/kg DF. Data are means ± SD, n = 5. Inserts in the panels show the area under the curve from 0-6 hr (AUC_{0-6}) for DF (*A*) and DF-AG (*B*) in the different strains. *** $P < 0.001$, compared to WT mice.

mg.hr/L; Fig. 1B, insert). Furthermore, *Mrp2/Bcrp1*$^{-/-}$ mice had significantly higher DF-AG plasma concentrations than *Mrp2*$^{-/-}$ mice at 2 and 4 hr after oral administration, although the AUC_{0-6} was just not significantly different between these genotypes ($P = 0.06$; Fig. 2B). Deficiency of Mrp2 thus seems the main cause of the highly increased DF-AG plasma concentrations. The maximal plasma concentrations of DF as well as DF-AG were probably reached before the first sampling time point, i.e.15 min after oral administration (Fig. 2A and 2B), testifying to the rapid kinetics of these compounds.

Biliary excretion of DF and DF-AG in *Mrp2*$^{-/-}$, *Bcrp1*$^{-/-}$ and *Mrp2/Bcrp1*$^{-/-}$ mice. As the metabolic conversion of DF predominantly occurs in the liver (26), the highly increased plasma concentrations of DF-AG in *Mrp2*$^{-/-}$ and *Mrp2/Bcrp1*$^{-/-}$ mice might be the result of disrupted biliary elimination of DF-AG via Mrp2 and/or Bcrp1. We therefore measured the biliary excretion of DF-AG in *Mrp2*$^{-/-}$, *Bcrp1*$^{-/-}$ and *Mrp2/Bcrp1*$^{-/-}$ mice (Fig. 3; Table 1). DF was i.v. administered at 5 mg/kg to mice with a cannulated gall bladder and bile was collected for 60 minutes, immediately followed by isolation of plasma and liver.

Table 1. Diclofenac and three primary metabolites as determined in bile, livers and plasma of mice with cannulated gall bladder, 60 minutes after i.v. administration of diclofenac at 5 mg/kg.

Biological Matrix	Compound	Genotype			
		WT	*Mrp2*$^{-/-}$	*Bcrp1*$^{-/-}$	*Mrp2/Bcrp1*$^{-/-}$
Bile	Diclofenac	0.036 ± 0.033	0.033 ± 0.007	0.042 ± 0.014	0.044 ± 0.010
(% of dose)	Diclofenac AG	4.22 ± 1.39	2.12 ± 0.33*	1.96 ± 0.72*	1.11 ± 0.22**/#/†
	4'-hydroxy diclofenac	0.140 ± 0.055	0.008 ± 0.004**	0.145 ± 0.034	0.007 ± 0.002***/††
	5-hydroxy diclofenac	0.053 ± 0.024	0.022 ± 0.008*	0.039 ± 0.010	0.017 ± 0.003**/†
Liver	Diclofenac	4.57 ± 2.00	2.88 ± 1.23	3.92 ± 2.09	4.32 ± 1.44
(% of dose)	Diclofenac AG	0.47 ± 0.23	0.36 ± 0.31	0.84 ± 0.28*/#	1.76 ± 0.40***/##/†
	4'-hydroxy diclofenac	0.46 ± 0.17	0.42 ± 0.18	0.44 ± 0.20	0.42 ± 0.15
	5-hydroxy diclofenac	1.31 ± 0.59	0.77 ± 0.38	1.28 ± 0.45	0.94 ± 0.28
Plasma	Diclofenac	6.74 ± 3.06	3.75 ± 1.71	5.06 ± 3.39	6.54 ± 1.74
(mg/l)	Diclofenac AG	0.23 ± 0.10	0.95 ± 0.16***	0.30 ± 0.11	1.64 ± 0.49***/#/††
	4'-hydroxy diclofenac	0.23 ± 0.11	0.19 ± 0.08	0.22 ± 0.16	0.21 ± 0.07
	5-hydroxy diclofenac	0.90 ± 0.30	0.58 ± 0.15	0.82 ± 0.32	0.63 ± 0.15

Plasma concentrations are expressed as mg/l and liver and bile concentrations are given as percentage of the dose. Data are given as means ± SD, n = 4-6. * $P < 0.05$, ** $P < 0.01$ and *** $P < 0.001$, compared to WT mice. # $P < 0.05$ and ## $P < 0.01$, compared to *Mrp2*$^{-/-}$ mice. † $P < 0.05$ and †† $P < 0.01$, compared to *Bcrp1*$^{-/-}$ mice.

The amounts of DF recovered in bile, liver and plasma were not affected by Mrp2 and/or Bcrp1 deficiency (Fig. 3A, C and E). The amount of DF occurring in bile was also very small (< 0.05% of the dose), in spite of considerable accumulation in the liver (~4% of the dose). In contrast, the considerably higher biliary output of DF-AG (~4% of the dose) was ~2-fold reduced in both single *Mrp2*$^{-/-}$ or *Bcrp1*$^{-/-}$ mice compared to WT mice, and approximately 4-fold in compound *Mrp2/Bcrp1*$^{-/-}$ mice (Fig. 3B). Interestingly, the ~2-fold lower biliary excretion of DF-AG in *Mrp2*$^{-/-}$ and *Bcrp1*$^{-/-}$ mice was associated with elevated DF-AG plasma but not liver concentrations in *Mrp2*$^{-/-}$ mice, whereas the inverse was true for *Bcrp1*$^{-/-}$ mice (Fig. 3D and 3F). We will return to this difference in the discussion. Furthermore, the fact that biliary output of DF-AG was not completely abrogated in *Mrp2/Bcrp1*$^{-/-}$ mice points towards additional efflux mechanism(s) for DF-AG in the canalicular membrane, other than Mrp2 and Bcrp1. Nonetheless, the lower biliary excretion of DF-AG in *Mrp2/Bcrp1*$^{-/-}$ mice was associated with both increased liver concentrations (Fig. 3D) and higher plasma concentrations (Fig. 3F).

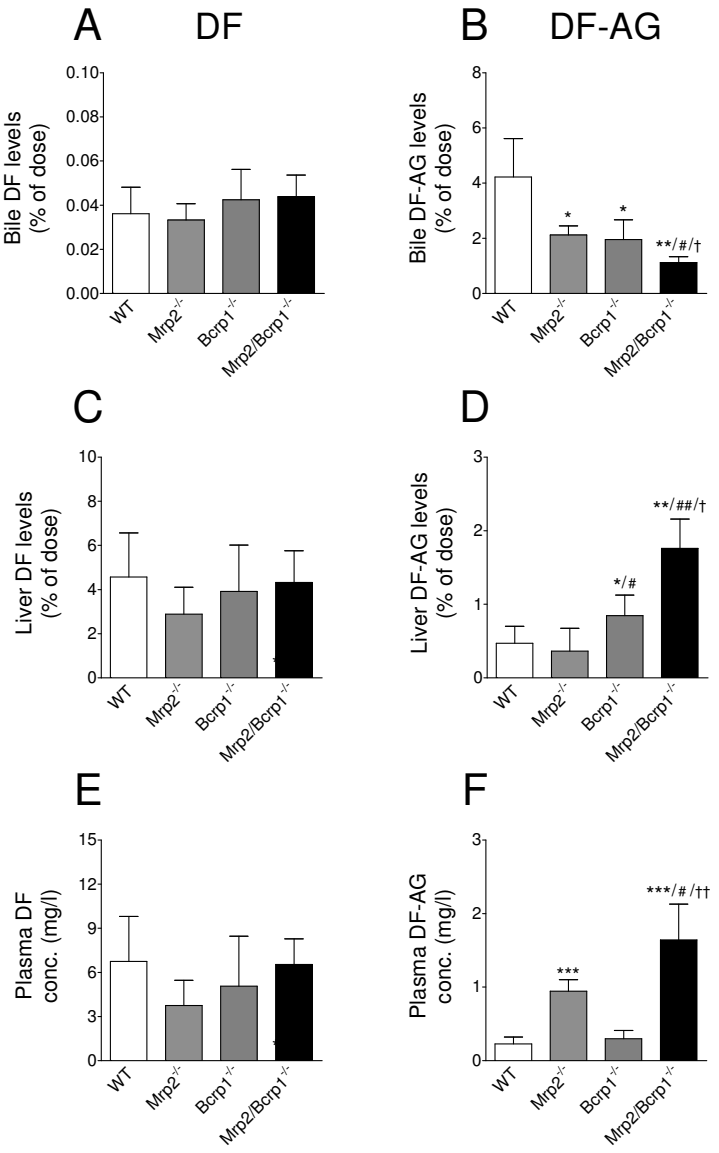

Fig. 3. Levels of DF and DF-AG in bile (*A*, *B*), liver (*C*, *D*) and plasma (*E*, *F*) of male WT, *Mrp2*$^{-/-}$, *Bcrp1*$^{-/-}$ and *Mrp2/Bcrp1*$^{-/-}$ mice, with a cannulated gall bladder. After ligation of the common bile duct and cannulation of the gall bladder DF (5 mg/kg) was given i.v. followed by bile collection for 60 min and tissue isolation at 60 min. Data represent means ± SD (n = 5 per strain). * $P < 0.05$, ** $P < 0.01$ and *** $P < 0.001$, compared to WT mice. # $P < 0.05$ and ## $P < 0.01$, compared to *Mrp2*$^{-/-}$ mice. † $P < 0.05$ and †† $P < 0.01$, compared to *Bcrp1*$^{-/-}$ mice.

Biliary excretion of 4OH-DF and 5OH-DF in *Mrp2*$^{-/-}$, *Bcrp1*$^{-/-}$ and *Mrp2/Bcrp1*$^{-/-}$ mice. The levels of the two principal hydroxylated metabolites of DF, 4OH-DF and 5OH-DF (Fig. 1), were also measured in plasma, bile and liver (Table 1). Interestingly, although liver and plasma levels of these metabolites were not significantly different, the biliary output of 4OH-DF was 17.3- and 19.2-fold decreased in *Mrp2*$^{-/-}$ and *Mrp2/Bcrp1*$^{-/-}$ mice, respectively ($P < 0.01$; Table 1). Furthermore, the excretion of 5OH-DF in the bile was 2.4- and 3.2-fold lower in *Mrp2*$^{-/-}$ and *Mrp2/Bcrp1*$^{-/-}$ mice, respectively ($P < 0.05$; Table 1). In single *Bcrp1*$^{-/-}$ mice, the biliary excretion of these metabolites was not different from WT mice. The biliary output of these hydroxylated DF metabolites, particularly of 4OH-DF, thus seems to depend largely on Mrp2. However, the impact of this process on liver and plasma levels of these metabolites was negligible, in line with the modest amounts excreted into bile.

Biliary excretion of DF glucuronide metabolites other than DG-AG in *Mrp2*$^{-/-}$, *Bcrp1*$^{-/-}$ and *Mrp2/Bcrp1*$^{-/-}$ mice. To determine the total biliary output of DF and its metabolites in mice, we i.v. administered 5 mg/kg DF, supplemented with a tracer amount of [^{14}C]DF, to WT mice and we measured the biliary excretion. Over a period of 60 minutes, 42.6 ± 4.4% of the dose was excreted into the bile as ^{14}C-label. This is consistent with a study in rats with a cannulated bile duct that received 3 mg/kg [^{14}C]DF i.v. and excreted 57% of the dose as ^{14}C-label into the bile within 90 min (18). As depicted in Table 1, the biliary excretion of DF and DF-AG in WT mice was 0.04 and 4.2% of the dose, respectively. In addition, the excretion of 4OH-DF and 5OH-DF into the bile accounted for 0.14 and 0.053% of the dose, respectively (Table 1). Together, DF and its primary metabolites represent only ~10% of the ^{14}C-label excreted into bile. The majority of the radioactivity in the bile must thus originate from DF metabolites other than DF-AG, 4OH-DF or 5OH-DF. When analyzed with LC-MS/MS, we indeed observed additional peaks in the chromatograms of the bile samples. Based on mass, retention time, and fragmentation patterns, 4OH-DF-AG and 5OH-DF-AG could be identified. Another peak represented isomer(s) of DF-AG, which originated from epimerization of the 1-*O*-glucuronide by acyl migration to 2-, 3- or 4-*O*-glucuronide (10;13). Acyl migration especially occurs at alkaline pH, and since mouse bile has a pH of ~9, it is possible that a significant amount of the DF-AG was converted to isomeric isoforms before we could stabilize the compound with acetic acid. As we do not have reference standards for these compounds, these metabolites could not be quantified and therefore their biliary output is given in arbitrary units (Fig. 4). Notably, the excretion patterns of 4OH-DF-AG, 5OH-DF-AG and the isomers of DF-AG are qualitatively similar to that of DF-AG,

indicating that biliary excretion of these glucuronide metabolites is predominantly mediated by Mrp2 and Bcrp1.

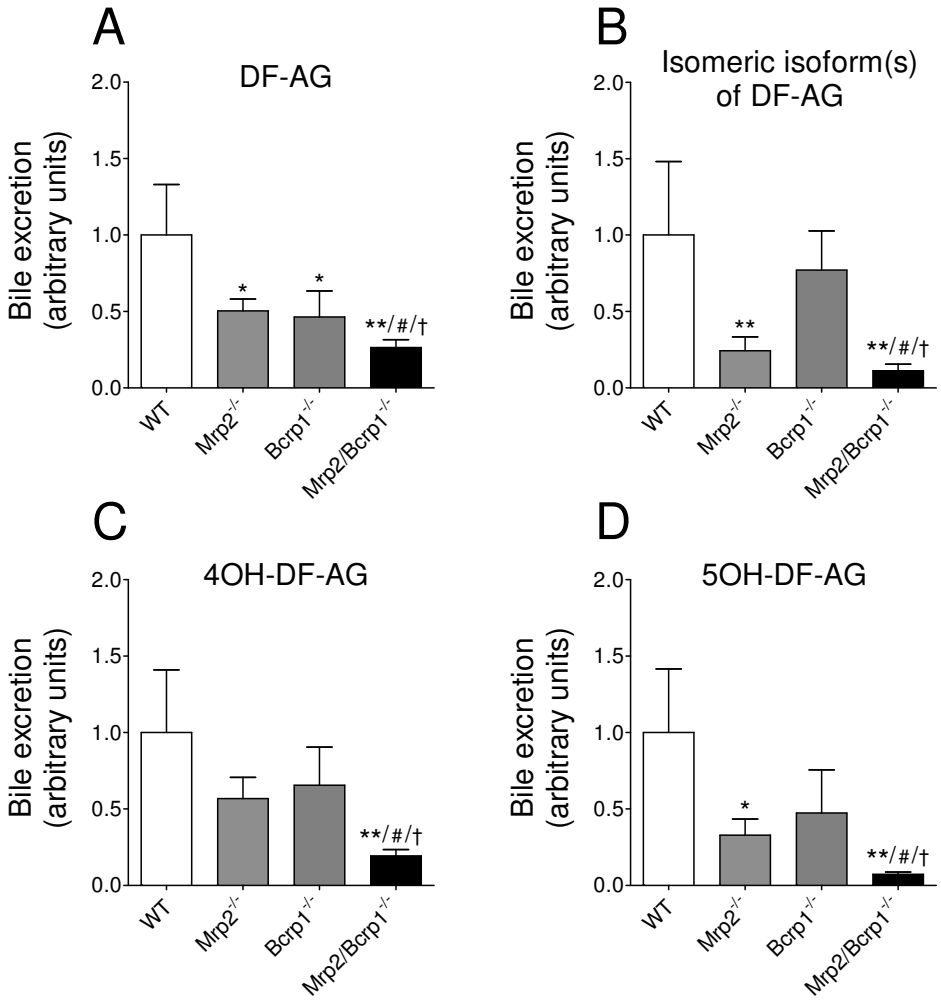

Fig. 4. Levels of DF-AG (*A*), isomeric isoform(s) of DF-AG (*B*), 4OH-DF-AG (*C*) and 5OH-DF-AG (*D*) in bile of male gall bladder cannulated WT, *Mrp2*$^{-/-}$,*Bcrp1*$^{-/-}$ and *Mrp2/Bcrp1*$^{-/-}$ mice. After ligation of the common bile duct and cannulation of the gall bladder DF (5 mg/kg) was given i.v. followed by bile collection for 60 min. Levels are given in arbitrary units. Data represent means ± SD (n = 5 per strain). * $P < 0.05$ and ** $P < 0.01$, compared to WT mice. # $P < 0.05$, compared to *Mrp2*$^{-/-}$ mice. † $P < 0.01$, compared to *Bcrp1*$^{-/-}$ mice.

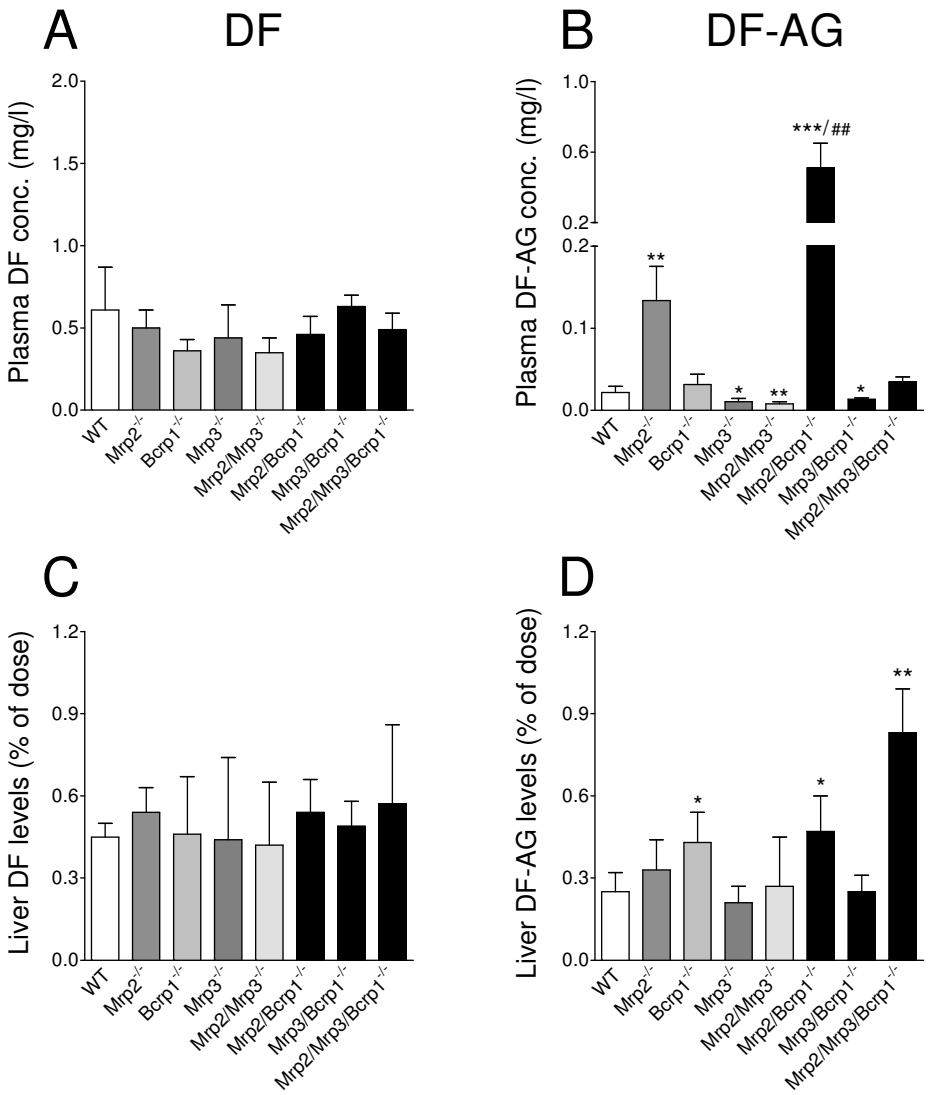

Fig. 5. Levels of DF and DF-AG in plasma (*A*, *B*) and liver (*C*, *D*) of male WT, *Mrp2*$^{-/-}$, *Mrp3*$^{-/-}$, *Bcrp1*$^{-/-}$, *Mrp2/Mrp3*$^{-/-}$, *Mrp2/Bcrp1*$^{-/-}$, *Mrp3/Bcrp1*$^{-/-}$ and *Mrp2/Mrp3/Bcrp1*$^{-/-}$ mice. DF (5 mg/kg) was given i.v. followed by plasma collection and tissue isolation at 60 min. Data represent means ± SD (n = 5 per strain). * $P < 0.05$, ** $P < 0.01$ and *** $P < 0.001$, compared to WT mice. ## $P < 0.01$, compared to *Mrp2*$^{-/-}$mice.

Basolateral efflux of DF-AG in the liver is mediated by Mrp3. In the liver, Mrp3 is expressed at the sinusoidal membranes of hepatocytes and it transports its substrates towards the blood circulation. Because Mrp3 is a typical organic anion transporter with a preference for glucuronidated substrates [reviewed in (19)], we tested whether Mrp3 was involved in the basolateral efflux of DF-AG from the liver. DF (5 mg/kg) was i.v. administered at to conscious, freely moving WT, *Mrp2*$^{-/-}$, *Mrp3*$^{-/-}$ and *Bcrp1*$^{-/-}$ mice and all possible combinations of these single knockout strains, and plasma and livers were collected 60 minutes after injection. As shown in figures 5A and 5C, plasma and liver concentrations of DF were not affected by single and combined transporter deficiencies. In contrast, plasma concentrations of DF-AG were 6.2-fold increased in *Mrp2*$^{-/-}$ mice and 24-fold in *Mrp2/Bcrp1*$^{-/-}$ mice (Fig. 5B), consistent with the results obtained after oral administration (Fig 2B). Strikingly, the highly increased plasma concentrations in *Mrp2/Bcrp1*$^{-/-}$ mice were restored to WT levels in *Mrp2/Mrp3/Bcrp1*$^{-/-}$ mice (Fig. 5B), and a similar shift was seen between *Mrp2*$^{-/-}$ and *Mrp2/Mrp3*$^{-/-}$ mice. This suggests that Mrp3 is mainly responsible for the efflux of DF-AG across the basolateral membrane. The observation that plasma DF-AG levels in single *Mrp3*$^{-/-}$ mice and in combination *Mrp2/Mrp3*$^{-/-}$ and *Mrp3/Bcrp1*$^{-/-}$ mice were even significantly lower than in WT mice further supports a functional role of Mrp3 for the efflux of DF-AG from the liver towards the blood (Fig. 5B). Accordingly, the DF-AG concentrations in the liver, determined at 60 minutes after administration, were ~1.8-fold elevated in *Bcrp1*$^{-/-}$ and *Mrp2/Bcrp1*$^{-/-}$ mice, and 3.3-fold in *Mrp2/Mrp3/Bcrp1*$^{-/-}$ mice (Fig. 5D). Interestingly, in the livers of *Mrp2/Mrp3/Bcrp1*$^{-/-}$ mice, but not in WT livers, also substantial accumulation of 4OH-DF-AG, 5OH-DF-AG and of DF-AG isomers was observed (not shown). As mentioned above, the lack of reference compounds made it impossible to quantify these metabolites. However, as DF acyl glucuronide metabolites are associated with idiosyncratic hepatotoxicity [reviewed in (4;17)] we hypothesized that *Mrp2/Mrp3/Bcrp1*$^{-/-}$ mice might be more prone to DF-induced liver toxicity than WT mice.

***Mrp2/Mrp3/Bcrp1*$^{-/-}$ mice develop mild DF-induced acute hepatotoxicity.** To test whether *Mrp2/Mrp3/Bcrp1*$^{-/-}$ mice were more sensitive to DF-induced liver toxicity, DF was i.p. administered at 25 mg/kg to WT and *Mrp2/Mrp3/Bcrp1*$^{-/-}$ mice (n = 4) and ALAT levels in plasma were determined 3 and 24 hr after administration (Fig. 6). WT mice had slightly, but not significantly higher ALAT levels 3 hr after administration, which were restored to control levels at 24 hr. In contrast, treatment of *Mrp2/Mrp3/Bcrp1*$^{-/-}$ mice with DF resulted in significant ~2-fold higher ALAT levels at both time points, suggesting that these mice displayed acute, albeit mild, liver toxicity.

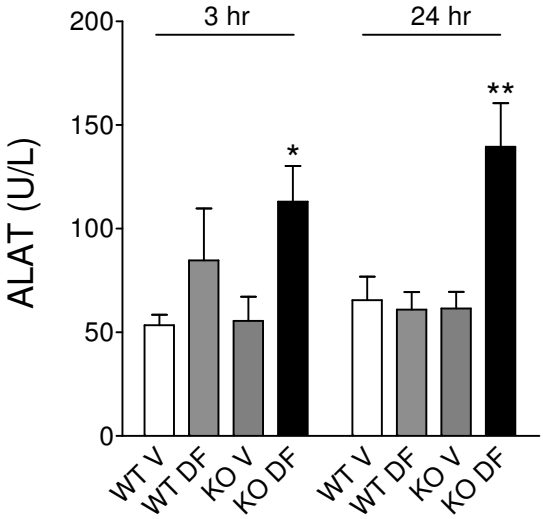

Fig. 6. Plasma levels of alanine aminotransferase (ALAT) in WT and KO (*Mrp2/Mrp3/Bcrp1*$^{-/-}$) mice. Mice were i.p. injected with vehicle (V) or DF (25 mg/kg) and blood was collected 3 hr and 24 hr after administration. Data represent means ± SD (n = 4 per strain). * $P < 0.05$ and ** $P < 0.01$, compared to WT mice receiving vehicle.

DISCUSSION

In this study we identify Mrp2, Mrp3 and Bcrp1 in the mouse as important determinants for the pharmacokinetics of reactive glucuronide metabolites of DF. Mrp2 and Bcrp1 are involved in the biliary excretion of DF glucuronides, whereas Mrp3 is a major hepatic transporter for the extrusion of DF-AG across the sinusoidal membrane towards the blood circulation. Simultaneous loss of Mrp2, Mrp3 and Bcrp1 results in substantial accumulation of reactive glucuronide metabolites in the liver, with acute but mild hepatotoxicity as a consequence.

We recently demonstrated that mouse Bcrp1 can transport DF *in vitro* (20). In this study, however, loss of Bcrp1 in mice did not affect the oral uptake or biliary excretion of DF. On the other hand, deficiencies in Bcrp1 and Mrp2 resulted in impaired biliary output of DF glucuronides. In addition to glucuronides, we also found that Mrp2, but not Bcrp1, mediates the biliary excretion of the hydroxylated DF metabolites, 4OH-DF and 5OH-DF.

From studies in rats, Mrp2 was already known to mediate the biliary excretion of DF glucuronides (10;18). Moreover, hepatobiliary excretion of DF glucuronides in TR$^-$ rats, a spontaneous mutant lacking Mrp2, is almost completely abrogated (18). In contrast, in mice we show that the biliary excretion of DF glucuronides is

mainly dependent on both Mrp2 and Bcrp1. This species difference is in line with previous findings showing that the biliary excretion of 4-methylumbelliferyl glucuronide in rats is primarily mediated by Mrp2, whereas in mice both Mrp2 and Bcrp1 play a role in this process (27;28). Our observation that the biliary output of DF-AG was not completely abrogated in *Mrp2/Bcrp1*$^{-/-}$ mice may point towards the existence of other efflux mechanism(s) in the canalicular membrane, in addition to MRP2 and BCRP. Nonetheless, simultaneous loss of Mrp2 and Bcrp1 resulted in increased liver concentrations (Figs 3D and 5D) and, presumably as a consequence, highly increased plasma concentrations (Figs 2B, 3F and 5B) of DF-AG.

Notably, after oral DF administration, maximal plasma concentrations of DF-AG are reached within 15 minutes after administration (Fig 2B). This might suggest that the glucuronidation of DF already occurs in the gastrointestinal tract, as the gut, in addition to the liver, is an important organ for glucuronidation (29). However, studies in rats demonstrate that DF is predominantly glucuronidated in the liver and not in the gut (18;26;30). The glucuronidation of DF in rats is catalyzed by Ugt2b1 (5) and since rat and mouse Ugt2b1 proteins share >85% homology (www.ensembl.org), murine Ugt2b1 may also be primarily responsible for the glucuronidation of DF. In rats and mice, the liver is the predominant tissue for the expression of Ugt2b1, whereas expression in the intestine is low (31;32). We find that approximately 40% of an DF i.v. dose is excreted as glucuronide metabolites in the bile of WT mice within 60 minutes, indicating that the liver indeed is the major tissue for DF glucuronidation in mice. We therefore believe that the early C_{max} of DF-AG (Fig. 2B) may be explained by very fast oral absorption of DF (Fig. 2A), enabling rapid hepatic uptake and subsequent conversion to DF-AG. The fact that DF was given as an aqueous solution in combination with temporary food deprivation before administration may explain the rapid absorption of the drug. Indeed, in humans the T_{max} of an aqueous DF solution was reached in 10-30 min, whereas this was ~2 hr for a tablet with the same DF dose (8).

Mrp3 has a preference for glucuronidated compounds and plays a dominant role in the transport of glucuronides across the sinusoidal membrane of hepatocytes [reviewed in (19)]. Our results suggest that Mrp3 also predominantly mediates the transport of DF-AG from the liver toward the blood circulation. We have recently shown that Mrp3 is upregulated in livers of *Mrp2*$^{-/-}$ and *Mrp2/Bcrp1*$^{-/-}$ mice (22 and Vlaming et al., in press). This likely explains that, although the biliary DF-AG excretion is impaired in *Mrp2*$^{-/-}$ and *Mrp2/Bcrp1*$^{-/-}$ mice, substantial hepatic accumulation of DF-AG is not observed (Fig. 5D). Instead, plasma concentrations of DF-AG are highly elevated in *Mrp2*$^{-/-}$ and *Mrp2/Bcrp1*$^{-/-}$ mice (Figs 2B, 3F and 5B). In contrast, in *Bcrp1*$^{-/-}$ mice, which do not have altered Mrp3 expression in

their liver (Vlaming *et al*, in press), impaired biliary excretion of DF-AG results in liver accumulation without elevated plasma concentration (Figs 3D and 3F).

Acyl glucuronides are electrophilic, chemically reactive compounds that can form protein adduct via non-enzymatic reactions (13). Hepatic protein adducts of DF acyl glucuronides, including hydroxylated DF-AG metabolites and DF-AG isomers, are believed to play an important role in DF-induced idiosyncratic hepatotoxicity [reviewed in (4;17)]. Seitz and colleagues showed that the formation of these hepatic adducts is critically dependent on Mrp2 (18). This makes sense, as perfusion of rat livers with gemfibrozil acyl glucuronide, which is also excreted into the bile by Mrp2 (33), resulted in a significant concentration gradient between the sinusoid circulation (blood), hepatocytes and bile in the order of 1:50:5000 (34;35). As a consequence of Mrp2-mediated canalicular export, acyl glucuronide concentrations in the biliary tree are high, which likely explains why intra-hepatic protein adduct formation most frequently occurs with proteins that are exposed to the canalicular lumen [(13) and references therein]. Reduced MRP2 activity, or complete loss of MRP2, might thus prevent the formation of protein adducts by reactive acyl glucuronides in the biliary tree, thereby preventing liver toxicity. Interestingly, Daly and co-workers (2007) found that a C-24T polymorphism in the ABCC2 gene (coding for MRP2) was significantly more common in patients who suffered from DF-induced hepatotoxicity than in hospital controls (patients on DF without any signs of liver toxicity) or healthy controls (36). The functional significance of this mutation is still not clear, and Daly and colleagues argued that decreased expression and/or activity of MRP2 would lead to accumulation of DF glucuronides within the hepatocytes (36). However, our data suggest that even complete loss of Mrp2 in mice does not result in hepatic accumulation of DF-AG. We therefore argue that the ABCC2 C-24T variant might lead to increased hepatic expression and/or activity of MRP2, resulting in increased DF glucuronide levels in the biliary tree, with subsequent adduct formation and hepatotoxicity (*vide supra*). Interestingly, in humans DF acyl glucuronides are predominantly excreted from the liver to the blood circulation and subsequently excreted in the urine (2;7;8). This could mean that MRP3 in the sinusoidal membrane of human hepatocytes has a higher affinity for DF acyl glucuronides than canalicular MRP2. In that case, decreased hepatic MRP3 expression and/or activity might result in increased MRP2-mediated biliary excretion of reactive acyl glucuronides and possibly lead to increased hepatotoxicity.

The 24-fold increased plasma level of DF-AG in *Mrp2/Bcrp1*$^{-/-}$ mice (Fig. 5B) was restored to WT levels in *Mrp2/Mrp3/Bcrp1*$^{-/-}$ mice. We therefore had expected that DF-AG would be highly accumulated in the livers of in *Mrp2/Mrp3/Bcrp1*$^{-/-}$ mice, but hepatic levels of DF-AG in this strain were only 3.3-fold higher than in

WT mice (Fig. 5D). The relatively low accumulation of DF-AG in the liver of *Mrp2/Mrp3/Bcrp1*$^{-/-}$ mice might partially be explained by the fact that biliary excretion of DF-AG in *Mrp2/Bcrp1*$^{-/-}$ mice is not completely abrogated, but reduced by ~75% (Fig. 3B). There must thus be other canalicular efflux system(s) for DF-AG, possibly with low affinity and high capacity. However, subsequent hydroxylation of DF-AG and/or acyl migration of DF-AG may also contribute to the relatively low DF-AG concentration in the liver of *Mrp2/Mrp3/Bcrp1*$^{-/-}$ mice. Indeed, DF-AG can undergo further hydroxylation in the liver (6). In fact, in rats the biliary excretion of metabolites that were hydroxylated and glucuronidated was approximately equal to that of DF-AG (10). Furthermore, substantial acyl migration has been observed *in vivo* as well (13;17). Our results suggest that the majority of radioactivity in the bile of WT mice can be attributed to 4OH-DF-AG, 5OH-DF-AG and DF-AG isomer(s). Unfortunately, these metabolites could not be quantified, but the biliary efflux of these compounds was largely dependent on Mrp2 and Bcrp1 (Fig. 4). Furthermore, these metabolites are putative substrates for Mrp3, which is supported by their presence in *Mrp2/Mrp3/Bcrp1*$^{-/-}$ livers, whereas they could not be detected in WT livers. Overall, circumstantial evidence thus suggests that *Mrp2/Mrp3/Bcrp1*$^{-/-}$ mice accumulate substantial amounts of DF acyl glucuronides in addition to DF-AG in their livers. We therefore tested if these mice were more prone to DF-induced hepatotoxicity. Indeed, *Mrp2/Mrp3/Bcrp1*$^{-/-}$ mice displayed 2-fold elevated plasma ALAT levels, whereas WT did not, suggesting that *Mrp2/Mrp3/Bcrp1*$^{-/-}$ mice experienced some acute, albeit mild liver toxicity.

On the other hand, intra-hepatic protein adduct formation by DF-AG in rats was shown to be dependent on Mrp2 (*vide supra*) (18). This suggests that Mrp2 deficiency might protect the liver form DF-induced toxicity and possibly explains why *Mrp2/Mrp3/Bcrp1*$^{-/-}$ mice do not display severe hepatotoxicity. Furthermore, in humans, the rare idiosyncratic hepatotoxicity that can be induced by DF is characterized by a delayed onset of symptoms and usually occurs between 1 and 6 months after starting the treatment (4;17). There are many indications that, in addition to hepatic adduct formation by reactive metabolites, other factors, including immune-mediated responses, contribute to the liver toxicity (4;17). Our results suggest some acute but mild liver toxicity in *Mrp2/Mrp3/Bcrp1*$^{-/-}$ mice, and although it was beyond the scope of this study, it might be interesting to investigate this toxicity in more detail or in a much longer time frame in these transporter deficient mouse models.

In conclusion, our results show that Mrp2, Mrp3 and Bcrp1 play an important role in the distribution and elimination of DF acyl glucuronides in mice, both after oral and intravenous administration. We expect that acyl glucuronide metabolites of more drugs will be similarly handled by these ABC transporters.

ACKNOWLEDGMENTS

We thank Mr. Enver Dilec of the Department of Clinical Chemistry at the NKI-AVL for technical assistance, and our colleagues for critical reading of the manuscript.

REFERENCES

(1) Davies NM, Anderson KE. Clinical pharmacokinetics of diclofenac. Therapeutic insights and pitfalls. Clin Pharmacokinet 1997;33:184-213.

(2) Stierlin H, Faigle JW, Sallmann A, Kung W, Richter WJ, Kriemler HP et al. Biotransformation of diclofenac sodium (Voltaren) in animals and in man. I. Isolation and identification of principal metabolites. Xenobiotica 1979;9:601-10.

(3) Peris-Ribera JE, Torres-Molina F, Garcia-Carbonell MC, Aristorena JC, Pla-Delfina JM. Pharmacokinetics and bioavailability of diclofenac in the rat. J Pharmacokinet Biopharm 1991;19:647-65.

(4) Tang W. The metabolism of diclofenac--enzymology and toxicology perspectives. Curr Drug Metab 2003;4:319-29.

(5) King C, Tang W, Ngui J, Tephly T, Braun M. Characterization of rat and human UDP-glucuronosyltransferases responsible for the in vitro glucuronidation of diclofenac. Toxicol Sci 2001;61:49-53.

(6) Kumar S, Samuel K, Subramanian R, Braun MP, Stearns RA, Chiu SH et al. Extrapolation of diclofenac clearance from in vitro microsomal metabolism data: role of acyl glucuronidation and sequential oxidative metabolism of the acyl glucuronide. J Pharmacol Exp Ther 2002;303:969-78.

(7) Willis JV, Kendall MJ, Flinn RM, Thornhill DP, Welling PG. The pharmacokinetics of diclofenac sodium following intravenous and oral administration. Eur J Clin Pharmacol 1979;16:405-10.

(8) John VA. The pharmacokinetics and metabolism of diclofenac sodium (Voltarol) in animals and man. Rheumatol Rehabil 1979;Suppl 2:22-37.

(9) Willis JV, Kendall MJ, Jack DB. A study of the effect of aspirin on the pharmacokinetics of oral and intravenous diclofenac sodium. Eur J Clin Pharmacol 1980;18:415-8.

(10) Seitz S, Boelsterli UA. Diclofenac acyl glucuronide, a major biliary metabolite, is directly involved in small intestinal injury in rats. Gastroenterology 1998;115:1476-82.

(11) Dickinson RG, King AR. Studies on the reactivity of acyl glucuronides-II. Interaction of diflunisal acyl glucuronide and its isomers with human serum albumin in vitro. Biochem Pharmacol 1991;42:2301-6.

(12) Ding A, Ojingwa JC, McDonagh AF, Burlingame AL, Benet LZ. Evidence for covalent binding of acyl glucuronides to serum albumin via an imine mechanism as revealed by tandem mass spectrometry. Proc Natl Acad Sci U S A 1993;90:3797-801.

(13) Sallustio BC, Sabordo L, Evans AM, Nation RL. Hepatic disposition of electrophilic acyl glucuronide conjugates. Curr Drug Metab 2000;1:163-80.

(14) Borst P, Oude Elferink RP. Mammalian ABC transporters in health and disease. Annu Rev Biochem 2002;71:537-92.

(15) Schinkel AH, Jonker JW. Mammalian drug efflux transporters of the ATP binding cassette (ABC) family: an overview. Adv Drug Deliv Rev 2003;55:3-29.

(16) Borst P, Zelcer N, van de Wetering K. MRP2 and 3 in health and disease. Cancer Lett 2006;234:51-61.

(17) Boelsterli UA. Diclofenac-induced liver injury: a paradigm of idiosyncratic drug toxicity. Toxicol Appl Pharmacol 2003;192:307-22.

(18) Seitz S, Kretz-Rommel A, Oude Elferink RP, Boelsterli UA. Selective protein adduct formation of diclofenac glucuronide is critically dependent on the rat canalicular conjugate export pump (Mrp2). Chem Res Toxicol 1998;11:513-9.

(19) Borst P, de Wolf C, van de Wetering K. Multidrug resistance-associated proteins 3, 4, and 5. Pflugers Arch 2007;453:661-73.

(20) Lagas JS, van der Kruijssen CM, van de Wetering K, Beijnen JH, Schinkel AH. Transport of diclofenac by breast cancer resistance protein (ABCG2) and stimulation of multidrug resistance protein 2 (ABCC2)-mediated drug transport by diclofenac and benzbromarone. Drug Metab Dispos 2009;37:129-36.

(21) Jonker JW, Buitelaar M, Wagenaar E, Van Der Valk MA, Scheffer GL, Scheper RJ et al. The breast cancer resistance protein protects against a major chlorophyll-derived dietary phototoxin and protoporphyria. Proc Natl Acad Sci U S A 2002;99:15649-54.

(22) Vlaming ML, Mohrmann K, Wagenaar E, de Waart DR, Elferink RP, Lagas JS et al. Carcinogen and anticancer drug transport by Mrp2 in vivo: studies using Mrp2 (Abcc2) knockout mice. J Pharmacol Exp Ther 2006;318:319-27.

(23) Zelcer N, van de Wetering K, Hillebrand M, Sarton E, Kuil A, Wielinga PR et al. Mice lacking multidrug resistance protein 3 show altered morphine pharmacokinetics and morphine-6-glucuronide antinociception. Proc Natl Acad Sci U S A 2005;102:7274-9.

(24) van de Wetering K, Zelcer N, Kuil A, Feddema W, Hillebrand M, Vlaming ML et al. Multidrug resistance proteins 2 and 3 provide alternative routes for hepatic excretion of morphine-glucuronides. Mol Pharmacol 2007;72:387-94.

(25) Sparidans RW, Lagas JS, Schinkel AH, Schellens JH, Beijnen JH. Liquid chromatography-tandem mass spectrometric assay for diclofenac and three primary metabolites in mouse plasma. J Chromatogr B Analyt Technol Biomed Life Sci 2008;872:77-82.

(26) Vargas M, Franklin MR. Intestinal UDP-glucuronosyltransferase activities in rat and rabbit. Xenobiotica 1997;27:413-21.

(27) Zamek-Gliszczynski MJ, Hoffmaster KA, Humphreys JE, Tian X, Nezasa K, Brouwer KL. Differential involvement of Mrp2 (Abcc2) and Bcrp (Abcg2) in biliary excretion of 4-methylumbelliferyl glucuronide and sulfate in the rat. J Pharmacol Exp Ther 2006;319:459-67.

(28) Zamek-Gliszczynski MJ, Nezasa K, Tian X, Kalvass JC, Patel NJ, Raub TJ et al. The important role of Bcrp (Abcg2) in the biliary excretion of sulfate and glucuronide metabolites of acetaminophen, 4-methylumbelliferone, and harmol in mice. Mol Pharmacol 2006;70:2127-33.

(29) Tukey RH, Strassburg CP. Human UDP-glucuronosyltransferases: metabolism, expression, and disease. Annu Rev Pharmacol Toxicol 2000;40:581-616.

(30) Ware JA, Graf ML, Martin BM, Lustberg LR, Pohl LR. Immunochemical detection and identification of protein adducts of diclofenac in the small intestine of rats: possible role in allergic reactions. Chem Res Toxicol 1998;11:164-71.

(31) Shelby MK, Cherrington NJ, Vansell NR, Klaassen CD. Tissue mRNA expression of the rat UDP-glucuronosyltransferase gene family. Drug Metab Dispos 2003;31:326-33.

(32) Buckley DB, Klaassen CD. Tissue- and gender-specific mRNA expression of UDP-glucuronosyltransferases (UGTs) in mice. Drug Metab Dispos 2007;35:121-7.

(33) Kim MS, Liu DQ, Strauss JR, Capodanno I, Yao Z, Fenyk-Melody JE et al. Metabolism and disposition of gemfibrozil in Wistar and multidrug resistance-associated protein 2-deficient TR- rats. Xenobiotica 2003;33:1027-42.

(34) Sabordo L, Sallustio BC, Evans AM, Nation RL. Hepatic disposition of the acyl glucuronide1-O-gemfibrozil-beta-D-glucuronide: effects of dibromosulfophthalein on membrane transport and aglycone formation. J Pharmacol Exp Ther 1999;288:414-20.

(35) Sabordo L, Sallustio BC, Evans AM, Nation RL. Hepatic disposition of the acyl glucuronide 1-O-gemfibrozil-beta-D-glucuronide: effects of clofibric acid, acetaminophen, and acetaminophen glucuronide. J Pharmacol Exp Ther 2000;295:44-50.

(36) Daly AK, Aithal GP, Leathart JB, Swainsbury RA, Dang TS, Day CP. Genetic susceptibility to diclofenac-induced hepatotoxicity: contribution of UGT2B7, CYP2C8, and ABCC2 genotypes. Gastroenterology 2007;132:272-81.

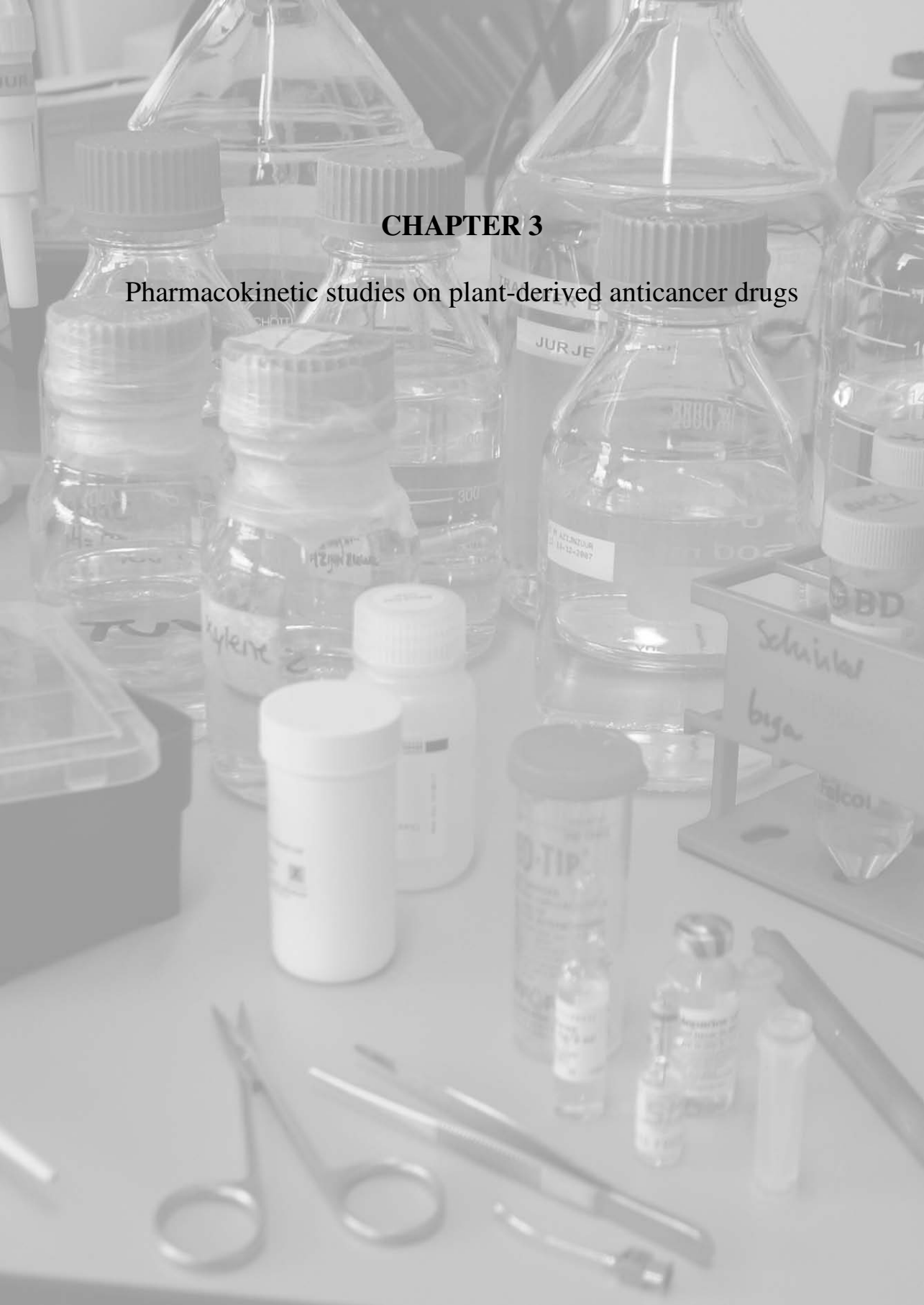

CHAPTER 3

Pharmacokinetic studies on plant-derived anticancer drugs

CHAPTER 3.1

Multidrug resistance protein 2 (MRP2/*ABCC2*) is an important determinant of paclitaxel pharmacokinetics

Jurjen S. Lagas, Maria L. Vlaming, Olaf van Tellingen, Els Wagenaar, Robert S. Jansen, Hilde Rosing, Jos H. Beijnen and Alfred H. Schinkel

Clinical Cancer Research 2006; 12:6125-6132

ABSTRACT

Purpose: P-glycoprotein (*ABCB1*, P-gp) efficiently transports lipophilic amphipathic drugs, including the widely used anti-cancer drug paclitaxel (Taxol). We previously found that human MRP2 (*ABCC2)* also transports paclitaxel *in vitro*, and although we expected that paclitaxel pharmacokinetics would be dominated by P-gp, the impact of Mrp2 was tested *in vivo*. *Experimental design:* We generated and characterized *Mdr1a/b/Mrp2*$^{-/-}$ mice, allowing assessment of the distinct roles of Mrp2 and Mdr1a/1b P-gp in paclitaxel pharmacokinetics. *Results:* Surprisingly, the impact of Mrp2 upon intravenous administration of paclitaxel was as great as that of P-gp. The $AUC_{i.v.}$ in both *Mrp2*$^{-/-}$ and *Mdr1a/1b*$^{-/-}$ mice was 1.3-fold higher than in wild-type mice, and in *Mdr1a/b/Mrp2*$^{-/-}$ mice a 1.7-fold increase was found. In spite of this similar impact, Mrp2 and P-gp had mostly complementary functions in paclitaxel elimination. Mrp2 dominated the hepatobiliary excretion, which was reduced by 80% in *Mrp2*$^{-/-}$ mice. In contrast, P-gp dominated the direct intestinal excretion, with a minor role for Mrp2. The AUC_{oral} of paclitaxel was 8.5-fold increased by Mdr1a/1b deficiency, but not affected by Mrp2 deficiency. However, in the absence of Mdr1a/1b P-gp, additional Mrp2 deficiency increased the AUC_{oral} another 1.7-fold. *Conclusions:* Thusfar, Mrp2 was thought to mainly affect organic anionic drugs *in vivo*. Our data show that Mrp2 can also be a major determinant of the pharmacokinetic behavior of highly lipophilic anti-cancer drugs, even in the presence of other efficient transporters. Variation in MRP2 activity might thus directly affect the effective exposure to paclitaxel, upon intravenous administration, but also upon oral administration, especially when P-gp activity is inhibited.

INTRODUCTION

ATP-binding cassette (ABC) multidrug transporters, like P-glycoprotein (P-gp, *ABCB1*), BCRP (*ABCG2*) and MRP2 (*ABCC2*) can have an important impact on chemotherapy. These proteins share a strategic localization at apical membranes of important epithelial barriers and at the canalicular membrane of hepatocytes, where they facilitate excretion of transported drugs via liver, intestine and kidneys, and limit their distribution to tissues such as brain or testis (1). In addition, (over-) expression of these transporters in tumor cells can lead to drug resistance through active efflux of cytostatic drugs. Many inhibitors of P-gp and/or BCRP have therefore been developed and applied to potentially improve chemotherapy response of such tumors (2).

Paclitaxel is an excellent P-gp substrate that is widely used in treatment of breast and ovarian cancer, non-small cell lung cancer and Kaposi's sarcoma (3).

We showed earlier that P-gp in epithelial cells of the small intestine actively effluxes its substrates, including paclitaxel, directly from the blood into the intestinal lumen. Moreover, using paclitaxel as model substrate, P-gp was shown to drastically limit intestinal absorption of orally administered substrates (4;5). Based on these findings, numerous mouse studies and clinical trials have been performed, showing that the poor oral availability of paclitaxel could be dramatically improved by coadministration of a P-gp inhibitor (6-10). This is of importance, because oral administration of paclitaxel would be preferred over i.v. administration, as it is convenient to patients, reduces administration costs and facilitates the use of more chronic treatment regimes (11).

Despite virtually complete absorption of paclitaxel from the gastro-intestinal tract in *Mdr1a/1b*$^{-/-}$ mice, bioavailability does not approach 100% (5;6). Similar results were found in patients, when paclitaxel was combined with the potent P-gp inhibitors Cyclosporine A (CsA) or GF120918 (Elacridar®) (10;12). This might be explained by the fact that besides absorption, first-pass metabolism and elimination also affect the bioavailability of a drug. In addition to the P-gp-mediated excretion of paclitaxel from blood directly into the gut lumen (5), excretion into the bile is another important route of elimination, both in rodents and in humans (13;14). Given its presence in the canalicular membrane of hepatocytes, P-gp seemed to be a good candidate for this elimination pathway. However, studies with *Mdr1a*$^{-/-}$ and *Mdr1a/1b*$^{-/-}$ mice (5;15) failed to demonstrate a significant role for P-gp in hepatobiliary excretion of paclitaxel and its hydroxylated metabolites.

We recently identified human MRP2 as a transporter for taxanes *in vitro* (16), and we hypothesized that MRP2 may also play a role *in vivo*, affecting absorption, distribution and/or elimination of paclitaxel. As MRP2 is expressed at the apical membrane of epithelial cells of the small intestine (17), it might limit oral absorption of paclitaxel, similar to P-gp. Furthermore, MRP2 is found at the canalicular membrane of hepatocytes (18), and could thus mediate biliary excretion of paclitaxel and/or its principal hydroxylated metabolites. Thus, absence or reduced activity of MRP2 might increase absorption or decrease elimination of paclitaxel and hence increase overall paclitaxel exposure, potentially influencing therapeutic efficacy and risks of toxic side effects. Involvement of MRP2 in the pharmacokinetics of paclitaxel could be highly relevant for chemotherapy in patients, and possible interpatient variability. Many MRP2 polymorphisms have been described in the human population that affect MRP2 transport activity, including fully deficient variants that occur in homozygous form in Dubin-Johnson patients (19). We have recently generated *Mrp2*$^{-/-}$ mice (20) and crossed them with *Mdr1a/1b*$^{-/-}$ mice (15) to obtain *Mdr1a/1b/Mrp2*$^{-/-}$ mice. The availability of these

strains allowed us to address the relative impact of Mrp2 and P-gp on paclitaxel pharmacokinetics.

MATERIALS AND METHODS

Chemicals. Paclitaxel, 2'-methylpaclitaxel and paclitaxel formulated as a 6 mg/ml solution (Taxol®) in Cremophor EL and dehydrated alcohol (1:1, v/v) were from Bristol-Myers Squibb (Princeton, NJ, USA). [^{3}H]Paclitaxel (4.8 Ci/mmol) was from Moravek Biochemicals (Brea, CA, USA). Paclitaxel metabolites 3'*p*-hydroxypaclitaxel and 6α-hydroxypaclitaxel were purified from patient feces as described (21) or purchased from Gentest Corporation (Woburn, MA, USA). Ketamine (Ketanest-S®) was from Pfizer (Cappelle a/d IJssel, The Netherlands). Xylazine was from Sigma Chemical Co (St. Louis, MO, USA). Methoxyflurane (Metofane®) was from Medical Developments Australia (Springvale, Victoria, Australia). Heparin (5000 IE/ml) was from Leo Pharma BV (Breda, the Netherlands). Bovine serum albumin (BSA), fraction V, was from Roche (Mannheim, Germany). The organic solvents methanol, acetonitril (both HPLC grade) and diethyl ether were from Merck (Darmstadt, Germany). Blank human plasma was from healthy volunteers.

Animals. Mice were housed and handled according to institutional guidelines complying with Dutch legislation. Animals used were male *Mdr1a/1b*$^{-/-}$ (15), *Mrp2*$^{-/-}$ (20), *Mdr1a/1b/Mrp2*$^{-/-}$ and wild-type mice, all of a >99% FVB genetic background, between 9 and 15 weeks of age. Animals were kept in a temperature-controlled environment with a 12-hour light / 12-hour dark circle and received a standard diet (AM-II, Hope Farms, Woerden, The Netherlands) and acidified water *ad libitum*.

Plasma pharmacokinetics. For oral administration, paclitaxel formulated in Cremophor EL and dehydrated alcohol (1:1, v/v, 6mg/ml, Taxol®) was diluted with saline to 1 mg/ml and dosed at 10 mg/kg body weight (10 ml/kg). To minimize variation in absorption, mice were fasted for 3 hours, before paclitaxel was administered by gavage into the stomach, using a blunt-ended needle. Multiple blood samples (~30 µl) were collected from the tail vein at 15 and 30 min and 1, 2, 4, 6, and 8 h, using heparinized capillary tubes (Oxford Labware, St. Louis, USA). Blood samples were centrifuged at 2100 g for 10 min at 4°C, the plasma fraction was collected, completed to 200 µl with blank human plasma and stored at -20°C until analysis. For intravenous studies, paclitaxel was formulated in ethanol and polysorbate 80 (1:1, v/v, 6 mg/ml). This solution was diluted with saline to 2 mg/ml and injected as single bolus at a dose of 10 mg/kg (5 ml/kg) into the tail vein. Blood samples were collected by cardiac puncture under methoxyflurane anesthesia. Animals were sacrificed at 7.5, 15 and 30 min and 1, 2, 4 and 8 hr after

paclitaxel administration, with 3-4 animals per time point. Blood samples were centrifuged at 2100 g for 10 min at 4°C, the plasma fraction was collected and stored at -20°C until analysis.

Fecal and urinary excretion. Mice were individually housed in Ruco Type M/1 stainless-steel metabolic cages (Valkenswaard, the Netherlands). They were allowed 2 days to adapt, before 10 mg/kg paclitaxel, supplemented with [^{3}H]paclitaxel (~0.5 μCi per animal), was injected into a tail vein. Feces and urine were collected over a 24 h period; urine was diluted 5-fold with blank human plasma and feces were homogenized in 4% BSA (1 ml per 100 mg feces). Part of the sample was used to determine levels of radioactivity by liquid scintillation counting; the rest was stored at -20°C until analysis.

Biliary excretion. In gall bladder cannulation experiments, mice were anesthetised by intraperitoneal injection of a combination of ketamine (100 mg/kg) and xylazine (6.7 mg/kg), in a volume of 4.33 μl per gram body weight. After opening the abdominal cavity and distal ligation of the common bile duct, a polythene catheter (Portex limited, Hythe, UK) with an inner diameter of 0.28 mm, was inserted into the incised gallbladder and fixed with an additional ligation. Bile was collected for 60 min after i.v. injection of paclitaxel. For gall bladder cannulation experiments 5 mg/kg was used, as 10 mg/kg paclitaxel in combination with anesthesia and surgery can result in cardiac and respiratory insufficiency (5). At the end of the experiment, blood was collected by cardiac puncture and mice were sacrificed by cervical dislocation. Several tissues were removed and homogenized in 4% BSA; intestinal contents were separated from intestinal tissues prior to homogenization. Tissue homogenates, bile and plasma were stored at -20°C until analysis.

Drug analysis. Amounts of paclitaxel and its hydroxylated metabolites 3'*p*-hydroxypaclitaxel and 6α-hydroxypaclitaxel in small plasma samples, obtained by sampling from the tail vein, were determined using a previously described sensitive and specific LC-MS/MS assay (22). All other samples were processed using liquid-liquid and solid-phase extraction, followed by reversed-phase HPLC with UV detection (23), with minor modifications. We adjusted the mobile phase for HPLC analysis of bile samples and tissue- and feces homogenate-extracts (acetonitrile-methanol-0.2 M ammonium acetate buffer (pH 5.0) (42:65:93, v/v/v)) to obtain successful separation of drug peaks and interfering peaks.

Clinical-chemical analysis of plasma. Standard clinical chemistry analyses on plasma of wild-type, *Mdr1a/1b*$^{-/-}$, *Mrp2*$^{-/-}$ and *Mdr1a/1b/Mrp2*$^{-/-}$ mice (n = 6, males and females) were performed on a Roche Hitachi 917 analyzer (Roche diagnostics, Basel, Switzerland) to determine levels of total and conjugated bilirubin, alkaline phosphatase, aspartate aminotransferase, alanine aminotrans-

ferase, lactate dehydrogenase, creatinine, urea, Na^+, K^+, Cl^-, Ca^{2+}, phosphate, total protein and albumin.

Haematological analysis. Haemoglobin, haematocrit, mean corpuscular volume, red blood cells, white blood cells, lymphocytes, monocytes, granulocytes and platelets were determined in EDTA blood on a Beckman Coulter Ac·T Diff analyzer.

Pharmacokinetic calculations and statistical analysis. Pharmacokinetic parameters were calculated by noncompartimental methods using the software package WinNonlin Professional version 5.0. The area under plasma concentration-time curves (AUC) was calculated using the trapezoidal rule, without extrapolating to infinity. Elimination half-lives ($t_{½,\ el}$) were calculated by linear regression analysis of the log-linear part of the plasma concentration-time curves. Plasma clearance (Cl) after i.v. paclitaxel administration was calculated by the formula Cl = Dose/$AUC_{i.v.}$ and the oral bioavailability (F) was calculated by the formula $F = AUC_{oral} / AUC_{i.v.} \times 100\%$. The two-sided unpaired Student's t-test was used for statistical analysis. Data obtained with single- and combination knockout mice were compared to data obtained with wild-type mice, unless stated otherwise. Differences were considered statistically significant when $P < 0.05$. Data are presented as means ± SD.

RESULTS

Generation and characterization of *Mdr1a/1b/Mrp2*$^{-/-}$ mice. We generated *Mdr1a/1b/Mrp2*$^{-/-}$ mice by cross-breeding *Mdr1a/1b* $^{-/-}$ and *Mrp2*$^{-/-}$ mice (15;20). *Mdr1a/1b/Mrp2*$^{-/-}$ mice were fertile and had normal life spans and body weights. Similar to *Mrp2*$^{-/-}$ mice (20), they had a ~25% increased liver weight (6.1 ± 0.4% of body weight in *Mdr1a/1b/Mrp2*$^{-/-}$ vs. 4.8 ± 0.3% in wild-type, n = 5-6, P = 0.0003). No other macroscopic or microscopic anatomic abnormalities were evident. The bile flow in *Mdr1a/1b/Mrp2*$^{-/-}$ mice was reduced to 40-50% of wild-type levels ($P < 0.01$), and not significantly different from that in *Mrp2*$^{-/-}$ mice (20). *Mdr1a/1b/Mrp2*$^{-/-}$ mice had a moderately increased (~3-fold) plasma level of total bilirubin compared to wild-type mice, which could be attributed to elevated levels of conjugated bilirubin (3.2 ± 1.6 μM in males, 2.7 ± 0.8 μM in females, n = 6). Conjugated bilirubin levels in wild-type plasma were below the detection limit (<1 μM). Conjugated and total bilirubin levels in *Mdr1a/1b/Mrp2*$^{-/-}$ mice were not significantly different from those in *Mrp2*$^{-/-}$ mice. The other clinical-chemical parameters measured in plasma (see Materials and Methods) showed no significant differences between wild-type and *Mdr1a/1b/Mrp2*$^{-/-}$ mice. Haemoglobin levels were moderately but significantly decreased in both male and female *Mdr1a/1b/Mrp2*$^{-/-}$ mice (males: 7.0 ± 0.1 mM in knockout vs. 7.4 ± 0.1 mM in

wild-type mice, n = 3-4, $P = 0.017$; females: 7.2 ± 0.5 mM in knockout vs. 7.6 ± 0.1 mM in wild-type mice, n = 5-6, $P = 0.016$). These results are qualitatively similar to those for *Mrp2*$^{-/-}$ mice. None of the other haematological parameters measured revealed significant differences between wild-type and *Mdr1a/1b/Mrp2*$^{-/-}$ mice. *Mdr1a/1b/Mrp2*$^{-/-}$ mice thus appear in many respects very similar to *Mrp2*$^{-/-}$ mice (20), and they are likely as amenable to pharmacological analyses.

Impact of Mrp2 and P-gp on plasma pharmacokinetics of paclitaxel. To investigate the relative roles of Mrp2 and P-gp in absorption, distribution and elimination of paclitaxel, we studied oral and intravenous plasma pharmacokinetics in wild-type, *Mrp2*$^{-/-}$, *Mdr1a/1b*$^{-/-}$ and *Mdr1a/1b/Mrp2*$^{-/-}$ mice. Upon oral administration of 10 mg/kg paclitaxel, plasma concentrations and area under the plasma concentration-time curve (AUC_{oral}) were not different between *Mrp2*$^{-/-}$ and wild-type mice (Fig. 1A and Table 1). For *Mdr1a/1b*$^{-/-}$ mice the AUC_{oral} was about 8.5-fold higher, in line with previous results (5;6), but the elimination half life of the drug was not changed (Table 1).

Table 1. Plasma pharmacokinetic parameters after oral or i.v. administration of paclitaxel at 10 mg/kg.

	Strain			
	Wild-type	*Mdr1a/1b*$^{-/-}$	*Mrp2*$^{-/-}$	*Mdr1a/1b/Mrp2*$^{-/-}$
Oral				
$AUC_{(0\text{-}8)}$, hr.mg/l	0.44 ± 0.19	3.75 ± 0.38***	0.40 ± 0.08	6.23 ± 0.60***/†
C_{max}, mg/l	0.13 ± 0.11	1.05 ± 0.19***	0.12 ± 0.04	1.53 ± 0.19***/†
$t_{½,\,el}$, hr	1.96 ± 0.28	1.69 ± 0.16	1.74 ± 0.11	2.42 ± 0.28*/†
i.v.				
$AUC_{(0\text{-}8)}$, hr.mg/l	5.57 ± 0.26	7.08 ± 0.31*	7.33 ± 0.34*	9.41 ± 0.57**
C_{max}, mg/l	6.17 ± 0.21	7.09 ± 0.30	6.89 ± 0.89	6.17 ± 0.68
$t_{½,\,el}$, hr	1.65 ± 0.11	1.79 ± 0.10	1.61 ± 0.11	2.08 ± 0.12*
Cl, l/hr.kg	1.80 ± 0.08	1.41 ± 0.06*	1.36 ± 0.06*	1.06 ± 0.06**
F, %	7.9 ± 3.4	53.0 ± 5.8**	5.5 ± 1.1	66.2 ± 7.5**

$AUC_{(0\text{-}8)}$, area under plasma concentration-time curve up to 8 hr; C_{max}, maximum plasma levels; $t_{½,\,el}$, elimination half life, calculated from 2-8 hr for both oral and i.v. administration; Cl, plasma clearance; *F*, oral bioavailability. Data are means ± SD, n = 5-6 for oral and n = 3-4 for i.v. administration. * $P < 0.05$, ** $P < 0.01$ and *** $P < 0.001$, compared to wild-type mice. † $P < 0.01$, compared to *Mdr1a/1b*$^{-/-}$ mice.

Interestingly, however, in *Mdr1a/1b/Mrp2*$^{-/-}$ mice the AUC_{oral} was increased another 1.7-fold compared to *Mdr1a/1b* $^{-/-}$ mice (and 14.2-fold compared to wild-type mice), the C_{max} was 1.5-fold increased, and a 1.4-fold extended elimination half life was found ($P < 0.01$ for each parameter) (Fig. 1A, Table 1). These results confirm that P-gp is a major factor in limiting the paclitaxel AUC after oral administration, but that, in the absence of P-gp, Mrp2 also has a marked impact on oral paclitaxel plasma pharmacokinetics.

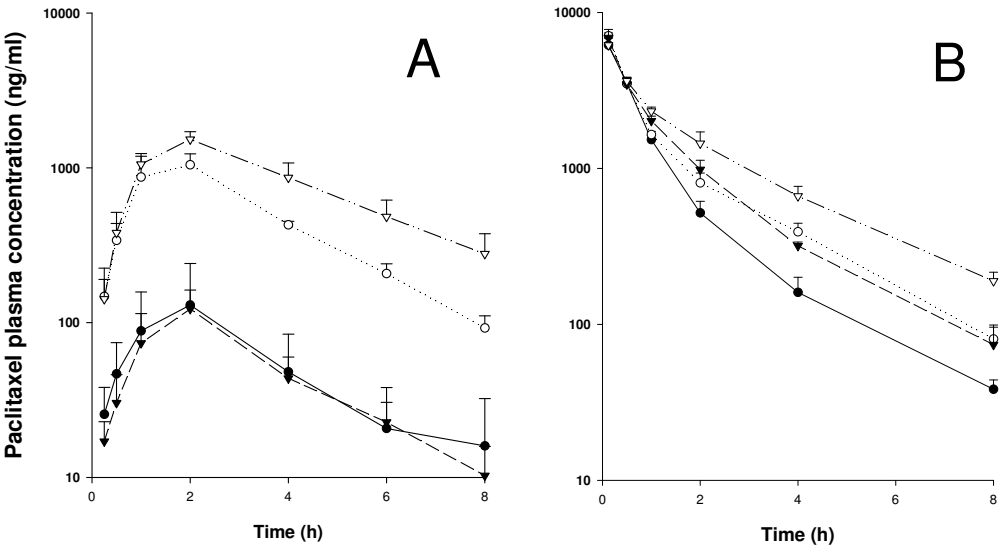

Fig. 1. Plasma concentration-time curves of paclitaxel in male FVB wild-type (●), *Mdr1a/1b*$^{-/-}$ (o), *Mrp2*$^{-/-}$ (▼) and *Mdr1a/1b/Mrp2*$^{-/-}$ (∇) mice, after oral (*A*) and i.v. (*B*) administration of paclitaxel at a dose of 10 mg/kg. Data represent mean concentrations ± SD, n = 5-6 for oral and n = 3-4 for i.v. administration.

The relative impact of Mrp2 versus P-gp was even more pronounced after intravenous administration of paclitaxel. The $AUC_{i.v.}$ was 1.3-fold higher in *Mrp2*$^{-/-}$ mice than in wild-type mice (Fig. 1B, Table 1). A similar 1.3-fold increase in $AUC_{i.v.}$ was found for *Mdr1a/1b*$^{-/-}$ mice, consistent with our previous results (5;6). This similarity in impact of Mrp2 and P-gp on paclitaxel plasma levels after i.v. administration is striking, since paclitaxel is an excellent P-gp substrate (24;25). Nonetheless, even with P-gp present, Mrp2 is an important determinant for the disposition of paclitaxel *in vivo*. Absence of both Mrp2 and Mdr1a/1b resulted in a 1.7- fold higher $AUC_{i.v.}$ than in wild-type mice, and a significantly prolonged elimination half life (Fig. 1B, Table 1).

Table 2. Levels of paclitaxel and monohydroxylated metabolites in plasma and liver at t = 8 hr after i.v. administration of 10 mg/kg paclitaxel.

Biological Matrix	Compound	Strain			
		Wild-type	*Mdr1a/1b*$^{-/-}$	*Mrp2*$^{-/-}$	*Mdr1a/1b/Mrp2*$^{-/-}$
Plasma (ng/ml)	Paclitaxel	38.3 ± 5.8	80.5 ± 8.9**	73.9 ± 12.6*	189.6 ± 13.1***
	3'*p*-hydroxypaclitaxel	ND	2.3 ± 0.4	2.0 ± 0.5	6.5 ± 0.79
	6α-hydroxypaclitaxel	ND	0.6 ± 0.7	1.0 ± 0.7	4.4 ± 1.5
Liver (% of dose)	Paclitaxel	5.8 ± 0.8	9.3 ± 1.0**	9.2 ± 1.5*	12.3 ± 1.6**
	3'*p*-hydroxypaclitaxel	0.3 ± 0.04	0.5 ± 0.08**	1.8 ± 0.3***	4.1 ± 0.4***
	6α-hydroxypaclitaxel	ND	0.1 ± 0.02	0.5 ± 0.3	4.4 ± 0.3

Plasma levels of paclitaxel and metabolites are expressed as ng/ml (mean ± SD, n = 3-4) and liver levels of paclitaxel and metabolites are expressed as percentage of the dose (mean ± SD, n = 3-4). ND: not detectable. * $P < 0.05$, ** $P < 0.01$ and *** $P < 0.001$, compared to wild-type mice.

Role of Mrp2 and P-gp in plasma and liver levels of 3'*p*-hydroxypaclitaxel and 6α-hydroxypaclitaxel. Because metabolism is an important detoxification pathway for paclitaxel, we also studied its primary metabolites: 3'*p*-hydroxypaclitaxel and 6α-hydroxypaclitaxel. Plasma levels of these monohydroxylated metabolites at t = 8 hr after i.v. administration of paclitaxel at 10 mg/kg were below the limits of detection in wild-type mice (Table 2). However, substantial levels were detected in plasma of *Mdr1a/1b*$^{-/-}$ and *Mrp2*$^{-/-}$ mice, and for *Mdr1a/1b/Mrp2*$^{-/-}$ mice the levels were another 3 to 4-fold higher. Similar results were obtained for metabolite levels in liver at t = 8 hr (Table 2), suggesting an interrelatedness of plasma and liver metabolite levels. The same might apply to unchanged paclitaxel, as its accumulation in liver and plasma concentration were also markedly higher in each of the separate and especially the combined knockout strains.

Impact of Mrp2 and P-gp on fecal and urinary excretion of paclitaxel. In both humans and mice, fecal excretion is the main route of elimination for paclitaxel, whereas almost no parent compound is found in the urine (14;26-28). We collected urine and feces for 24 hours after i.v. administration of 10 mg/kg [^{3}H]paclitaxel and determined cumulative excretion of total radioactivity as well as unchanged paclitaxel and its monohydroxylated metabolites (Table 3). 68.2% of the radioactivity was recovered from the feces in wild-type mice. In *Mdr1a/1b*$^{-/-}$

and *Mrp2*$^{-/-}$ mice this was reduced to 49.0% and 46.8%, respectively, whereas only 21.6% was found in the feces of *Mdr1a/1b/Mrp2*$^{-/-}$ mice ($P < 0.001$ for each parameter). For urinary excretion of radioactivity, a reverse pattern was found, ranging from 3.3% in wild-type mice to 27.1% in *Mdr1a/1b/Mrp2*$^{-/-}$ mice. The combined radioactivity data revealed a shift from almost exclusively fecal excretion in wild-type mice to roughly equal fecal and urinary excretion in *Mdr1a/1b/Mrp2*$^{-/-}$ mice.

Table 3. Cumulative fecal and urinary excretion (0-24 hr) of paclitaxel, 3'*p*-hydroxypaclitaxel and 6α-hydroxypaclitaxel in intact mice after i.v. administration of [^{3}H]paclitaxel at 10 mg/kg.

		Strain			
Biological Matrix	Compound	Wild-type	*Mdr1a/1b*$^{-/-}$	*Mrp2*$^{-/-}$	*Mdr1a/1b/Mrp2*$^{-/-}$
Feces	Paclitaxel	49.0 ± 4.4	1.4 ± 0.6***	30.8 ± 8.1**	1.0 ± 0.3***
	3'*p*-hydroxypaclitaxel	14.8 ± 1.2	17.2 ± 1.3*	9.9 ± 1.9**	1.6 ± 0.5***
	6α-hydroxypaclitaxel	8.4 ± 0.6	9.7 ± 0.8*	5.1 ± 1.6**	0.6 ± 0.2***
	[^{3}H] label	68.2 ± 1.6	49.0 ± 4.5***	46.8 ± 7.8***	21.6 ± 3.2***
Urine	Paclitaxel	0.66 ± 0.18	0.58 ± 0.21	0.73 ± 0.07	0.77 ± 0.13
	3'*p*-hydroxypaclitaxel	ND	ND	0.02 ± 0.01	0.02 ± 0.01
	6α-hydroxypaclitaxel	ND	ND	0.04 ± 0.02	0.15 ± 0.01
	[^{3}H] label	3.3 ± 0.6	5.4 ± 0.8**	14.5 ± 1.7***	27.1 ± 3.3***

Excretion is given as percentage of the dose (mean ± SD, n = 5). ND, not detectable. * $P < 0.05$, ** $P < 0.01$ and *** $P < 0.001$, compared to wild-type mice.

HPLC-UV analyses showed that fecal excretion of unmodified paclitaxel in wild-type mice was 49% of the administered dose (Table 3). In *Mdr1a/1b*$^{-/-}$ and *Mdr1a/1b/Mrp2*$^{-/-}$ mice, less than 2% was excreted in the feces. For *Mrp2*$^{-/-}$ mice, a less pronounced but still marked reduction in fecal excretion was found (to 30.8%, $P = 0.002$), indicating that Mrp2 in liver and/or intestine also contributes substantially to the fecal excretion of paclitaxel (about 18% of the dose). Yet, in *Mdr1a/1b*$^{-/-}$ mice, where Mrp2 is still present, paclitaxel was nearly absent from feces. This suggests that P-gp helps to keep paclitaxel, initially excreted by Mrp2, in the intestinal lumen, presumably by limiting reabsorption of the drug.

Role of Mrp2 and P-gp in fecal and urinary excretion of monohydroxylated Metabolites. The fecal excretion pattern of the hydroxylated paclitaxel metabolites was quite different from that of the parent compound (Table 3). Wild-type mice excreted 15% of the dose as 3'*p*-hydroxypaclitaxel and 8.5% as 6α-hydroxypaclitaxel. In *Mdr1a/1b*$^{-/-}$ mice, the fecal excretion of both metabolites was moderately but significantly increased compared to wild-type mice ($P < 0.05$ for both), and accounted for more than half of the excreted radioactivity. *Mrp2*$^{-/-}$ mice, however, displayed a reduced excretion of 3'*p*-hydroxypaclitaxel and 6α-hydroxypaclitaxel to 67% and 61% of wild-type levels, respectively. In *Mdr1a/1b/Mrp2*$^{-/-}$ mice, fecal excretion of these metabolites was nearly abolished. The latter result suggests that, in addition to Mrp2, Mdr1a/1b P-gp is also important in the fecal excretion of the hydroxylated metabolites, in spite of their increased excretion in the *Mdr1a/1b*$^{-/-}$ mice. This may result from strongly increased formation of the metabolites due to the extended residence time of paclitaxel in *Mdr1a/1b*$^{-/-}$ mice, more than compensating for a partial reduction in their excretion capacity due to P-gp deficiency. Mrp2 appeared to be responsible for nearly all of the fecal excretion of the metabolites in the *Mdr1a/1b*$^{-/-}$ mice. In the urine of *Mdr1a/1b*$^{-/-}$, and especially *Mrp2*$^{-/-}$ and *Mdr1a/1b/Mrp2*$^{-/-}$ mice, a highly significant increase in excreted radioactivity was found. Paclitaxel and its primary hydroxylated metabolites only represented a minor fraction (Table 3), so other hydrophilic metabolites likely accounted for the majority of this excreted radioactivity.

Impact of Mrp2 and P-gp on biliary and direct intestinal excretion of paclitaxel and its hydroxylated metabolites. We performed gall bladder cannulation experiments to clarify the roles of Mrp2 and Mdr1a/1b in biliary and direct intestinal excretion. Previous experiments suggest that P-gp does not primarily mediate biliary excretion of paclitaxel or its hydroxylated metabolites (5;15). We measured the biliary excretion for 1 hour in anesthetized mice with a cannulated gall bladder and a ligated common bile duct, receiving i.v. [^{3}H]paclitaxel at 5 mg/kg. In wild-type mice, 3.3% ± 0.8% of the dose was excreted over 1 hour as unchanged paclitaxel (Table 4). *Mdr1a/1b*$^{-/-}$ mice did not show a significant reduction in biliary excretion of paclitaxel, in line with previous findings (5;15). In contrast, in *Mrp2*$^{-/-}$ mice biliary excretion of paclitaxel was reduced by 80% compared to wild-type mice, whereas in *Mdr1a/1b/Mrp2*$^{-/-}$ mice the excretion was almost totally abolished (97% reduction). A similar excretory pattern was found for the principal metabolites (Table 4). This indicates that Mrp2 is the predominant factor in the biliary excretion of paclitaxel and its hydroxylated metabolites and that Mdr1a/1b plays a minor role in this process. Furthermore, in *Mrp2*$^{-/-}$ and *Mdr1a/1b/Mrp2*$^{-/-}$ mice, very similar and significantly increased levels

of paclitaxel in plasma (by 51% and 53%) and in liver (by 38% and 34%) and increased levels of metabolites in liver were found at the end of the cannulation experiment (Table 4). This probably reflects the decreased hepatobiliary elimination of paclitaxel and monohydroxylated metabolites owing to Mrp2 absence. The biliary radioactivity data indicate that the majority of other paclitaxel metabolites was also primarily transported into the bile by Mrp2, since in wild-type and *Mdr1a/1b* $^{-/-}$ mice about 20% of the radioactive dose was recovered in bile, whereas this was only ~4% in *Mrp2*$^{-/-}$ and *Mdr1a/1b/Mrp2*$^{-/-}$ bile.

Table 4. Paclitaxel and its monohydroxylated metabolites as determined in bile, plasma and different tissues of mice with cannulated gall bladder, 60 minutes after i.v. administration of [^{3}H]paclitaxel at 5 mg/kg.

		Strain			
Biological Matrix	Compound	Wild-type	*Mdr1a/1b*$^{-/-}$	*Mrp2*$^{-/-}$	*Mdr1a/1b/Mrp2*$^{-/-}$
Plasma†	Paclitaxel	546 ± 43	534 ± 65	825 ± 128**	837 ± 99**
	[^{3}H] label	936 ± 94	1068 ± 160	1324 ± 126**	1532 ± 111**
Bile	Paclitaxel	3.25 ± 0.83	2.21 ± 0.50	0.66 ± 0.17**	0.10 ± 0.05***
	3'*p*- hydroxypaclitaxel	0.95 ± 0.33	1.41 ± 0.33	0.10 ± 0.05***	ND
	6α-hydroxypaclitaxel	0.40 ± 0.15	0.66 ± 0.17	0.03 ± 0.03	ND
	[^{3}H] label	19.0 ± 3.64	22.1 ± 3.02	4.26 ± 0.43***	3.91 ± 0.92***
Liver	Paclitaxel	27.5 ± 1.69	27.0 ± 1.15	37.9 ± 4.86**	36.8 ± 5.73*
	3'*p*- hydroxypaclitaxel	0.77 ± 0.32	1.03 ± 0.18	1.46 ± 0.38*	1.76 ± 0.53*
	6α-hydroxypaclitaxel	0.27 ± 0.16	0.44 ± 0.08	0.73 ± 0.26*	0.74 ± 0.28*
	[^{3}H] label	24.6 ± 1.13	25.4 ± 1.16	37.2 ± 3.58***	39.7 ± 5.13***
S.I.C.	Paclitaxel	4.94 ± 0.93	2.00 ± 0.75**	3.59 ± 0.76*	1.63 ± 0.29**
	3'*p*- hydroxypaclitaxel	2.05 ± 0.33	3.90 ± 1.24*	0.70 ± 0.38***	0.86 ± 0.25***
	6α-hydroxypaclitaxel	0.28 ± 0.07	0.55 ± 0.04**	0.14 ± 0.07*	0.23 ± 0.14
	[^{3}H] label	7.55 ± 0.70	4.28 ± 0.71***	6.60 ± 1.05	2.78 ± 0.49***

Levels are given as percentage of the dose (means ± SD, n = 4-6). ND: not detectable; S.I.C.: small intestinal contents. †Plasma levels of paclitaxel are expressed as ng/ml and tritium plasma levels as ng-equivalent/ml. Metabolites were not detectable in plasma at t = 60 minutes. * $P < 0.05$, ** $P < 0.01$ and *** $P < 0.001$, compared to wild-type mice.

Other than through biliary excretion, paclitaxel can reach the gut lumen by excretion directly across the intestinal wall. P-gp is known to play a major role in this process (5;15). We analyzed the small intestinal contents at the end of the 1 hr gall bladder cannulation experiments. Since the common bile duct was ligated, paclitaxel and metabolites could only reach the intestinal lumen by excretion from the blood across the gut wall. In the small intestinal contents of wild-type mice 4.9 ± 0.9% of the administered dose was recovered as unchanged drug (Table 4). For *Mrp2*$^{-/-}$ mice this was 3.6 ± 0.8%, a modest but significant reduction (P = 0.035), also in view of the higher paclitaxel plasma concentration. Markedly less paclitaxel was detected in the intestinal lumen of *Mdr1a/1b*$^{-/-}$ and *Mdr1a/1b/Mrp2*$^{-/-}$ mice: 2.0% ± 0.8% and 1.6% ± 0.3%, respectively. These data confirm the dominant role of P-gp in the direct intestinal excretion of paclitaxel, while Mrp2 may contribute modestly to this process. Different results were obtained for the hydroxylated metabolites. *Mdr1a/1b*$^{-/-}$ mice showed a significantly increased intestinal excretion of 3'*p*-hydroxypaclitaxel and 6α-hydroxypaclitaxel, presumably owing to higher plasma levels of these compounds. In contrast, clearly reduced amounts of these metabolites were found in the intestinal contents of *Mrp2*$^{-/-}$ and *Mdr1a/1b/Mrp2*$^{-/-}$ mice (Table 4). These data suggest that Mrp2 has a predominant function in the direct intestinal excretion of the hydroxylated paclitaxel metabolites.

DISCUSSION

In this study we describe the generation and characterization of *Mdr1a/1b/Mrp2*$^{-/-}$ mice, and their utilization in the analysis of the separate and combined impact of Mrp2 and P-gp on the pharmacokinetics of paclitaxel. Extensive analysis of the *Mdr1a/1b/Mrp2*$^{-/-}$ mice suggests that they are very similar to *Mrp2*$^{-/-}$ mice, displaying mild physiological abnormalities such as increased liver weight, mild conjugated hyperbilirubinemia, reduced bile flow and a modest decrease in blood haemoglobin levels. No severe deficiencies due to the combination of *Mrp2* and *Mdr1a/1b* knockout were observed. Consequently, the *Mdr1a/1b/Mrp2*$^{-/-}$ mice appear as suitable for pharmacological analyses as the separate *Mrp2*$^{-/-}$ and *Mdr1a/1b*$^{-/-}$ mice (15;20). These mice thus provide a powerful tool to study redundant or overlapping, but also complementary functions of Mrp2 and P-gp in pharmacology, toxicology and physiology.

Although we had previously demonstrated that paclitaxel is transported by human MRP2 (16), we were surprised to find that the impact of Mrp2 on the pharmacokinetics of paclitaxel after intravenous administration was at least as great as that of Mdr1a/1b P-gp. Paclitaxel is an excellent P-gp substrate, so we had expected that its pharmacokinetics would be dominated by P-gp, as is indeed the case upon oral administration of the drug. However, upon intravenous

administration, even in the presence of P-gp, Mrp2 has a marked effect on paclitaxel plasma levels and excretion, at least equal to the P-gp effects. As paclitaxel is currently primarily administered to patients intravenously, variation in MRP2 activity might directly affect their effective paclitaxel exposure.

The pronounced impact of P-gp on (oral) paclitaxel pharmacokinetics appears to be determined primarily by the capability of P-gp to reduce net (re-)absorption of paclitaxel from the intestinal lumen, and, related to this, its capability to mediate direct intestinal excretion (5). Especially upon oral administration in P-gp-proficient mice, very little paclitaxel enters the circulation, leaving little room for a significant contribution of Mrp2. We observed earlier that Mrp2 has a more pronounced pharmacokinetic impact at relatively high plasma drug concentrations of methotrexate, presumably because at lower plasma concentrations alternative, more high-affinity elimination systems dominate drug removal (20). The same might apply for elimination of the comparatively low paclitaxel levels after oral administration in P-gp-proficient animals (Fig. 1).

The results from Tables 3 and 4 indicate that Mrp2 and P-gp have rather complementary roles in hepatobiliary and intestinal excretion of paclitaxel after i.v. administration. Mrp2 is the dominant factor in biliary excretion of paclitaxel, and P-gp contributes modestly. In contrast, P-gp dominates the direct intestinal excretion of paclitaxel, while Mrp2 plays a minor role here. Table 3 shows that Mrp2 activity accounts for at least 18% of the dose being excreted in the feces over 24 hr, which must result mainly from hepatobiliary and perhaps some direct intestinal excretion. In spite of this, in the absence of P-gp in the *Mdr1a/1b*$^{-/-}$ mice, very little paclitaxel is retrieved in the feces (Table 3). This must mean that the paclitaxel initially excreted by Mrp2 into the intestinal lumen of these mice is readily reabsorbed from the gut due to P-gp absence. This continued reabsorption of unchanged paclitaxel results in prolonged metabolism, explaining why very little unmetabolized paclitaxel leaves the body when P-gp is absent.

It is interesting to note that, in spite of the qualitatively different primary functions of P-gp and Mrp2 affecting paclitaxel pharmacokinetics, the quantitative effect of absence of both proteins on the $AUC_{i.v.}$ was very similar (1.3-fold each). The combination of both deficiencies had rather an additive than a synergistic effect on the paclitaxel $AUC_{i.v.}$. (1.3 x 1.3 = 1.69, corresponding well with the 1.7-fold increased $AUC_{i.v.}$ in the combination knockout mice).

In the past, MRP2/Mrp2 has been considered primarily as an organic anion transporter, and earlier experiments in Mrp2-deficient rats and mice indicated that Mrp2 could have a marked effect on pharmacokinetics of the anionic anti-cancer drug methotrexate (20;29). Our data show that Mrp2 can also be a major determinant of the pharmacokinetic behavior of a highly lipophilic anti-cancer

drug, even in the presence of other very efficient transporters for this drug. As it is now clear that several other non-anionic and lipophilic (anti-cancer) drugs, including docetaxel, etoposide and various HIV protease inhibitors, are markedly transported by MRP2 in vitro (16;30), it may well be that these other drugs are equally affected in their (i.v.) pharmacokinetics. This could mean that MRP2 activity has a much broader significance for pharmacokinetic behavior of anti-cancer and other drugs than previously appreciated. This is of importance, as extensive genetic polymorphisms in human MRP2 are known that affect functionality, some even resulting in full homozygous deficiency for MRP2 (19). In a recent study, six known allelic variants in genes involved in paclitaxel metabolism (*CYP2C8*, *CYP3A4*, *CYP3A5*) and in the gene coding for P-gp (*ABCB1*) were evaluated, but could not explain the substantial interindividual variability in paclitaxel pharmacokinetics (31). It will be of interest to test whether polymorphisms in the *ABCC2* gene contribute to these variations.

Furthermore, factors affecting MRP2 expression, like hepatic diseases, renal failure or exposure to certain drugs, can result in inter-individual differences in disposition of drugs eliminated via MRP2 (19). Such variation in MRP2 activity might thus affect the therapeutic plasma levels and toxic side effects of a much broader range of anti-cancer drugs than previously realized and this should be taken into account during chemotherapy treatment of patients.

Our study shows that Mrp2 has a marked impact on both i.v. and oral paclitaxel AUC when P-gp activity is absent (Fig. 1). In a variety of clinical trials, highly efficacious P-gp inhibitors such as PSC-833 (Valspodar®), GF120918 (Elacridar®), and others are co-administered with paclitaxel or other MRP2 substrate drugs, to counteract multidrug resistance in tumors, or to improve the oral bioavailability of the anti-cancer drug (7;10;12;32). Under these circumstances, variation in MRP2 activity due to genetic polymorphisms might have even more pronounced effects on effective availability of the drug, with implications for therapeutic efficacy and the risk of toxic side effects. It will thus be important to be well aware of the impact of MRP2 on the pharmacokinetic behavior of many anti-cancer drugs when P-gp is inhibited. The mouse models we have generated will provide useful tools to qualitatively assess this impact for a variety of drugs. This information can subsequently be used for rational translation of the insights to the (clinical) situation in humans, which may ultimately lead to more constant and reliable chemotherapy regimens.

ACKNOWLEDGMENTS

We thank our colleagues for critical reading of the manuscript and Tessa Buckle and Anita van Esch for excellent technical assistance.

REFERENCES

(1) Borst P, Oude Elferink RP. Mammalian ABC transporters in health and disease. Annu Rev Biochem 2002;71:537-92.

(2) Lee CH. Reversing agents for ATP-binding cassette (ABC) transporters: application in modulating multidrug resistance (MDR). Curr Med Chem Anticancer Agents 2004;4:43-52.

(3) Jordan MA, Wilson L. Microtubules as a target for anticancer drugs. Nat Rev Cancer 2004;4:253-65.

(4) Mayer U, Wagenaar E, Beijnen JH, Smit JW, Meijer DK, van Asperen J et al. Substantial excretion of digoxin via the intestinal mucosa and prevention of long-term digoxin accumulation in the brain by the mdr 1a P-glycoprotein. Br J Pharmacol 1996;119:1038-44.

(5) Sparreboom A, van Asperen J, Mayer U, Schinkel AH, Smit JW, Meijer DK et al. Limited oral bioavailability and active epithelial excretion of paclitaxel (Taxol) caused by P-glycoprotein in the intestine. Proc Natl Acad Sci U S A 1997;94:2031-5.

(6) Bardelmeijer HA, Beijnen JH, Brouwer KR, Rosing H, Nooijen WJ, Schellens JH et al. Increased oral bioavailability of paclitaxel by GF120918 in mice through selective modulation of P-glycoprotein. Clin Cancer Res 2000;6:4416-21.

(7) Meerum Terwogt JM, Beijnen JH, Bokkel Huinink WW, Rosing H, Schellens JH. Co-administration of cyclosporin enables oral therapy with paclitaxel. Lancet 1998;352:285.

(8) van Asperen J, van Tellingen O, van der Valk MA, Rozenhart M, Beijnen JH. Enhanced oral absorption and decreased elimination of paclitaxel in mice cotreated with cyclosporin A. Clin Cancer Res 1998;4:2293-7.

(9) van Asperen J, van Tellingen O, Sparreboom A, Schinkel AH, Borst P, Nooijen WJ et al. Enhanced oral bioavailability of paclitaxel in mice treated with the P-glycoprotein blocker SDZ PSC 833. Br J Cancer 1997;76:1181-3.

(10) Malingre MM, Beijnen JH, Rosing H, Koopman FJ, Jewell RC, Paul EM et al. Co-administration of GF120918 significantly increases the systemic exposure to oral paclitaxel in cancer patients. Br J Cancer 2001;84:42-7.

(11) Schellens JH, Malingre MM, Kruijtzer CM, Bardelmeijer HA, van Tellingen O, Schinkel AH et al. Modulation of oral bioavailability of anticancer drugs: from mouse to man. Eur J Pharm Sci 2000;12:103-10.

(12) Meerum Terwogt JM, Malingre MM, Beijnen JH, Bokkel Huinink WW, Rosing H, Koopman FJ et al. Coadministration of oral cyclosporin A enables oral therapy with paclitaxel. Clin Cancer Res 1999;5:3379-84.

(13) Monsarrat B, Alvinerie P, Wright M, Dubois J, Gueritte-Voegelein F, Guenard D et al. Hepatic metabolism and biliary excretion of Taxol in rats and humans. J Natl Cancer Inst Monogr 1993;39-46.

(14) Sparreboom A, van Tellingen O, Nooijen WJ, Beijnen JH. Tissue distribution, metabolism and excretion of paclitaxel in mice. Anticancer Drugs 1996;7:78-86.

(15) Schinkel AH, Mayer U, Wagenaar E, Mol CA, van Deemter L, Smit JJ et al. Normal viability and altered pharmacokinetics in mice lacking mdr1-type (drug-transporting) P-glycoproteins. Proc Natl Acad Sci U S A 1997;94:4028-33.

(16) Huisman MT, Chhatta AA, van Tellingen O, Beijnen JH, Schinkel AH. MRP2 (ABCC2) transports taxanes and confers paclitaxel resistance and both processes are stimulated by probenecid. Int J Cancer 2005;116:824-9.

(17) Mottino AD, Hoffman T, Jennes L, Vore M. Expression and localization of multidrug resistant protein mrp2 in rat small intestine. J Pharmacol Exp Ther 2000;293:717-23.

(18) Buchler M, Konig J, Brom M, Kartenbeck J, Spring H, Horie T et al. cDNA cloning of the hepatocyte canalicular isoform of the multidrug resistance protein, cMrp, reveals a novel conjugate export pump deficient in hyperbilirubinemic mutant rats. J Biol Chem 1996;271:15091-8.

(19) Suzuki H, Sugiyama Y. Single nucleotide polymorphisms in multidrug resistance associated protein 2 (MRP2/ABCC2): its impact on drug disposition. Adv Drug Deliv Rev 2002;54:1311-31.

(20) Vlaming ML, Mohrmann K, Wagenaar E, de Waart DR, Elferink RP, Lagas JS et al. Carcinogen and anticancer drug transport by Mrp2 in vivo: studies using Mrp2 (Abcc2) knockout mice. J Pharmacol Exp Ther 2006;318:319-27.

(21) Sparreboom A, Huizing MT, Boesen JJ, Nooijen WJ, van Tellingen O, Beijnen JH. Isolation, purification, and biological activity of mono- and dihydroxylated paclitaxel metabolites from human feces. Cancer Chemother Pharmacol 1995;36:299-304.

(22) Vainchtein LD, Thijssen B, Stokvis E, Rosing H, Schellens JH, Beijnen JH. A simple and sensitive assay for the quantitative analysis of paclitaxel and metabolites in human plasma using liquid chromatography/tandem mass spectrometry. Biomed Chromatogr 2006;20:139-48.

(23) Sparreboom A, van Tellingen O, Nooijen WJ, Beijnen JH. Determination of paclitaxel and metabolites in mouse plasma, tissues, urine and faeces by semi-automated reversed-phase high-performance liquid chromatography. J Chromatogr B Biomed Appl 1995;664:383-91.

(24) Greenberger LM, Lothstein L, Williams SS, Horwitz SB. Distinct P-glycoprotein precursors are overproduced in independently isolated drug-resistant cell lines. Proc Natl Acad Sci U S A 1988;85:3762-6.

(25) Mickisch GH, Merlino GT, Galski H, Gottesman MM, Pastan I. Transgenic mice that express the human multidrug-resistance gene in bone marrow enable a rapid identification of agents that reverse drug resistance. Proc Natl Acad Sci U S A 1991;88:547-51.

(26) Wiernik PH, Schwartz EL, Strauman JJ, Dutcher JP, Lipton RB, Paietta E. Phase I clinical and pharmacokinetic study of taxol. Cancer Res 1987;47:2486-93.

(27) Walle T, Walle UK, Kumar GN, Bhalla KN. Taxol metabolism and disposition in cancer patients. Drug Metab Dispos 1995;23:506-12.

(28) Longnecker SM, Donehower RC, Cates AE, Chen TL, Brundrett RB, Grochow LB et al. High-performance liquid chromatographic assay for taxol in human plasma and urine and pharmacokinetics in a phase I trial. Cancer Treat Rep 1987;71:53-9.

(29) Masuda M, I'izuka Y, Yamazaki M, Nishigaki R, Kato Y, Ni'inuma K et al. Methotrexate is excreted into the bile by canalicular multispecific organic anion transporter in rats. Cancer Res 1997;57:3506-10.

(30) Huisman MT, Smit JW, Crommentuyn KM, Zelcer N, Wiltshire HR, Beijnen JH et al. Multidrug resistance protein 2 (MRP2) transports HIV protease inhibitors, and transport can be enhanced by other drugs. AIDS 2002;16:2295-301.

(31) Henningsson A, Marsh S, Loos WJ, Karlsson MO, Garsa A, Mross K et al. Association of CYP2C8, CYP3A4, CYP3A5, and ABCB1 polymorphisms with the pharmacokinetics of paclitaxel. Clin Cancer Res 2005;11:8097-104.

(32) Boote DJ, Dennis IF, Twentyman PR, Osborne RJ, Laburte C, Hensel S et al. Phase I study of etoposide with SDZ PSC 833 as a modulator of multidrug resistance in patients with cancer. J Clin Oncol 1996;14:610-8.

CHAPTER 3.2

P-glycoprotein (P-gp/*ABCB1*), ABCC2 and ABCC3 determine the pharmacokinetics of etoposide

Jurjen S. Lagas, Lin Fan, Els Wagenaar, Maria L.H. Vlaming, Olaf van Tellingen, Jos H. Beijnen and Alfred H. Schinkel

To be submitted

ABSTRACT

Purpose: Etoposide is a semisynthetic podophyllotoxin derivative that is widely used for the treatment of different malignant neoplasms. Despite extensive use, its main pharmacokinetic determinants are still not completely defined. The aim of this study was to investigate the impact of P-glycoprotein (P-gp/MDR1) and the multidrug transporters ABCC2 (MRP2) and ABCC3 (MRP3) on the pharmacokinetics of etoposide. *Experimental design: Abcb1a/1b*$^{-/-}$, *Abcc2*$^{-/-}$, *Abcc3*$^{-/-}$, *Abcb1a/1b;Abcc2*$^{-/-}$ and *Abcc2;Abcc3*$^{-/-}$ mice were used to study the separate and combined impact of P-gp, Abcc2 and Abcc3 on the *in vivo* behavior of etoposide. *Results:* We show that the hepatobiliary excretion of etoposide is almost entirely dependent on Abcc2. Furthermore, P-gp was found to restrict the oral (re)uptake of etoposide, and to mediate its excretion across the gut wall. We also show that Abcc2 is responsible for the hepatobiliary excretion of etoposide glucuronide, the main metabolite, whereas Abcc3 mediates the efflux of etoposide glucuronide from the liver to the blood circulation. *Conclusions:* P-gp, ABCC2 and ABCC3 thus importantly affect the pharmacokinetics of etoposide and/or etoposide glucuronide. For each of these transporters polymorphisms have been described, affecting their transporter activity. Variation in transporter expression or activity may therefore directly affect the efficacy and toxicity of the drug, and explain the high variation in oral availability of etoposide (25-80%) that is observed among cancer patients. These results may be used to improve pharmacotherapy with etoposide and possibly other related drugs.

INTRODUCTION

ATP binding cassette (ABC) multidrug transporters, like P-glycoprotein (P-gp, *ABCB1*) and Multidrug Resistance Proteins 2 and 3 (*ABCC2* and *ABCC3*), can have an important impact on cancer chemotherapy. These efflux pumps have broad and substantially overlapping substrate specificities. P-gp and ABCC2 are localized at apical membranes of important epithelial barriers, such as kidney and intestine and at the canalicular membrane of hepatocytes. Consequently, they can extrude their substrates into bile, urine and feces, and restrict the (re)uptake of their substrates from the gut. In addition, P-gp and ABCC2 are localized at the blood-brain, blood-testis, and blood-placenta barriers, where they restrict the penetration of potentially harmful compounds. In contrast, ABCC3 is situated at the basolateral membrane of epithelial cells of kidney and intestine and at the sinusoidal membrane of hepatocytes, and therefore ABCC3 pumps its substrates towards the blood circulation. Additionally, both apical and basolateral ABC transporters can

be expressed in tumor cells where they can actively efflux a broad spectrum of different anticancer drugs and thus contribute to multidrug resistance (1).

Etoposide is a semisynthetic derivative of podophyllotoxin and since many years this drug is widely used for the treatment of different malignant neoplasms, including leukemia, and tumors of the brain, lung, testis and stomach (2). Despite its extensive use, the main pharmacokinetic determinants of etoposide are still not completely defined. Knowledge of these pharmacokinetic determinants is necessary to optimize the pharmacotherapeutic parameters of etoposide, including dose, therapeutic schedule and route of administration (2). For instance, oral administration of etoposide in general has comparable efficacy as i.v. administration, but because the oral bioavailability of etoposide can vary highly among patients (25-80%), unpredictable and serious adverse reactions can occur (2). Therefore, defining the factors that contribute to the pharmacokinetic behavior of etoposide is necessary to further optimize drug therapy with etoposide.

P-gp efficiently transports lipophilic amphipathic drugs, including etoposide. Using *Abcb1a/1b*$^{-/-}$ mice, we previously found that P-gp can restrict the uptake of etoposide from the gut (3). In addition, etoposide is also a good ABCC1 substrate and Abcc1 deficient mice display an increased sensitivity for etoposide-induced toxicity (4). Furthermore, *in vitro* data show that both ABCC2 and ABCC3 can moderately transport etoposide (5;6). However, *Abcc3*$^{-/-}$ mice do not show any signs of increased toxicity compared to wild-type (WT) mice, when challenged with etoposide (7). In vivo data on the impact of ABCC2 on etoposide disposition and toxicity are thus far lacking.

In the present study we used *Abcb1a/1b*$^{-/-}$, *Abcc2*$^{-/-}$, *Abcc3*$^{-/-}$, *Abcb1a/1b;Abcc2*$^{-/-}$ and *Abcc2;Abcc3*$^{-/-}$ mice to study the separate and combined impact of these drug transporters on the *in vivo* behavior of etoposide.

MATERIALS AND METHODS

Chemicals. Etoposide, formulated as solution for intravenous injection (Toposin, 20 mg/ ml) originated from Pharmachemie, Haarlem, The Netherlands. Teniposide, formulated as solution for intravenous injection (Vumon, 10 mg/ ml) was from Bristol-Myers Squibb, Woerden, The Netherlands. [^{3}H]etoposide (specific activity 5 Ci/mmol) was obtained from Campro Scientific, Veenendaal, The Netherlands. Ketamine (Ketanest-S®) was from Pfizer (Cappelle a/d IJssel, the Netherlands). Xylazine was from Sigma Chemical Co (St. Louis, MO, USA). Methoxyflurane (Metofane®) was from Medical Developments Australia (Springvale, Victoria, Australia). Heparin (5000 IE/ml) was from Leo Pharma BV (Breda, the Netherlands). β-Glucuronidase from *Helix pomatia* (aqueous solution, ≥ 85,000 units/ml) originated from Sigma-Aldrich (Steinheim, Germany). Bovine

serum albumin (BSA), fraction V, was from Roche (Mannheim, Germany). The organic solvents methanol, acetonitril (both HPLC grade) and 1,2-dichloroethane were from Merck (Darmstadt, Germany). Blank human plasma was from healthy volunteers. All other chemicals and reagents were obtained from Sigma-Aldrich (Steinheim, Germany).

Animals. Mice were housed and handled according to institutional guidelines complying with Dutch legislation. Animals used in this study were male *Abcb1a/1b*$^{-/-}$ (8), *Abcc2*$^{-/-}$ (9), *Abcc3*$^{-/-}$ (10), *Abcb1a/1b;Abcc2*$^{-/-}$ (11), *Abcc2;Abcc3*$^{-/-}$ (12) and wild-type mice (WT), all of a >99% FVB genetic background, between 9 and 15 weeks of age. Animals were kept in a temperature-controlled environment with a 12-hour light / 12-hour dark cycle and received a standard diet (AM-II, Hope Farms, Woerden, The Netherlands) and acidified water *ad libitum*.

Plasma pharmacokinetics. For oral administration, etoposide (Toposin, 20 mg/ml) was 6.7-fold diluted with a 5% glucose solution in water and a total volume of 10 ml/kg (30 mg/kg) body weight was administered by gavage into the stomach, using a blunt-ended needle. To minimize variation in absorption, mice were fasted 3 hours before drug administration. For i.v. administration, etoposide (Toposin, 20 mg/ml) was 3.3-fold diluted with a saline solution (0.9% NaCl) and a total volume of 5 ml/kg (30 mg/kg) body weight was injected into a tail vein. Blood samples were collected by cardiac puncture under methoxyflurane anesthesia. Animals were sacrificed at 7.5 (i.v.), 15 (oral) and 30 min and 1, 2 and 4 hr (both series) after etoposide administration. Blood samples were centrifuged at 2,100 g for 6 min at 4°C, the plasma fraction was collected and stored at -20°C until analysis.

Fecal and urinary excretion. Excretion of etoposide in urine and feces was studied as previously described (11). Briefly, mice were individually housed in Ruco Type M/1 stainless-steel metabolic cages (Valkenswaard, the Netherlands). They were allowed 2 days to adapt, before 30 mg/kg etoposide, supplemented with [^{3}H]etoposide (~0.5 μCi per animal), was injected into a tail vein. Feces and urine were collected over a 24 h period and feces were homogenized in 4% BSA (1 ml per 100 mg feces). Part of the samples was used to determine levels of radioactivity by liquid scintillation counting and the rest was stored at -20°C until analysis.

Biliary excretion. In gall bladder cannulation experiments mice were anesthetized by intraperitoneal injection of a combination of ketamine (100 mg/kg) and xylazine (6.7 mg/kg), in a volume of 4.33 μl per gram body weight. After opening the abdominal cavity and distal ligation of the common bile duct, a polythene catheter (Portex limited, Hythe, UK) with an inner diameter of 0.28 mm, was inserted into the incised gallbladder and fixed with an additional ligation. Bile was collected for 60 min after i.v. injection of 30 mg/kg etoposide, supplemented with [^{3}H]etoposide (~0.5 μCi per animal). At the end of the experiment, blood was

collected by cardiac puncture and mice were sacrificed by cervical dislocation. Several tissues were removed and homogenized in 4% BSA. Intestinal contents were separated from intestinal tissues prior to homogenization. Part of the tissue homogenates, bile and plasma samples was used to determine levels of radioactivity. The rest was stored at -20°C until analysis.

Drug analysis. Etoposide concentrations were measured with a previously described HPLC method with minor modifications (13). A volume of 20 µl bile or 50 µl plasma, urine or tissue homogenate was completed to 500 µl with drug-free human plasma. Teniposide (Vumon, 10 mg/ml) was 500-fold diluted with methanol to 20 µg/ml and 100 µl of this solution was added as internal standard. Etoposide was extracted with 2 ml of 1,2-dichloroethane and after thoroughly shaking for 5 min, the mixture was centrifuged at 2,000 rpm × 3 min. The aqueous layer was removed and the organic extract was transferred to a clean glass tube and evaporated to dryness under a constant nitrogen flow. The residue was reconstituted in 200 µl solvent (25% acetonitril and 75% water), and subjected to reversed-phase HPLC analysis with UV detection (282 nm), using a 3.9 × 300 mm, 10 µm, µBondapak Phenyl Column (Waters, Etten-Leur, The Netherlands) and a mobile phase consisting of water:acetonitril:acetic acid (71:28:1).

Deglucuronidation of etoposide glucuronide. To obtain etoposide glucuronide concentrations in plasma, bile, urine and liver homogenates, ß-glucuronidase (*Helix pomatia*) was used for deglucuronidation. The pH was set to pH 4.5 - 5.0 by adding 3 µl 0.3 M acetic acid buffer pH 4.5 (urine and bile and liver homogenates) or 10 µl 0.4 M acetic acid (plasma) to 50 µl of the different matrices and the samples were incubated with 20 µl ß-glucuronidase (final concentration 2000 Unit/ml) at 37 °C for 24 hours. After this incubation, samples were completed to 500 µl with drug-free human plasma and processed as described above. The etoposide glucuronide concentration was calculated by subtracting the original etoposide concentration from the etoposide concentration after deglucuronidation. Etoposide glucuronide concentrations are expressed in etoposide mass equivalents.

RNA isolation, cDNA synthesis and real-time RT PCR. Mouse livers were excised and immediately placed in an appropriate volume of RNAlater (QIAGEN, Venlo, The Netherlands). They were stored at 4°C for several days until RNA was extracted using the RNeasy mini kit (QIAGEN) according to the manufacturer's protocol. Subsequently, cDNA was generated using 5 µg of total RNA in a synthesis reaction using random hexamers (Applied Biosystems, Foster City, CA) and SuperScript II reverse transcriptase (Invitrogen, Carlsbad, CA) according to the supplier's protocols. The reverse transcription reaction was performed for 60 min at 42°C with a deactivation step of 15 min at 70°C. cDNA was stored at -20°C until

use. Real-time RT-PCR was performed using specific primers (QIAGEN) on an Applied Biosystems 7500 real-time cycler system as previously described (14). Analysis of the results was done by the comparative C_t method as described (15) and statistic analysis was performed on ΔCt values as previously described (16).

Pharmacokinetic calculations and statistical analysis. Pharmacokinetic parameters were calculated by noncompartmental methods using the software package WinNonlin Professional version 5.0. The area under the plasma concentration-time curve (AUC) was calculated using the trapezoidal rule, with extrapolating to infinity. Elimination half-lives ($t_{½,\ el}$) were calculated by linear regression analysis of the log-linear part of the plasma concentration-time curves. The peak plasma concentration (C_{max}) and the time of maximum plasma concentration (T_{max}) were estimated from the original data. Plasma clearance (CL) after i.v. administration was calculated by the formula CL = Dose/$AUC_{i.v.}$ and the oral bioavailability (*F*) was calculated by the formula $F = AUC_{oral} / AUC_{i.v.} \times 100\%$. The two-sided unpaired Student's *t*-test was used for statistical analysis. Data obtained with single and combination knockout mice were compared to data obtained with wild-type mice, unless stated otherwise. Differences were considered statistically significant when $P < 0.05$. Data are presented as means ± SD.

RESULTS

Impact of Abcc2 and P-gp on plasma pharmacokinetics of etoposide and its glucuronide. To investigate the separate and combined impact of Abcc2 and P-gp on absorption, distribution and elimination of etoposide, we studied plasma pharmacokinetics in WT, *Abcc2*$^{-/-}$, *Abcb1a/1b*$^{-/-}$ and *Abcb1a/1b;Abcc2*$^{-/-}$ mice. After oral administration of etoposide (30 mg/kg body weight) the plasma concentrations and the area under the oral plasma concentration-time curve (AUC_{oral}) were not different between WT and *Abcc2*$^{-/-}$ mice (Fig. 1A and Table 1). *Abcb1a/1b*$^{-/-}$ mice had a 2.7-fold greater AUC_{oral} and the C_{max} was 3.3-fold increased (Table 1). Combined deficiencies of Abcc2 and P-gp resulted in another 1.3-fold higher AUC_{oral} compared to *Abcb1a/1b*$^{-/-}$ mice (and 3.5-fold compared to WT mice) and C_{max} was 1.3-fold greater than for *Abcb1a/1b*$^{-/-}$ mice ($P < 0.05$ for both parameters; Table 1 and Fig 1A). These results suggest that P-gp restricts the (re)uptake of etoposide from the gut, whereas single Abcc2 deficiency does not affect the oral etoposide plasma pharmacokinetics. However, when P-gp is absent, Abcc2 can also have an impact on oral etoposide plasma pharmacokinetics.

After i.v. administration of 30 mg/kg etoposide, Abcc2 deficiency had a modest effect on the $AUC_{i.v.}$ (Fig. 1B and Table 1). In contrast, absence of P-gp resulted in a 1.4-fold higher $AUC_{i.v.}$ and combined deficiencies led to a 1.6-fold increased $AUC_{i.v.}$ (Table 1).

Table 1. Plasma pharmacokinetic parameters after oral or i.v. administration of etoposide at 30 mg/kg.

		Strain			
		WT	*Abcb1a/1b*$^{-/-}$	*Abcc2*$^{-/-}$	*Abcb1a/1b;Abcc2*$^{-/-}$
Etoposide					
Oral	$AUC_{(0-\infty)}$, hr.mg/l	4.19 ± 0.38	11.3 ± 0.75**	4.17 ± 0.14	14.8 ± 0.45***/††
	C_{max}, mg/l	1.92 ± 0.16	6.38 ± 0.61***	2.17 ± 0.50	8.35 ± 1.08***/†
	T_{max}, hr	0.5	0.5	0.5	0.5
i.v.	$AUC_{(0-\infty)}$, hr.mg/l	16.1 ± 0.58	23.0 ± 1.00**	18.8 ± 0.78*	25.9 ± 1.10***/†
	$t_{½,\ el}$, hr	0.35 ± 0.02	0.50 ± 0.02*	0.41 ± 0.04	0.52 ± 0.04*
	CL, l/hr.kg	1.86 ± 0.07	1.31 ± 0.10**	1.60 ± 0.08*	1.16 ± 0.09**
F, %		26.0 ± 2.5	49.4 ± 5.4**	22.2 ± 1.2	57.3 ± 3.0**
Etoposide glucuronide					
i.v.	$AUC_{(0-\infty)}$, hr.mg/l	14.9 ± 0.81	18.5 ± 0.74**	28.3 ± 0.75***	33.0 ± 1.80***/††
Etoposide and etoposide glucuronide					
i.v.	$AUC_{(0-\infty)}$, hr.mg/l	31.0 ± 1.21	41.5 ± 1.37**	47.1 ± 1.18**	58.9 ± 1.52***/††

AUC, area under plasma concentration-time curve; C_{max}, maximum plasma concentration; T_{max}, time of maximum plasma concentration; $t_{½,\ el}$, elimination half life; CL, plasma clearance; *F*, oral bioavailability. Etoposide glucuronide concentrations are expressed in etoposide mass equivalents. Data are means ± SD, n = 4 for both oral and i.v. administration. * $P < 0.05$, ** $P < 0.01$ and *** $P < 0.001$, compared to WT mice. † $P < 0.01$, †† $P < 0.001$ compared to *Abcb1a/1b*$^{-/-}$ mice.

Conjugation of etoposide to glucuronic acid plays a major role in its elimination in humans, rats and rabbits (13;17;18). We therefore determined the etoposide glucuronide concentrations in plasma after i.v. administration of etoposide (Fig. 2A and Table 1). Abcc2 deficiency resulted in a 1.9-fold higher $AUC_{i.v.}$ for etoposide glucuronide compared to WT mice, whereas mice lacking P-gp had only a 1.2-fold higher $AUC_{i.v.}$ (Table 1). Absence of both transporters had an additive effect on the etoposide glucuronide $AUC_{i.v.}$, which was 2.2-fold higher than in WT mice. Our data indicate that upon i.v. administration, P-gp seems mainly important for the parent compound, whereas Abcc2 deficiency primarily affects the plasma pharmacokinetics of the glucuronide metabolite.

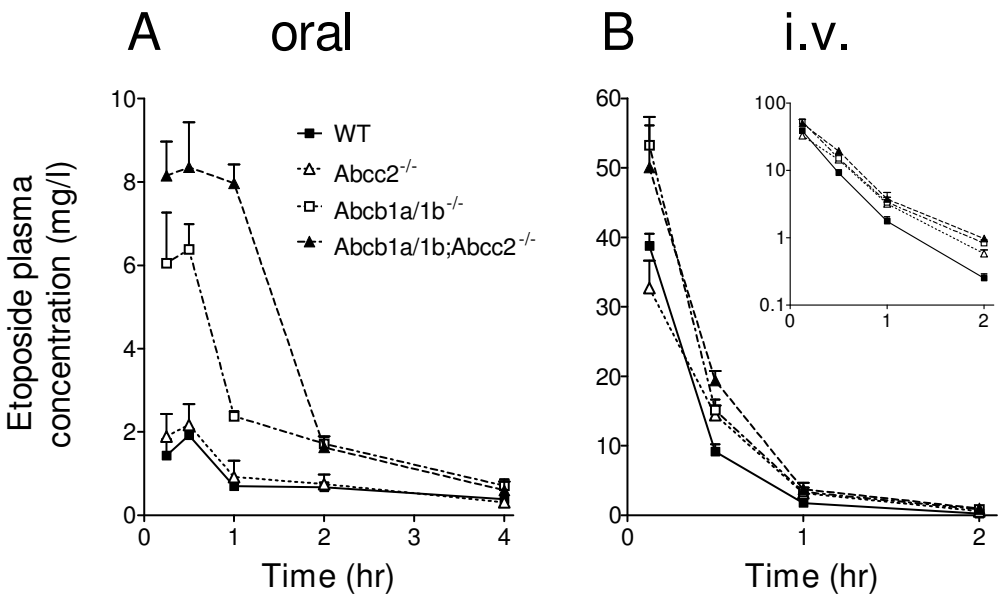

Fig. 1. Plasma concentration-time curves for etoposide in male FVB WT (■), *Abcc2*$^{-/-}$ (Δ), *Abcb1a/1b*$^{-/-}$ (□), and *Abcb1a/1b;Abcc2*$^{-/-}$ (▲) mice, after oral (*A*) and i.v. (*B*) administration of 30 mg/kg etoposide. Data are means ± SD, n = 4 for both oral and i.v. administration. Insert in panel *B* shows a semilogarithmic representation of the data. Note the difference in concentrations and time scales between panels *A* and *B*.

To compare the impact of P-gp and Abcc2 on the total etoposide plasma pharmacokinetics (etoposide + etoposide glucuronide), we also plotted the etoposide plasma concentration-time curves after deglucuronidation (Fig. 2B) and calculated the total $AUC_{i.v.}$ (Table 1). The total $AUC_{i.v.}$ was 1.3-fold elevated in *Abcb1a/1b*$^{-/-}$ mice and 1.5-fold increased in *Abcc2*$^{-/-}$ mice. Combination knockout animals had a 1.9-fold higher total $AUC_{i.v.}$, which is additive compared to both single knockout strains (Table 1). These results indicate that upon i.v. administration, P-gp and Abcc2 equally contribute to the overall disposition and elimination of etoposide, P-gp primarily through etoposide itself, and Abcc2 primarily through etoposide glucuronide.

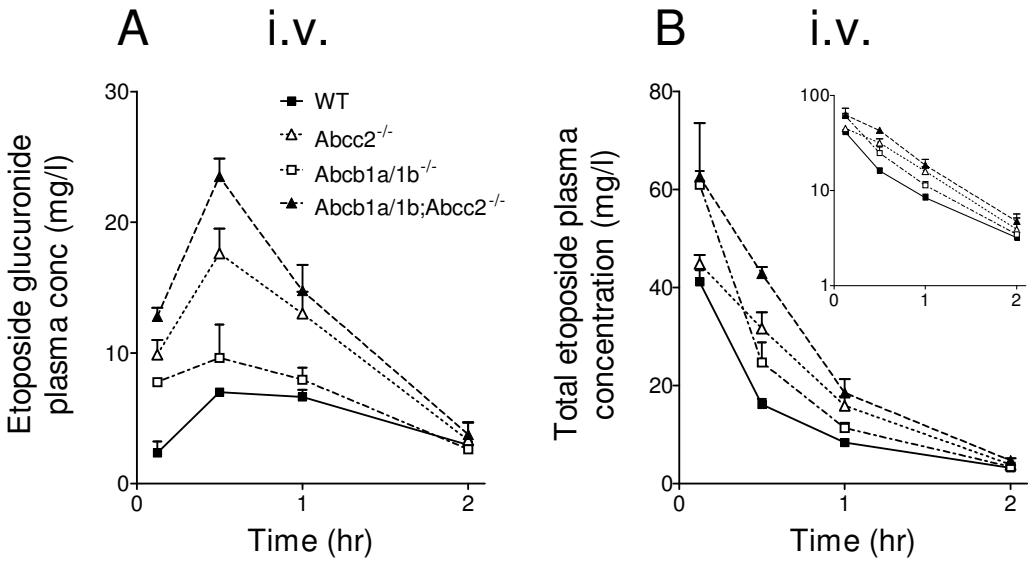

Fig. 2. Plasma concentration-time curves in male FVB WT (■), *Abcc2*$^{-/-}$ (Δ), *Abcb1a/1b*$^{-/-}$ (□), and *Abcb1a/1b;Abcc2*$^{-/-}$ (▲) mice, for etoposide glucuronide (*A*) and for total etoposide after deglucuronidation (*B*), determined after i.v. administration of 30 mg/kg etoposide. Etoposide glucuronide concentrations are expressed in etoposide mass equivalents. Data are means ± SD; n = 4. Insert in B shows semilogarithmic representation of the data. Note the difference in concentration scales between panels *A* and *B*.

Effect of Abcc2 and P-gp on the urinary and fecal excretion of etoposide and its glucuronide. In humans, rats and rabbits, elimination of etoposide mainly occurs via urinary excretion of unchanged etoposide and etoposide glucuronide (13;17;18). Since P-gp and Abcc2 markedly affected the plasma pharmacokinetics of etoposide and its glucuronide, we next assessed the overall excretion of these compounds in the same panel of knockout mice. Urine and feces were collected for 24 hours after i.v. administration of 30 mg/kg [^{3}H]etoposide and cumulative excretion of unchanged etoposide and total radioactivity was determined (Fig. 3). For P-gp-deficient animals, excretion of unchanged etoposide and total radioactivity in urine and feces was not different from WT mice (Fig. 3A and 3B). Urinary excretion of unchanged etoposide in mice lacking Abcc2 and/or P-gp was not different compared to WT mice, but the amount of total radioactivity in urine was highly increased in *Abcc2*$^{-/-}$ and *Abcb1a/1b;Abcc2*$^{-/-}$ mice. Given the higher plasma concentrations of etoposide glucuronide in *Abcc2*$^{-/-}$ and *Abcb1a/1b;Abcc2*$^{-/-}$ mice (Fig. 2A) we investigated the urinary output of this metabolite. Indeed, etoposide glucuronide accounted for an important part (~21-23% of the given dose)

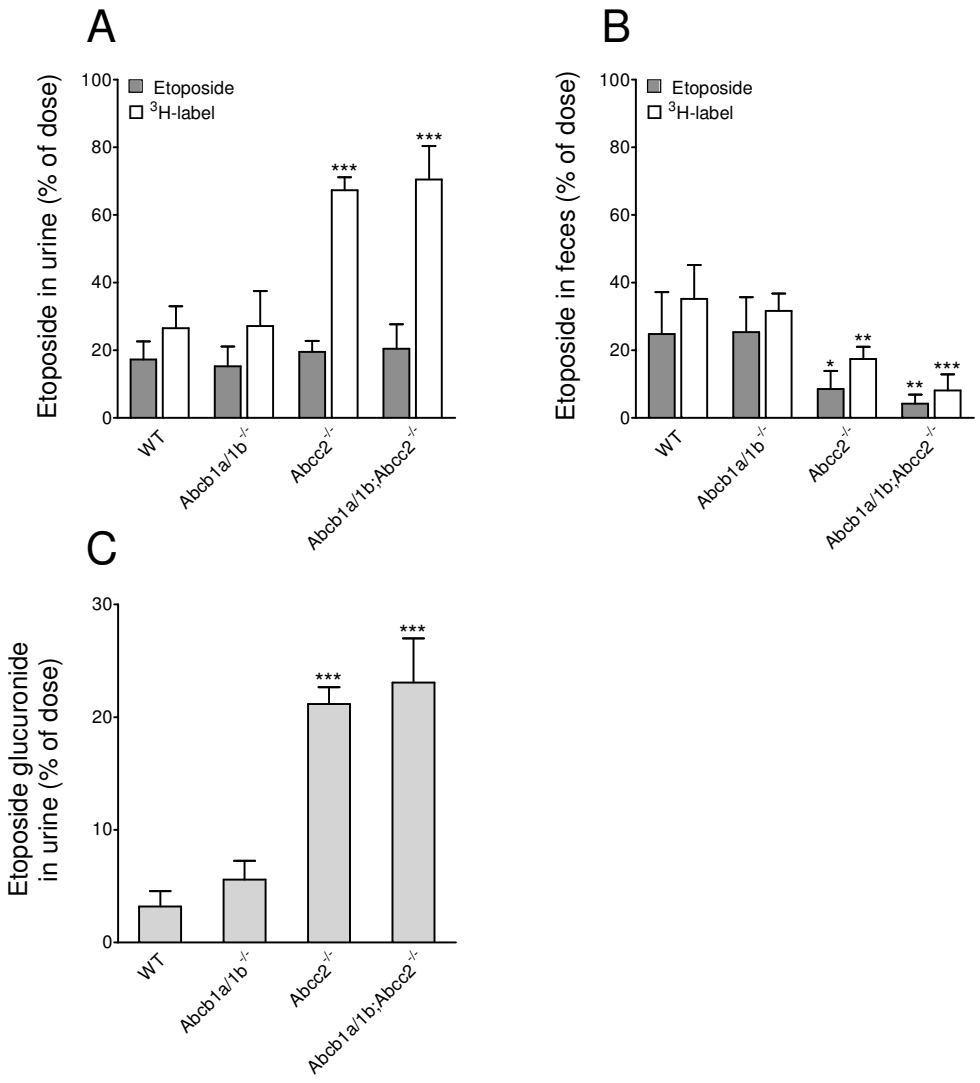

Fig. 3. Urinary and fecal excretion of etoposide in male FVB WT, *Abcc2*$^{-/-}$, *Abcb1a/1b*$^{-/-}$, and *Abcb1a/1b;Abcc2*$^{-/-}$ mice, over 24 hr after i.v. administration of 30 mg/kg [^{3}H]etoposide. In feces and urine (*A* and *B*), total radioactivity (^{3}H label) and unchanged etoposide were measured, whereas etoposide glucuronide was determined only in urine (*C*). Etoposide glucuronide concentrations are expressed in etoposide mass equivalents. Data are means ± SD; n = 5. * $P < 0.05$, ** $P < 0.01$ and *** $P < 0.001$, compared to WT mice. Note the difference in concentration scales between the panels.

of urinary radioactivity in these strains, versus 3-6% in WT and *Abcb1a/1b*$^{-/-}$ mice (Fig. 3A and 3C). Roughly a third of the total radioactivity in the Abcc2-deficient strains could not be directly ascribed to either unchanged etoposide or its glucuronide, suggesting that additional etoposide metabolite(s) are excreted in the urine when Abcc2 is absent. In contrast to the urinary excretion, the fecal excretion of unchanged etoposide and total radioactivity was strongly reduced in *Abcc2*$^{-/-}$ mice, and especially *Abcb1a/1b;Abcc2*$^{-/-}$ mice (Fig. 3B).

Impact of Abcc2 and P-gp on biliary and direct intestinal excretion of etoposide. To investigate the roles of Abcc2 and P-gp in biliary and direct intestinal excretion we performed gall bladder cannulation experiments. Anesthetized mice with a cannulated gall bladder and a ligated common bile duct were i.v. injected with 30 mg/kg [^{3}H]etoposide and the biliary output was measured for 1 hour. WT mice excreted 12.0 ± 1.3% of the dose as unchanged etoposide in their bile (Fig. 4A). In P-gp deficient mice this was not different (14.5 ± 3.9%; P = 0.2). In contrast, biliary excretion of etoposide in *Abcc2*$^{-/-}$ and *Abcb1a/1b;Abcc2*$^{-/-}$ mice was 5.7 and 6.1-fold reduced, respectively (to 2.1 ± 0.7% and 2.0 ± 0.7% of the dose; Fig. 4A). This demonstrates that Abcc2 dominates the biliary excretion of unchanged etoposide, whereas P-gp contributes very little, if anything to this excretion.

In WT mice the biliary excretion of unchanged etoposide was not different from total radioactivity output, indicating that virtually only etoposide was excreted. However, in *Abcb1a/1b* $^{-/-}$ mice, the biliary output of total radioactivity was markedly higher than that of unchanged etoposide (the difference being ~12% of the dose), indicating that etoposide metabolite(s) were present in the bile. Etoposide glucuronide in the bile of these mice was determined and accounted for 10.1 ± 2.4% of the dose. This means that the higher output of total radioactivity in this strain (Fig. 4A) represents mainly etoposide glucuronide. The observation that the biliary excretion of radioactivity other than parent etoposide in combination *Abcb1a/1b;Abcc2*$^{-/-}$ mice was negligible (Fig. 4A), suggests that Abcc2 is also primarily responsible for biliary excretion of etoposide glucuronide in the *Abcb1a/1b* $^{-/-}$ mice.

Because in gall bladder cannulation experiments the common bile duct is ligated, drug found in the gut can be solely attributed to direct excretion across the intestinal wall. In the small intestinal contents of WT mice ~10% of the dose was found as unchanged etoposide and levels of total radioactivity (also ~10% of the dose) revealed that little metabolite was present in the small intestinal contents of these mice (Fig 4B). Both *Abcb1a/1b*$^{-/-}$ and *Abcb1a/1b;Abcc2*$^{-/-}$ mice had markedly less unchanged etoposide in their gut, indicating that P-gp mediates the direct intestinal excretion of etoposide.

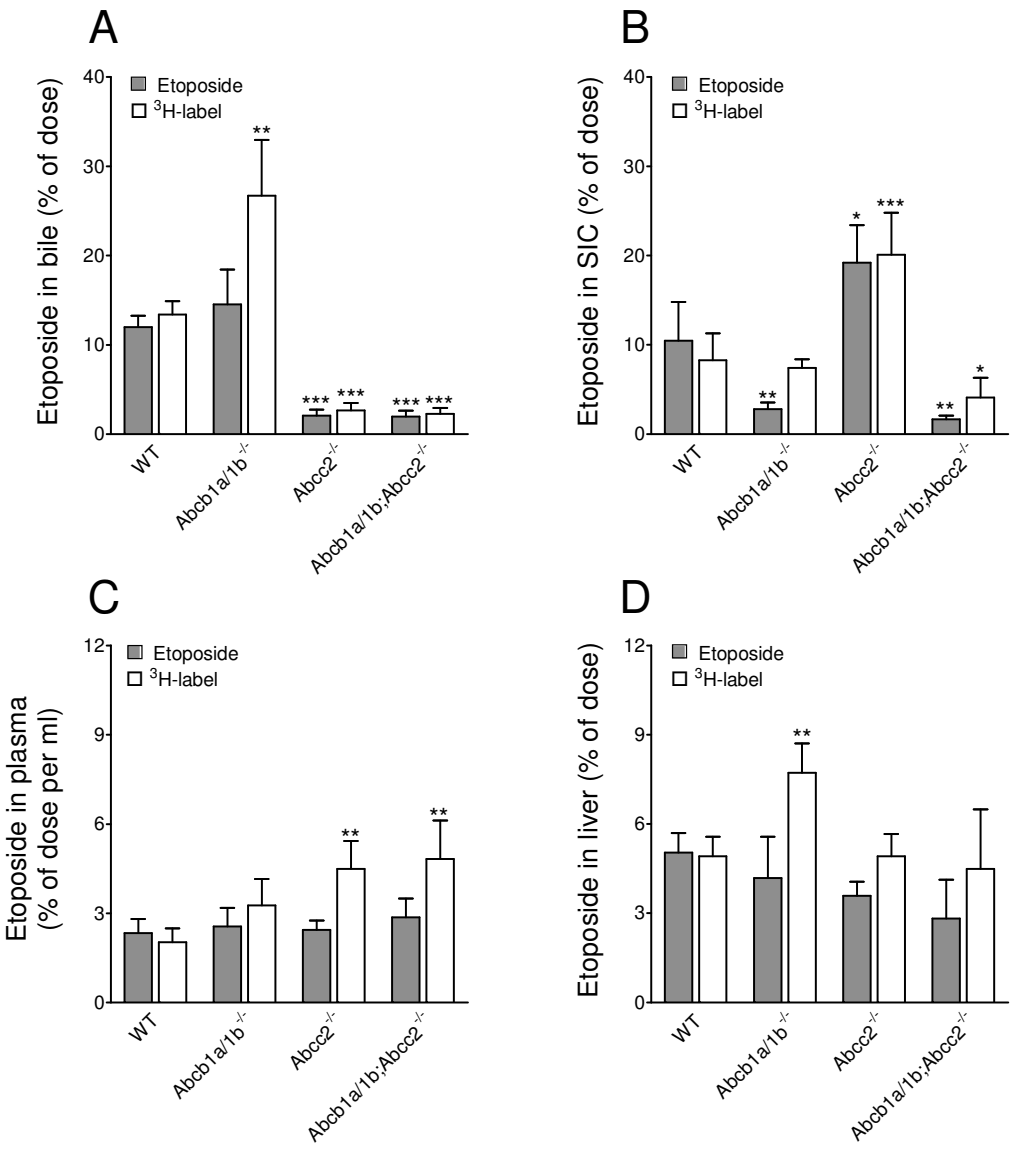

Fig. 4. Biliary and intestinal excretion of etoposide in gall bladder cannulated male FVB WT, *Abcc2*$^{-/-}$, *Abcb1a/1b*$^{-/-}$, and *Abcb1a/1b;Abcc2*$^{-/-}$ mice, over 60 min after i.v. administration of 30 mg/kg [^{3}H]etoposide. In addition to bile (*A*), total radioactivity (^{3}H label) and unchanged etoposide were also measured in the small intestinal contents (SIC; *B*), plasma (*C*) and liver (*D*), which were collected 60 minutes after the [^{3}H]etoposide administration. Data are means ± SD; n = 5. * $P < 0.05$, ** $P < 0.01$ and *** $P < 0.001$, compared to WT mice.

The decrease in direct intestinal excretion of etoposide from ~19% of the dose in *Abcc2*$^{-/-}$ mice to ~2% of the dose in *Abcb1a/1b;Abcc2*$^{-/-}$ mice illustrates the profound impact of P-gp in this process. These observations are in line with the data presented in Fig. 1A, which showed that P-gp drastically restricts the intestinal (re)uptake of etoposide. Interestingly, *Abcc2*$^{-/-}$ mice had highly increased levels of radioactivity in their guts (~20% of the dose), which could entirely be attributed to unchanged etoposide (Fig 4B). We note that the decrease in biliary output as well as the increase in direct intestinal excretion in *Abcc2*$^{-/-}$ mice was ~10% of the dose (Fig. 4A and 4B). It is therefore tempting to speculate that impaired biliary excretion in *Abcc2*$^{-/-}$ mice results in higher levels of etoposide in the systemic circulation and subsequent excretion of etoposide across the intestinal wall into the gut, presumably via P-gp. If this is indeed the case, this process must occur quite efficiently and shortly after i.v. injection while plasma concentrations of etoposide are still high, because at 60 min after i.v. injection plasma concentrations were not elevated in cannulated *Abcc2*$^{-/-}$ mice (Fig. 4C).

The total radioactivity, but not the unchanged etoposide concentration, in the liver of P-gp deficient mice was significantly higher than in WT mice (Fig. 4D). Together with the increased biliary excretion of etoposide glucuronide, these results suggest that *Abcb1a/1b*$^{-/-}$ mice have an increased hepatic formation and subsequently a higher biliary excretion of etoposide glucuronide.

Accumulation of etoposide glucuronide in livers of *Abcc2;Abcc3*$^{-/-}$ mice. ABCC3 was previously found to efficiently transport etoposide glucuronide *in vitro* (19), whereas the affinity of ABCC2 towards this metabolite was not reported. To investigate the impact of Abcc2 and Abcc3 on etoposide glucuronide transport *in vivo*, we studied liver accumulation in conscious, freely moving WT, *Abcc2*$^{-/-}$, *Abcc3*$^{-/-}$ and *Abcc2;Abcc3*$^{-/-}$ mice, 1 hour after i.v. administration of 30 mg/kg etoposide. We also included *Abcb1a/1b*$^{-/-}$ and *Abcb1a/1b;Abcc2*$^{-/-}$ mice to obtain a complete picture. Importantly, in contrast to single *Abcc2*$^{-/-}$ or *Abcc3*$^{-/-}$ mice, in the livers of *Abcc2;Abcc3*$^{-/-}$ mice a highly increased amount of etoposide glucuronide was found (Fig. 5). This indicates that excretion of etoposide glucuronide from the liver to the systemic blood circulation is primarily dependent on Abcc3, whereas its excretion into the bile occurs predominantly via Abcc2.

Liver accumulation of etoposide glucuronide in *Abcc2*$^{-/-}$ and *Abcb1a/1b;Abcc2*$^{-/-}$ mice was markedly lower than in WT mice (Fig. 5B). We previously observed that hepatic protein expression of Abcc3 is upregulated in male *Abcc2*$^{-/-}$ mice (9) and in the present study we also found higher Abcc3 mRNA expression in livers of in male *Abcc2*$^{-/-}$ and *Abcb1a/1b;Abcc2*$^{-/-}$ mice (Fig. 6, described below). Higher hepatic expression and activity of Abcc3 likely results in an elevated efflux of etoposide glucuronide to the blood circulation and

accordingly lower liver accumulation in these strains. The increased plasma concentrations of etoposide glucuronide in *Abcc2*$^{-/-}$ and *Abcb1a/1b;Abcc2*$^{-/-}$ mice (Fig. 5A) are consistent with this idea.

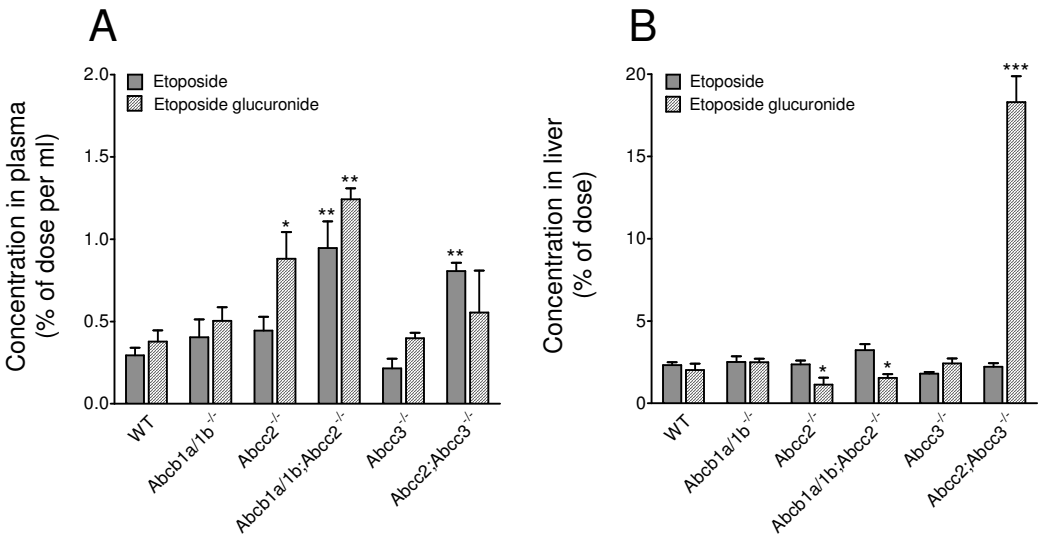

Fig. 5. Plasma (*A*) and liver concentrations (*B*) of etoposide and etoposide glucuronide in male FVB WT, *Abcc2*$^{-/-}$, *Abcb1a/1b*$^{-/-}$, *Abcb1a/1b;Abcc2*$^{-/-}$, *Abcc3*$^{-/-}$ and *Abcc2;Abcc3*$^{-/-}$ mice, 60 min after i.v. administration of 30 mg/kg etoposide. Data are means ± SD, n = 5. * $P < 0.05$, ** $P < 0.01$ and *** $P < 0.001$, compared to WT mice. Note the difference in concentration scales between the panels.

Hepatic mRNA expression of Ugt1a1 and Abcc3. The highly elevated concentrations of etoposide glucuronide in the bile of *Abcb1a/1b*$^{-/-}$ mice (Fig. 4A) may be the result of increased hepatic formation of etoposide glucuronide. A possible cause for increased etoposide glucuronide formation would be upregulation of UDP-glucuronosyltransferase (UGT) enzyme(s) in liver. In human liver microsomes, conjugation of etoposide to glucuronic acid is mainly mediated by UGT1A1 (20;21). We therefore evaluated hepatic mRNA levels of Ugt1a1 in WT, *Abcc2*$^{-/-}$, *Abcb1a/1b*$^{-/-}$ and *Abcb1a/1b;Abcc2*$^{-/-}$ mice. Indeed, Ugt1a1 mRNA was 2-3-fold increased in single and combination P-gp deficient mice (Fig. 6). This may explain the higher output of etoposide glucuronide in the bile of *Abcb1a/1b*$^{-/-}$ mice. In contrast, the highly increased plasma concentration and urinary output of

etoposide glucuronide in *Abcc2*$^{-/-}$ mice (Fig. 2A and 3C) were not associated with elevated hepatic Ugt1a1 expression (Fig. 6). Presumably, as there is little biliary excretion of etoposide from the *Abcc2*$^{-/-}$ liver, there is more opportunity for conversion to etoposide glucuronide.

The finding that *Abcb1a/1b;Abcc2*$^{-/-}$ mice had elevated Ugt1a1 expression, but strongly reduced biliary excretion of etoposide glucuronide (≤ 0.5% of the dose) compared to *Abcb1a/1b*$^{-/-}$ mice (10% of the dose; Fig. 4A), indicates that Abcc2 is responsible for the biliary output of the glucuronide metabolite.

We previously reported that Abcc3 protein was upregulated in the livers of male *Abcc2*$^{-/-}$ mice compared to WT mice (9). Because Abcc3 plays an important role in the efflux of etoposide glucuronide from the liver to the blood, we evaluated hepatic mRNA expression in the same panel of knockout mice. Abcc3 (Abcc3) was upregulated in the livers of P-gp (2.2-fold) and Abcc2 (3.2-fold) deficient animals, with the highest mRNA expression in *Abcb1a/1b;Abcc2*$^{-/-}$ mice (5.3-fold; Fig. 6).

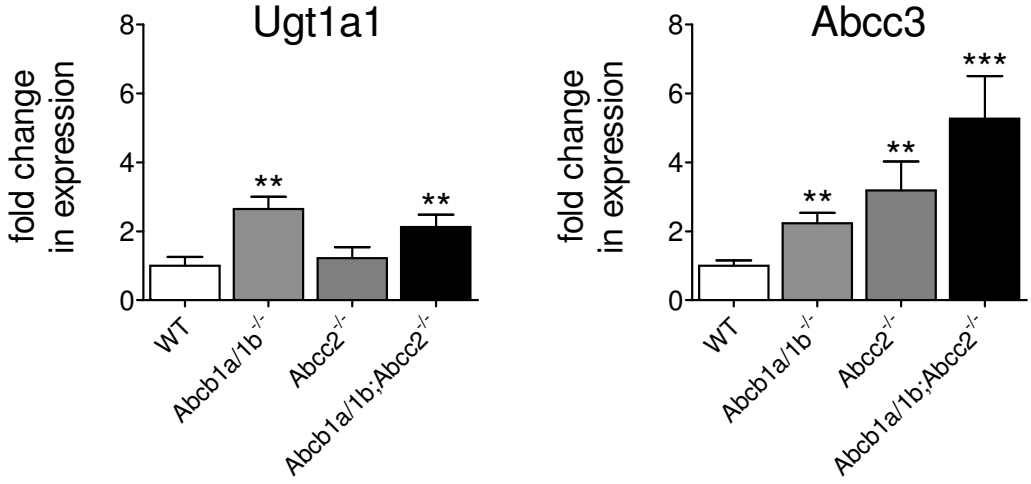

Fig. 6. Expression levels of Ugt1a1 and Abcc3 in livers of male WT, *Abcc2*$^{-/-}$, *Abcb1a/1b*$^{-/-}$ and *Abcb1a/1b;Abcc2*$^{-/-}$ mice, as determined by real-time RT-PCR. Data are normalized to GAPDH expression. Values represent mean fold change ± SD, compared to WT mice; n = 4. * $P < 0.05$, ** $P < 0.01$ and *** $P < 0.001$, compared to WT ΔCt values.

DISCUSSION

In the present study we show that the hepatobiliary output of both etoposide and etoposide glucuronide is almost entirely dependent on Abcc2, and not on P-gp. Furthermore, P-gp was found to restrict the oral (re)uptake of unchanged etoposide (as shown before (3)), and to mediate substantial direct intestinal excretion across the gut wall. We also show that Abcc3 is responsible for the efflux of etoposide glucuronide from the liver to the systemic blood circulation, especially when Abcc2 is absent.

Although Abcc2 almost exclusively mediates the biliary excretion of parent drug, liver and plasma concentrations of unchanged etoposide upon i.v. administration were not elevated in Abcc2 deficient mice (Fig. 4A). This may be explained by increased hepatic formation of the main metabolite etoposide glucuronide. Yet, *Abcc2*$^{-/-}$ mice did not display higher levels of etoposide glucuronide in their livers than WT mice (Fig. 4D), whereas plasma levels were highly increased (Fig. 2A). Apparently, when the canalicular transporter Abcc2 is absent, the (upregulated) basolateral Abcc3 takes over and efficiently extrudes etoposide glucuronide from the liver to the blood circulation. The highly elevated glucuronide levels in the livers of *Abcc2;Abcc3*$^{-/-}$ mice confirm this idea (Fig. 5B).

We previously observed that protein expression of Abcc3 is upregulated in the livers of male *Abcc2*$^{-/-}$ mice (9). In the present study we show that Abcc3 mRNA is increased in the livers of male *Abcc2*$^{-/-}$ as well as *Abcb1a/1b;Abcc2*$^{-/-}$ mice. Elevated hepatic Abcc3 expression in Abcc2-deficient animals likely contributes to efficient extrusion of etoposide glucuronide from the liver to the blood. Subsequently, the glucuronide metabolite can be eliminated in the urine. Indeed, Abcc2 deficient mice had up to 7-fold increased urinary output of etoposide glucuronide compared to their WT counterparts (Fig. 3C). Our observation in mice that disrupted hepatobiliary excretion of etoposide results in increased hepatic formation and subsequent urinary excretion of etoposide metabolites, may also apply to etoposide pharmacokinetics in humans. In fact, this may explain why many pharmacokinetic studies in patients with elevated plasma levels of bilirubin or even with obstructive jaundice, failed to demonstrate differences in total clearance, elimination half-life or volume of distribution of unchanged etoposide (17;22-25). The *Abcc2*$^{-/-}$ mice show very similar results when only unchanged etoposide is considered (Fig 1A, 1B, 3A, 4C).

Although Abcc3 is also more highly expressed in *Abcb1a/1b*$^{-/-}$ mice (Fig. 6), there is no marked increase in urinary etoposide glucuronide excretion (Fig. 3A, 3C). This suggests that Abcc2 is considerably more efficient than Abcc3 in

removing etoposide glucuronide from the liver, allowing very little etoposide glucuronide to leave the liver over the sinusoidal membrane.

Ugt1a1 was not more highly expressed in livers of *Abcc2*$^{-/-}$ mice, despite the highly increased plasma and urine levels of etoposide glucuronide in this strain (Fig. 2A and 3C). The formation of etoposide glucuronide in the liver of *Abcc2*$^{-/-}$ mice thus seems not to be limited by the capacity of the UGT enzyme, but rather by the hepatic residence time of etoposide, which is presumably increased in the absence of hepatobiliary excretion of etoposide by Abcc2. Interestingly, in humans receiving 80-120 mg/m^2 etoposide, approximately 8% of the dose was excreted as etoposide glucuronide in the urine within 24 hours (17). Another study revealed that the urinary excretion of etoposide glucuronide in patients receiving up to 3500 mg/m^2 etoposide (~35-fold higher dose) was still 8.3-17.3% of the dose (18). Assuming that the patients in these two studies had comparable UGT1A1 expression, enhanced formation of etoposide glucuronide is thus not necessarily dependent on higher UGT1A1 expression.

Both human ABCC2 and ABCC3 were previously shown to moderately transport etoposide *in vitro* (5;6). However, *Abcc3*$^{-/-}$ mice did not display an enhanced lethality when exposed to etoposide (7). Furthermore, etoposide glucuronide was reported to be an excellent substrate for human ABCC3 (19), whereas information on the transport of etoposide glucuronide by ABCC2 is lacking. Our data indicate that etoposide is an excellent substrate of Abcc2 *in vivo*. In fact, biliary excretion of etoposide, which plays an important role in the elimination of etoposide in WT mice, is ~6-fold decreased in *Abcc2*$^{-/-}$ mice. We further found that mice deficient for both Abcc2 and Abcc3 had highly increased levels of etoposide glucuronide in their livers. Additionally, in single *Abcc3*$^{-/-}$ mice the hepatic etoposide glucuronide concentrations were not different from WT mice, whereas these concentrations in single *Abcc2*$^{-/-}$ and combination *Abcb1a/1b;Abcc2*$^{-/-}$ mice were even somewhat lower than in WT mice (Fig. 5B). The latter might well be explained by the upregulated Abcc3 in the livers of *Abcc2*$^{-/-}$ and *Abcb1a/1b;Abcc2*$^{-/-}$ mice [(9) and Fig. 6]. Collectively, these results indicate that etoposide glucuronide is a good substrate for both Abcc2 and Abcc3 and that the elimination of this metabolite from the liver is almost completely dependent on these efflux pumps. However, if both Abcc2 and Abcc3 are present, like in the *Abcb1a/1b*$^{-/-}$ mice (Fig. 4A and 4C), Abcc2 appears to be more efficient than Abcc3.

In this study we show that Abcc2, and not P-gp, dominates the biliary excretion of etoposide. Previously, we found that the biliary excretion of the anticancer agent paclitaxel also was dominated by Abcc2, whereas P-gp played a minor role (11). In addition, ABCC2 was shown to be overexpressed in

hepatocellular carcinoma (HCC) (27;28), and silencing of ABCC2 in HepG2 tumor cells (hepatoma cells) with an ABCC2 antisense construct resulted in a highly increased sensitivity towards etoposide (25-fold), doxorubicin (12-fold), vincristine (50-fold) and cisplatin (25-fold) (29). ABCC2 thus seems to play an important role in the liver, under physiological and pathological conditions. On the one hand ABCC2 dominates the hepatobiliary drug excretion, and on the other hand ABCC2 can confer multidrug resistance in HCC.

Our findings may be relevant for patients treated with etoposide, because for P-gp, ABCC2 and ABCC3 polymorphisms have been described that affect their transport activity. Variation in transporter expression might explain why the oral availability of etoposide varies widely among patients (25-80%). Knowledge of factors that affect the pharmacokinetics may help to improve pharmacotherapy with etoposide and possibly other related drugs.

ACKNOWLEGMENTS

We thank Dr. Piet Borst (The Netherlands Cancer Institute, Amsterdam, The Netherlands) for providing the *Abcc3*$^{-/-}$ mice. We further acknowledge our colleagues for critical reading of the manuscript.

REFERENCES

(1) Borst P, Oude Elferink RP. Mammalian ABC transporters in health and disease. Annu Rev Biochem 2002;71:537-92.

(2) Toffoli G, Corona G, Basso B, Boiocchi M. Pharmacokinetic optimisation of treatment with oral etoposide. Clin Pharmacokinet 2004;43:441-66.

(3) Allen JD, Van Dort SC, Buitelaar M, van Tellingen O, Schinkel AH. Mouse breast cancer resistance protein (Bcrp1/Abcg2) mediates etoposide resistance and transport, but etoposide oral availability is limited primarily by P-glycoprotein. Cancer Res 2003;63:1339-44.

(4) Wijnholds J, Scheffer GL, van der Valk M, van der Valk P, Beijnen JH, Scheper RJ et al. Multidrug resistance protein 1 protects the oropharyngeal mucosal layer and the testicular tubules against drug-induced damage. J Exp Med 1998;188:797-808.

(5) Cui Y, Konig J, Buchholz JK, Spring H, Leier I, Keppler D. Drug resistance and ATP-dependent conjugate transport mediated by the apical multidrug resistance protein, MRP2, permanently expressed in human and canine cells. Mol Pharmacol 1999;55:929-37.

(6) Kool M, van der Linden M, de Haas M, Scheffer GL, de Vree JM, Smith AJ et al. MRP3, an organic anion transporter able to transport anti-cancer drugs. Proc Natl Acad Sci U S A 1999;96:6914-9.

(7) Belinsky MG, Dawson PA, Shchaveleva I, Bain LJ, Wang R, Ling V et al. Analysis of the in vivo functions of Mrp3. Mol Pharmacol 2005;68:160-8.

(8) Schinkel AH, Mayer U, Wagenaar E, Mol CA, van Deemter L, Smit JJ et al. Normal viability and altered pharmacokinetics in mice lacking mdr1-type (drug-transporting) P-glycoproteins. Proc Natl Acad Sci U S A 1997;94:4028-33.

(9) Vlaming ML, Mohrmann K, Wagenaar E, de Waart DR, Elferink RP, Lagas JS et al. Carcinogen and anticancer drug transport by Mrp2 in vivo: studies using Mrp2 (Abcc2) knockout mice. J Pharmacol Exp Ther 2006;318:319-27.

(10) Zelcer N, van de Wetering K, Hillebrand M, Sarton E, Kuil A, Wielinga PR et al. Mice lacking multidrug resistance protein 3 show altered morphine pharmacokinetics and morphine-6-glucuronide antinociception. Proc Natl Acad Sci U S A 2005;102:7274-9.

(11) Lagas JS, Vlaming ML, van Tellingen O, Wagenaar E, Jansen RS, Rosing H et al. Multidrug resistance protein 2 is an important determinant of paclitaxel pharmacokinetics. Clin Cancer Res 2006;12:6125-32.

(12) van de Wetering K, Zelcer N, Kuil A, Feddema W, Hillebrand M, Vlaming ML et al. Multidrug resistance proteins 2 and 3 provide alternative routes for hepatic excretion of morphine-glucuronides. Mol Pharmacol 2007;72:387-94.

(13) Hande K, Anthony L, Hamilton R, Bennett R, Sweetman B, Branch R. Identification of etoposide glucuronide as a major metabolite of etoposide in the rat and rabbit. Cancer Res 1988;48:1829-34.

(14) van Waterschoot RA, van Herwaarden AE, Lagas JS, Sparidans RW, Wagenaar E, van der Kruijssen CM et al. Midazolam metabolism in cytochrome P450 3A knockout mice can be attributed to up-regulated CYP2C enzymes. Mol Pharmacol 2008;73:1029-36.

(15) Schmittgen TD, Livak KJ. Analyzing real-time PCR data by the comparative C(T) method. Nat Protoc 2008;3:1101-8.

(16) Yuan JS, Reed A, Chen F, Stewart CN, Jr. Statistical analysis of real-time PCR data. BMC Bioinformatics 2006;7:85.

(17) D'Incalci M, Rossi C, Zucchetti M, Urso R, Cavalli F, Mangioni C et al. Pharmacokinetics of etoposide in patients with abnormal renal and hepatic function. Cancer Res 1986;46:2566-71.

(18) Holthuis JJ, Postmus PE, Van Oort WJ, Hulshoff B, Verleun H, Sleijfer DT et al. Pharmacokinetics of high dose etoposide (VP 16-213). Eur J Cancer Clin Oncol 1986;22:1149-55.

(19) Zelcer N, Saeki T, Reid G, Beijnen JH, Borst P. Characterization of drug transport by the human multidrug resistance protein 3 (ABCC3). J Biol Chem 2001;276:46400-7.

(20) Watanabe Y, Nakajima M, Ohashi N, Kume T, Yokoi T. Glucuronidation of etoposide in human liver microsomes is specifically catalyzed by UDP-glucuronosyltransferase 1A1. Drug Metab Dispos 2003;31:589-95.

(21) Wen Z, Tallman MN, Ali SY, Smith PC. UDP-glucuronosyltransferase 1A1 is the principal enzyme responsible for etoposide glucuronidation in human liver and intestinal microsomes: structural characterization of phenolic and alcoholic glucuronides of etoposide and estimation of enzyme kinetics. Drug Metab Dispos 2007;35:371-80.

(22) Aita P, Robieux I, Sorio R, Tumolo S, Corona G, Cannizzaro R et al. Pharmacokinetics of oral etoposide in patients with hepatocellular carcinoma. Cancer Chemother Pharmacol 1999;43:287-94.

(23) Arbuck SG, Douglass HO, Crom WR, Goodwin P, Silk Y, Cooper C et al. Etoposide pharmacokinetics in patients with normal and abnormal organ function. J Clin Oncol 1986;4:1690-5.

(24) Hande KR, Wolff SN, Greco FA, Hainsworth JD, Reed G, Johnson DH. Etoposide kinetics in patients with obstructive jaundice. J Clin Oncol 1990;8:1101-7.

(25) Stewart CF, Arbuck SG, Fleming RA, Evans WE. Changes in the clearance of total and unbound etoposide in patients with liver dysfunction. J Clin Oncol 1990;8:1874-9.

(26) Chu XY, Strauss JR, Mariano MA, Li J, Newton DJ, Cai X et al. Characterization of mice lacking the multidrug resistance protein MRP2 (ABCC2). J Pharmacol Exp Ther 2006;317:579-89.

(27) Bonin S, Pascolo L, Croce LS, Stanta G, Tiribelli C. Gene expression of ABC proteins in hepatocellular carcinoma, perineoplastic tissue, and liver diseases. Mol Med 2002;8:318-25.

(28) Zollner G, Wagner M, Fickert P, Silbert D, Fuchsbichler A, Zatloukal K et al. Hepatobiliary transporter expression in human hepatocellular carcinoma. Liver Int 2005;25:367-79.

(29) Folmer Y, Schneider M, Blum HE, Hafkemeyer P. Reversal of drug resistance of hepatocellular carcinoma cells by adenoviral delivery of anti-ABCC2 antisense constructs. Cancer Gene Ther 2007;14:875-84.

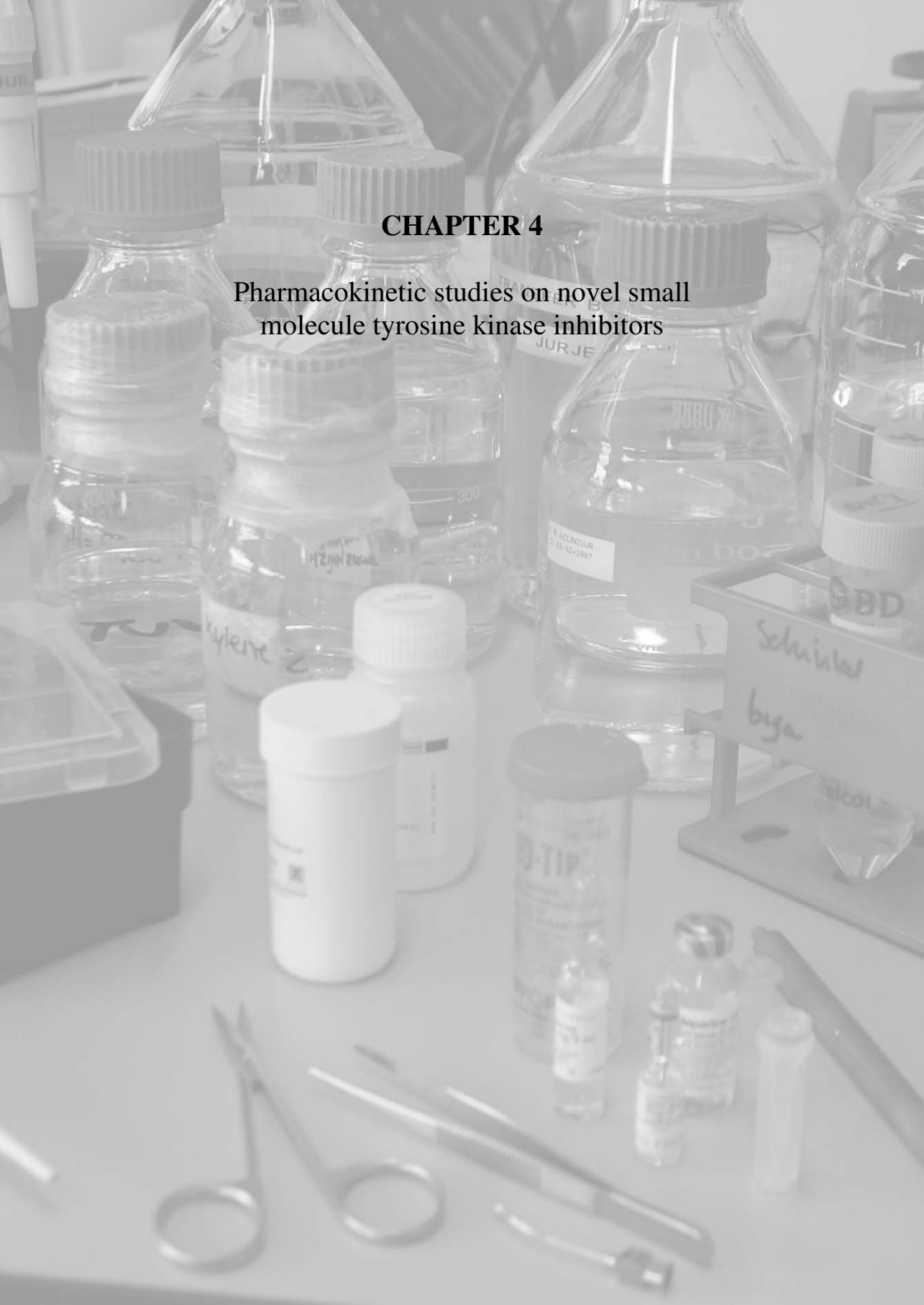

CHAPTER 4

Pharmacokinetic studies on novel small molecule tyrosine kinase inhibitors

CHAPTER 4.1

Brain accumulation of dasatinib is restricted by P-glycoprotein (ABCB1) and ABCG2 (BCRP) and can be enhanced by elacridar treatment

Jurjen S. Lagas, Robert A.B. van Waterschoot, Vicky A.C.J. van Tilburg, Michel J. Hillebrand, Nienke Lankheet, Hilde Rosing, Jos H. Beijnen and Alfred H. Schinkel

Clinical Cancer Research 2009; 15:2344-2351

ABSTRACT

Purpose: Imatinib, a BCR-ABL tyrosine kinase inhibitor, is a substrate of the efflux transporters P-glycoprotein (P-gp, *ABCB1*) and ABCG2 (BCRP), and its brain accumulation is restricted by both transporters. For dasatinib, an inhibitor of SCR/BCR-ABL kinases, *in vivo* interactions with P-gp and ABCG2 are not fully established yet. *Experimental design:* We used *Abcb1a/1b*$^{-/-}$, *Abcg2*$^{-/-}$ and *Abcb1a/1b;Abcg2*$^{-/-}$ mice to establish the roles of P-gp and ABCG2 in the pharmacokinetics and brain accumulation of dasatinib. *Results:* We found that oral uptake of dasatinib is limited by P-gp. Furthermore, relative brain accumulation, 6 hr after administration, was not affected by Abcg2 deficiency, but absence of P-gp resulted in a 3.6-fold increase after oral and 4.8-fold higher accumulation after i.p. administration. *Abcb1a/1b;Abcg2*$^{-/-}$ mice had the most pronounced increase in relative brain accumulation, which was 13.2-fold higher after oral and 22.7-fold increased after i.p. administration. Moreover, coadministration to WT mice of dasatinib with the dual P-gp and ABCG2 inhibitor elacridar resulted in a similar dasatinib brain accumulation as observed for *Abcb1a/1b;Abcg2*$^{-/-}$ mice. *Conclusions:* Brain accumulation of dasatinib is primarily restricted by P-gp, but Abcg2 can partly take over this protective function at the blood-brain barrier. Consequently, when both transporters are absent or inhibited, brain uptake of dasatinib is highly increased. These findings might be clinically relevant for patients with central nervous system Philadelphia chromosome positive leukemia, as coadministration of an inhibitor of P-gp and ABCG2 with dasatinib might result in better therapeutic responses in these patients.

INTRODUCTION

Multidrug efflux transporters of the ATP binding cassette (ABC) transporter family, like P-glycoprotein (P-gp, *ABCB1*), Breast Cancer Resistance Protein (BCRP, *ABCG2*) and Multidrug Resistance Protein 2 (MRP2, *ABCC2*) can have an important impact on chemotherapy. These efflux pumps have a broad and overlapping substrate specificity and are expressed at apical membranes of important epithelial barriers and at the canalicular membrane of hepatocytes. Consequently, these proteins can facilitate excretion of transported drugs via liver, intestine and kidneys, and restrict the intestinal uptake of orally encountered substrates. In addition, ABC transporters are localized at the so-called sanctuary site barriers, such as blood-brain, blood-testis, and blood-placenta barrier, where they restrict accumulation of potentially harmful compounds. Moreover, (over-) expression of these efflux pumps in tumor cells can lead to multi-drug resistance (MDR) through active efflux of cytostatic drugs (1).

Imatinib, a first-generation, orally active inhibitor of BCR-ABL kinase, is currently used as frontline therapy for Philadelphia chromosome positive (Ph+) leukemia (defined by the fusion of the BCR- and ABL genes), including chronic myeloid leukemia (CML) and Ph+ acute lymphoblastic leukemia. Imatinib has revolutionized the treatment of CML by its impressive therapeutic responses in the chronic phase of the disease. However, patients with advanced disease show generally lower and more transient responses to imatinib. In addition, accumulating evidence indicates that resistance to imatinib in a significant proportion of patients in all disease stages results in failure to achieve an optimal response (2-4). Thus far, several mechanism of resistance have been reported, including point mutations in the BCR-ABL kinase domain, amplification of the gene and imatinib binding to α_1-acid glycoprotein (5-9).

Dasatinib is a second generation, oral, multi-targeted inhibitor of BCR-ABL and SRC family kinases, rationally designed for CML treatment (10). Compared to imatinib, dasatinib has 325-fold greater *in vitro* potency against cells expressing "wild-type" BCR-ABL (11). Furthermore, dasatinib effectively inhibits the growth of clones of a leukemic cell line expressing all known imatinib-resistant BCR-ABL isoforms, with the exception of T315I (12). Importantly, dasatinib has shown significant activity in imatinib-resistant or imatinib-intolerant patients with CML or Ph+ acute lymphoblastic leukemia (13-17).

Imatinib is a substrate of the efflux transporters P-gp and ABCG2 and accumulation of imatinib through the blood-brain barrier is markedly restricted by both transporters (18-27). This might explain why up to 20% of the imatinib-treated patients with either lymphoid or myeloid blast crisis-chronic myelogenous leukemia (BC-CML) or Ph+ acute lymphoblastic leukemia develop central nervous system (CNS) relapses (28;29). In contrast, dasatinib was recently found to have antitumor activity in a mouse model of intracranial CML and in patients with CNS Ph+ leukemia dasatinib induced substantial responses (30). Moreover, in K562 leukemic cells that overexpress P-gp, dasatinib showed significant antiproliferation activity, in contrast to imatinib (31). These findings may indicate that dasatinib is not seriously affected by P-gp and/or ABCG2 at the blood-brain barrier or by P-gp in the K562 cells. Nonetheless, it was recently found that the accumulation of dasatinib was decreased in P-gp and ABCG2 overexpressing leukemic cells, and that dasatinib was transported in P-gp overexpressing MDCK-II cells, suggesting that dasatinib is a substrate of P-gp and ABCG2 (32;33).

To further study the interaction of dasatinib with drug transporters, we used *in vitro* transwell transport assays. In addition, *Abcb1a/1b*$^{-/-}$, *Abcg2*$^{-/-}$ and *Abcb1a/1b;Abcg2*$^{-/-}$ mice were used to investigate the *in vivo* roles of P-gp and ABCG2 in the pharmacokinetics and brain accumulation of dasatinib.

MATERIALS AND METHODS

Chemicals. Dasatinib monohydrate originated from Sequoia Research Products (Pangbourne, UK). GlaxoSmithKline (Uxbridge, UK) kindly provided Elacridar (GF120918). [^{14}C]Inulin was from Amersham (Little Chalfont, UK). Methoxyflurane (Metofane®) was from Medical Developments Australia (Springvale, Victoria, Australia). Bovine serum albumin (BSA), fraction V, was from Roche (Mannheim, Germany).All other chemicals and reagents were obtained from Sigma-Aldrich (Steinheim, Germany).

Transport assays. Polarized canine kidney MDCK-II cell lines were used in transport assays. MDCK-II cells transduced with human ABCB1 or ABCC2 or murine Abcg2 were described previously (34;35). Transepithelial transport assays using Transwell plates were carried out as described previously with minor modifications (36). Experiments with cells transfected with human ABCC2 were performed in the presence of 5 μM of elacridar, to inhibit any endogenous P-glycoprotein activity. Elacridar does not affect ABCC2 activity. When elacridar was applied, it was present in both compartments during 2 hr preincubation and during the transport experiment. After preincubation, experiments were started (t = 0) by replacing the medium in either the apical or basolateral compartment with fresh OptiMEM medium (Invitrogen, Breda, The Netherlands), either with or without 5 μM elacridar and containing 5 μM of dasatinib. Cells were incubated at 37°C in 5% CO_2, and 50 μl aliquots were taken at t = 2 and 4 h. Transport was calculated as the fraction of drug found in the acceptor compartment relative to the total amount added to the donor compartment at the beginning of the experiment. Transport is given as mean percentage ± SD (n = 3). Membrane tightness was assessed in parallel, using the same cells seeded on the same day and at the same density, by analyzing transepithelial [^{14}C]inulin (approx. 3 kBq /well) leakage. Leakage had to remain <1% of the total added radioactivity per hour.

Relative transport ratio. Active transport was expressed by the relative transport ratio (r), defined as: r = percentage apically directed transport divided by percentage basolaterally directed translocation, after 4 hr (37).

Animals. Mice were housed and handled according to institutional guidelines complying with Dutch legislation. Animals used were male wild-type (WT), *Abcb1a/1b*$^{-/-}$ (38), *Abcg2*$^{-/-}$ (35) and *Abcb1a/1b;Abcg2*$^{-/-}$ (39) mice, all of a >99% FVB genetic background, between 10 and 12 weeks of age. Animals were kept in a temperature-controlled environment with a 12-hour light / 12-hour dark cycle and received a standard diet (AM-II, Hope Farms, Woerden, The Netherlands) and acidified water *ad libitum*.

Plasma pharmacokinetics. Dasatinib was dissolved in DMSO (25 mg/ml) and 25-fold diluted with 50 mM sodium acetate buffer (pH 4.6). For oral studies, dasatinib was dosed at 10 mg/kg body weight (10 ml/kg). To minimize variation in absorption, mice were fasted 3 hours before dasatinib was administered by gavage into the stomach, using a blunt-ended needle. For plasma pharmacokinetic studies after systemic exposure, dasatinib was applied by intraperitoneal (i.p.) injection, because i.v. injection into a tail vein compromises multiple blood sampling from the tail. For i.p. studies, dasatinib was dosed at 5 mg/kg body weight (5 ml/kg). We used a 2-fold lower dose for i.p. than for oral studies, to obtain plasma concentrations and AUC values that are in the same range for both administration routes. Multiple blood samples (~50 µl) were collected from the tail vein at 7.5 min (i.p.) or 15 min (oral) and 30 min and 1, 2, 4 and 6 h (both series), using heparinized capillary tubes (Oxford Labware, St. Louis, USA). At the last time point, mice were anesthetized with methoxyflurane and blood was drawn by cardiac puncture. Immediately thereafter, mice were sacrificed by cervical dislocation and brains were rapidly removed, homogenized on ice in 4% BSA and stored at -20°C until analysis. Blood samples were centrifuged at 2100 *g* for 6 min at 4°C, the plasma fraction was collected, completed to 200 µl with drug-free human plasma and stored at -20°C until analysis.

Brain accumulation of dasatinib in combination with elacridar. Elacridar was dissolved in a mixture of ethanol, polyethylene glycol 200 and 5% glucose (2:6:2) and i.v. injected into a tail vein at 10 mg/kg (2.5 ml/kg). Dasatinib dissolved in DMSO (25 mg/ml), was 25-fold diluted with 50 mM sodium acetate buffer (pH 4.6) and injected as a single i.v. bolus at 5 mg/kg body weight (5 ml/kg). Dasatinib was administered 15 min after an injection with either elacridar or with the vehicle used to dissolve elacridar. Blood and brains were isolated 60 minutes after dasatinib administration and processed and stored as described above.

Relative brain accumulation. Brain concentrations were corrected for the amounts of drug in the brain vasculature, i.e. 1.4% of the plasma concentration right before the brains were isolated (22). Subsequently, brain accumulation after oral or i.p. dasatinib administration was calculated by determining the dasatinib brain concentration relative to the area under plasma concentration-time curve from 0-6 hr (AUC_{0-6}). For studies with i.v. dasatinib in combination with elacridar, blood was collected only just before the brains were isolated, 60 min after dasatinib administration. Therefore, brain-to-plasma ratios were calculated to assess the relative brain accumulation.

Drug Analysis. Dasatinib concentrations in OptiMEM cell culture medium (Invitrogen), and in plasma samples and brain homogenates were determined using a sensitive and specific LC-MS/MS assay. Chromatography was carried out using a Solvent delivery system LC-20AD Prominence (Shimadzu, Kyoto, Japan), consisting of a binary pump, auto sampler, degasser, and column oven. Chromatographic separations of the analytes were carried out on a Gemini C18 column, 50 x 2.0 mm ID, 5µm (Phenomenex, Torrance, CA, USA). A mobile phase consisting of eluent A (10 mM ammonium hydroxide in water) and eluent B (1 mM ammonium hydroxide in methanol) was pumped through the column with a flow of 0.25 ml/min. The following gradient was used:

Time (min)	0.0	0.5	3.0	6.0	6.1	8.0	8.1	12.0
Eluent B (%)	55	55	80	80	100	100	55	55

The respective retention time for dasatinib was 3.8 min. The mass spectrometric analyses were performed using a Finnigan TSQ Quantum Ultra Triple Quadrupole Spectrometer equipped with an electrospray (ESI) ion source (Thermo Fisher, Walthan, MA, USA). The mass spectrometers were operating in positive ESI selective reaction monitoring (MRM), three MRM channels were monitored at unit resolution corresponding to dasatinib m/z 488 to 401, and the stable 13C-isotope of imatinib m/z 498 to 394 (used as internal standard). Samples were pretreated by protein precipitation with acetonitril, the supernatants were diluted 1:1, v/v (sample extract: Eluent A) prior to injection (10 µL).

Pharmacokinetic calculations and statistical analysis. Pharmacokinetic parameters were calculated by noncompartmental methods using the software package WinNonlin Professional version 5.0. The area under plasma concentration-time curve (AUC) was calculated using the trapezoidal rule, without extrapolating to infinity. Elimination half-lives ($t_{½,\ el}$) were calculated by linear regression analysis of the log-linear part of the plasma concentration-time curves. The peak plasma concentration (C_{max}) and the time of maximum plasma concentration (T_{max}) were estimated from the original data. Apparent clearance (CL_{app} or CL/F) was calculated by the formula CL_{app} = Dose/AUC. The formula $F_{rel} = (AUC_{oral} \times Dose_{i.p.})/(AUC_{i.p.} \times Dose_{oral}) \times 100\%$ was used to calculated the relative oral bioavailability (F_{rel}). The two-sided unpaired Student's *t*-test was used for statistical analysis. Data obtained with single- and combination knockout mice were compared to data obtained with WT mice. Differences were considered statistically significant when $P < 0.05$. Data are presented as means ± SD.

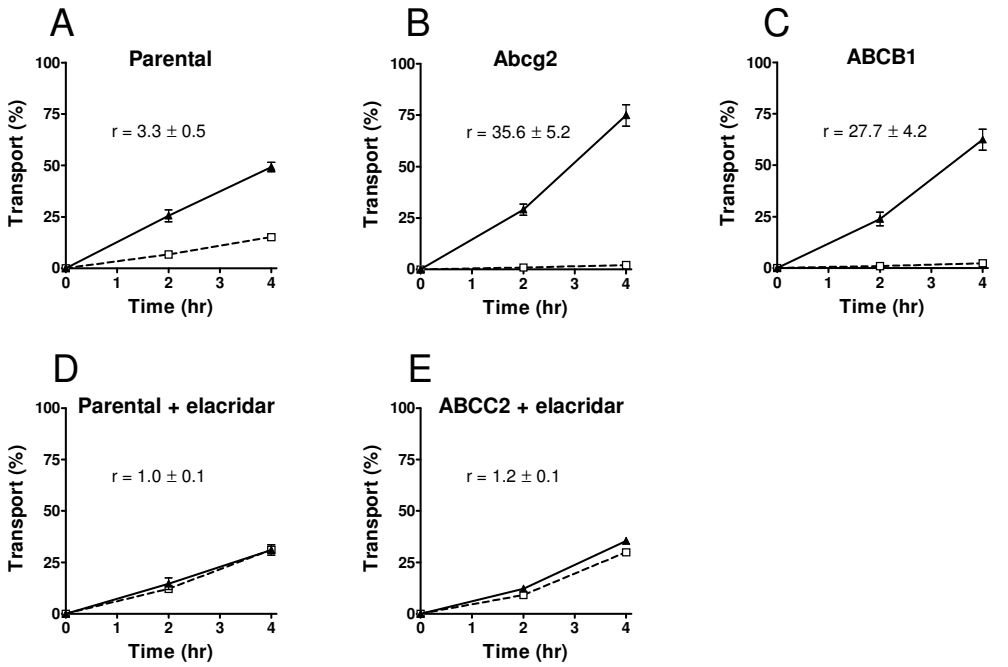

Fig. 1. Transepithelial transport of dasatinib (5 μM) was assessed in MDCK-II cells either non-transduced (*A, D*) or transduced with murine Abcg2 (*B*) or human ABCB1 (*C*) or ABCC2 (*E*) cDNA. At t = 0 h, dasatinib was applied in one compartment (apical or basolateral), and the concentration in the opposite compartment at t = 2 and 4 h was measured by LC-MS/MS and plotted as the percentage of initial drug concentration (n = 3). Elacridar (5 μM) was applied to inhibit endogenous P-gp (*D, E*). Translocation from the basolateral to the apical compartment (▲); translocation from the apical to the basolateral compartment (□). Data are means ± SD. At t = 4 hr, 1% of transport is approximately equal to an apparent permeability coefficient (P_{app}) of 0.30 * 10^{-6} cm/sec.

RESULTS

In vitro transport of dasatinib. We used monolayers of the polarized canine kidney cell line MDCK-II and its subclones transduced with human ABCB1 or ABCC2 or murine Abcg2 to study transepithelial vectorial transport of 5 μM dasatinib. Dasatinib was modestly but actively transported in the apical direction in the MDCK-II parental cell line (Fig. 1A), which is known to have relatively high expression of functional endogenous canine P-gp (40). Transport in the parental cells could be completely inhibited with elacridar, a potent inhibitor of P-gp (Fig. 1D), suggesting that indeed endogenous P-gp was responsible for dasatinib transport in the parental cells. In cells transfected with murine Abcg2 or human ABCB1 P-gp, transport of dasatinib was markedly increased, resulting in 10.8-fold

and 8.4-fold higher transport ratios (*r*, defined under the material and methods section) compared to parental cells, respectively (Fig. 1B and 1C). In cells transduced with human ABCC2, no transport of dasatinib was observed (Fig. 1E).

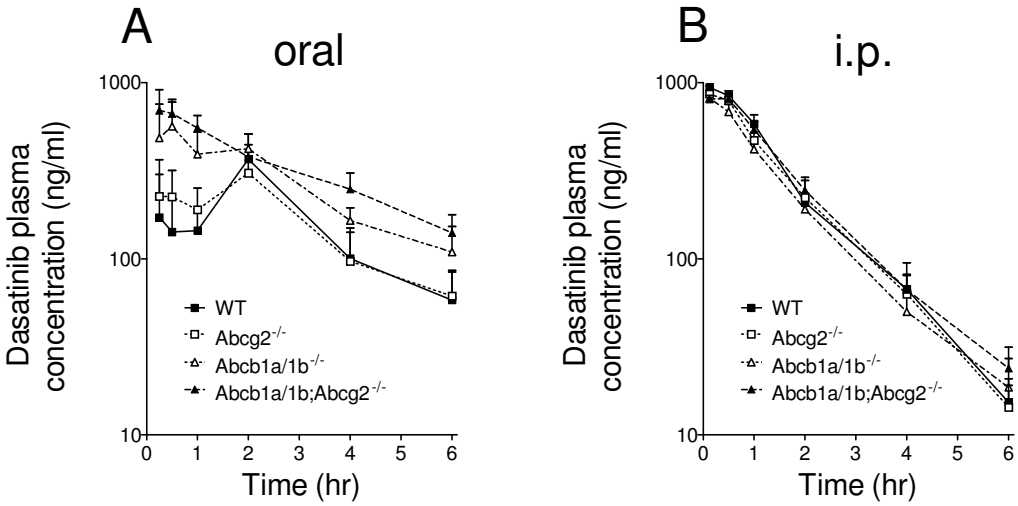

Fig. 2. Plasma concentration-time curves of dasatinib in male FVB WT (■), *Abcg2*$^{-/-}$ (□), *Abcb1a/1b*$^{-/-}$ (Δ), and *Abcb1a/1b;Abcg2*$^{-/-}$ (▲) mice, after oral (*A*) and i.p. (*B*) administration of dasatinib at a dose of 10 mg/kg (oral) and 5 mg/kg (i.p.). Data are means ± SD, n = 5 for oral and n = 4 for i.p. administration.

Impact of ABCG2 and P-gp on Plasma Pharmacokinetics of Dasatinib in Mice. Because our data indicated that both ABCG2 and P-gp have a profound impact on dasatinib transport *in vitro*, we further investigated their separate and combined impact *in vivo*. In the clinic, dasatinib is administered p.o. to cancer patients, and therefore we first studied plasma dasatinib concentrations after oral administration of 10 mg/kg to WT, *Abcb1a/1b*$^{-/-}$, *Abcg2*$^{-/-}$ and *Abcb1a/1b;Abcg2*$^{-/-}$ mice. *Abcb1a/1b*$^{-/-}$ mice displayed a 1.7-fold higher $AUC_{p.o.}$ compared to WT mice ($P < 0.05$, Fig. 2A, Table 1), and the maximal plasma levels in *Abcb1a/1b*$^{-/-}$ mice were reached markedly faster than in WT mice. In WT mice, the relatively late C_{max}, ~2 hr after oral administration, might partly be explained by enterohepatic circulation of dasatinib. The fact that this late C_{max} was absent in P-gp deficient animals may indicate that P-gp restricts rapid absorption from the intestine and/or mediates substantial hepatobiliary excretion and thus contributes to enterohepatic circulation of dasatinib. Deficiency of only Abcg2 did not affect plasma pharmacokinetics after oral administration (Fig. 2A, Table 1). *Abcb1a/1b;Abcg2*$^{-/-}$

mice had 2.0-fold higher $AUC_{p.o.}$ ($P < 0.01$), and the C_{max} was 1.9-fold higher compared to WT mice ($P < 0.05$, Fig. 2A, Table 1). Collectively, these results indicate that P-gp, and not Abcg2, restricts the oral uptake of dasatinib in mice. To study the plasma pharmacokinetics after systemic administration, dasatinib was given by i.p. injection at 5 mg/kg. At this dose, plasma concentrations were in the same range as in oral experiments with 10 mg/kg. *Abcb1a/1b*$^{-/-}$ mice had slightly, but significantly lower plasma concentrations 0.5 and 1 hr after administration, resulting in a 1.3-fold lower $AUC_{i.p.}$ compared to WT mice ($P < 0.05$, Fig. 2B, Table 1). The $AUC_{i.p.}$ values for *Abcg2*$^{-/-}$ and *Abcb1a/1b;Abcg2*$^{-/-}$ mice were not different from WT mice. These results indicate that both transporters do not strongly affect the systemic distribution and elimination of dasatinib. Because we do not know if the availability after i.p. administration is complete, we used the $AUC_{i.p.}$ as a relative standard to calculate the relative oral bioavailability (F_{rel}) in the different mouse strains. WT and *Abcg2*$^{-/-}$ mice displayed a relative oral bioavailability of ~30% and P-gp deficiency increased the relative oral availability in both *Abcb1a/1b*$^{-/-}$ and *Abcb1a/1b;Abcg2*$^{-/-}$ mice to ~68% ($P < 0.01$, Table 1).

Table 1. Plasma pharmacokinetic parameters after oral (10 mg/kg) or i.p. (5 mg/kg) administration of dasatinib.

	Strain			
	WT	*Abcb1a/1b*$^{-/-}$	*Abcg2*$^{-/-}$	*Abcb1a/1b;Abcg2*$^{-/-}$
Oral				
$AUC_{(0-6)}$, mg/l.hr	1.02 ± 0.27	1.70 ± 0.42 *	1.00 ± 0.35	2.05 ± 0.25 **
C_{max}, mg/l	0.37 ± 0.08	0.49 ± 0.27	0.31 ± 0.21	0.70 ± 0.22 *
T_{max}, hr	2	0.5	2	0.25
CL_{app}, l/hr.kg	10.4 ± 2.40	6.15 ± 1.38 **	11.0 ± 3.61	4.94 ± 0.58 **
i.p.				
$AUC_{(0-6)}$, mg/l.hr	1.59 ± 0.10	1.25 ± 0.15 *	1.69 ± 0.32	1.52 ± 0.16
C_{max}, mg/l	0.94 ± 0.07	0.81 ± 0.06	0.86 ± 0.07	0.81 ± 0.03 *
$t_{½, el}$, hr	0.93 ± 0.04	1.43 ± 0.49	0.98 ± 0.28	1.33 ± 0.12 *
CL_{app}, l/hr.kg	3.16 ± 0.20	4.05 ± 0.50 *	3.05 ± 0.66	3.31 ± 0.36
F_{rel}, %	32.0 ± 1.74	68.0 ± 3.72 **	29.6 ± 2.39	67.3 ± 2.13 **

$AUC_{(0-6)}$, area under plasma concentration-time curve up to 6 hr; C_{max}, maximum plasma levels; $t_{½, el}$, elimination half life, calculated from 2-6 hr; CL_{app}, apparent clearance (CL/*F*); F_{rel}, relative oral bioavailability. Data are means ± SD, n = 5 for oral and n = 4 for i.p. administration. All parameters obtained for knockout mice were compared to those for WT mice. * $P < 0.05$ and ** $P < 0.01$, compared to WT mice.

Impact of ABCG2 and P-gp on brain accumulation of dasatinib in mice. As shown in Fig. 3, the relative brain accumulation, determined 6 hr after administration and corrected for the plasma AUC_{0-6}, was not different between *Abcg2*$^{-/-}$ and WT mice, either after oral (Fig. 3A) or i.p. (Fig. 3B) administration. However, in *Abcb1a/1b*$^{-/-}$ mice, the relative brain accumulation was 3.6-fold increased after oral and 4.8-fold after i.p. administration. *Abcb1a/1b;Abcg2*$^{-/-}$ mice had the most pronounced increases in relative brain accumulation, 13.2-fold after oral and 22.7-fold after i.p. administration. The relative brain accumulation values, as well as the uncorrected brain concentrations are listed in Table 2. Correction for plasma concentration at t = 6 hr yielded qualitatively the same results for relative brain accumulation as correction for AUC_{0-6} (data not shown).These results demonstrate that P-gp almost completely controls the dasatinib brain accumulation, no matter whether Abcg2 is present or not. However, in *Abcb1a/1b*$^{-/-}$ mice Abcg2 can partly but not completely take over the function of P-gp at the blood-brain barrier. These results further show that when both transporters are absent, brain accumulation of dasatinib is highly increased.

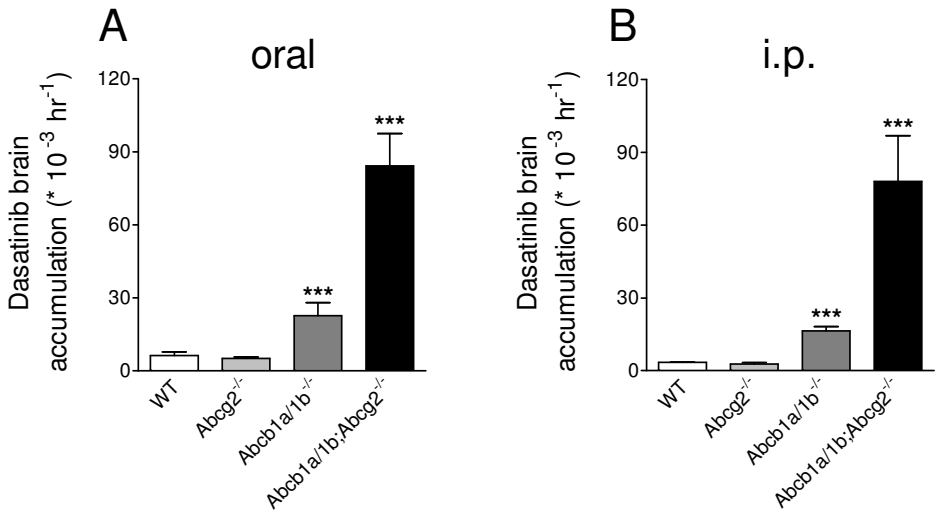

Fig. 3. Relative brain accumulation of dasatinib in male FVB WT, *Abcg2*$^{-/-}$, *Abcb1a/1b*$^{-/-}$, and *Abcb1a/1b;Abcg2*$^{-/-}$ mice, after oral (*A*) or i.p. (*B*) administration of dasatinib at a dose of 10 mg/kg (oral) or 5 mg/kg (i.p.). Relative brain accumulation was calculated by determining the brain concentration relative to the area under plasma concentration-time curve from 0-6 hr (AUC_{0-6}). Means ± SD, n = 5 (oral) and n = 4 (i.p.). *** $P < 0.001$.

Table 2. Brain concentrations and relative brain accumulation after oral (10 mg/kg) or i.p. (5 mg/kg) administration of dasatinib.

	Strain			
	WT	*Abcb1a/1b*$^{-/-}$	*Abcg2*$^{-/-}$	*Abcb1a/1b;Abcg2*$^{-/-}$
Oral				
C_{brain}, ng/g	6.50 ± 2.10	37.2 ± 5.38***	4.93 ± 1.13	171.6 ± 30.9***
P_{brain}, (*10^{-3} hr^{-1})	6.39 ± 1.39	22.7 ± 5.41***	5.11 ± 0.68	84.3 ± 13.3***
i.p.				
C_{brain}, ng/g	5.47 ± 0.38	25.6 ± 3.56***	5.15 ± 1.73	116.7 ± 15.2***
P_{brain}, (*10^{-3} hr^{-1})	3.44 ± 0.17	16.4 ± 1.71***	2.78 ± 0.65	78.1 ± 18.8***

C_{brain}, brain concentration at 6 hr after administration; P_{brain}, relative brain accumulation at 6 hr after administration, calculated by determining the dasatinib brain concentration relative to the area under plasma concentration-time curve from 0-6 hr (AUC_{0-6}). Data are means ± SD, n = 5 for oral and n = 4 for i.p. administration. All parameters obtained for knockout mice were compared to those for WT mice. *** $P < 0.001$, compared to WT mice.

Impact of the dual P-gp and ABCG2 inhibitor elacridar on dasatinib brain accumulation. Because both P-gp and ABCG2 markedly restricted the brain accumulation of dasatinib, we investigated if inhibition of both efflux transporters at the blood-brain barrier would result in an increased brain accumulation of dasatinib. We used the dual P-gp and ABCG2 inhibitor elacridar. Figure 4A shows that the dasatinib plasma concentration, 60 min after i.v. administration, was 1.7-fold higher in *Abcb1a/1b;Abcg2*$^{-/-}$ compared to WT mice ($P < 0.05$). In the presence of elacridar, plasma concentrations of dasatinib in WT and *Abcb1a/1b;Abcg2*$^{-/-}$ mice were not different anymore, suggesting that elacridar inhibits the systemic elimination of dasatinib via P-gp and/or Abcg2. In contrast to the modest effect on plasma concentrations, elacridar drastically increased brain concentration in WT mice by 10-fold ($P < 0.001$; Fig. 4B). Brain concentrations in *Abcb1a/1b;Abcg2*$^{-/-}$ mice appeared also somewhat increased when elacridar was applied, but the difference was not statistically significant ($P = 0.11$; Fig 4B) and probably reflects the modestly higher plasma levels (Fig. 4A). Figure 4C shows the brain-to-plasma ratios, which were calculated to correct for the differences in plasma concentrations. For WT mice, the ratio was 4.4-fold increased with elacridar, resulting in a similar dasatinib brain accumulation as observed for *Abcb1a/1b;Abcg2*$^{-/-}$ mice. For *Abcb1a/1b;Abcg2*$^{-/-}$ mice, elacridar did not affect

brain-to-plasma ratios. Overall, these results show that elacridar can completely inhibit P-gp and ABCG2 at the blood-brain barrier, leading to highly increased dasatinib concentrations in the brain.

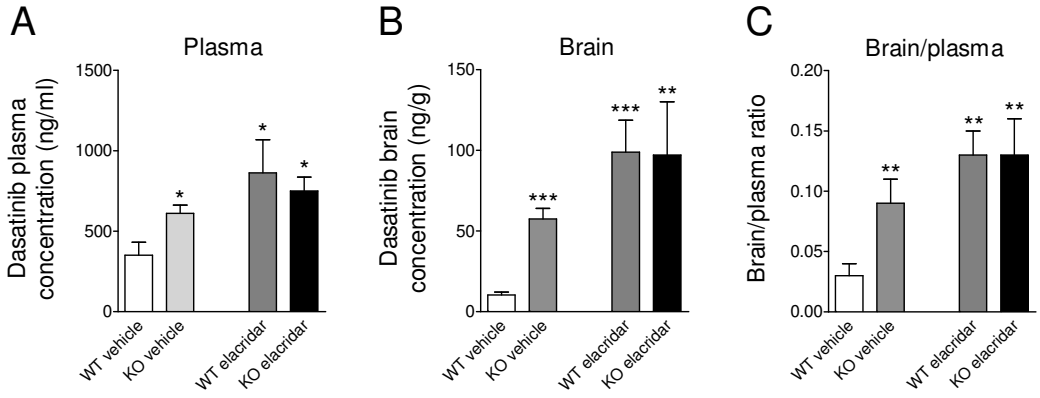

Fig. 4. Plasma (*A*) and brain (*B*) concentrations and brain-to-plasma ratios (*C*) for FVB WT and *Abcb1a/1b;Abcg2*$^{-/-}$ (KO) mice, 60 minutes after i.v. administration of 5 mg/kg dasatinib. Dasatinib was given 15 minutes after the i.v. administration of either vehicle or elacridar (10 mg/kg). Data are means ± SD, n = 4 for WT and n = 3 for KO. * $P < 0.05$, ** $P < 0.01$ and *** $P < 0.001$, compared to WT mice treated with vehicle.

DISCUSSION

In this study we show that the second generation tyrosine kinase inhibitor dasatinib is efficiently transported *in vitro* by P-gp and Abcg2. We extended these observations *in vivo* and found that relative oral availability is limited by P-gp. We further demonstrate that the brain accumulation of dasatinib is primarily restricted by P-gp, but that Abcg2 can partly take over this protective function at the blood-brain barrier. Consequently, when both efflux transporters are absent, brain uptake of dasatinib is highly increased. And finally, we show that the brain accumulation of dasatinib in WT mice can be markedly increased by applying the dual P-gp and ABCG2 inhibitor elacridar.

It was recently reported that the cellular accumulation of dasatinib in P-gp or ABCG2 overexpressing leukemic cells was significantly lower than in control cells (32). In addition, active transport of dasatinib in P-gp overexpressing MDCK-II cells was recently shown (41). Our *in vitro* data on the transport of dasatinib by human P-gp are consistent with these observations and we further show that, in

addition to the reported transport by human ABCG2 (32), also mouse Abcg2 is an efficient transporter for dasatinib. Based on the reported *in vitro* data and our own *in vitro* results, we further investigated the impact of P-gp and Abcg2 on the pharmacokinetics of dasatinib. We found that *Abcb1a/1b*$^{-/-}$ mice had 1.7-fold higher plasma $AUC_{p.o.}$ than WT mice. In a recent study, no difference in $AUC_{p.o.}$ between WT and P-gp deficient mice was observed (42). However, the limited number of animals used in that study (n = 3) may have resulted in substantial variation (the variation was not reported). In addition, we know from experience that variation in absorption after oral administration can be markedly reduced by food deprivation for 3 hours prior to administration. We did so and we used 5 animals per group, resulting in more statistical power to detect differences in $AUC_{p.o.}$ We found no difference in $AUC_{p.o.}$ between *Abcg2*$^{-/-}$ and WT mice, despite our observation that dasatinib is a good Abcg2 substrate *in vitro*. Moreover, *Abcb1a/1b;Abcg2*$^{-/-}$ mice had a similar $AUC_{p.o.}$ compared to *Abcb1a/1b* $^{-/-}$ mice, indicating that P-gp, and not Abcg2, restricts the oral uptake of dasatinib in mice. We have shown earlier that there is not a higher level of P-gp RNA in the intestine of *Abcg2*$^{-/-}$ mice (unpublished), so possible P-gp upregluation cannot explain the lack of effect of Abcg2. We further show that the relative oral bioavailability of dasatinib of ~32% in WT mice was more than doubled to ~68% in P-gp deficient mice. This might be clinically relevant, because dasatinib is taken orally by cancer patients, and intestinal uptake in humans might be limited by P-gp as well.

In addition to the impact of P-gp on the relative oral availability, we show that P-gp, together with ABCG2, drastically restricts the brain accumulation of dasatinib in mice. It is interesting to note that P-gp seems to have a dominant role compared to Abcg2 in both intestine and blood-brain barrier, whereas in vitro both transporters appear to efficiently transport dasatinib. A possible explanation of this apparent discrepancy could be that Abcg2 is more lowly expressed in intestine and blood-brain barrier than P-gp, something that is difficult to assess with the currently available tools. This would make P-gp the dominant player, and, at least in the blood-brain barrier, only when P-gp is absent the contribution of Abcg2 becomes visible. As mentioned above, we have shown earlier that there is not a higher level of P-gp RNA in Abcg2 knockout intestine. Although it therefore seems unlikely, we cannot completely exclude that there is increased expression of blood-brain barrier P-gp in Abcg2 knockout mice. Be that as it may, it is clear that both P-gp and Abcg2 can contribute to decreased brain accumulation of dasatinib. The relevance of this finding may be put in perspective by the recent findings of Porkka *et al.*, who showed that dasatinib has antitumor activity in a mouse model of intracranial CML (30). Dasatinib also induced substantial responses in patients with CNS Ph+ leukemia and showed a considerably higher CNS accumulation than

imatinib in mice and humans (30). Interestingly, imatinib failed to show any antitumor activity in their mouse model of intracranial CML, which is consistent with several clinical and preclinical findings (22;28;43;44). This difference between dasatinib and imatinib cannot simply be explained by the fact that brain accumulation of imatinib is limited by P-gp and ABCG2 (21;22;27;43;44). In fact, our data show that P-gp and Abcg2 also profoundly restrict the brain accumulation of dasatinib in mice. Moreover, compared to other agents that have a good accumulation of the blood-brain barrier, such as cytarabine, the CNS accumulation of dasatinib is still low (45). Therefore, other factors, such as its far higher potency (325-fold) compared to imatinib (11), may explain the antitumor effects of dasatinib within the CNS.

We further demonstrated that the brain accumulation of dasatinib in WT mice could be markedly increased with the dual P-gp and ABCG2 inhibitor elacridar. Moreover, WT mice pretreated with elacridar had similar dasatinib brain-to-plasma ratios as observed for *Abcb1a/1b;Abcg2*$^{-/-}$ mice that received either vehicle or elacridar. These results suggest that elacridar can fully inhibit P-gp and ABCG2 at the blood-brain barrier. We realize that results obtained in mice cannot simply be transferred to the clinical situation. However, we believe that our observations provide a rationale for combining dasatinib with a dual P-gp and ABCG2 inhibitor to increase the dasatinib brain accumulation and further improve its therapeutic efficacy in patients with CNS Ph+ leukemia. Clearly, further preclinical and clinical research is warranted to assess the feasibility of this approach.

ACKNOWLEGMENTS

We thank Evita van de Steeg and Marijn Vlaming for critical reading of the manuscript.

REFERENCES

(1) Borst P, Oude Elferink RP. Mammalian ABC transporters in health and disease. Annu Rev Biochem 2002;71:537-92.

(2) O'Brien SG, Guilhot F, Larson RA, Gathmann I, Baccarani M, Cervantes F et al. Imatinib compared with interferon and low-dose cytarabine for newly diagnosed chronic-phase chronic myeloid leukemia. N Engl J Med 2003;348:994-1004.

(3) Druker BJ, Sawyers CL, Kantarjian H, Resta DJ, Reese SF, Ford JM et al. Activity of a specific inhibitor of the BCR-ABL tyrosine kinase in the blast crisis of chronic myeloid leukemia and acute lymphoblastic leukemia with the Philadelphia chromosome. N Engl J Med 2001;344:1038-42.

(4) Talpaz M, Silver RT, Druker BJ, Goldman JM, Gambacorti-Passerini C, Guilhot F et al. Imatinib induces durable hematologic and cytogenetic responses in patients with accelerated phase chronic myeloid leukemia: results of a phase 2 study. Blood 2002;99:1928-37.

(5) Shannon KM. Resistance in the land of molecular cancer therapeutics. Cancer Cell 2002;2:99-102.

(6) McCormick F. New-age drug meets resistance. Nature 2001;412:281-2.

(7) Heinrich MC, Corless CL, Blanke CD, Demetri GD, Joensuu H, Roberts PJ et al. Molecular correlates of imatinib resistance in gastrointestinal stromal tumors. J Clin Oncol 2006;24:4764-74.

(8) Sleijfer S, Wiemer E, Seynaeve C, Verweij J. Improved insight into resistance mechanisms to imatinib in gastrointestinal stromal tumors: a basis for novel approaches and individualization of treatment. Oncologist 2007;12:719-26.

(9) Gambacorti-Passerini C, Zucchetti M, Russo D, Frapolli R, Verga M, Bungaro S et al. Alpha1 acid glycoprotein binds to imatinib (STI571) and substantially alters its pharmacokinetics in chronic myeloid leukemia patients. Clin Cancer Res 2003;9:625-32.

(10) Lombardo LJ, Lee FY, Chen P, Norris D, Barrish JC, Behnia K et al. Discovery of N-(2-chloro-6-methyl- phenyl)-2-(6-(4-(2-hydroxyethyl)- piperazin-1-yl)-2-methylpyrimidin-4-ylamino)thiazole-5-carboxamide (BMS-354825), a dual Src/Abl kinase inhibitor with potent antitumor activity in preclinical assays. J Med Chem 2004;47:6658-61.

(11) O'Hare T, Walters DK, Stoffregen EP, Jia T, Manley PW, Mestan J et al. In vitro activity of Bcr-Abl inhibitors AMN107 and BMS-354825 against clinically relevant imatinib-resistant Abl kinase domain mutants. Cancer Res 2005;65:4500-5.

(12) Shah NP, Tran C, Lee FY, Chen P, Norris D, Sawyers CL. Overriding imatinib resistance with a novel ABL kinase inhibitor. Science 2004;305:399-401.

(13) Hochhaus A, Kantarjian HM, Baccarani M, Lipton JH, Apperley JF, Druker BJ et al. Dasatinib induces notable hematologic and cytogenetic responses in chronic-phase chronic myeloid leukemia after failure of imatinib therapy. Blood 2007;109:2303-9.

(14) Cortes J, Rousselot P, Kim DW, Ritchie E, Hamerschlak N, Coutre S et al. Dasatinib induces complete hematologic and cytogenetic responses in patients with imatinib-resistant or -intolerant chronic myeloid leukemia in blast crisis. Blood 2007;109:3207-13.

(15) Guilhot F, Apperley J, Kim DW, Bullorsky EO, Baccarani M, Roboz GJ et al. Dasatinib induces significant hematologic and cytogenetic responses in patients with imatinib-resistant or -intolerant chronic myeloid leukemia in accelerated phase. Blood 2007;109:4143-50.

(16) Kantarjian H, Pasquini R, Hamerschlak N, Rousselot P, Holowiecki J, Jootar S et al. Dasatinib or high-dose imatinib for chronic-phase chronic myeloid leukemia after failure of first-line imatinib: a randomized phase 2 trial. Blood 2007;109:5143-50.

(17) Ottmann O, Dombret H, Martinelli G, Simonsson B, Guilhot F, Larson RA et al. Dasatinib induces rapid hematologic and cytogenetic responses in adult patients with Philadelphia chromosome positive acute lymphoblastic leukemia with resistance or intolerance to imatinib: interim results of a phase 2 study. Blood 2007;110:2309-15.

(18) Hamada A, Miyano H, Watanabe H, Saito H. Interaction of imatinib mesilate with human P-glycoprotein. J Pharmacol Exp Ther 2003;307:824-8.

(19) Burger H, van Tol H, Boersma AW, Brok M, Wiemer EA, Stoter G et al. Imatinib mesylate (STI571) is a substrate for the breast cancer resistance protein (BCRP)/ABCG2 drug pump. Blood 2004;104:2940-2.

(20) Houghton PJ, Germain GS, Harwood FC, Schuetz JD, Stewart CF, Buchdunger E et al. Imatinib mesylate is a potent inhibitor of the ABCG2 (BCRP) transporter and reverses resistance to topotecan and SN-38 in vitro. Cancer Res 2004;64:2333-7.

(21) Breedveld P, Pluim D, Cipriani G, Wielinga P, van Tellingen O, Schinkel AH et al. The effect of Bcrp1 (Abcg2) on the in vivo pharmacokinetics and brain penetration of imatinib mesylate (Gleevec): implications for the use of breast cancer resistance protein and P-glycoprotein inhibitors to enable the brain penetration of imatinib in patients. Cancer Res 2005;65:2577-82.

(22) Dai H, Marbach P, Lemaire M, Hayes M, Elmquist WF. Distribution of STI-571 to the brain is limited by P-glycoprotein-mediated efflux. J Pharmacol Exp Ther 2003;304:1085-92.

(23) Bihorel S, Camenisch G, Lemaire M, Scherrmann JM. Influence of breast cancer resistance protein (Abcg2) and p-glycoprotein (Abcb1a) on the transport of imatinib mesylate (Gleevec) across the mouse blood-brain barrier. J Neurochem 2007;102:1749-57.

(24) Bihorel S, Camenisch G, Lemaire M, Scherrmann JM. Modulation of the brain distribution of imatinib and its metabolites in mice by valspodar, zosuquidar and elacridar. Pharm Res 2007;24:1720-8.

(25) Mahon FX, Belloc F, Lagarde V, Chollet C, Moreau-Gaudry F, Reiffers J et al. MDR1 gene overexpression confers resistance to imatinib mesylate in leukemia cell line models. Blood 2003;101:2368-73.

(26) Nakanishi T, Shiozawa K, Hassel BA, Ross DD. Complex interaction of BCRP/ABCG2 and imatinib in BCR-ABL-expressing cells: BCRP-mediated resistance to imatinib is attenuated by imatinib-induced reduction of BCRP expression. Blood 2006;108:678-84.

(27) Oostendorp RL, Buckle T, Beijnen JH, van Tellingen O, Schellens JH. The effect of P-gp (Mdr1a/1b), BCRP (Bcrp1) and P-gp/BCRP inhibitors on the in vivo absorption, distribution, metabolism and excretion of imatinib. Invest New Drugs 2009; 27:31-40.

(28) Pfeifer H, Wassmann B, Hofmann WK, Komor M, Scheuring U, Bruck P et al. Risk and prognosis of central nervous system leukemia in patients with Philadelphia chromosome-positive acute leukemias treated with imatinib mesylate. Clin Cancer Res 2003;9:4674-81.

(29) Leis JF, Stepan DE, Curtin PT, Ford JM, Peng B, Schubach S et al. Central nervous system failure in patients with chronic myelogenous leukemia lymphoid blast crisis and Philadelphia chromosome positive acute lymphoblastic leukemia treated with imatinib (STI-571). Leuk Lymphoma 2004;45:695-8.

(30) Porkka K, Koskenvesa P, Lundan T, Rimpilainen J, Mustjoki S, Smykla R et al. Dasatinib crosses the blood-brain barrier and is an efficient therapy for central nervous system Philadelphia chromosome-positive leukemia. Blood 2008;112:1005-12.

(31) Deguchi Y, Kimura S, Ashihara E, Niwa T, Hodohara K, Fujiyama Y et al. Comparison of imatinib, dasatinib, nilotinib and INNO-406 in imatinib-resistant cell lines. Leuk Res 2008;32:980-3.

(32) Hiwase DK, Saunders V, Hewett D, Frede A, Zrim S, Dang P et al. Dasatinib cellular uptake and efflux in chronic myeloid leukemia cells: therapeutic implications. Clin Cancer Res 2008;14:3881-8.

(33) Giannoudis A, Davies A, Lucas CM, Harris RJ, Pirmohamed M, Clark RE. Effective dasatinib uptake may occur without human organic cation transporter 1 (hOCT1): implications for the treatment of imatinib resistant chronic myeloid leukaemia. Blood 2008;112:3348-54.

(34) Evers R, Kool M, van Deemter L, Janssen H, Calafat J, Oomen LC et al. Drug export activity of the human canalicular multispecific organic anion transporter in polarized kidney MDCK cells expressing cMOAT (MRP2) cDNA. J Clin Invest 1998;101:1310-9.

(35) Jonker JW, Buitelaar M, Wagenaar E, Van Der Valk MA, Scheffer GL, Scheper RJ et al. The breast cancer resistance protein protects against a major chlorophyll-derived dietary phototoxin and protoporphyria. Proc Natl Acad Sci U S A 2002;99:15649-54.

(36) Schinkel AH, Wagenaar E, van Deemter L, Mol CA, Borst P. Absence of the mdr1a P-Glycoprotein in mice affects tissue distribution and pharmacokinetics of dexamethasone, digoxin, and cyclosporin A. J Clin Invest 1995;96:1698-705.

(37) Huisman MT, Chhatta AA, van Tellingen O, Beijnen JH, Schinkel AH. MRP2 (ABCC2) transports taxanes and confers paclitaxel resistance and both processes are stimulated by probenecid. Int J Cancer 2005;116:824-9.

(38) Schinkel AH, Mayer U, Wagenaar E, Mol CA, van Deemter L, Smit JJ et al. Normal viability and altered pharmacokinetics in mice lacking mdr1-type (drug-transporting) P-glycoproteins. Proc Natl Acad Sci U S A 1997;94:4028-33.

(39) Jonker JW, Freeman J, Bolscher E, Musters S, Alvi AJ, Titley I et al. Contribution of the ABC transporters Bcrp1 and Mdr1a/1b to the side population phenotype in mammary gland and bone marrow of mice. Stem Cells 2005;23:1059-65.

(40) Goh LB, Spears KJ, Yao D, Ayrton A, Morgan P, Roland Wolf C et al. Endogenous drug transporters in in vitro and in vivo models for the prediction of drug disposition in man. Biochem Pharmacol 2002;64:1569-78.

(41) Giannoudis A, Davies A, Lucas CM, Harris RJ, Pirmohamed M, Clark RE. Effective dasatinib uptake may occur without human organic Cation Transporter 1 (hOCT1): implications for the treatment of imatinib resistant chronic myeloid leukaemia. Blood 2008 ;112:3348-54.

(42) Kamath AV, Wang J, Lee FY, Marathe PH. Preclinical pharmacokinetics and in vitro metabolism of dasatinib (BMS-354825): a potent oral multi-targeted kinase inhibitor against SRC and BCR-ABL. Cancer Chemother Pharmacol 2008;61:365-76.

(43) Takayama N, Sato N, O'Brien SG, Ikeda Y, Okamoto S. Imatinib mesylate has limited activity against the central nervous system involvement of Philadelphia chromosome-positive acute lymphoblastic leukaemia due to poor penetration into cerebrospinal fluid. Br J Haematol 2002;119:106-8.

(44) Bornhauser M, Jenke A, Freiberg-Richter J, Radke J, Schuler US, Mohr B et al. CNS blast crisis of chronic myelogenous leukemia in a patient with a major cytogenetic response in bone marrow associated with low levels of imatinib mesylate and its N-desmethylated metabolite in cerebral spinal fluid. Ann Hematol 2004;83:401-2.

(45) Slevin ML, Piall EM, Aherne GW, Johnston A, Lister TA. The pharmacokinetics of cytosine arabinoside in the plasma and cerebrospinal fluid during conventional and high-dose therapy. Med Pediatr Oncol 1982;10 Suppl 1:157-68.

CHAPTER 4.2

Breast cancer resistance protein (ABCG2) and P-glycoprotein (P-gp/MDR1) limit sorafenib brain penetration

Jurjen S. Lagas, Robert A.B. van Waterschoot, Rolf W. Sparidans, Els Wagenaar, Jos H. Beijnen and Alfred H. Schinkel

Submitted for publication

ABSTRACT
Sorafenib is a second generation, orally active multikinase inhibitor, approved for the treatment of patients with advanced renal cell carcinoma and patients with unresectable hepatocellular carcinoma. We studied active transport of sorafenib in MDCK-II cells and its subclones expressing the multidrug transporters P-gp or Abcg2. Sorafenib was found to be a moderate P-gp substrate and an efficiently transported Abcg2 substrate. Subsequently, because sorafenib is taken orally by cancer patients, we investigated the impact of P-gp and ABCG2 on oral plasma pharmacokinetics and brain penetration of sorafenib, using wild-type, *Abcb1a/1b*$^{-/-}$, *Abcg2*$^{-/-}$ and *Abcb1a/1b;Abcg2*$^{-/-}$ mice. The oral availability was not different among all strains. However, the brain penetration, 6 hr after oral administration, was 4.3-fold increased in *Abcg2*$^{-/-}$ mice, and not altered in *Abcb1a/1b*$^{-/-}$ mice. Brain penetration in *Abcb1a/1b;Abcg2*$^{-/-}$ mice was further increased (9.3-fold) compared to wild-type levels. These results demonstrate that the brain penetration of sorafenib is primarily restricted by ABCG2. This is in contrast with previous studies using shared ABCG2 and P-gp substrates, which all suggested that P-gp dominates at the blood-brain barrier, and that an effect of ABCG2 is only evident when both transporters are lacking. Interestingly, for sorafenib it is the other way around, i.e. ABCG2, and not P-gp, plays the dominant role in restricting brain penetration. Clinically, our findings may have implications for the treatment of renal cell carcinoma patients with CNS relapses, as a dual ABCG2 and P-gp inhibitor might drastically improve the CNS entry and thereby the therapeutic efficacy of sorafenib.

INTRODUCTION
The ATP binding cassette (ABC) drug transporters P-glycoprotein (P-gp, *ABCB1*) and Breast Cancer Resistance Protein (*ABCG2*) are localized at several so-called sanctuary site barriers, such as blood-brain, blood-testis, and blood-placenta barrier. At these barriers, the drug transporters restrict the penetration of many harmful compounds, thereby protecting the sanctuary tissues (1). However, their protective function becomes a disadvantage when penetration of substrate drugs into sanctuary tissues is desired, for instance for the treatment of brain tumors. An example that illustrates this disadvantage is the low brain penetration of imatinib, a first-generation, orally active inhibitor of BCR-ABL kinase, that is used as frontline therapy for Philadelphia chromosome positive (Ph+) leukemia. Because imatinib is a good substrate of both P-gp and ABCG2 (2;3), its penetration into the central nervous system (CNS) is markedly restricted by both transporters (4-6).

Sorafenib (BAY 43-9006; Nexavar; Fig. 1) is a second generation, orally active multikinase inhibitor, recently approved for the treatment of patients with advanced renal cell carcinoma (RCC) and patients with unresectable hepatocellular carcinoma (7). Interactions of sorafenib with P-gp or ABCG2 are thus far not reported. However, a few case reports indicated that sorafenib can achieve partial remission in RCC patients with brain metastases (8;9). Although brain metastases may contain leaky blood vessels due to neovascularization, they are often protected from adequate chemotherapy because they are still mostly behind an intact blood-brain barrier [reviewed in (10)]. It is thus important to establish whether the entry of sorafenib into the brain is limited by P-gp and/or ABCG2, because this information may be used to further optimize the treatment of RCC patients with CNS metastases. Therefore, we studied *in vitro* transport of sorafenib by P-gp and Abcg2 and we investigated plasma pharmacokinetics and brain penetration after oral sorafenib administration to wild-type, *Abcb1a/1b*$^{-/-}$, *Abcg2*$^{-/-}$ and *Abcb1a/1b;Abcg2*$^{-/-}$ mice.

MATERIALS AND METHODS

Chemicals. Sorafenib tosylate originated from Sequoia Research Products (Pangbourne, UK). Methoxyflurane (Metofane®) was from Medical Developments Australia (Springvale, Victoria, Australia). Bovine serum albumin (BSA), fraction V, was from Roche (Mannheim, Germany). Cremophor EL was supplied by Fluka Biochemica (Steinheim, Germany). All other chemicals and reagents were obtained from Sigma-Aldrich (Steinheim, Germany).

Transport assays. Polarized canine kidney MDCK-II cell lines were used in transport assays. MDCK-II cells transduced with human P-gp or murine Abcg2 were described previously (11;12) . Transepithelial transport assays using transwell plates were carried out as described previously (13). Experiments were started by replacing the medium in either the apical or basolateral compartment with fresh OptiMEM medium (Invitrogen, Breda, The Netherlands), containing 5 µM of sorafenib. Cells were incubated at 37°C in 5% CO_2, and 50 µl aliquots were taken at t = 4 hr. The apparent permeability coefficient (P_{app}) was calculated using the equation: P_{app} (cm/s) = dC/dt * 1/A * V/C_o [cm/s], where dC/dt (µM.sec^{-1}) represents the flux across the monolayer (permeability rate), A (cm^2) the surface area of the monolayer, V (cm^3) the volume of the receiver chamber and C_o (µM) the initial concentration in the donor compartment (14). Results are presented as mean P_{app} ± SD (n = 3). Membrane tightness was assessed in parallel, using the same cells seeded on the same day and at the same density, by analyzing transepithelial [^{14}C]inulin (approx. 3 kBq /well) leakage. Leakage had to remain <1% of the total added radioactivity per hour.

Animals. Mice were housed and handled according to institutional guidelines complying with Dutch legislation. Animals used were male wild-type (WT), *Abcb1a/1b*$^{-/-}$ (15), *Abcg2*$^{-/-}$ (16) and *Abcb1a/1b;Abcg2*$^{-/-}$ (17) mice, all of a >99% FVB genetic background, between 9 and 12 weeks of age. Animals were kept in a temperature-controlled environment with a 12-hour light / 12-hour dark cycle and received a standard diet (AM-II, Hope Farms, Woerden, The Netherlands) and acidified water *ad libitum*.

Plasma pharmacokinetics. Sorafenib tosylate was dissolved in Cremophor EL/95% Ethanol/water (12.5/12.5/75, v/v/v) and orally administered at 10 mg/kg (10 µl/g). To minimize variation in absorption, mice were fasted 3 h before sorafenib was given by gavage into the stomach, using a blunt-ended needle. Multiple blood samples (~30 µl) were collected from the tail vein at 15 and 30 min and 1, 2, 4 and 6 h, using heparinized capillary tubes (Oxford Labware, St. Louis, USA). At the last time point, mice were anesthetized with methoxyflurane and blood was collected by cardiac puncture. Immediately thereafter, mice were sacrificed by cervical dislocation and brains were rapidly removed, homogenized on ice in 1 ml 4% BSA and stored at -30°C until analysis. Blood samples were centrifuged at 2,100 x *g* for 6 min at 4°C, the plasma fraction was collected and stored at -20°C until analysis.

Relative brain penetration. Brain concentrations were corrected for the amounts of drug in the brain vasculature, i.e. 1.4% of the plasma concentration right before the brains were isolated (18). Subsequently, brain penetration after oral administration was calculated by determining the sorafenib brain concentration relative to the area under plasma concentration-time curve from 0-6 hr (AUC_{0-6}). The AUC_{0-6} was used instead of plasma concentration at 6 hr, because the AUC better reflects the overall sorafenib exposure of the brain.

Drug analysis. Sorafenib concentrations in OptiMEM cell culture medium, plasma samples and brain homogenates were determined using a sensitive and specific LC-MS/MS assay (19).

Pharmacokinetic calculations and statistical analysis. Pharmacokinetic parameters were calculated by noncompartmental methods using the software package WinNonlin Professional version 5.0. The area under plasma concentration-time curve (AUC) was calculated using the trapezoidal rule, without extrapolating to infinity. The peak plasma concentration (C_{max}) and the time of the maximum plasma concentration (T_{max}) were estimated from the original data. The two-sided unpaired Student's *t*-test was used for statistical analysis. Differences were considered statistically significant when $P < 0.05$. Data are presented as means ± SD.

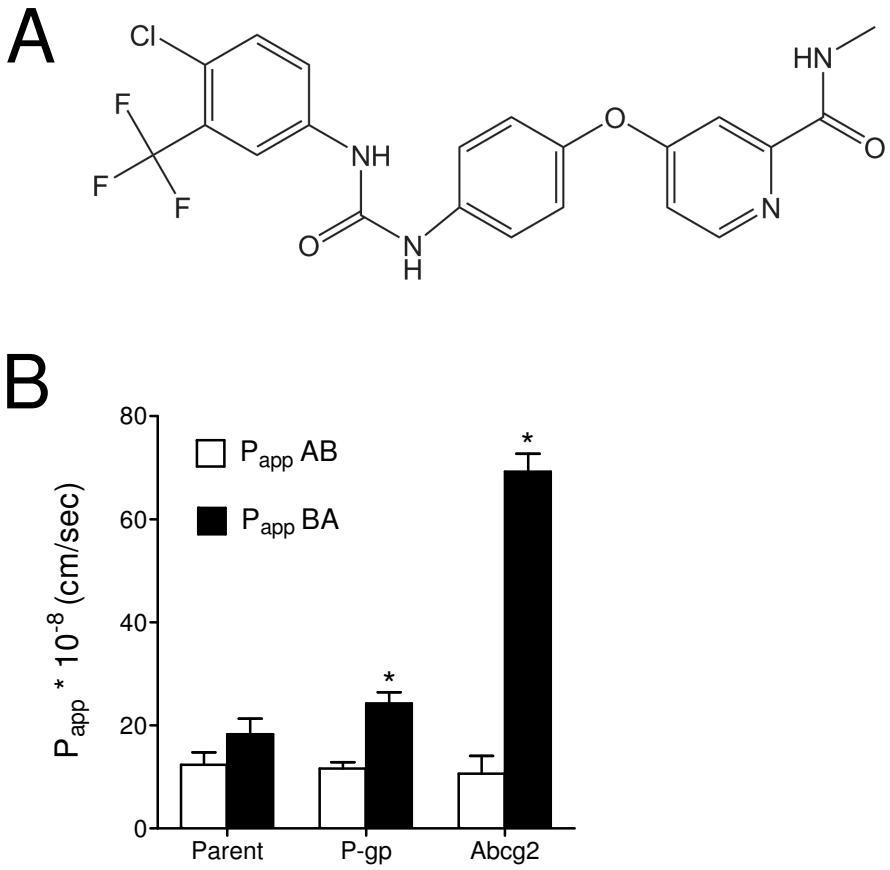

Fig. 1. Molecular structure of sorafenib (*A*) and apparent permeability coefficients (*B*) for sorafenib in MDCK-II parent cells, and in P-gp- or Abcg2-transduced subclones. P_{app} was calculated 4 hr after the application of sorafenib to the apical compartment (P_{app} AB) or to the basolateral compartment (P_{app} AB). Data are mean P_{app} ± SD (n = 3). * $P < 0.01$, when P_{app} BA was compared to P_{app} AB for parental cells and each transfected subclone.

RESULTS AND DISCUSSION

Thus far, interactions of sorafenib with either ABCG2 or P-gp have not been described. However, for a number of tyrosine kinase inhibitors (TKIs), including imatinib (2;3), erlotinib (20), dasatinib (21) and lapatinib (22), transport by ABCG2 and P-gp was reported, while other TKIs were shown to inhibit ABCG2- and/or P-gp mediated transport, e.g. gefitinib (23-25), nilotinib (26;27) and sunitinib (28). We therefore anticipated that sorafenib could be a substrate of P-gp

and/or ABCG2 as well, and we studied the *in vitro* transport of sorafenib in MDCK-II cells and subclones of these cells transfected with P-gp or Abcg2. In the parental cells, the apparent permeability coefficient (P_{app}) was not different for apically or basolaterally applied sorafenib, indicating that sorafenib was not actively transported in these cells (Fig. 1B). In the MDCK-II cells transfected with P-gp, the P_{app} for basolaterally applied sorafenib was 2.1-fold higher than for apically applied sorafenib, whereas for Abcg2 transfected cells the P_{app} was 6.5-fold higher when sorafenib was basolaterally applied ($P < 0.001$; Fig. 1B). Sorafenib appears thus to be actively transported by P-gp and ABCG2, and the P_{app} values indicate that sorafenib is a moderate P-gp and a good ABCG2 substrate.

Table 1. Pharmacokinetic parameters, brain concentrations and relative brain penetration of sorafenib after oral administration at 10 mg/kg.

	Genotype			
	WT	*Abcb1a/1b*$^{-/-}$	*Abcg2*$^{-/-}$	*Abcb1a/1b/Abcg2*$^{-/-}$
$AUC_{(0-6)}$, µg/ml.hr	24.0 ± 4.8	19.6 ± 0.7	22.2 ± 1.5	21.2 ± 2.3
C_{max}, µg/ml	6.9 ± 1.3	6.7 ± 0.8	7.1 ± 0.6	6.0 ± 0.8
T_{max}, hr	1	1	1	2
C_{brain}, µg/g	0.12 ± 0.04	0.11 ± 0.04	0.50 ± 0.13 *	1.04 ± 0.08 */†
Fold increase	1.0	0.9	4.2	8.7
P_{brain}, ($*10^{-3}$ hr^{-1})	5.3 ± 2.7	5.8 ± 2.2	22.6 ± 5.0 *	49.4 ± 5.2 */†
Fold increase	1.0	1.1	4.3	9.3

$AUC_{(0-6)}$, area under plasma concentration-time curve up to 6 hr; C_{max}, maximum plasma concentration; T_{max}, time of maximal plasma concentration; C_{brain}, brain concentration at 6 hr after oral administration; P_{brain}, relative brain penetration at 6 hr after oral administration, calculated by determining the sorafenib brain concentration relative to the area under plasma concentration-time curve from 0-6 hr (AUC_{0-6}). Data are means ± SD, n = 5. * $P < 0.001$, compared to WT mice, † $P < 0.01$, compared to *Abcg2*$^{-/-}$ mice.

Because sorafenib is taken orally by cancer patients, we next studied oral sorafenib plasma pharmacokinetics and we investigated whether the entry of sorafenib into the brain was restricted by either one or both transporters. We orally administered 10 mg/kg sorafenib to WT, *Abcb1a/1b*$^{-/-}$, *Abcg2*$^{-/-}$ and *Abcb1a/1b;Abcg2*$^{-/-}$ mice. As

shown in Fig. 2A and in Table 1, plasma concentrations and areas under the plasma concentration-time curves (AUCs) were not different among all strains. This suggests that Abcg2 and P-gp do not limit oral uptake or contribute significantly to first-pass elimination upon oral administration of sorafenib in mice. Furthermore, the brain penetration of sorafenib, 6 hr after oral administration, was not different between *Abcb1a/1b*$^{-/-}$ and WT mice (Fig 2B). In contrast, *Abcg2*$^{-/-}$ mice had a 4.3-fold increased brain penetration (Fig. 2B). *Abcb1a/1b;Abcg2*$^{-/-}$ mice had an even further increase in relative brain penetration, which was 2.2-fold higher than in *Abcg2*$^{-/-}$ mice and 9.3-fold increased compared to WT mice (Fig. 2B, Table 1).

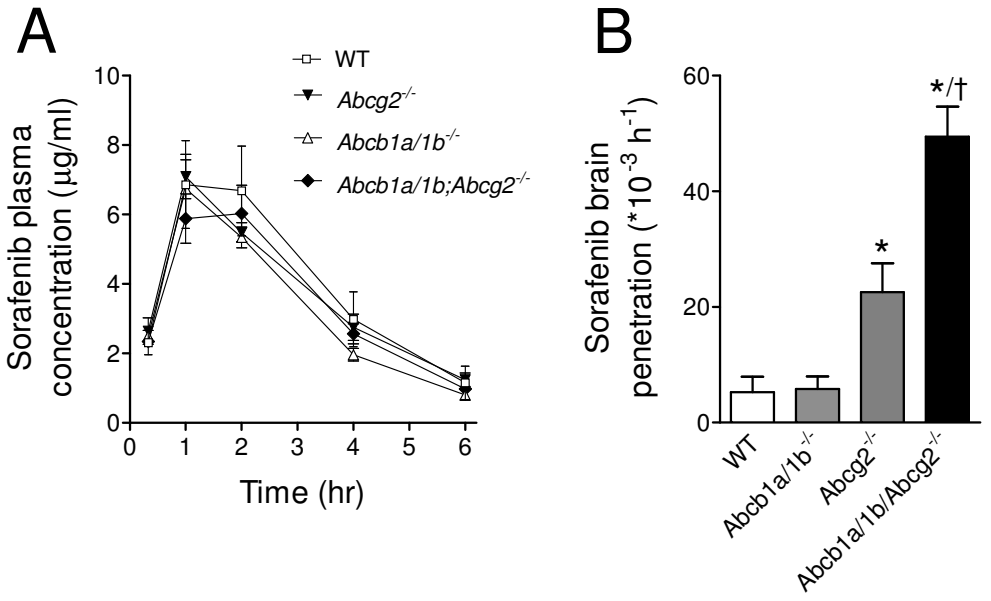

Fig. 2. Plasma concentration-time curves (*A*) and relative brain penetration (*B*) of sorafenib in male FVB WT, *Abcg2*$^{-/-}$, *Abcb1a/1b*$^{-/-}$, and *Abcb1a/1b;Abcg2*$^{-/-}$ mice after oral administration of 10 mg/kg sorafenib. Relative brain penetration was calculated by dividing brain concentration by the area under plasma concentration-time curve from 0-6 hr (AUC_{0-6}). Data are means ± SD, n = 5. * $P < 0.001$, compared to WT mice, † $P < 0.01$, compared to *Abcg2*$^{-/-}$ mice.

Abcg2 thus markedly restricts the brain penetration of sorafenib, both in P-gp proficient and deficient mice. However, in *Abcg2*$^{-/-}$ mice, P-gp can partly but not completely take over the function of Abcg2 at the BBB. Moreover, when both transporters are absent, brain penetration of sorafenib is highly increased. Uncorrected brain concentrations and values for the relative brain penetration essentially yielded the same results (Table 1). The apparent discrepancy, i.e. that the loss of P-gp and Abcg2 does not affect the oral uptake of sorafenib, whereas the brain penetration is highly increased, has been observed for other compounds, including the TKI imatinib (6). It could be that there are efficient uptake transporter(s) for these drugs in the gut, which may be absent from the BBB, or perhaps that passive diffusion of these compounds occurs more easily across the intestinal wall than through the BBB. It is of interest to note that Abcg2 RNA was not differentially expressed in the brain of P-gp deficient and WT mice (29). Vice versa, in the present study we checked the Mdr1a P-gp RNA expression in the brain of *Abcg2*$^{-/-}$ mice by real-time quantitative PCR, and found no difference compared to WT mice (data not shown). Thus, the relative contribution of P-gp or Abcg2 at the BBB of Abcg2- or P-gp-deficient mice, respectively, seems not to be obscured by altered expression of either P-gp or Abcg2.

Collectively, our results show that sorafenib is a substrate of both ABCG2 and P-gp, which however has little impact on sorafenib oral availability. Interestingly, single P-gp deficiency did not affect the entry of sorafenib to the brain, whereas absence of Abcg2 resulted in a markedly higher brain penetration. This observation is of particular interest, because previous reports, studying shared substrates in *Abcb1a/1b*$^{-/-}$, *Abcg2*$^{-/-}$ and compound *Abcb1a/1b;Abcg2*$^{-/-}$ mice, all indicated that P-gp, and not ABCG2, plays a dominant role at the BBB. This was first shown by de Vries and colleagues (30), who investigated the brain penetration of the anticancer agent topotecan. The brain-to-plasma AUC ratios of i.v. administered topotecan were 2.0-fold increased in *Abcb1a/1b*$^{-/-}$ mice, 0.65-fold in *Abcg2*$^{-/-}$ mice, and 3.2-fold in *Abcb1a/1b;Abcg2*$^{-/-}$ mice. These results are striking, because topotecan is a comparatively weak P-gp substrate and a good substrate for Abcg2 (31;32) and accordingly, also the oral availability of topotecan in mice seems to be more affected by Abcg2 than by P-gp (29;33). In a second study, Oostendorp et al. investigated the brain penetration of 100 mg/kg orally administered imatinib, a good substrate for both P-gp and Abcg2 (2;4;6). The brain-to-plasma ratio in *Abcb1a/1b*$^{-/-}$ mice was 2.3-fold increased after 1 hr. For *Abcg2*$^{-/-}$ mice brain-to-plasma ratios were not different from WT mice, whereas *Abcb1a/1b;Abcg2*$^{-/-}$ mice had a 13.3-fold increased ratio after 1 hr. Thirdly, a study with *Abcb1a/1b;Abcg2*$^{-/-}$ mice was reported, that investigated the brain penetration of the TKI lapatinib, a good substrate of P-gp and an intermediate ABCG2 substrate (22;34). Lapatinib

was i.v. infused at 0.3 or 3 mg/kg/hr, and after 24 hr infusion the brain-to-plasma ratios were determined. In *Abcb1a/1b*$^{-/-}$ mice, the ratios were 3- to 4-fold higher, whereas *Abcg2*$^{-/-}$ mice had similar ratios as WT mice. The brain-to-plasma ratios in *Abcb1a/1b;Abcg2*$^{-/-}$ mice, however, were about 40-fold increased. And finally, while we were finalizing our manuscript, Zhou et al. reported a study, in which they tried to gain more insight into the role of ABCG2 at the BBB (35). In that study more than 1000 compounds were screened *in vitro* for their affinity for P-gp and ABCG2, in order to find a substrate with good affinity for ABCG2/Abcg2 and negligible affinity for P-gp. Only one compound, PF-407288, was classified as a specific ABCG2/Abcg2 substrate. This compound was used to study the brain penetration in *Abcb1a/1b*$^{-/-}$, *Abcg2*$^{-/-}$ and *Abcb1a/1b;Abcg2*$^{-/-}$ mice. However, the brain penetration was not considerably increased in single *Abcg2*$^{-/-}$ or *Abcb1a/1b*$^{-/-}$ mice, and only about 2-fold higher in *Abcb1a/1b;Abcg2*$^{-/-}$ mice.

Taken together, these previous studies in *Abcb1a/1b;Abcg2*$^{-/-}$ mice and many other studies in single *Abcb1a/1b*$^{-/-}$ and/or *Abcg2*$^{-/-}$ mice suggested that P-gp, and not Abcg2, plays a dominant role at the BBB. Moreover, in all studies reported thus far on shared P-gp and ABCG2 substrates an impact of Abcg2 deficiency on brain penetration only became evident when P-gp was absent too, i.e. in *Abcb1a/1b;Abcg2*$^{-/-}$ mice [reviewed in (36)]. To the best of our knowledge, the present study is therefore the first to show that the brain penetration of a shared P-gp and ABCG2 substrate is not noticeably affected by single P-gp deficiency, whereas Abcg2 plays a leading role in restricting the entry into the brain.

Apart from the basic mechanistic aspects of the individual contribution of these efflux transports at the BBB, the drastically increased brain penetration of sorafenib in *Abcb1a/1b;Abcg2*$^{-/-}$ mice upon oral administration may provide a rationale for combining sorafenib with a dual P-gp and ABCG2 inhibitor. This approach may result in increased brain penetration and improved therapeutic efficacy in cancer patients with CNS relapses. Based on the interactions of many TKIs with P-gp and ABCG2, and strengthened by the recently reported data on the highly increased brain penetration of lapatinib in *Abcb1a/1b;Abcg2*$^{-/-}$ mice (34), we expect that this concept might be applicable to other TKIs as well.

ACKNOWLEGMENTS

We thank our colleagues for critical reading of the manuscript.

REFERENCES

(1) Borst P, Oude Elferink RP. Mammalian ABC transporters in health and disease. Annu Rev Biochem 2002;71:537-92.

(2) Hamada A, Miyano H, Watanabe H, Saito H. Interaction of imatinib mesilate with human P-glycoprotein. J Pharmacol Exp Ther 2003;307:824-8.

(3) Burger H, van Tol H, Boersma AW, Brok M, Wiemer EA, Stoter G et al. Imatinib mesylate (STI571) is a substrate for the breast cancer resistance protein (BCRP)/ABCG2 drug pump. Blood 2004;104:2940-2.

(4) Breedveld P, Pluim D, Cipriani G, Wielinga P, van Tellingen O, Schinkel AH et al. The effect of Bcrp1 (Abcg2) on the in vivo pharmacokinetics and brain penetration of imatinib mesylate (Gleevec): implications for the use of breast cancer resistance protein and P-glycoprotein inhibitors to enable the brain penetration of imatinib in patients. Cancer Res 2005;65:2577-82.

(5) Bihorel S, Camenisch G, Lemaire M, Scherrmann JM. Influence of breast cancer resistance protein (Abcg2) and p-glycoprotein (Abcb1a) on the transport of imatinib mesylate (Gleevec) across the mouse blood-brain barrier. J Neurochem 2007;102:1749-57.

(6) Oostendorp RL, Buckle T, Beijnen JH, van Tellingen O, Schellens JH. The effect of P-gp (Mdr1a/1b), BCRP (Bcrp1) and P-gp/BCRP inhibitors on the in vivo absorption, distribution, metabolism and excretion of imatinib. Invest New Drugs 2009;27:31-40.

(7) Wilhelm SM, Adnane L, Newell P, Villanueva A, Llovet JM, Lynch M. Preclinical overview of sorafenib, a multikinase inhibitor that targets both Raf and VEGF and PDGF receptor tyrosine kinase signaling. Mol Cancer Ther 2008;7:3129-40.

(8) Ranze O, Hofmann E, Distelrath A, Hoeffkes HG. Renal cell cancer presented with leptomeningeal carcinomatosis effectively treated with sorafenib. Onkologie 2007;30:450-1.

(9) Valcamonico F, Ferrari V, Amoroso V, Rangoni G, Simoncini E, Marpicati P et al. Long-lasting successful cerebral response with sorafenib in advanced renal cell carcinoma. J Neurooncol 2009;91:47-50.

(10) de Vries NA, Beijnen JH, Boogerd W, van Tellingen O. Blood-brain barrier and chemotherapeutic treatment of brain tumors. Expert Rev Neurother 2006;6:1199-209.

(11) Evers R, Kool M, van Deemter L, Janssen H, Calafat J, Oomen LC et al. Drug export activity of the human canalicular multispecific organic anion transporter in polarized kidney MDCK cells expressing cMOAT (MRP2) cDNA. J Clin Invest 1998;101:1310-9.

(12) Jonker JW, Buitelaar M, Wagenaar E, van der Valk MA, Scheffer GL, Scheper RJ et al. The breast cancer resistance protein protects against a major chlorophyll-derived dietary phototoxin and protoporphyria. Proc Natl Acad Sci U S A 2002;99:15649-54.

(13) Schinkel AH, Wagenaar E, van Deemter L, Mol CA, Borst P. Absence of the mdr1a P-Glycoprotein in mice affects tissue distribution and pharmacokinetics of dexamethasone, digoxin, and cyclosporin A. J Clin Invest 1995;96:1698-705.

(14) Irvine JD, Takahashi L, Lockhart K, Cheong J, Tolan JW, Selick HE et al. MDCK (Madin-Darby canine kidney) cells: A tool for membrane permeability screening. J Pharm Sci 1999;88:28-33.

(15) Schinkel AH, Mayer U, Wagenaar E, Mol CA, van Deemter L, Smit JJ et al. Normal viability and altered pharmacokinetics in mice lacking mdr1-type (drug-transporting) P-glycoproteins. Proc Natl Acad Sci U S A 1997;94:4028-33.

(16) Jonker JW, Buitelaar M, Wagenaar E, van der Valk MA, Scheffer GL, Scheper RJ et al. The breast cancer resistance protein protects against a major chlorophyll-derived dietary phototoxin and protoporphyria. Proc Natl Acad Sci U S A 2002;99:15649-54.

(17) Jonker JW, Freeman J, Bolscher E, Musters S, Alvi AJ, Titley I et al. Contribution of the ABC transporters Bcrp1 and Mdr1a/1b to the side population phenotype in mammary gland and bone marrow of mice. Stem Cells 2005;23:1059-65.

(18) Dai H, Marbach P, Lemaire M, Hayes M, Elmquist WF. Distribution of STI-571 to the brain is limited by P-glycoprotein-mediated efflux. J Pharmacol Exp Ther 2003;304:1085-92.

(19) Sparidans RW, Vlaming ML, Lagas JS, Schinkel AH, Schellens JH, Beijnen JH. Liquid chromatography-tandem mass spectrometric assay for sorafenib and sorafenib-glucuronide in mouse plasma and liver homogenate and identification of the glucuronide metabolite. J Chromatogr B Analyt Technol Biomed Life Sci 2009;877:269-76.

(20) Marchetti S, de Vries NA, Buckle T, Bolijn MJ, van Eijndhoven MA, Beijnen JH et al. Effect of the ATP-binding cassette drug transporters ABCB1, ABCG2, and ABCC2 on erlotinib hydrochloride (Tarceva) disposition in in vitro and in vivo pharmacokinetic studies employing Bcrp1-/-/Mdr1a/1b-/- (triple-knockout) and wild-type mice. Mol Cancer Ther 2008;7:2280-7.

(21) Hiwase DK, Saunders V, Hewett D, Frede A, Zrim S, Dang P et al. Dasatinib cellular uptake and efflux in chronic myeloid leukemia cells: therapeutic implications. Clin Cancer Res 2008;14:3881-8.

(22) Polli JW, Humphreys JE, Harmon KA, Castellino S, O'Mara MJ, Olson KL et al. The role of efflux and uptake transporters in lapatinib disposition and drug interactions. Drug Metab Dispos 2008;36:695-701.

(23) Ozvegy-Laczka C, Hegedus T, Varady G, Ujhelly O, Schuetz JD, Varadi A et al. High-affinity interaction of tyrosine kinase inhibitors with the ABCG2 multidrug transporter. Mol Pharmacol 2004;65:1485-95.

(24) Nakamura Y, Oka M, Soda H, Shiozawa K, Yoshikawa M, Itoh A et al. Gefitinib ("Iressa", ZD1839), an epidermal growth factor receptor tyrosine kinase inhibitor, reverses breast cancer resistance protein/ABCG2-mediated drug resistance. Cancer Res 2005;65:1541-6.

(25) Kitazaki T, Oka M, Nakamura Y, Tsurutani J, Doi S, Yasunaga M et al. Gefitinib, an EGFR tyrosine kinase inhibitor, directly inhibits the function of P-glycoprotein in multidrug resistant cancer cells. Lung Cancer 2005;49:337-43.

(26) Mahon FX, Hayette S, Lagarde V, Belloc F, Turcq B, Nicolini F et al. Evidence that resistance to nilotinib may be due to BCR-ABL, Pgp, or Src kinase overexpression. Cancer Res 2008;68:9809-16.

(27) Brendel C, Scharenberg C, Dohse M, Robey RW, Bates SE, Shukla S et al. Imatinib mesylate and nilotinib (AMN107) exhibit high-affinity interaction with ABCG2 on primitive hematopoietic stem cells. Leukemia 2007;21:1267-75.

(28) Shukla S, Robey RW, Bates SE, Ambudkar SV. Sunitinib (Sutent, SU11248), a small-molecule receptor tyrosine kinase inhibitor, blocks function of the ATP-binding cassette (ABC) transporters P-glycoprotein (ABCB1) and ABCG2. Drug Metab Dispos 2009;37:359-65.

(29) Jonker JW, Smit JW, Brinkhuis RF, Maliepaard M, Beijnen JH, Schellens JH et al. Role of breast cancer resistance protein in the bioavailability and fetal penetration of topotecan. J Natl Cancer Inst 2000;92:1651-6.

(30) de Vries NA, Zhao J, Kroon E, Buckle T, Beijnen JH, van Tellingen O. P-glycoprotein and breast cancer resistance protein: two dominant transporters working together in limiting the brain penetration of topotecan. Clin Cancer Res 2007;13:6440-9.

(31) Hendricks CB, Rowinsky EK, Grochow LB, Donehower RC, Kaufmann SH. Effect of P-glycoprotein expression on the accumulation and cytotoxicity of topotecan (SK&F 104864), a new camptothecin analogue. Cancer Res 1992;52:2268-78.

(32) Maliepaard M, van Gastelen MA, de Jong LA, Pluim D, van Waardenburg RC, Ruevekamp-Helmers MC et al. Overexpression of the BCRP/MXR/ABCP gene in a topotecan-selected ovarian tumor cell line. Cancer Res 1999;59:4559-63.

(33) Jonker JW, Buitelaar M, Wagenaar E, van der Valk MA, Scheffer GL, Scheper RJ et al. The breast cancer resistance protein protects against a major chlorophyll-derived dietary phototoxin and protoporphyria. Proc Natl Acad Sci U S A 2002;99:15649-54.

(34) Polli JW, Olson KL, Chism JP, John-Williams LS, Yeager RL, Woodard SM et al. An unexpected synergist role of P-glycoprotein and breast cancer resistance protein on the central nervous system penetration of the tyrosine kinase inhibitor lapatinib. Drug Metab Dispos 2009;37:439-42.

(35) Zhou L, Schmidt K, Nelson FR, Zelesky V, Troutman MD, Feng B. The Effect of Breast Cancer Resistance Protein (Bcrp) and P-glycoprotein (Mdr1a/1b) on the Brain Penetration of Flavopiridol, Gleevec, Prazosin and PF-407288 in Mice. Drug Metab Dispos 2009; 37: 946-55.

(36) Vlaming ML, Lagas JS, Schinkel AH. Physiological and pharmacological roles of ABCG2 (BCRP): recent findings in Abcg2 knockout mice. Adv Drug Deliv Rev 2009;61:14-25.

CONCLUSIONS AND PERSPECTIVES

The studies described in this thesis show that mouse models that are deficient for multiple ATP-binding cassette (ABC) drug transporters are valuable tools to study the redundant, overlapping, and complementary functions of ABC transporters. Our studies, as well as the work of others on combination ABC transporter knockout mice, demonstrated that the relative contribution of each ABC transporter to the pharmacokinetics of (anticancer) drugs is not only dependent on the substrate and the route of administration, but also on the organ or tissue under investigation. Examples that are described in this thesis are discussed below. These findings illustrate that it is currently not possible to only use *in vitro* assays or in silico models to predict the impact of multiple ABC transporters on the *in vivo* behavior of (experimental) anticancer agents and other drugs. It is therefore expected that these combination ABC transporter knockout mouse models will be extensively used for preclinical studies in the future.

Nowadays, it is more and more recognized that ABC transporters can markedly affect the pharmacokinetics of anticancer drugs. For example, novel rationally designed small molecule anticancer agents for oral application are developed to have low affinity for P-glycoprotein (P-gp) and Breast Cancer Resistance Protein (ABCG2), because these transporters can drastically restrict the oral uptake of their substrates. On the other hand, the chemical structure of these drugs determines their interaction with target proteins, and structural modifications to reduce their affinity for drugs transporter may render these drugs less active. It is obvious that compromises must be made to meet both criteria. In this thesis, two examples of such drugs were studied, the second generation, orally active tyrosine kinase inhibitors dasatinib and sorafenib. Both compounds were found to be transported by P-g and ABCG2 *in vitro*, and the oral uptake of dasatinib, which appeared to be a better P-gp substrate than sorafenib, was limited by P-gp in mice. Nonetheless, preclinical studies have shown that the oral bioavailability of dasatinib ranges from 15-30% (1), and because the drug has a relatively wide therapeutic window, oral administration of dasatinib to cancer patients is not hampered by P-gp in the gut. On the other hand, it is also described in this thesis that mice knockout for P-gp and Abcg2 had highly increased brain penetration of dasatinib and sorafenib. The entry of both compounds into the central nervous system is thus drastically restricted by P-gp and ABCG2. Moreover, with the dual P-gp and ABCG2 inhibitor elacridar we were able to completely inhibit P-gp and Abcg2 at the blood-brain barrier (BBB) of wild-type mice, resulting in similar dasatinib brain penetration as observed in the combination knockout mice. These findings provide a rationale for combining dasatinib and sorafenib with a dual P-gp and ABCG2 inhibitor to improve their penetration into the central nervous system and target intracranial tumors.

Another interesting aspect that we came across in the studies on the tyrosine kinase inhibitors is the relative contribution of both transporters to the blood-brain barrier. The important function of P-gp at the BBB has been convincingly established years ago, using P-gp knockout mice (2). For ABCG2, however, it was not as straightforward to establish a functional role at the BBB, despite the availability of Abcg2-deficient mice. In fact, most studies used shared P-gp and ABCG2 substrates and failed to show higher brain penetration in single *Abcg2*$^{-/-}$ mice because P-gp often completely compensates for the loss of Abcg2 (reviewed in chapter 1.2 of this thesis). However, several recent studies, including those described in this thesis, have compared brain penetration of shared substrates in mice knockout for both P-gp and Abcg2 to that in single P-gp deficient mice, and could demonstrate a clear function of Abcg2 at the BBB in the absence of P-gp. For dasatinib we found that loss of P-gp resulted in markedly higher brain penetration, whereas single Abcg2 deficiency had no effect. However, when both transporters were absent the brain penetration was highly increased. These results showed that P-gp can fully compensate for the loss of Abcg2, whereas Abcg2 only partially compensates for the absence of P-gp. Interestingly, for sorafenib it was the other way around. To the best of our knowledge, this is the first example of a shared P-gp and ABCG2 substrate, for which the entry into the central nervous system is primarily restricted by Abcg2, and not P-gp.

The clinical significance of these insights was recently highlighted by a study on single nucleotide polymorphisms (SNPs) of both transporter genes in relation to toxic neurological complications of chemotherapy (3). In this study it was found that cancer patients with SNPs in both transporter genes, resulting in reduced expression and function of P-gp and ABCG2, developed disproportionally more toxic encephalopathy during chemotherapy with potentially neurotoxic anticancer agents than patients with either one or no SNP. These findings suggest that also at the human BBB P-gp and ABCG2 work in concert and restrict the penetration of potentially harmful compounds into the central nervous system. We therefore conclude that P-gp/Abcg2 combination knockout mice, together with the single P-gp and Abcg2 knockout mice, are valuable preclinical tools to study the functional overlap of P-gp and ABCG2 at the BBB.

The studies in this thesis on paclitaxel and etoposide, employing single and combination knockout mice for P-gp and multidrug resistance protein 2 (Mrp2), also illustrate that the relative contribution of each ABC transporter to the pharmacokinetics of drugs can be highly dependent on the substrate, the route of administration, and the organ or tissue under investigation. Paclitaxel and etoposide are bulky, lipophilic, amphipathic, plant-derived anticancer agents, and good to excellent substrates for P-gp. As a consequence, the absorption of these drugs from

the gut is largely restricted by P-gp, resulting in a low oral availability. Previously, *in vitro* studies showed that paclitaxel and etoposide are moderate substrate for MRP2, but the *in vivo* relevance of these findings remained unclear, as MRP2 was thought to mainly affect organic anionic drugs *in vivo*. MRP2, like P-gp, is highly expressed in the apical membrane of epithelial cells lining the gut and we studied the oral availability of paclitaxel and etoposide in Mrp2 deficient mice. However, loss of Mrp2 did not result in an increased oral uptake of either compound. On the other hand, both transporters are also expressed in the canalicular membrane of hepatocytes where they pump their substrates into the bile. We found that the biliary excretion of paclitaxel and etoposide was largely dependent on Mrp2, whereas P-gp played only a minor role. Interestingly, loss of Mrp2 resulted in markedly increased plasma concentrations of paclitaxel upon i.v. administration, which could be attributed to impaired hepatobiliary elimination. This finding may be relevant for cancer patients, because paclitaxel is given by i.v. infusion and variation in MRP2 activity might thus directly affect the effective exposure to paclitaxel. In contrast, our study on etoposide showed that impaired biliary excretion in Mrp2 deficient mice did not lead to higher etoposide plasma concentrations. Instead, hepatic formation of etoposide glucuronide was highly increased, and this metabolite was extruded from the liver to the blood and subsequently excreted in the urine. This finding might explain why a number of studies showed that cancer patients with impaired liver function displayed no altered etoposide plasma clearance. The single P-gp and Mrp2 deficient mice, together with the P-gp/Mrp2 combination knockout model enabled us to show that P-gp and MRP2 fulfill complementary functions in liver and intestine. These studies also revealed that the *in vivo* substrate specificity of MRP2 is broader than previously anticipated. In addition to organic anionic compounds, MRP2 thus also importantly affects the pharmacokinetics of lipophilic, amphipathic plant-derived anticancer drugs.

The study on salinomycin in this thesis showed that the substrate specificity of P-gp is also broader than previously thought. Salinomycin is a polyether antibiotic belonging to the group of ionophores, that is extensively used as a coccidiostat in poultry and other livestock and is commonly fed to ruminant animals to improve feed efficiency. However, salinomycin can also cause severe toxicity when accidentally fed to animals in relatively high doses. Our interest in salinomycin was sparked by the widespread poisoning of cats with salinomycin that occurred in 1996 in the Netherlands and in Switzerland (4). Two brands of cat food from one manufacturer were found to be contaminated with salinomycin, which resulted in an outbreak of acute polyneuropathy. We wondered if salinomycin could be a substrate of one or more of the apical efflux transporters, as these can restrict oral

uptake and reduce bioavailability of harmful substrate compounds, thus protecting the body. Because salinomycin is an organic anion, we had expected that salinomycin would be a substrate for MRP2 and/or BCRP, which are known to transport a broad spectrum of organic anions. However, we found that P-gp, which primarily transports hydrophobic neutral or positively charged compounds, actively transported salinomycin *in vitro*, and MRP2 and BCRP did not. Moreover, P-gp appeared to be a major determinant of the pharmacokinetic behavior and toxicity of salinomycin in mice.

This thesis also includes a chapter on *in vitro* drug-drug interaction studies that involve ABC transporters. Nowadays, it is well recognized that, in addition to metabolism-based drug-drug interactions, interactions at the level of drug transporters can profoundly affect the absorption, distribution and elimination of drugs. In a draft guidance on drug-drug interaction studies for the industry, the US Food and Drug Administration (FDA) has included *in vitro* assays to evaluate whether a drug is a substrate or an inhibitor of P-gp (5). In this guidance, decision trees are depicted that can be used to evaluate in vitro transport results to determine whether *in vivo* drug-drug interaction studies with an established P-gp substrate or an P-gp inhibitor are necessary. P-gp is the first discovered and most extensively studied mammalian ABC transporter, and its impact on the *in vivo* behavior of many drugs has been recognized for a long time. In recent years it has become clear that more ABC transporters importantly determine the pharmacokinetics of numerous (anticancer) drugs. It is therefore expected that *in vitro* screening assays for more ABC transporters will soon be recommended by the FDA. Moreover, single and combination ABC transporter knockout mice may also be applied during drug development, as these are valuable preclinical tools to determine the *in vivo* impact of ABC transporters.

In summary, the studies described in this thesis show that combination ABC transporter knockout models are valuable tools to unravel the pharmacological functions of ABC transporters and we expect that these model will be extensively used in future preclinical research.

REFERENCES

(1) Kamath AV, Wang J, Lee FY, Marathe PH. Preclinical pharmacokinetics and in vitro metabolism of dasatinib (BMS-354825): a potent oral multi-targeted kinase inhibitor against SRC and BCR-ABL. Cancer Chemother Pharmacol 2008;61:365-76.

(2) Schinkel AH, Smit JJ, van Tellingen O, Beijnen JH, Wagenaar E, van Deemter L et al. Disruption of the mouse mdr1a P-glycoprotein gene leads to a deficiency in the blood-brain barrier and to increased sensitivity to drugs. Cell 1994;77:491-502.

(3) Erdilyi DJ, Kamory E, Csokay B, Andrikovics H, Tordai A, Kiss C et al. Synergistic interaction of ABCB1 and ABCG2 polymorphisms predicts the prevalence of toxic encephalopathy during anticancer chemotherapy. Pharmacogenomics J 2008;8:321-7.

(4) van der Linde-Sipman JS, van den Ingh TS, van nes JJ, Verhagen H, Kersten JG, Beynen AC et al. Salinomycin-induced polyneuropathy in cats: morphologic and epidemiologic data. Vet Pathol 1999;36:152-6.

(5) Drug Interaction Studies - Study Design Data Analysis and Implications for Dosing and Labeling. (http://www.fda.gov/Cder/guidance/6695dft.pdf). FDA draft guidance 2006.

SUMMARY / SAMENVATTING

ATP-binding cassette (ABC) multidrug transporters are drug efflux pumps located in the plasma membrane that utilize the energy of ATP hydrolysis to extrude a wide spectrum of endogenous and exogenous compounds from cells, including numerous (anticancer) drugs and/or their metabolites. The studies described in this thesis focus on the pharmacological functions of the ABC transporters: P-glycoprotein (P-gp/ABCB1), the Multidrug Resistance Proteins 2 and 3 (MRP2/ABCC2 and MRP3/ABCC3) and the Breast Cancer Resistance Protein (BCRP/ABCG2). Most results presented in this thesis were obtained by studying single and combination ABC multidrug transporter knockout mice. As ABC multidrug transporters do not only have very broad, but also substantially overlapping substrate specificities, they can often partially, or sometimes even fully, compensate for the loss of each other. Combination ABC drug transporter knockout mice are therefore invaluable tools to study the separate roles and functional overlap of ABC multidrug transporters.

P-gp, MRP2 and BCRP are abundant in the liver, intestine and kidneys, where they facilitate the elimination of their substrates by active excretion into bile, feces and urine. Furthermore, these ABC multidrug transporters can also reduce the oral availability of drugs and xenotoxins by pumping these back from the enterocytes into the gut lumen. In addition, profound expression at important blood-tissue barriers such as the blood-brain, blood-testis and placental materno-fetal barrier has an important protective function, as these ABC multidrug transporters can drastically restrict the penetration of potentially harmful compounds into these tissues. MRP3 is also abundant in the liver, intestine and kidneys, but it is located in the basolateral cell membranes, i.e. opposite to the apical membranes were P-gp, MRP2 and BCRP are present. Therefore, MRP3 pumps its substrates towards the blood circulation.

Chapter 1 gives an overview of insights into the pharmacological and physiological functions of ABC multidrug transporters that were obtained by studying multidrug transporter knockout mice. In Chapter 1.1 the combination multidrug transporter knockout mice are discussed, whereas Chapter 1.2 primarily focuses on Bcrp1 knockout mice.

In **Chapter 2** studies on the interactions of ABC multidrug transporters with several anionic drugs are presented, including salinomycin, diclofenac and benzbromarone. The polyether antibiotic salinomycin (Chapter 2.1) is widely used as a coccidiostatic drug in poultry and commonly fed to ruminant animals to improve feed efficiency. However, salinomycin can also cause severe toxicity when accidentally fed to animals in high doses. A batch of dry cat food that was accidentally contaminated with salinomycin resulted in an outbreak of acute polyneuropathy among the exposed cats. This incident triggered us to investigate

whether salinomycin was a substrate of one of the apical ABC multidrug transporters, as these efflux pumps can importantly restrict the oral uptake of their substrates. Salinomycin was *in vitro* identified to be a P-gp substrate. Moreover, P-gp-deficient mice displayed markedly higher salinomycin plasma concentrations and the absence of P-gp was associated with increased susceptibility to salinomycin toxicity. This finding is especially of interest because P-gp was thus far thought to mainly affect hydrophobic, positively charged or neutral drugs *in vivo*. However, the results described in Chapter 2.1 show that P-gp can also be a major determinant of the pharmacokinetic behavior and toxicity of an organic anionic drug.

In Chapter 2.2 the results of various *in vitro* transport and drug-drug interaction studies are described. We show that the analgesic and anti-inflammatory drug diclofenac is actively transported by mouse Bcrp1 and human BCRP. In addition, diclofenac and the uricosuric drug benzbromarone markedly stimulated MRP2-mdiated transport of the anticancer agents docetaxel and paclitaxel and the HIV protease inhibitor saquinavir. These findings may be of interest for anticancer drug therapy, when drug concentrations are often critical and stimulation of drug elimination via MRP2 may result in suboptimal chemotherapeutic drug concentrations. Moreover, stimulation of MRP2 activity in tumors may lead to increased efflux of chemotherapeutic agents from the tumors, thereby rendering these tumors resistant to anticancer drugs.

Chapter 2.3 deals with the *in vivo* interactions of diclofenac acyl glucuronide, the primary metabolite of diclofenac, with the ABC multidrug transporters BCRP, MRP2 and MRP3. Diclofenac acyl glucuronide is chemically instable and reactive and in humans this metabolite is associated with rare but serious idiosyncratic liver toxicity. We show that complete loss of Mrp2 and Bcrp1 results in disrupted hepatobiliary excretion of diclofenac acyl glucuronide and consequently, in highly increased plasma levels of this metabolite. We further show that the efflux of diclofenac acyl glucuronide from liver to the blood circulation is largely dependent on Mrp3. This might explain why combination Mrp2/Mrp3/Bcrp1 knockout mice, which had markedly elevated liver concentrations of diclofenac acyl glucuronide, displayed acute, albeit mild, hepatotoxicity.

Chapter 3 describes the *in vivo* interactions of the plant-derived anticancer drugs paclitaxel (Chapter 3.1) and etoposide (Chapter 3.2) with ABC multidrug transporters. The Chapter on paclitaxel describes the generation and characterization of combination P-gp/Mrp2 knockout mice, which were subsequently used to assess the distinct roles of P-gp and Mrp2 in paclitaxel pharmacokinetics. Although paclitaxel is an excellent P-gp substrate, Mrp2 was found to almost exclusively mediate the excretion of paclitaxel from the liver into

the bile, whereas P-gp had little effect. This finding is especially interesting because Mrp2 was thus far thought to mainly affect organic anionic drugs *in vivo*. However, the results presented in Chapter 3.1 show that Mrp2 can also be a major determinant of the pharmacokinetic behavior of highly lipophilic anti-cancer drugs, even in the presence of other efficient transporters.

The aim of the study presented in Chapter 3.2 was to investigate the impact of P-gp, MRP2 and MRP3 on the pharmacokinetics of etoposide. P-gp was found to restrict the oral (re)uptake of etoposide, and to mediate its excretion across the gut wall. Furthermore, the excretion of etoposide into the bile was dominated by Mrp2, which was qualitatively similar to the results that were observed for paclitaxel (Chapter 3.1). However, for paclitaxel disrupted hepatobiliary excretion upon the loss of Mrp2 resulted in elevated plasma concentrations of unchanged drug, whereas for etoposide this was not the case. Instead, hampered biliary excretion in Mrp2 knockout mice led to an increased hepatic formation of etoposide glucuronide and markedly increased plasma levels of this metabolite. The efflux of etoposide glucuronide from the liver to the blood was found to be mediated by Mrp3 and simultaneous loss of Mrp2 and Mrp3 resulted in profound accumulation of etoposide glucuronide in the liver. This study nicely illustrates that the body is very flexible in protecting itself against harmful compounds. When the hepatobiliary excretion of etoposide via Mrp2 is disrupted, the glucuronidation pathway takes over, thereby protecting the body from exposure to toxic etoposide levels.

In **Chapter 4** P-gp and BCRP combination knockout mice enabled us to demonstrate that both multidrug transporters act in concert at the blood-brain barrier in restricting the brain penetration of the tyrosine kinase inhibitors dasatinib (Chapter 4.1) and sorafenib (Chapter 4.2). The brain penetration of dasatinib was primarily restricted by P-gp, whereas loss of BCRP had no effect. However, when both transporters were absent a disproportional increase in brain accumulation of dasatinib was observed. In contrast, for sorafenib it was the other way around, i.e. absence of P-gp had no effect while BCRP deficiency resulted in markedly elevated brain levels. Again, simultaneous loss of both transporters resulted in a highly increased brain penetration. These results provide a rationale for combining these tyrosine kinase inhibitors with a dual inhibitor of P-gp and BCRP to boost the brain penetration of these drugs. To test this concept, we combined dasatinib with the P-gp and BCRP inhibitor elacridar and found indeed that the brain penetration in wild-type mice could be increased to P-gp/BCRP knockout levels. These findings might be clinically relevant for patients with intracranial tumors, as concomitant administration of an inhibitor of P-gp and ABCG2 with dasatinib,

sorafenib or possibly other tyrosine kinase inhibitors might result in better therapeutic responses in these patients.

In conclusion, the studies described in this thesis demonstrate the power of combination ABC multidrug transporter knockout models to study the pharmacological functions of ABC multidrug transporters. Using these models it was found that P-gp can affect the in vivo behavior of an anionic drug, whereas MRP2 can be a major determinant of the pharmacokinetics of highly lipophilic and amphipathic drugs, thereby expanding the already broad substrate specificities of these ABC multidrug transporters. Furthermore, we show that, in addition to P-gp, also BCRP importantly contributes to the blood-brain barrier. We expect that combination transporter knockout mouse models will be extensively used as preclinical research tools in the future.

"ATP-binding cassette (ABC) multidrug transporters" zijn geneesmiddel efflux-pompen in het plasmamembraan van cellen, die met behulp van energie een breed scala aan lichaamseigen en lichaamsvreemde verbindingen de cel uit kunnen pompen, waaronder vele (antikanker) geneesmiddelen en/of metabolieten daarvan. De nadruk in de studies die worden beschreven in dit proefschrift ligt op de farmacologische functies van een viertal ABC transporters, te weten P-glycoprotein (P-gp/MDR1), de "Multidrug Resistance Proteins" 2 en 3 (MRP2/ABCC2 en MRP3/ABCC3) en "Breast Cancer Resistance Protein" (BCRP/ABCG2). De meeste resultaten die worden gepresenteerd in dit proefschrift zijn verkregen door bestudering van zogenaamde ABC transporter knockout muizen. Dit zijn muizen die deficiënt zijn voor één of meerdere ABC multidrug transporters. Omdat ABC multidrug transporters een zeer breed en vaak ook een substantieel overlappend spectrum aan substraten kunnen verpompen, kan bij afwezigheid van één ABC transporter een andere transporter de functie van de afwezige transporter vaak gedeeltelijk of soms zelfs helemaal overnemen. Combinatie transporter knockout muizen zijn daarom waardevolle modellen om zowel de separate als de overlappende functies van ABC multidrug transporters te bestuderen.

P-gp, MRP2 en BCRP komen veelvuldig voor in de lever, de dunne darm en de nieren, waar deze transporters een belangrijke rol spelen bij de eliminatie van hun substraten in de gal, feces and urine. Daarnaast kunnen deze ABC transpoters de orale beschikbaarheid van veel geneesmiddelen en andere lichaamsvreemde stoffen substantieel verlagen doordat ze hun substraten vanuit de epitheelcellen in de darm kunnen terugpompen naar het darmlumen. Ook komen deze transporters voor in bloed-weefsel barrières, zoals de bloed-hersen, de bloed-testis en de bloed-placenta barrière, waar ze een belangrijke beschermende functie hebben en de penetratie van potentieel gevaarlijke stoffen in deze weefsels kunnen tegengaan. MRP3 komt eveneens veelvuldig voor in de lever, de dunne darm en de nieren, maar dan in de basolaterale membraan, dat wil zeggen, de membraan tegenover de apicale membraan waar P-gp, MRP2 en BCRP aanwezig zijn. Het transport dat MRP3 verzorgt verloopt dan ook in de richting van de bloed circulatie.

Hoofdstuk 1 geeft een overzicht van recente inzichten in de farmacologische en fysiologische functies van ABC multidrug transporters, die verkregen zijn bij de bestudering van multidrug transporter knockout muizen. In hoofdstuk 1.1 worden combinatie multidrug transporter knockout muizen bediscussieerd, terwijl hoofdstuk 1.2 hoofdzakelijk ingaat op Bcrp1 knockout muizen.

In **hoofdstuk 2** worden studies beschreven over de interacties van ABC multidrug transporters met een aantal anionische verbindingen, waaronder salinomycine, diclofenac en benzbromaron. Salinomycine (hoofdstuk 2.1) is een polyether antibioticum dat veel wordt gebruikt als coccidiostaticum bij pluimvee en

ook vaak aan herkauwers wordt gegeven om de voedingsefficiëntie te verbeteren. Echter, salinomycine kan ook serieuze toxiciteit veroorzaken wanneer het per ongeluk in hoge dosering aan dieren wordt gegeven. Zo resulteerde een met salinomycine verontreinigde partij droog kattenvoer in een uitbraak van polyneuropathie in de blootgestelde katten. Dit incident was voor ons de aanleiding om te onderzoeken of salinomycine een substraat is voor één van de apicale ABC multidrug transporters, gezien het feit dat deze efflux pompen de orale beschikbaarheid van hun substraten in belangrijke mate kunnen beperken. *In vitro* hebben we laten zien dat salinomycine een substraat is van P-gp. Sterker nog, we vonden dat P-gp deficiënte muizen die met salinomycine behandeld waren substantieel hogere salinomycine plasma spiegels hadden dan controle muizen en de afwezigheid van P-gp leidde tot een hogere gevoeligheid voor salinomycine toxiciteit. Deze bevinding is met name van belang omdat van P-gp tot dusverre werd gedacht dat deze transporter voornamelijk invloed had op het gedrag van hydrofobe, positief geladen of neutrale verbindingen in het lichaam. Echter, de resultaten die in hoofdstuk 2.1 beschreven worden laten zien dat P-gp ook een belangrijke determinant kan zijn voor de farmacokinetiek en toxiciteit van een organisch anion.

In hoofdstuk 2.2 worden de resultaten van verscheidene *in vitro* transport en geneesmiddel interactie studies beschreven. We laten zien dat diclofenac, een pijnstillend en koortsverlagend geneesmiddel, actief getransporteerd wordt door muis Bcrp1 en humaan BCRP. Ook vonden we dat diclofenac en benzbromaron het MRP2-gemedieerde transport van de antikanker geneesmiddelen docetaxel en paclitaxel en van de HIV protease remmer saquinavir kan stimuleren. Deze bevindingen kunnen van belang zijn voor de behandeling van patiënten met antikanker geneesmiddelen, omdat deze middelen vaak een smal therapeutisch venster hebben en stimulatie van de eliminatie van deze geneesmiddelen via Mrp2 zou kunnen leiden tot suboptimale geneesmiddel concentraties. Sterker nog, stimulatie van de activiteit van Mrp2 in tumoren zou kunnen resulteren in actieve efflux van antikanker geneesmiddelen uit tumor cellen, en daarmee tot geneesmiddel resistentie.

Hoofdstuk 2.3 behandelt de *in vivo* interacties van diclofenac acyl glucuronide, de belangrijkste metaboliet van diclofenac, met de ABC multidrug transporters BCRP, MRP2 en MRP3. Diclofenac acyl glucuronide is chemisch instabiel en reactief en deze metaboliet wordt in mensen geassocieerd met sporadische maar ernstige idiosyncratische levertoxiciteit. We laten zien dat complete afwezigheid van Mrp2 en Bcrp1 leidt tot een verstoorde galuitscheiding van diclofenac acyl glucuronide en dientengevolge, tot sterk verhoogde plasmaconcentraties van deze metaboliet. Ook laten we zien dat de efflux van diclofenac acyl glucuronide vanuit

de lever naar de bloedcirculatie in sterke mate afhankelijk is van Mrp3. Dit zou kunnen verklaren waarom combinatie Mrp2/Mrp3/Bcrp1 knockout muizen, die substantieel verhoogde leverconcentraties van diclofenac acyl glucuronide hadden, acute, zij het milde, levertoxiciteit ondervonden.

Hoofdstuk 3 beschrijft de *in vivo* interacties van de plant afgeleide antikanker geneesmiddelen paclitaxel (hoofdstuk 3.1) en etoposide (hoofdstuk 3.2) met ABC multidrug transporters. Het hoofdstuk over paclitaxel beschrijft het genereren en karakteriseren van combinatie P-gp/Mrp2 knockout muizen die vervolgens gebruikt werden om de specifieke impact van P-gp en Mrp2 op de farmacokinetiek van paclitaxel te bestuderen. Alhoewel paclitaxel een uitstekend P-gp substraat is, was het Mrp2 dat de excretie van paclitaxel vanuit de lever naar de gal bijna geheel voor zijn rekening nam, terwijl P-gp weinig effect had op dit proces. Dit is een belangrijke bevinding omdat van Mrp2 tot op heden gedacht werd dat deze transporter voornamelijk effect had op het *in vivo* gedrag van organische anionen. Echter, de resultaten die in hoofdstuk 3.1 gepresenteerd worden laten zien dat Mrp2 ook belangrijk kan zijn voor de farmacokinetiek van een zeer lipofiel antikanker geneesmiddel, zelfs in de aanwezigheid van andere efficiënte transporters voor dit geneesmiddel.

Het doel van de studie die beschreven wordt in hoofdstuk 3.2 was om te onderzoeken in welke mate P-gp, MRP2 en MRP3 de farmacokinetiek van etoposide kunnen beïnvloeden. P-gp bleek de (her)opname van etoposide vanuit de darmen te beperken en was verantwoordelijk voor de uitscheiding van etoposide over de darmwand. Daarnaast werd de uitscheiding van etoposide in de gal gedomineerd door Mrp2. Deze resultaten waren kwalitatief vergelijkbaar met de bevindingen voor paclitaxel (hoofdstuk 3.1). Echter, verstoorde uitscheiding van paclitaxel in de gal door afwezigheid van Mrp2 leidde tot verhoogde plasmaconcentraties van onveranderd geneesmiddel, terwijl voor etoposide dit niet het geval was. In plaats daarvan resulteerde verstoorde galuitscheiding in Mrp2 knockout muizen tot een verhoogde formatie van etoposide glucuronide in de lever met substantieel verhoogde plasmaconcentraties van deze metaboliet als gevolg. De uitscheiding van etoposide glucuronide vanuit de lever naar het bloed werd voornamelijk door Mrp3 verzorgd en gelijktijdige afwezigheid van Mrp2 en Mrp3 leidde tot een uitgesproken accumulatie van etoposide glucuronide in de lever. Deze studie laat zien dat het lichaam zeer flexibel is en zich op meerdere manieren kan beschermen tegen potentieel schadelijk verbindingen. Zo kan etoposide, wanneer de galuitscheiding van deze stof via Mrp2 is verstoord, in verhoogde mate geglucuronideerd worden en met de urine worden geëlimineerd.

In **hoofdstuk 4** werd met behulp van P-gp/BCRP combinatie knockout muizen aangetoond dat deze multidrug transporters samenwerken in de bloed-hersen barrière en de penetratie van de tyrosine kinase remmers dasatinib (hoofdstuk 4.1) en sorafenib (hoofdstuk 4.2) kunnen tegenwerken. De hersenpenetratie van dasatinib werd vooral gelimiteerd door P-gp, terwijl afwezigheid van BCRP geen effect had. Echter, wanneer beide transporters afwezig waren, werd een disproportionele verhoging in de hersenaccumulatie waargenomen. Voor sorafenib was het andersom, dat wil zeggen dat afwezigheid van P-gp geen effect had, terwijl afwezigheid van Bcrp1 leidde tot een substantieel verhoogde hersenconcentratie. Wederom leidde afwezigheid van beide transporters tot een disproportionele verhoging in de hersenaccumulatie. Deze resultaten vormen een rationele basis om deze tyrosine kinase remmers te combineren met een remmer voor zowel P-gp als BCRP met het doel om de hersenpenetratie van deze antikanker geneesmiddelen te verhogen. Om dit principe te bestuderen hebben we dasatinib gecombineerd met de P-gp en BCRP remmer elacridar en we vonden dat de hersenpenetratie in controle muizen inderdaad verhoogd kon worden tot het niveau dat in P-gp/BCRP knockout muizen werd gevonden. Deze bevindingen kunnen klinisch relevant zijn voor patiënten met hersentumoren, omdat de combinatie van een remmer van P-gp en BCRP met dasatinib, sorafenib en mogelijk andere tyrosine kinase remmers zou kunnen leiden tot een betere therapeutische respons in deze patiënten.

Op basis van de studies die in dit proefschrift worden beschreven kunnen we concluderen dat combinatie ABC multidrug transporter knockout muizen bruikbare modellen zijn om de farmacologische functies van ABC multidrug transporters te bestuderen. Met behulp van deze modellen hebben we gevonden dat P-gp het *in vivo* gedrag van een organisch anion kan beïnvloeden, terwijl MRP2 een belangrijke rol kan spelen bij de farmacokinetiek van zeer lipofiele en amfipatische geneesmiddelen. Deze studies laten zien dat de reeds brede substraat specificiteit van deze ABC multidrug transporters dus nog breder blijkt te zijn dan tot nu toe werd aangenomen. Daarnaast laten we zien dat niet alleen P-gp maar ook BCRP een belangrijke beschermende functie heeft in de bloed-hersen barrière. We verwachten dat deze combinatie transporter knockout muis modellen veelvuldig gebruikt zullen worden bij toekomstig preklinisch onderzoek.

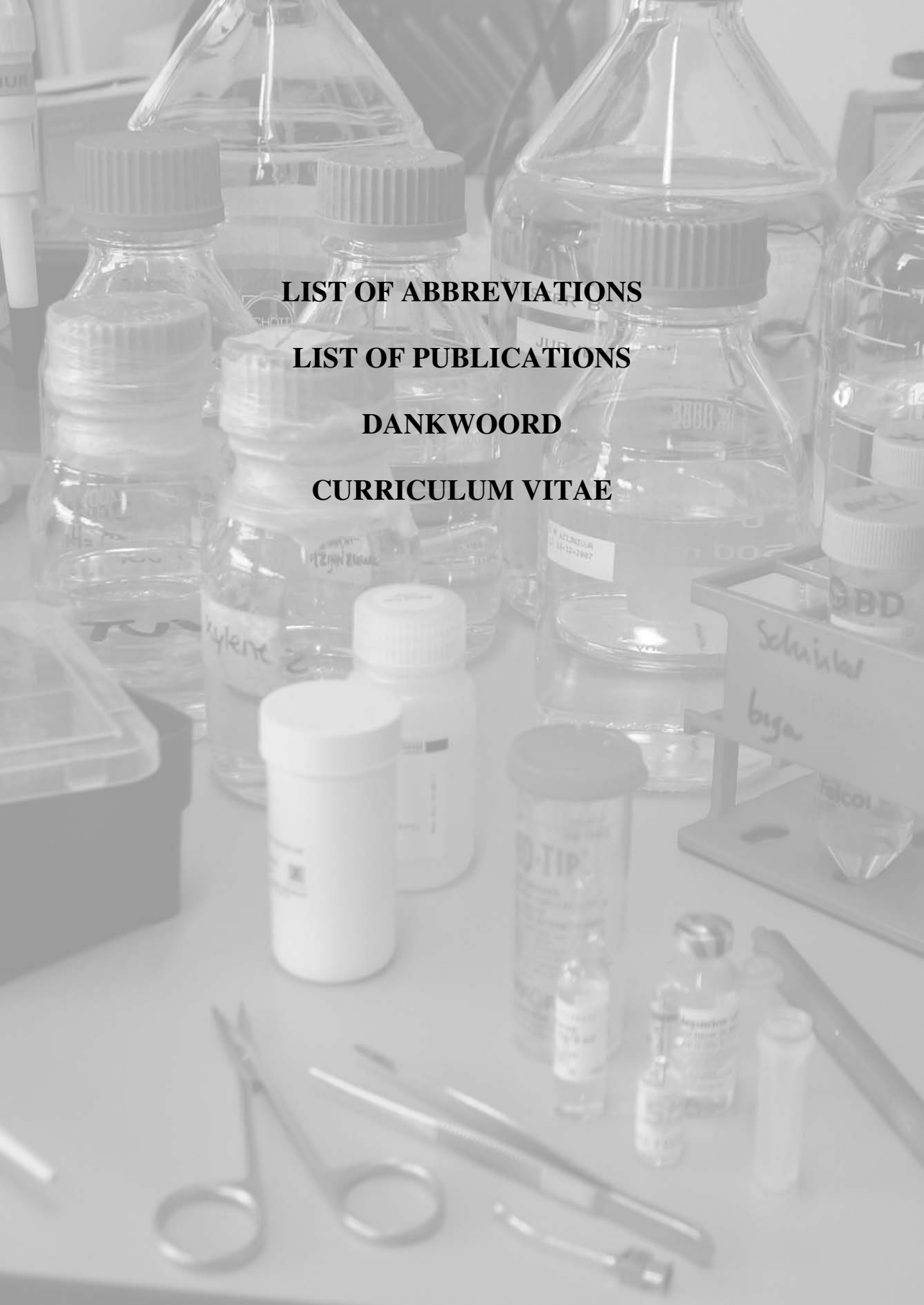

LIST OF ABBREVIATIONS

LIST OF PUBLICATIONS

DANKWOORD

CURRICULUM VITAE

LIST OF ABBREVIATIONS

ABC	ATP-binding cassette
ABCB	ATP-binding cassette transporter family B
ABCC	ATP-binding cassette transporter family C
ABCG	ATP-binding cassette transporter family G
ALAT	alanine aminotransferase
AUC	area under the plasma concentration-time curve
BBB	blood-brain barrier
BCRP	breast cancer resistance protein
BSA	bovine serum albumin
Ci	Curie
CL	clearance
C_{max}	maximum drug concentration in plasma
CSF	cerebrospinal fluid
CYP	cytochrome P450
DHEAS	dehydroepiandrosterone sulfate
DMSO	dimethylsulfoxide
DNA	desoxyribonucleic acid
$E_2$17βG	estradiol-17β-glucuronide
GSH	glutathione
HIV	human immunodeficiency virus
HPLC	high performance liquid chromatography
IC_{50}	half-maximal inhibitory concentration
ID	internal diameter
i.v.	intravenous
i.p.	intraperitoneal
KO	knockout
LC-MS/MS	liquid chromatography with tandem mass spectrometry detection
LTC_4	leukotriene C4
MDCK	Madin-Darby canine kidney
MDR	multidrug resistance
MRP	Multidrug-resistance protein
mRNA	messenger ribonucleic acid
MTX	methotrexate
P-gp	P-glycoprotein
PK	pharmacokinetics
RNA	ribonucleic acid
RT-PCR	reverse transcriptase polymerase chain reaction
SD	standard deviation

SI	small intestine
SIC	small intestinal contents
SNP	single nucleotide polymorphism
SP	side population
TKO	triple knockout mice
T_{max}	time to maximum drug concentration in plasma
$t_{½}$	terminal half-life
UDP	Uridine diphosphate
UGT	UDP-glucuronosyltransferase
UV	ultraviolet
WT	wild-type

LIST OF PUBLICATIONS

1. Lagas JS*, Vlaming ML*, Schinkel AH. Compound transporter knockout mice: powerful tools to unravel the pharmacological and physiological functions of ATP-binding cassette drug transporters. *Invited, to be submitted. *contributed equally*

2. Lagas JS, Sparidans RW, Wagenaar W, Beijnen JH, Schinkel AH. Hepatic clearance of reactive glucuronide metabolites of diclofenac is dependent on multiple ATP-binding cassette efflux transporters. *To be submitted*

3. Lagas JS, Fan L, Wagenaar E, Vlaming ML, van Tellingen O, Beijnen JH, Schinkel AH. P-glycoprotein (P-gp/*ABCB1*), ABCC2 and ABCC3 determine the pharmacokinetics of etoposide. *To be submitted*

4. Lagas JS, van Waterschoot RA, Sparidans RW, Wagenaar E, Beijnen JH, Schinkel AH. Breast cancer resistance protein (BCRP/ABCG2) and P-glycoprotein (P-gp/MDR1) limit sorafenib brain penetration. *Submitted for publication*

5. Van Waterschoot RA, Lagas JS, Wagenaar E, van der Kruijssen CM, van Herwaarden AE, Rooswinkel RW, van Tellingen O, Rosing H, Beijnen JH, Schinkel AH. Highly efficient detoxification by Cytochrome P450 3A and P-glycoprotein is based on additive but not synergistic collaboration. *Submitted for publication*

6. Damen CW, Lagas JS, Rosing H, Schellens JH, Beijnen JH. The bioanalysis of vinorelbine and 4-*O*-deacetylvinorelbine in human and mouse plasma using high-performance liquid chromatography coupled with heated electrospray ionization tandem mass spectrometry. *Biomed Chrom, accepted for publication*

7. Lagas JS, van Waterschoot RA, van Tilburg AC, Hillebrand MJ, Lankheet N, Rosing H, Beijnen JH, Schinkel AH. Brain accumulation of dasatinib is restricted by P-glycoprotein (MDR1) and breast cancer resistance protein (ABCG2) and can be enhanced by elacridar treatment. *Clin Cancer Res. 2009; 15:2344-2351*

8. Vlaming ML*, Lagas JS*, Schinkel AH. Physiological and pharmacological roles of ABCG2 (BCRP): recent findings in Abcg2 knockout mice. *Adv Drug Deliv Rev. 2009; 61:14-25. * contributed equally*

9. Sparidans RW, Vlaming ML, Lagas JS, Schinkel AH, Schellens JH, Beijnen JH. Liquid chromatography-tandem mass spectrometric assay for sorafenib and sorafenib-glucuronide in mouse plasma and liver homogenate and identification of the glucuronide metabolite. *J Chromatogr B Analyt Technol Biomed Life Sci. 2009; 877:269-276*

10. Lagas JS, van der Kruijssen CM, van de Wetering K, Beijnen JH, Schinkel AH. Transport of diclofenac by BCRP (ABCG2) and stimulation of MRP2 (ABCC2)-mediated drug transport by diclofenac and benzbromarone. *Drug Metab Dispos. 2009; 37:129-136*

11. Sparidans RW, Lagas JS, Schinkel AH, Schellens JH, Beijnen JH. Liquid chromatography-tandem mass spectrometric assay for diclofenac and three primary metabolites in mouse plasma. *J Chromatogr B Analyt Technol Biomed Life Sci. 2008; 872:77-82*

12. Damen CW, Rosing H, Tibben MM, van Maanen MJ, Lagas JS, Schinkel AH, Schellens JH, Beijnen JH. A sensitive assay for the quantitative analysis of vinorelbine in mouse and human EDTA plasma by high-performance liquid chromatography coupled with electrospray tandem mass spectrometry. *J Chromatogr B Analyt Technol Biomed Life Sci. 2008; 868:102-109*

13. Lagas JS, Sparidans RW, van Waterschoot RA, Wagenaar E, Beijnen JH, Schinkel AH. P-glycoprotein limits oral availability, brain penetration, and toxicity of an anionic drug, the antibiotic salinomycin. *Antimicrob Agents Chemother. 2008; 5 2:1034-103.*

14. van Waterschoot RA, van Herwaarden AE, Lagas JS, Sparidans RW, Wagenaar E, van der Kruijssen CM, Goldstein JA, Zeldin DC, Beijnen JH, Schinkel AH. Midazolam metabolism in cytochrome P450 3A knockout mice can be attributed to up-regulated CYP2C enzymes. *Mol Pharmacol. 2008; 73:1029-1036*

15. Sparidans RW, Lagas JS, Schinkel AH, Schellens JH, Beijnen JH. Liquid chromatography-tandem mass spectrometric assays for salinomycin in mouse plasma, liver, brain and small intestinal contents and in OptiMEM cell culture medium. *J Chromatogr B Analyt Technol Biomed Life Sci. 2007; 855:200-210*

16. Lagas JS, Vlaming ML, van Tellingen O, Wagenaar E, Jansen RS, Rosing H, Beijnen JH, Schinkel AH. Multidrug resistance protein 2 is an important determinant of paclitaxel pharmacokinetics. *Clin Cancer Res. 2006; 12:6125-6132*

17. Vlaming ML, Mohrmann K, Wagenaar E, de Waart DR, Elferink RP, Lagas JS, van Tellingen O, Vainchtein LD, Rosing H, Beijnen JH, Schellens JH, Schinkel AH. Carcinogen and anticancer drug transport by Mrp2 in vivo: studies using Mrp2 (Abcc2) knockout mice. *J Pharmacol Exp Ther. 2006; 318:319-327*

DANKWOORD

Mijn boekje is af! Met veel voldoening en plezier kijk ik terug op een voor mij zeer vruchtbare en bovenal leerzame periode. Omdat ik dit proefschrift nooit had kunnen realiseren zonder inspiratie, motivatie, support en samenwerking wil ik iedereen die hieraan een bijdrage heeft geleverd graag hartelijk danken.

Allereerst mijn co-promotor Dr. Alfred Schinkel. Beste Alfred, met heel veel plezier heb ik onderzoek gedaan in je groep. Ik heb het bijzonder gewaardeerd dat ik altijd bij je kon binnenlopen voor overleg. Je feedback op mijn presentaties en kritische commentaar op mijn manuscripten was altijd opbouwend en ik vond het fijn dat je me de ruimte gaf om tijdens mijn onderzoek mijn eigen koers te varen.

Mijn promotor Prof. Dr. Jos Beijnen. Beste Jos, ik heb niet heel vaak met je overlegd, maar je enthousiasme voor wetenschappelijk onderzoek in het algemeen heb ik als zeer plezierig ervaren. Ook je snelle respons op mijn manuscripten en de mogelijkheden die je hebt gecreëerd ter analytische ondersteuning van mijn projecten door je laboratoria in Amsterdam en Utrecht heb ik zeer gewaardeerd.

De leden van mijn beoordelingscommissie, Prof. Dr. P. Borst, Prof. Dr. J.H.M. Schellens, Prof. Dr. Ir. A.C. Beynen, Prof. Dr. R.P.J. Oude Elferink en Dr. G.H.M. Engels ben ik zeer erkentelijk voor het kritisch doorlezen en beoordelen van het manuscript.

Al mijn (ex-) collega's uit de Schinkel groep, evenals mijn ex-kamergenoten uit andere groepen, wil ik heel hartelijk danken voor alle hulp, wetenschappelijke discussies en natuurlijk voor alle gezelligheid. Hans, Gracia, Sandra, Teun, Christie, Sigga, Francesco, Christiaan, Corina, Marijn, Els, Evita, Robert, Anita, Dilek en Seng Chuan, allen bedankt!

Dan de studenten die in het kader van hun wetenschappelijke stage aan dit onderzoek meewerkten, Vicky van Tilburg en Lin Fan. Bijzonder bedankt voor jullie inzet en bijdrage aan mijn onderzoek! Ik vond het erg motiverend en leerzaam om jullie te begeleiden.

Olaf van Tellingen ben ik veel dank verschuldigd voor alle hulp bij de HPLC analyses die ik heb uitgevoerd op zijn lab. Tessa Buckle wil ik hartelijk danken voor de i.v. injecties bij mijn eerste proeven, toen ik deze techniek nog niet in de vingers had. Ook wil ik Nienke, Tessa en Roos bedanken voor de gezelligheid wanneer ik op het 'van Tellingen Research Lab' aan het werk was.

Rolf Sparidans uit de onderzoeksgroep van Jos Beijnen in Utrecht ben ik zeer erkentelijk voor de plezierige samenwerking. Ik denk met genoegen terug aan het diclofenac project, waarin we uiteindelijk met succes het instabiele diclofenac acyl glucuronide hebben kunnen stabiliseren en kwantificeren.

Dan wil ik een aantal collega OIO's uit het Slotervaart Ziekenhuis bedanken. Robert Jansen, Nienke Lankheet en Carola Damen, reuze bedankt voor alle monsters die jullie voor mij gemeten hebben! Ook wil ik Hilde Rosing en Michel Hillebrand hartelijk danken voor de analytische ondersteuning.

Alle proefdierverzorgers wil ik bedanken voor de goede zorg voor de muizen. Marius bedankt voor al je verhalen en Stephane voor je hulp bij een aantal van mijn experimenten. Met betrekking tot het muiswerk wil ik in het bijzonder Els Wagenaar uit onze groep bedanken voor haar bijdrage aan de ontwikkeling van de muismodellen waarmee ik heb gewerkt. Ook dank ik Els oprecht voor het inzetten en zorgvuldig controleren van de muizenfok, zodat we altijd een aanzienlijke en betrouwbare muizenpopulatie hadden. Het hanteren van de muizen en een aantal belangrijke experimentele muistechnieken heb ik geleerd van Loes Rijswijk en Ton Schrauwers, waarvoor hartelijk dank!

Henny en Theo van het radionucliden lab dank ik voor hun interesse in mijn werk, het toezicht wanneer ik alleen in de kelder aan het werk was en bovendien, voor de gezelligheid.

De mensen van het klinisch chemisch lab, in het bijzonder Enver Dilec en Rob Lodewijks, wil ik bedanken voor al hun analyses.

Alle mensen van de afdeling Experimentele Therapie (H6), waarvan de groep Schinkel de meeste tijd van mijn promotie deel uitmaakte, wil ik bedanken voor de gezelligheid tijdens de koffie, labstaps en kerstdiners. Een aantal mensen wil ik in het bijzonder noemen. Jimmy, bedankt voor alle potjes squash die helaas stopten toen jij met je opleiding begon. Sander, wij vormden waarlijk een goed duo toen we op de OIO-retreat op Texel een sessie voorzaten en later ook in Cambridge. Dick bedankt voor al je computerhulp. Conchita bedankt voor je hulp bij de rt-PCR. Hans bedankt voor het bestellen van al die pH meters. Thea bedankt voor je hulp op administratief vlak. Sari, Saske, Marion, Monique, Maarten en Lotte, en iedereen die ik vergeten mocht zijn te noemen, bedankt voor de gezellige gesprekken tijdens de lunch.

Stefan Harmsen uit de groep van Jan Schellens in Utrecht wil ik bedanken voor de gezelligheid tijdens het congres in San Diego. Gelukkig heb je in het lab meer succes met CAR, dan jullie hadden met de CAR in San Diego!

Evita en Robert, ons uitstapje naar Tijuana in Mexico op de vooravond aan het congres in San Diego was bij uitstek de plek om jullie te vragen mijn paranimfen te zijn. Een uitermate geslaagd masterplan! Evita, ik heb jouw positieve instelling, behulpzaamheid en gezelligheid altijd enorm kunnen waarderen. Robert, onze samenwerking heb ik als zeer plezierig ervaren, evenals het feit dat je een goed klankbord voor me was. Bedankt dat jullie mijn paranimfen willen zijn!

Mijn volleybalvrienden, jaarclub en mijn schoolvriend Machiel Kouwenberg, die ik al ken zolang ik mij kan heugen, wil ik bedanken voor de gezellige uitstapjes en etentjes de afgelopen jaren. Mijn zus Deirdre en broer Lourens Jan en hun partners evenals mijn schoonouders en mijn zwager en schoonzus, met aanhang, wil ik hartelijk danken voor hun interesse in mijn onderzoek en de gezelligheid tijdens familie bijeenkomsten.

Mijn ouders ben ik zeer veel dank verschuldigd voor alle support en hun vertrouwen in mij. Ik draag dan ook met trots dit boekje aan hen op. Mijn vader ben ik bovendien zeer erkentelijk voor de prachtige tekeningen die op de omslag prijken.

Tenslotte mijn vrouw. Lieve Willemien, bedankt voor al je liefde, steun, motivatie, geduld en bovenal voor de twee prachtige jongens die je me geschonken hebt tijdens mijn promotieonderzoek. Zoals ik in de inleiding van dit dankwoord al aangaf kijk ik met veel voldoening en plezier terug op een zeer vruchtbare periode.

Jurjen

CURRICULUM VITAE

Jurjen Sebastiaan Lagas was born on October 10th 1975 in Groningen. He followed his secondary education at the Willem Lodewijk Gymnasium in Groningen and received his VWO diploma in 1995. In 1997 he passed the propedeutic exam in Architecture at the University of Technology in Delft. In the same year, he enrolled in the study Pharmacy at the University of Groningen. During this study, Jurjen performed an internship at the department of Molecular Pharmacology of the University of Groningen under supervision of Prof. Dr. H. Meurs and Prof. Dr. J. Zaagsma. His project was entitled: "Competition between neuronal NO synthase and arginase for L-arginine in iNANC-mediated airway dilatation." He did a second internship at the National Heart and Lung Institute (London, UK) under supervision of Prof. Dr. P.J. Barnes and Dr. J.C.W. Mac and this project was entitled: "Effects of H_2O_2 on β_2-adrenoceptors and glucocorticoid receptors in the airways." In 2001 he received his Masters degree in Pharmacy and enrolled in the specialization to become a pharmacist. In 2003 he received his Doctor of Pharmacy degree and started working in a public pharmacy. In October 2004, Jurjen started a PhD project at the Division of Experimental Therapy at the Netherlands Cancer Institute in Amsterdam in the lab of Dr. A.H. Schinkel. This project was in collaboration with the research lab of Prof. Dr. J.H. Beijnen at the Department of Pharmacy and Pharmacology at the Slotervaart Hospital in Amsterdam.

Jurjen Sebastiaan Lagas werd op 10 oktober 1975 geboren in Groningen. Zijn middelbare schoolopleiding volgde hij aan het Willem Lodewijk Gymnasium in Groningen en in 1995 slaagde hij voor zijn VWO examen. In 1997 behaalde hij zijn propedeuse van de studie bouwkunde aan de Technische Universiteit in Delft en in datzelfde jaar begon hij met de studie farmacie aan de Rijks Universiteit van Groningen. Aan het einde van deze opleiding verrichtte Jurjen een afstudeer-onderzoek bij de vakgroep Moleculaire Farmacologie onder leiding van Prof. Dr. H. Meurs en Prof. Dr. J. Zaagsma en zijn project was getiteld: "Competitie tussen neuronaal NO synthase en arginase om L-arginine bij iNANC-gemediëerde luchtweg dilatatie". Hij deed een tweede afstudeerstage aan "the National Heart and Lung Institute (London, UK)" onder supervisie van Prof. Dr. P.J. Barnes and Dr. J.C.W. Mac en dit project was getiteld: "Effecten van H_2O_2 op β_2-adrenoceptoren en glucocorticoid receptoren in de luchtwegen." In 2001 haalde hij zijn Masters titel farmacie en startte hij met de vervolgopleiding tot apotheker. Zijn apothekersdiploma behaalde hij in 2003 en hij ging eerst aan de slag als openbaar apotheker. In oktober 2004 begon Jurjen met een promotieonderzoek bij de afdeling Experimentele Therapie van het Nederlands Kanker Instituut te Amsterdam in de groep van Dr. A.H. Schinkel. Dit onderzoek werd uitgevoerd in samenwerking met het onderzoekslaboratorium van Prof. Dr. J.H. Beijnen van de afdeling Farmacie and Farmacologie van het Slotervaart Ziekenhuis te Amsterdam.